Molecular and developmental characterization of the *Echinococcus multilocularis* stem cell system

Molekulare und entwicklungsbiologische Charakterisierung des *Echinococcus multilocularis* Stammzellsystems

Doctoral thesis for a doctoral degree at the Graduate School of Life Sciences,

Julius-Maximilians-Universität Würzburg,

Section Infection and Immunity

submitted by

Uriel Koziol

from

Montevideo

Würzburg, 2014

Submitted on: ……..……..

Office stamp

Members of the *Promotionskomitee*:

Chairperson: Prof. Dr. Markus Engstler

Primary Supervisor: Prof. Dr. Klaus Brehm

Supervisor (Second): Prof. Dr. Joachin Morschhäuser

Supervisor (Third): Dr. Daniel Lopez

Supervisor (Fourth): ……

(If applicable)

Date of Public Defence: ……..……

Date of Receipt of Certificates: ……..

Affidavit

I hereby confirm that my thesis entitled "**Molecular and developmental characterization of the *Echinococcus multilocularis* stem cell system**" is the result of my own work. I did not receive any help or support from commercial consultants. All sources and / or materials applied are listed and specified in the thesis.

Furthermore, I confirm that this thesis has not yet been submitted as part of another examination process neither in identical nor in similar form.

Würzburg, 10th June 2014 Uriel Koziol

Acknowledgements

First of all, I would like to thank Prof. Klaus Brehm, for accepting me into his Lab, and for his patience, enthusiasm, frankness and support (even for crazy ideas and projects). This lab is an excellent place to work and to learn, and I can´t remember a single Monday morning in which I was not motivated to start my week. I have learned a lot in my almost 4 years in Würzburg, and I believe I have also matured as a professional, thanks to his guidance and support.

I would also like to thank all of the members of my thesis committee: Prof. Klaus Brehm, Prof. Joachim Morschhäuser, and Dr. Daniel Lopez, for accepting to be my supervisors and for their accessibility and their help. Likewise, I am very grateful to the Graduate School of Life Sciences, for their support (including my doctoral fellowship) and for always looking for new ways to help us students.

I am very thankful to all the members of the "Echis" Lab (a.k.a. AG Brehm), especially to Monika Bergmann (Moni) and Dirk Radloff (Dirkules). Their excellent work and constant good mood is what keeps the lab alive, and I would have had to keep on doing my PhD until the 2018 World Cup if it was not for their help. Also, Dirk was "der offizielle Übersetzer" for old German papers, bank letters, thesis abstracts, and much more. Many thanks to my fellow students (many of whom are now doctors): Andreas, Anna, Dominick, Emilia, Ferenc, Julian, Justin, Luis, Marcela, Nadine, Raphaël, Sarah, Serrana, Silvia, Theresa, Tim; to the Azubis for their help in the laboratory (Daniella, Olivia, Lea, Regina); and to all of the IHM Mitarbeiter, especially to the Friday beering crew, as well as Reiner, Michael and Gunther, for providing us with jirds and with Helles.

Last, but definitively not least, I want to thank my family (pero esto tiene que ser en español). A mi esposa Ceci, lo mejor que me pasó en la vida, y espero que nunca más tengamos que estar lejos. A mi familia en Uruguay, que siempre me apoyaron; tanto allá como acá, siempre supe que ellos están conmigo. A todos ustedes, gracias por su cariño, apoyo, y paciencia.

Table of contents

1. Summary

The metacestode larva of *Echinococcus multilocularis* is the causative agent of alveolar echinococcosis (AE), one of the most dangerous zoonotic diseases in the Northern Hemisphere. Unlike "typical" metacestode larvae from other tapeworms, it grows as a mass of interconnected vesicles which infiltrates the liver of the intermediate host, continuously forming new vesicles in the periphery. From these vesicles, protoscoleces (the infective form for the definitive host) are generated by asexual budding. It is thought that in *E. multilocularis*, as in other flatworms, undifferentiated stem cells (so-called germinative cells in cestodes and neoblasts in free-living flatworms) are the sole source of new cells for growth and development. Therefore, this cell population should be of central importance for the progression of AE.

In this work, I characterized the germinative cells of *E. multilocularis*, and demonstrate that they are indeed the only proliferating cells in metacestode vesicles. The germinative cells are a population of undifferentiated cells with similar morphology, and express high levels of transcripts of a novel non-autonomous retrotransposon family (*ta-TRIM*s). Experiments of recovery after hydroxyurea treatment suggest that individual germinative cells have extensive self-renewal capabilities. However, germinative cells also display heterogeneity at the molecular level, since only some of them express conserved homologs of *fgfr*, *nanos* and *argonaute* genes, suggesting the existence of several distinct sub-populations. Unlike free-living flatworms, cestode germinative cells lack chromatoid bodies. Furthermore, *piwi* and *vasa* orthologs are absent from the genomes of cestodes, and there is widespread expression of some conserved neoblast markers in *E. multilocularis* metacestode vesicles. All of these results suggest important differences between the stem cell systems of free-living flatworms and cestodes.

1. Summary

Furthermore, I describe molecular markers for differentiated cell types, including the nervous system, which allow for the tracing of germinative cell differentiation. Using these molecular markers, a previously undescribed nerve net was discovered in metacestode vesicles. Because the metacestode vesicles are non-motile, and the nerve net of the vesicle is independent of the nervous system of the protoscolex, we propose that it could serve as a neuroendocrine system. By means of bioinformatic analyses, 22 neuropeptide genes were discovered in the *E. multilocularis* genome. Many of these genes are expressed in metacestode vesicles, as well as in primary cell preparations undergoing complete metacestode regeneration. This suggests a possible role for these genes in metacestode development. In line with this hypothesis, one putative neuropeptide (RGFI-amide) was able to stimulate the proliferation of primary cells at a concentration of 10^{-7} M, and the corresponding gene was upregulated during metacestode regeneration.

2. Zusammenfassung

Das Metazestoden Larvenstadium von *Echinococcus multilocularis* ist die Ursache für die alveoläre Echinokokkose (AE), eine der gefährlichsten Zoonosen in der nördlichen Hemisphäre. Im Gegensatz zu Metazestoden anderer Bandwürmer wächst es zu einem Labyrinth verknüpfter Vesikel, die in der Peripherie permanent neu gebildet werden und dabei die Leber des Wirts infilitrieren. In diesen Vesikeln werden die Protoskolizes (das infizierende Stadium für den Endwirt) durch asexuelle Knospung aus der Vesikelwand heraus gebildet. Man geht davon aus dass in *E. multilocularis*, wie in anderen Plattwürmen, undifferenzierte Stammzellen (so gennante „*Germinative cells*" in Bandwürmern und Neoblasten in Turbellarien) der einzige Ursprung neuer Zellen für Wachstum und Entwicklung sind. Deshalb sollte diese Zellpopulation eine zentrale Rolle im Fortschritt der AE spielen.

In dieser Arbeit habe ich die Germinative cells von *E. multilocularis* charakterisiert und zeige, dass sie tatsächlich die einzigen sich vermehrenden Zellen in Metazestodenvesikeln sind. Die Germinative cells sind eine Population von undifferenzierten Zellen mit ähnlicher Morphologie, die eine hohe Zahl an Transkripten einer neuen Retrotransposonfamilie (*ta-TRIMs*) exprimieren. Experimente nach Behandlung mit Hydroxyurea deuten darauf hin, dass einzelne Germinative cells die Fähigkeit haben sich selbst zu erneuern. Allerdings, zeigen die Germinative cells auch Heterogenität auf molekurarer Ebene, da nur manche von Ihnen konservierte Homologe von *fgfr*, *nanos* und *argonaute* Genen exprimieren, was auf die Existenz eindeutiger Subpopulationen hinweist. Im Gegensatz zu Turbellarien fehlen den Germinative cells von Zestoden "*Chromatoid bodies*", weiterhin fehlen dem Genom der Zestoden Orthologe von *piwi* und *vasa* und es werden einige Neoblastenmarker in den Metazestodenvesikeln von *E. multilocularis* umfassend exprimiert. All diese Ergebnisse zeigen deutliche Unterschiede zwischen den Stammzellsystemen von Turbellarien und Zestoden auf.

Ich beschreibe ausserdem molekulare Marker für differenzierte Zelltypen, inklusive solche des Nervensystems. Mit diesen Markern wurde ein Nervennetz in

2. Zusammenfassung

Metazestodenvesikeln endeckt, das bis dato unbeschrieben war. Da die Vesikel unbeweglich sind und ihr Nervennetz unabhängig vom Nervensystem des Protoscolex ist wird angenommen dass es als Neuroendokrinsystem dient. Mit Hilfe von Genomanalysen wurden 22 Neuropeptidgene im Genom von *E. multilocularis* entdeckt. Viele von ihnen werden sowohl in Metazestodenvesiklen exprimiert als auch in Primärzellpräparationen, die zu kompletten Vesikeln regenerieren. Das weist auf eine mögliche Rolle dieser Gene in der Metazestodenentwicklung hin. Einhergehend mit dieser Hypothese war ein putatives Neuropeptid (RGFIamide) in der Lage die Vermehrung von Primärzellen bei einer Konzentration von 10^{-7} M zu stimulieren, dabei war das korrespondierende Gen während der Metazestodenregeneration hochreguliert.

3. Introduction

3.1. Genus *Echinococcus* and Echinococcosis

The clinical term Echinococcosis is used to describe a group of zoonotic diseases caused by infection with the metacestode larvae of cestodes of the genus *Echinococcus* (order Cyclophyllidea, family Taeniidae). From the medical and veterinary point of view, the two most important species of this genus are *Echinococcus granulosus* (informally called the "dog tapeworm") and *Echinococcus multilocularis* (the so-called "fox tapeworm"), which are the causative agents of Cystic Echinococcosis (CE) and Alveolar Echinococcosis (AE), respectively (Eckert and Deplazes 2004). *E. granulosus* has a cosmopolitan distribution: it is present in over 100 countries from all continents except Antarctica, and is of medical and veterinary relevance (Eckert and Deplazes 2004; Moro and Schantz 2009). *E. multilocularis* on the other hand is restricted to endemic regions in the northern hemisphere (Figure I1 (Torgerson et al. 2010)), and has a much lower global incidence. However, as it will be described below, the characteristics of *E. multilocularis* makes AE more difficult to treat than CE. AE is almost impossible to cure when detected at late stages of development, and is typically lethal if left untreated (Craig 2003; Eckert and Deplazes 2004; Moro and Schantz 2009; Brunetti, Kern, and Vuitton 2010). This makes AE one the most dangerous zoonoses in the northern hemisphere, and it has been estimated that the global burden of AE is comparable to that of many other neglected tropical diseases such as Leishmaniasis and Trypanosomiasis, for which research efforts are much more intensive (Torgerson et al. 2010). Other species of *Echinococcus* have been described and are currently recognized, including *Echinococcus vogeli* and *Echinococcus oligarthrus*, which cause Polycystic Echinococcosis (PE). These two species are limited in distribution to the neotropical region in Central and South America and are of only limited medical relevance (Eckert and Deplazes 2004; D'Alessandro and Rausch 2008; Moro and Schantz 2009).

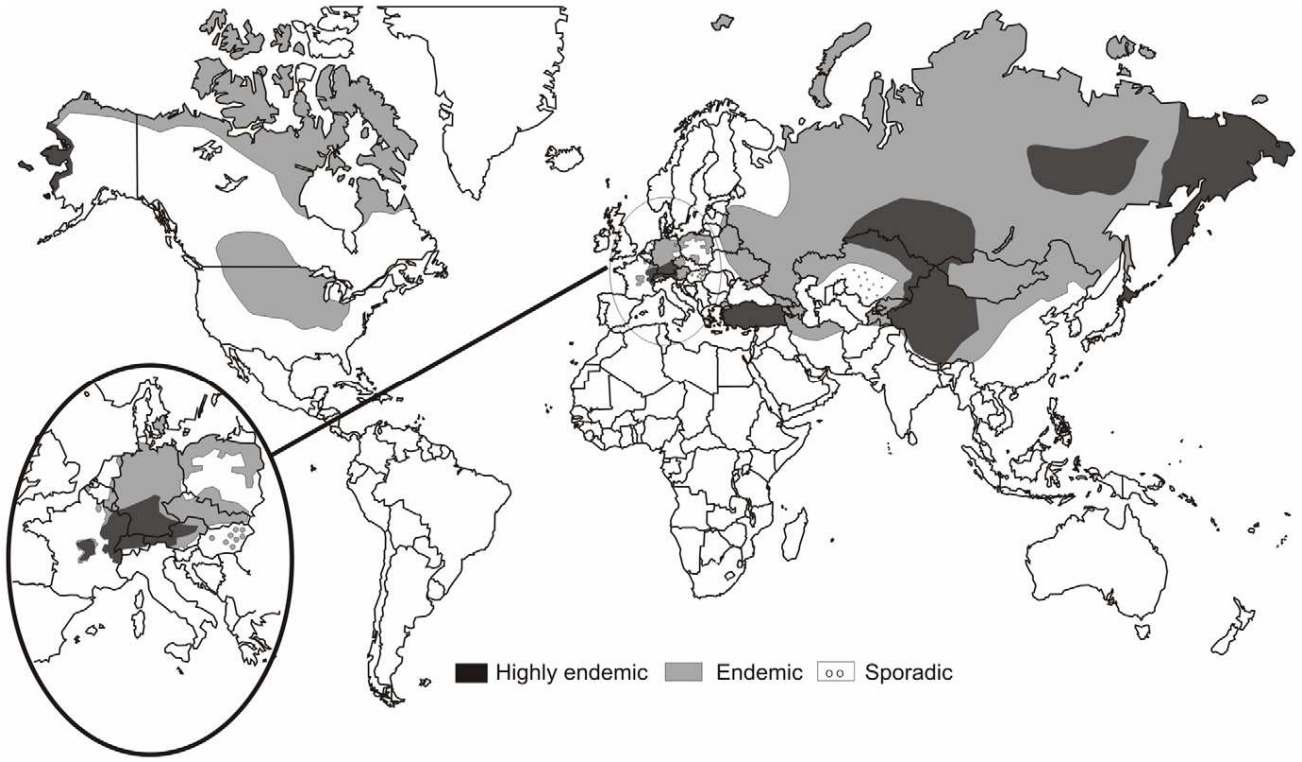

Figure I1. Distribution of AE in the world. Figure from Torgerson et al. (2010)

3.2. Life cycle and biology of *Echinococcus* spp.

The life cycle of *Echinococcus* spp. involves two mammalian hosts (Figure I2 for *E. granulosus* and Figure I3 for *E. multilocularis*). The adult worm develops in the small intestine of the definitive host (typically a canid for all species except for *Echinococcus felidis*), with a morphology that is relatively typical for cyclophyllidean cestodes, and which is very similar for all *Echinococcus* species (Thompson 1986; Eckert and Deplazes 2004). The anterior region of the adult is denominated the scolex and it contains the attachment organs (suckers and rostellum). Behind the scolex, the neck region proliferates extensively and continuously generates a chain of segments (proglottids), each one developing a complete set of male and female reproductive organs. The adults of *Echinococcus* spp. are unusual among cestodes in that, unlike other taeniids, they only have a very small number of proglottids (3 to 6). Furthermore, unlike some of the best known taeniids such as *Taenia solium*, the adult of *Echinococcus* spp. only lives in the intestine for a limited period of time (up to 12 months) after which the infection is lost (Craig 2003).

Within each proglottid, fertilization occurs. It is thought that *Echinococcus* spp. reproduce mostly by self-fertilization, but there is limited evidence indicating that occasional cross-fertilization can take place (Haag et al. 2011). Fertilization results in the production of thousands of infective eggs, that are released (within the mature proglottids) with the host´s feces to the environment. The eggs are then released from the proglottid and can survive for many months under ideal conditions (Craig 2003).

The released eggs contain the first larval stage, the oncosphere, a highly reduced organism with six small hooks and several protective layers around it. The eggs are accidentally ingested by the intermediate host and hatch in the intestine, where the larvae penetrate the intestinal wall and ingress into the portal vein, from which they are transported to the liver, and then to the rest of the body, *via* the blood stream. Most commonly, primary infections develop in the liver (especially in the case of *E. multilocularis*), but other organs can be primary infection sites for *E. granulosus* (especially the lungs and the brain) (Craig 2003; Eckert and Deplazes 2004; Brunetti, Kern, and Vuitton 2010).

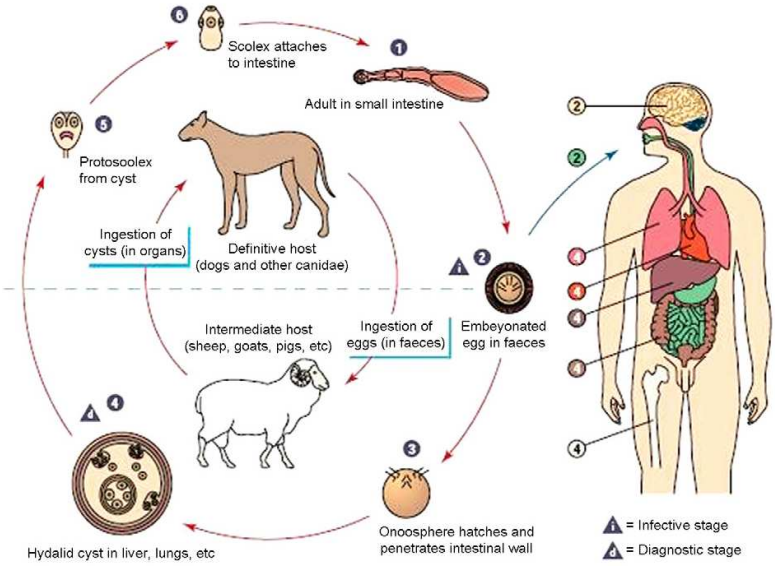

Figure I2. Life cycle of *E. granulosus*. Figure from the Center for Disease Control and Prevention (http://www.cdc.gov/parasites/echinococcosis/biology.html)

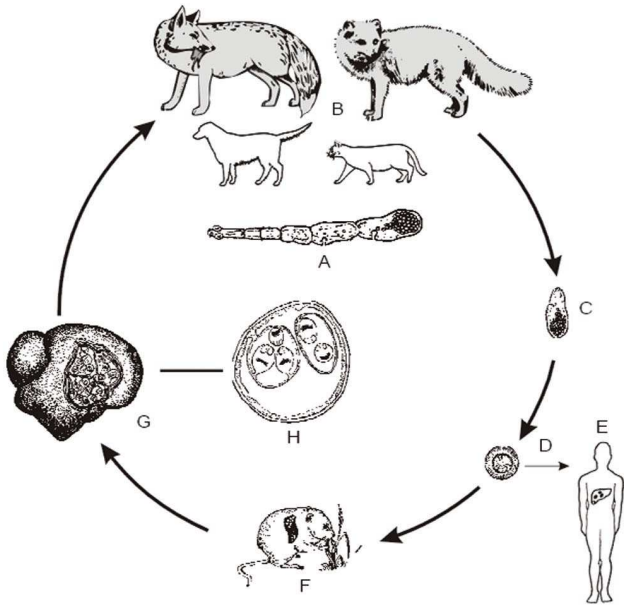

Figure I3. Life cycle of *E. multilocularis.* (A) Adult mature parasite. **(B)** Foxes (left, red fox; right, Arctic fox) are the principal definitive hosts; domestic animals such as dogs, other canids, and cats can also be involved in the cycle. **(C)** Proglottids with eggs are released with the feces of the fox. **(D)** Egg with oncosphere. **(E)** Accidental infection of humans. **(F)** Infection of rodents with oncospheres **(G)** Development of metacestodes in the liver of the rodent. **(H)** Detail of a metacestode vesicle with protoscoleces. Figure from Eckert and Deplazes (2004).

3. Introduction

Several different ungulate species are the typical intermediate hosts for the different lineages of the *E. granulosus* species complex, and most of them are domestic species. Indeed, each of the different lineages of *E. granulosus*, which can be distinguished on the basis of their mitochondrial DNA genotype (genotypes G1 to G10), have specific intermediate hosts for which they are highly infective and in which they can develop normally (*e.g. E. granulosus* genotypes G1 and G2 infect sheep, whereas G4 is infective for horses and G5 is infective for cattle) (Thompson 1986; Moro and Schantz 2009). It has been further proposed that several of these genotypes should be elevated to the rank of species, including genotypes G1 (as *E. granulosus sensu stricto*), G4 (as *Echinococcus equinuus*), and G5 (as *Echinococcus ortleppi*) (Moro and Schantz 2009; Nakao et al. 2010). The fact that all genotypes of *E. granulosus* except genotype G8 have a domestic life cycle between dogs and domestic ungulates makes control strategies that target the natural life cycle feasible, and has even lead to the eradication of the disease in some islands such as Iceland (Beard 1973; Moro and Schantz 2009). In contrast, several rodent species are the natural intermediate host for *E. multilocularis*, in particular species of the families Cricetidae and Arvicolidae (Rausch 1954; Craig 2003; Eckert and Deplazes 2004). Therefore, the natural life cycle of *E. multilocularis* is sylvatic, occurring between foxes and rodents. Because of this, control of the disease by monitoring and treatment of the natural hosts is very costly and difficult.

Humans can be an accidental host for *E. granulosus* and *E. multilocularis*, although they are an aberrant one and a dead-end for the life cycle of the parasite. In the case of *E. granulosus*, humans become exposed to the infective eggs when they come in contact with infected dogs and their feces (Moro and Schantz 2009). This is more common in the country-side of countries where cattle and sheep are raised (particularly in developing countries in which the dogs have access to the infected offal). For *E. multilocularis*, it is not completely clear how most humans become exposed to the parasite. Living in the country-side and owning dogs are risk factors for AE, suggesting that in many cases people become exposed to eggs released from their dogs, after they become infected from eating wild infected rodents. Also, ingestion of contaminated vegetables and fruits can be the source of *E. multilocularis* infection in men (Moro and Schantz 2009).

Once in the intermediate host, the oncosphere develops by metamorphosis into the next larval stage, the metacestode. The metacestode stage of the genus *Echinococcus*

is an evolutionary novelty that is quite divergent from the "typical" development of the metacestode stage of other cestodes (Freeman 1973; Slais 1973). In more typical cestodes, the metacestode is similar to a "juvenile" tapeworm, containing the scolex with the attachment organs, but lacking segmentation and the reproductive systems. In the case of *Echinococcus*, the metacestodes develop as fluid-filled vesicles. These metacestode vesicles comprise a thin layer of tissue (the germinal layer) covered by a syncitial tegument that secretes an acellular, carbohydrate-rich external layer (the laminated layer). The remaining volume of the vesicles is filled with fluid (hydatid fluid).

Within the germinal layer, thickenings (buds) occur that invaginate into the vesicle, resulting in the formation of brood capsules (Goldschmidt 1900; Thompson 1986; Leducq and Gabrion 1992; Koziol, Krohne, and Brehm 2013) (Figure I4). Within the brood capsules, a new budding process occurs, that results in the formation of protoscoleces, the infective form for the definitive host (Figure I4). The protoscolex already resembles the anterior region of the adult form, and remains quiescent with the scolex invaginated within a small posterior body (Figure I4). The life cycle of *Echinococcus* spp. is finally closed when the definitive host ingests an infected intermediate host. After ingestion of the protoscolex by the definitive host, it evaginates its scolex, attaches to the intestine and develops into the adult tapeworm. The formation of many protoscoleces in each metacestode represents a form of asexual propagation by the parasite. Asexual reproduction is very rare in cestodes, but it is relatively common within the family Taeniidae (genera *Echinococcus* and *Taenia*). It is possible that these processes are homologous between *Echinococcus* and *Taenia* species, although this is controversial (Freeman 1973; Slais 1973; Moore and Brooks 1987; Hoberg et al. 2000; Loos-Frank 2000; Trouvé, Morand, and Gabrion 2003; Swiderski et al. 2007).

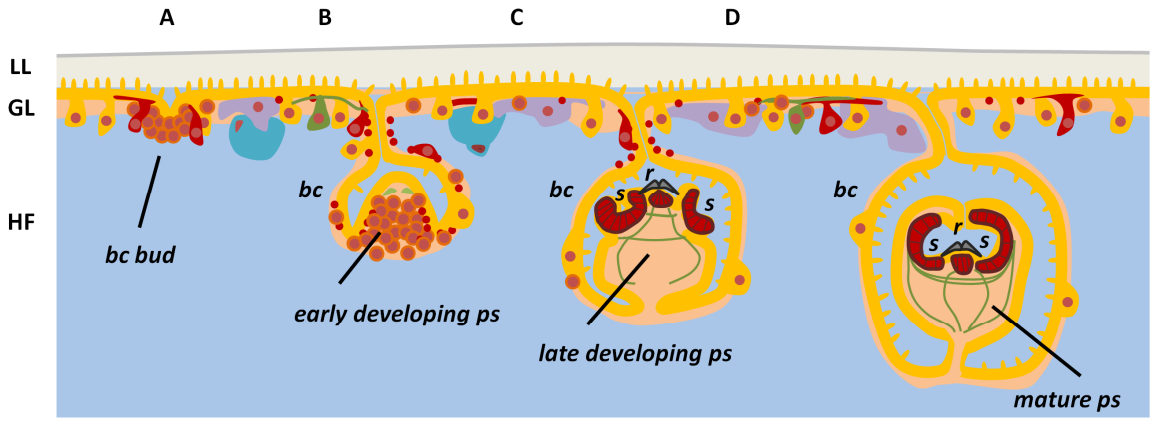

Figure I4. Schematic drawing showing the general organization and development of *E. multilocularis metacestodes*. A. Early brood capsule bud. **B.** Brood capsule with protoscolex bud. **C.** Brood capsule with protoscolex in late development. **D.** Brood capsule with invaginated protoscolex. The syncitial tegument is shown in orange, the germinative cells in brown, glycogen/lipid storage cells in violet, calcareous corpuscle cells in light blue, nerve cells in green and muscle cells and fibers in red. bc, brood capsule; GL, germinal layer; HF, hydatid fluid; LL, laminated layer; ps, protoscolex; r, rostellum; s, sucker. Figure and legend from Koziol et al. (2014).

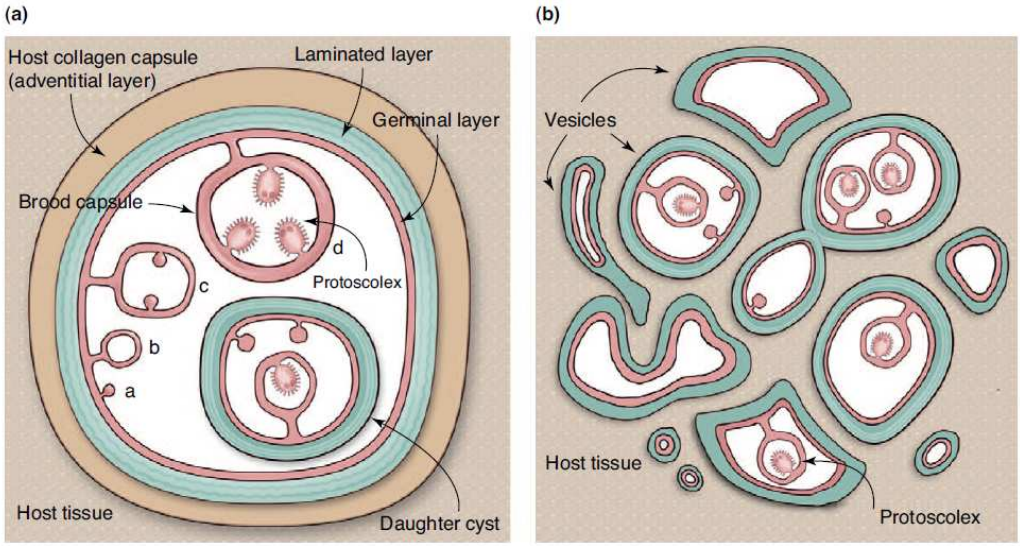

Figure I5. Diagrammatic comparison of *E. granulosus* (a) and *E. multilocularis* (b) metacestodes. Figure from Diaz et al., 2011.

3. Introduction

E. multilocularis and *E. granulosus* differ in the morphology and development of the metacestode stage (Thompson 1986; Eckert and Deplazes 2004) (Figure I5). In the case of *E. granulosus*, each oncosphere develops into a single vesicle (the hydatid cyst) covered by a thick laminated layer. This mode of development is denominated "unilocular". Each vesicle can grow to huge dimensions (exceeding 20 cm in diameter), and from the germinal layer brood capsules develop internally, each containing several protoscoleces. Rarely, endogenous formation of daughter cysts within the "mother" cyst occurs, by a process that is still incompletely understood (Fairley and Wright-Smith 1929; Rogan and Richards 1986). Exogenous formation of new vesicles is controversial for *E. granulosus*, and if it exists at all it must be very rare (Rausch and D'Alessandro 1999).

In contrast, development of *E. multilocularis* is only unilocular during the very early stages of development. After the first week of development, new vesicles are generated by exogenous budding of the metacestode, which therefore develops as a multilocular labyrinth of interconnected vesicles (Rausch 1954; Ohbayashi 1960; Sakamoto and Sugimura 1970). This process occurs continuously, and at later stages small protrusions of the metacestode tissue, devoid of laminated layer, have been described to emerge from the periphery of the metacestode mass and infiltrate the host tissues, resulting in the formation of new vesicles not only in the liver but also in neighboring organs (Eckert, Thompson, and Mehlhorn 1983; Mehlhorn, Eckert, and Thompson 1983). The metacetode tissue can even form metastases in distant organs during late stages of infection. It is thought that this occurs by infiltration of small vesicles or groups of parasite cells into the blood and lymph vessels, which are then distributed to other organs where they initiate the development of new metacestode tissue (Eckert, Thompson, and Mehlhorn 1983). When vesicles mature, they produce brood capsules, and from each brood capsule typically only one or a few protoscoleces develop. The mature, protoscolex-filled vesicles then cease to grow. Most of the metacestode vesicles in late infections have already ceased to grow, and can even become necrotic in the center of the metacestode tissue. Only the tissue in the periphery is still active, and continues to grow and infiltrate the organs of the host (Eckert, Thompson, and Mehlhorn 1983).

Growth of *E. multilocularis* is very fast in rodents, the natural intermediate hosts: after a few months the development of metacestodes is complete (*i.e.*, mature

protoscoleces are formed) and the host either dies from the infection or is easily preyed on by the definitive hosts (Rausch 1954; Craig 2003). In contrast, growth in humans is aberrant, since it is much slower, and usually no protoscoleces are produced (Craig 2003; Moro and Schantz 2009). Because of this, the parasite origin of the metacestode vesicles was not initially recognized by doctors, and AE was originally thought to be either a form of liver cancer or a necrosis of the liver tissue. It was Rudolf Virchow, working in the University of Würzburg, who showed in the 1850s that a species of *Echinococcus* is responsible for the etiology of AE (Tappe and Frosch 2007). Originally, it was thought that AE was caused by an aberrant form of *E. granulosus* in man. Only after more than 90 years of R. Virchow´s findings, when the natural intermediate hosts were discovered, was it shown that *E. multilocularis* is actually a distinct species (Rausch 1954; Tappe and Frosch 2007; Nakao et al. 2010).

Because of the slow growth and the infiltrative nature of *E. multilocularis* metacestodes, AE remains asymptomatic for up to 10 to 15 years after the initial infection, and only rather unspecific symptoms appear after this time (Moro and Schantz 2009). If discovered in time, AE can in principle be cured by radical resection of the infected region. However, it is usually discovered only at late stages, at which point complete resection is impossible, and microscopic portions of parasite tissue infiltrate the liver, resulting in recurrence if surgery is performed (Brunetti, Kern, and Vuitton 2010). Metastases are common in the lungs, peritoneal cavity and brain, making the surgical option impractical as well. The only option for most cases of late stage AE is chemotherapeutic treatment with benzamidazoles (BMZs: Albendazole or Mebendazole), but this treatment is only parasitostatic, and must be taken for many years, usually for the rest of the patient´s life (Brunetti, Kern, and Vuitton 2010). BMZs are toxic for a small proportion of patients, for whom there is no therapeutic option against AE (Eckert and Deplazes 2004). Furthermore, BMZs are largely unavailable for most of the infected population of the world, living in the least developed areas of China and Russia (Torgerson et al. 2010). If untreated, late stage AE is almost invariably deadly within 8 to 11 years (Eckert and Deplazes 2004).

3.3. Culture systems and the influence of host-derived factors on *E. multilocularis* metacestodes.

The metacestode stage of *E. multilocularis* is able to grow continuously by asexual formation of new vesicles within an appropriate host, and can be maintained indefinitely *in vivo* by serial passage of metacestode tissue from one host to the next (Norman and Kagan 1961; Spiliotis and Brehm 2009). In this sense, the metacestode larva of *E. multilocularis* can be considered immortal, similarly to the adult stage of other cestodes, which are able to grow and produce new segments for as long as the host survives. This implies that the metacestode tissue must contain cellular mechanisms for continuous tissue turnover and growth. That is, there must be a population or populations of cells that can self-renew and generate all of the cell types of metacestode vesicles, protoscoleces and eventually the adult if a protoscolex infects a definitive host.

The metacestode tissue and cells can also be cultured *in vitro*, by means of special culture conditions that were optimized in the laboratory of Dr. Klaus Brehm. The first methods developed for the robust culture of metacestode vesicles *in vitro* are the co-culture systems, in which metacestode vesicles are cultured in media optimized for mammalian cells in the presence of fetal calf serum and mammalian feeder cells (Jura et al. 1996; Brehm and Spiliotis 2008a; Spiliotis et al. 2008). Growth of the metacestode is absolutely dependent on the feeder cells, and different cell lines can serve this function, although the best cells identified so far are primary liver cells and hepatoma cell lines from rodents (Spiliotis et al. 2004). By a series of elegant experiments it was shown that these feeder cells were not only providing soluble factors required by the metacestode vesicles, but also eliminating toxic substances (likely reactive oxygen species) from the cell culture media, and that both processes were necessary for optimal metacestode growth (Brehm and Spiliotis 2008a; Brehm and Spiliotis 2008b; Spiliotis et al. 2008). Based on these experiments, an axenic culture system was developed in which the metacestode vesicles can grow in the absence of host cells, by culturing them in filtered media pre-conditioned by feeder cells, under microaerobic and reducing conditions (Spiliotis et al. 2004; Spiliotis et al. 2008). Furthermore, primary cells can be harvested from these axenic vesicles, and under similar conditions, these cells are able to completely regenerate metacestode vesicles

(Spiliotis et al. 2008; Spiliotis et al. 2010) (Figure I6). This shows that at least at the population level the primary cell preparations are multipotent, and allows for the first time to study the development of *E. multilocularis in vitro*.

The strict requirement for serum and soluble host factors indicates that some sort of molecular dialog is occurring between the metacestode and the host, in which the host cells provide *in vitro*, and also likely *in vivo*, signals that promote and regulate the development of the metacestode (Brehm 2010a). Because of the high evolutionary conservation of signaling pathways among metazoans, including signaling ligands and receptors, it is possible that this interaction occurs between the growth factors and cytokines of the host, and the cognate receptors of the parasite. One of the main lines of research in the laboratory of Dr. Klaus Brehm has therefore been the characterization of these conserved signaling pathways in *E. multilocularis*. It has been shown that host growth factors such as insulin and fibroblast growth factors (FGFs) are capable at a biochemical level of interacting with the parasite receptors and activating the downstream signaling cascades (Förster 2012; Hemer et al. 2014). Furthermore, addition of these growth factors at physiologically relevant concentrations promotes growth of metacestode vesicles and regeneration from primary cell preparations, thus showing an effect of host growth factors on metacestode development (Förster 2012; Hemer et al. 2014). However, it is not known how these host factors could promote the development of the metacestode at a cellular / tissular level, since it is not clear which cells express the parasite receptors and how they respond to the host factors.

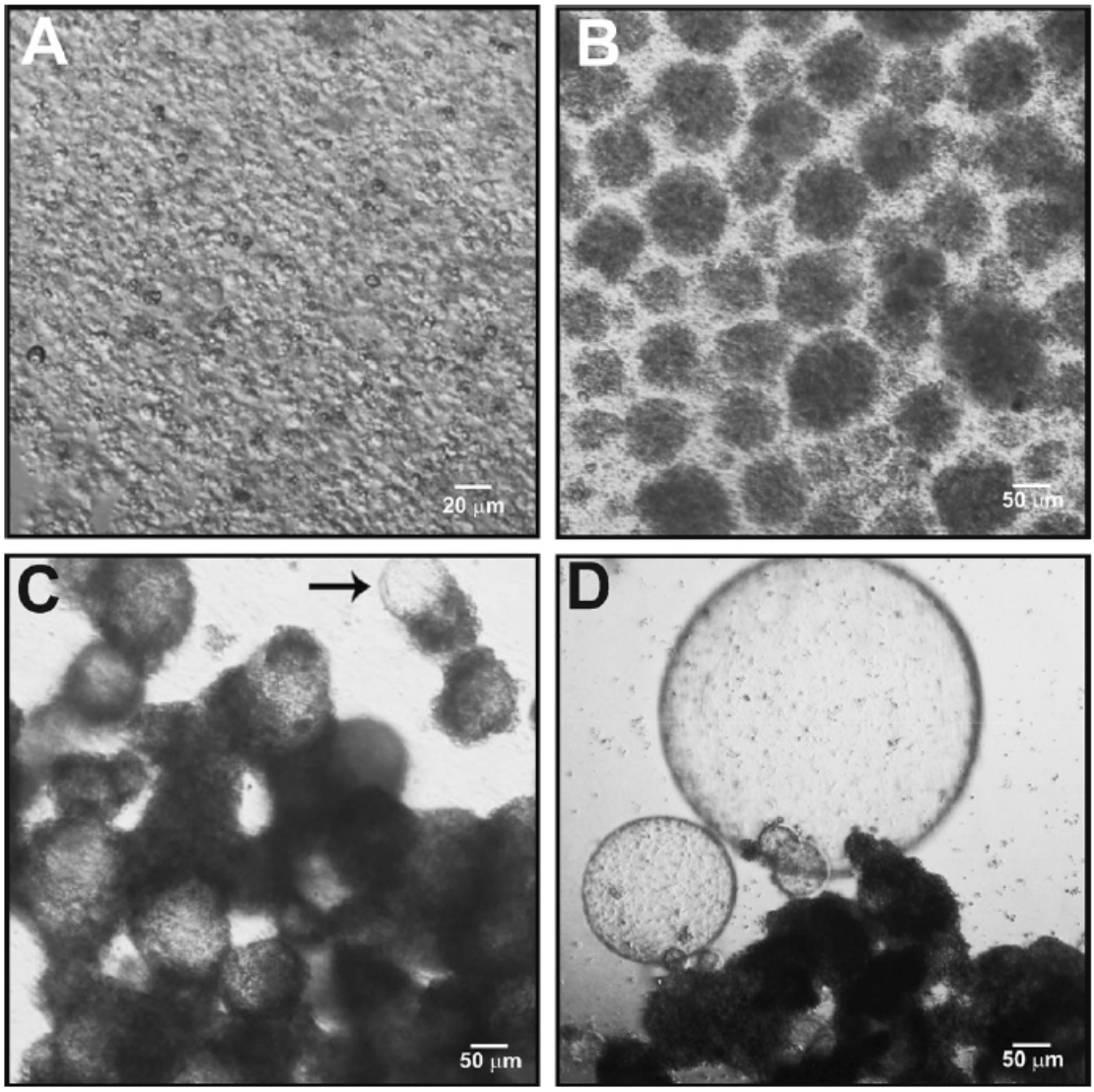

Figure I6. Regeneration of metacestode vesicles from *E. multilocularis* primary cell preparations. This primary culture was performed in the presence of Reuber RH rat hepatoma cells in a trans-well system. Progressive developmental stages are: **A.** Initial culture. **B.** Formation of cell aggregates. **C.** Appearance of cavities within the aggregates and release of the first vesicles (arrow). **D.** Completely developed vesicles with a laminated layer. Figure from Spiliotis et al., 2008.

3. Introduction

Cestodes are part of the phylum Platyhelminthes (flatworms), which contains many free-living groups and a large monophyletic clade of parasites, the Neodermata (Ax 1996; Baguñà and Riutort 2004; Olson and Tkach 2005). This clade includes the well known parasitic classes Cestoda, Trematoda and Monogenea. Flatworms are a highly diverse phylum in terms of morphology, development, and life-cycles. However, they have in common a unique population of undifferentiated stem cells, commonly known as "neoblasts". It is thought that neoblasts are the only proliferative cell population, and are therefore the source of new cells for normal tissue turnover, growth and regeneration, whereas all differentiated cells are post-mitotic (Gustafsson 1990; Peter et al. 2004; Reuter and Kreshchenko 2004; Koziol and Castillo 2011). This is an unusual cellular mechanism for tissue turnover, since in most animals several tissue-specific stem cells exist and many differentiated cell types are also able to proliferate (this subject is further developed in the following section). In cestodes, classical studies have described a population of undifferentiated stem cells similar to the neoblasts, the so-called germinative cells (see section 3.10). In particular, in *E. multilocularis* metacestodes, ultrastructural studies demonstrated the existence of germinative cells in the germinal layer, which proliferate and accumulate during brood capsule and protoscolex development (Sakamoto and Sugimura 1970). Because of the importance of conserved signaling pathways in stem cell biology in animals, and the presumed relevance of the germinative cells as the source of new cells for metacestode growth and development, they constitute a natural focus of research as the possible targets of host-derived growth factors. The main objective of this thesis is therefore the characterization of the stem cell system of *E. multilocularis*, and to investigate the possible role of previously characterized parasite signaling pathways in their physiology. In the following sections of the introduction, I will explore the subject of stem cells and the different mechanisms of tissue turnover in well studied models, and compare them to what is known and hypothesized for cestodes and other flatworms.

3.4. Stem cells and cell renewal mechanisms in metazoans

In many adult tissues in animals (particularly for tissues with fast cellular turnover), differentiated effector cells are post-mitotic, and have a limited lifetime. These cells are lost from the "wear and tear" of the tissue, or by programmed cell death, and are replaced from an undifferentiated pool of stem cells and their progeny (Bryder, Rossi, and Weissman 2006; Pellettieri and Sanchez Alvarado 2007). Stem cells are defined as cells that have the long-term ability to self-renew (that is, to generate new stem-cells by cell division) and that have the potency to differentiate into many cell types. This general definition is somewhat vague, in that "long-term self renewal" and "many cell types" are not explicitly defined. Usually, "long-term self-renewal" refers to the ability to self-renew for the duration of the life of the adult organism. As for the potency, stem cells and their progeny are defined as: 1) pluripotent, when they can give rise to all of the cells of an organism, from all three embryonic germinal layers (in mammals, the term totipotent is used specifically for cells that can give rise to all embryonic germinal layers as well as to extra-embryonic tissues); 2) multipotent, when they can differentiate into many different cell types; 3) oligopotent, when they can differentiate into a few, generally related cell types, and 4) unipotent, when they can only differentiate into one cell type (Seita and Weissman 2010).

In mammals, pluripotent stem cells are only known from the early embryonic stages (Hanna, Saha, and Jaenisch 2010). In adults, all of the well-characterized stem cell systems are actually tissue-specific, and their multipotency is generally defined as the ability to generate all of the main cell types of their tissue (Bryder, Rossi, and Weissman 2006). However, some of the best known stem cells in mammals and other animals are actually unipotent, such as the germ line stem cells (GSCs) of mice, *Drosophila* and *Caenorhabditis* which will only produce gametes throughout the life-span of the adult organism (Alberts 2000; Xie 2008).

In many systems, the stem cells give rise to progenitor cells. These progenitor cells can actively proliferate and differentiate into many cell types, but they no longer have the ability for long-term self renewal, and are therefore sometimes referred to as transit-amplifying cells. In some of the best studied stem cell systems, such as the murine hematopoietic stem cell (HSC) system, there is a gradient of self-renewal and

differentiation potency, in which stem cells give rise to multipotent progenitors, which in turn give rise to a hierarchy of progenitor cells with progressively reduced self-renewal and differentiation potency (Bryder, Rossi, and Weissman 2006) (see section 3.7.2).

In many other adult tissues, especially those with a slow cellular turnover, the source of normal cell renewal is not from undifferentiated stem cells, but from self-replication of differentiated effector cells (Yanger and Stanger 2011). Furthermore, in some systems it has been shown that committed progenitors and differentiated cells have the ability to function as stem cells (that is, they are the source of new cells for several different cell types), either by proliferation and trans-differentiation (direct transformation of a differentiated cell into another cell type) or by de-differentiation (transformation of a differentiated cell into an undifferentiated stem cell type). In particular, even in high-turnover tissues with canonical stem cell systems, some differentiated cells and committed progenitors have been shown to function as a reserve system which can take over the role of the stem cells under special conditions (such as stem cell depletion and during injury repair). Examples of these mechanisms are further explored in sections 3.7.3, 3.7.4 and 3.7.5.

In addition to self-renewal and differentiation, some other characteristics have been traditionally thought to be shared by all or most stem cells in different tissues, although the evidence was always limited to a few types of stem cells, in particular the HSCs (Alberts 2000). One characteristic is quiescence: stem cells in some models have been shown to proliferate only infrequently and to have low metabolic activity, which is thought to protect the stem cell, in particular to prevent its DNA from the incorporation of deleterious mutations. The stem cells could then become active when the tissue needs to be expanded or repaired. In addition, most stem cells were thought to divide primarily by asymmetric cell divisions, in which one daughter cell would retain the stem cell identity, whereas the other daughter cell would become a progenitor cell with limited self-renewal potency. This would give a straightforward mechanism for tissue homeostasis, since the number of stem cells would remain constant. However, recent developments in the study of mammalian stem cells have challenged these paradigms, and have shown that quiescence and asymmetric cell division are not necessary attributes of stem cells in all tissues (Barker, Bartfeld, and Clevers 2010; Barker and Clevers 2010; Klein and Simons 2011; Lander 2011). Many mammalian adult tissues

such as the intestinal epithelium, the inter-follicular skin epithelium and the germ line in the testis have been shown to be supported under conditions of normal homeostasis by actively proliferating stem cells, which divide in both symmetric and asymmetric ways, and whose fate is stochastic, depending on their interaction with their specific niche. As will be described in later sections, it is thought that in these and other tissues quiescent stem cells could be a separate population which normally remain inactive, but that may become active and have a specific role during injury repair and regeneration (Li and Clevers 2010; Doupe and Jones 2013). Even in the case of the *Drosophila* GSCs, which are known to divide by asymmetric divisions in which the daughter cell receives specific cytoplasmatic factors, these factors are neither necessary nor sufficient for the specification of the daughter cell fate. The fate of the daughter cell is instead defined by their interaction with the stem cell niche, since only those cells that remain within the niche maintain the stem cell identity (Losick et al. 2011) . In this way, homeostasis of the stem cell compartment is achieved at a population level by extrinsic signals so that in *average* half of the daughter cells remain as stem cells under normal conditions.

3.5. The stem cell niche concept and the importance of conserved signaling pathways for stem cell regulation

The stem cell niche is defined, in its most restrictive sense, as a localized microenvironment within tissues where stem cells reside, and which provides signals which promote self-renewal of the stem cells (Morrison and Spradling 2008; Lander et al. 2012). The niche must therefore consist of specific cells, the signals they produce, and the extracellular matrix (ECM) surrounding the stem cells. Furthermore, the niche environment may provide signals that regulate the proliferation and/or differentiation of the stem cells.

In order to identify the components of the niche, specific perturbation of defined cell types and signaling pathways can be performed, in order to assess the effect on the stem cell population. However, in order to show that these properties are important for a specific localized niche, and not a general property of the whole tissue, more precise experimental methods are needed (Morrison and Spradling 2008). The best examples of stem cell niches have been identified in invertebrates, in particular for the GSCs of *Drosophila* and *Caenorhabditis* (Xie 2008; Losick et al. 2011) (Figure I7). In both cases, the niche is composed of neighboring cells which make direct contact to the stem cells, and provide them with short-range signals that maintain the resident cells in an undifferentiated state. The specific ECM in those niches potentiates these signaling mechanisms and limits their diffusion, preventing activation of these signaling pathways outside of the niche. In the case of *Drosophila* male GSCs, it has been actually shown that removing a stem cell from the niche results in the loss of its stem cell identity, whereas re-incorporation of a daughter progenitor cell into the niche reinstates a stem cell identity to this cell (Brawley and Matunis 2004; Losick et al. 2011).

Theoretically, stem cells could instead maintain their identity by cell-autonomous mechanisms or from general signals provided in a non-localized fashion by the surrounding tissue, and this has been proposed to be the case for a few specific stem cell systems, such as the *Drosophila* intestinal stem cells. It is thought however that the stem cell niche can have specific regulatory functions which would not be achieved from non-localized signals, acting as a mechanism of feedback control in which limited niche space results in a limit in the expansion of stem cells (Lander et al. 2012). The

niche is also thought to function as a coordinator of signals for different cellular compartments within a tissue or organ, in particular in those with several different cell lineages as is the case of the hair follicle.

Metazoans employ a relatively small number of conserved signaling systems to regulate and coordinate their embryonic and adult development (Gilbert 2006). Some of these signaling pathways have been shown to be important for many stem cell types, and to be activated by specific niche signals in many tissues and organisms. These include in particular the canonical Wnt/beta-catenin pathway (Clevers 2006; Nusse et al. 2008), the Delta/Notch pathway (Koch, Lehal, and Radtke 2013), the BMP pathway (Watabe and Miyazono 2009), and signaling by fibroblast growth factors (FGFs) (Coutu and Galipeau 2011) (Figure I8). Although some common themes can be inferred about their function in stem cell biology, it is important to realize that their actual roles vary greatly between different stem cell systems, and even within one system, they may have several overlapping roles over the stem cells and their progeny. For instance, canonical Wnt, FGF and Notch signaling are generally associated with stem cell self-renewal, and in many cases with stem cell proliferation resulting in their expansion. However, these signals may also promote differentiation of progenitor daughter cells, and Notch in many cases promotes stem cell quiescence rather than proliferation (Koch, Lehal, and Radtke 2013). In the case of BMP signaling, it has been shown to inhibit stem cell proliferation and to promote differentiation in many mammalian tissues, working as an antagonist of Wnt signaling (Watabe and Miyazono 2009; Sato and Clevers 2013). In contrast, BMP signaling is one of the most important signals secreted by the niche cells in the *Drosophila* gonads, promoting the maintenance of stem cell identity in GSCs (Losick et al. 2011).

In addition to localized signals from the niche, long-range signals from the surrounding tissue and from the endocrine system may modulate the activity of the stem cells and their progeny, to match growth with the nutritional status and to coordinate growth and development throughout the organism. Among these, the insulin pathway regulates metabolism, growth and proliferation in response to nutritional status in metazoans cells (Siddle 2011), including stem cells (as occurs for example for *Drosophila* GSCs (Losick et al. 2011)). These signals are not considered part of the stem-cell niche proper, but are nonetheless of great importance for stem cell physiology.

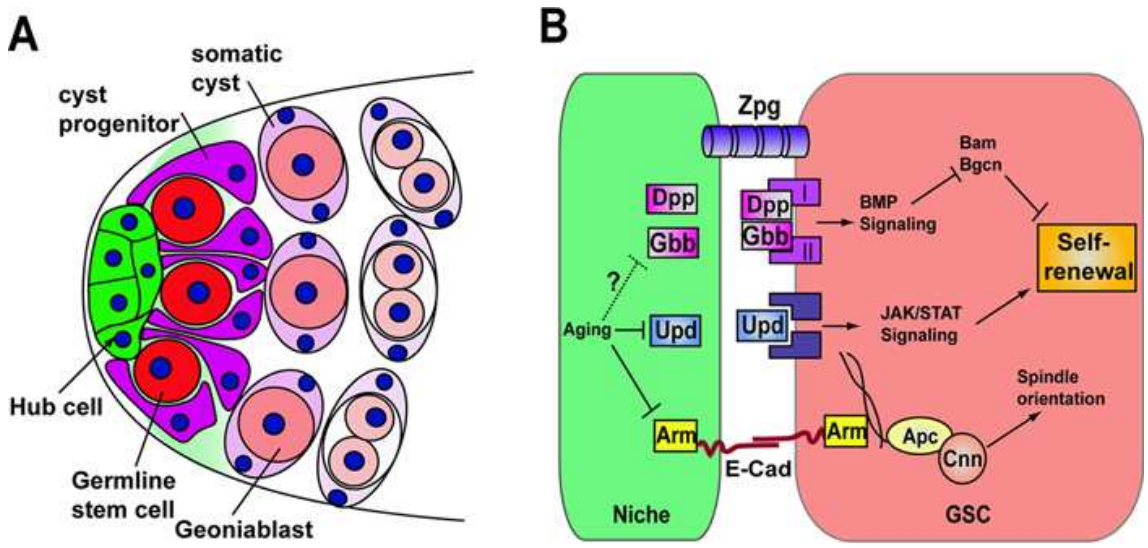

Figure I7. The *Drosophila melanogaster* testicular GSC niche. A. Anatomy of the testes and specific location of the GSC niche. GSCs are in direct contact with the apical hub cells, and surrounded by the cyst progenitor cells. Those GSCs that remain in contact with the hub cells after division retain the GSC identity, whereas those that do not remain in contact begin their differentiation into gonialblasts (which will further proliferate and differentiate into spermatozoa). The gonialblasts become enclosed by the derivatives of the cyst progenitor cells as they undergo proliferation and differentiation. **B.** Signaling in the GSC niche. Hub cells provide signals to the GSCs, including cell adhesion mediated by E-cadherins (which retains the GSCs within the niche, and may regulate the spindle orientation of dividing GSCs so that only one daughter cell remains in contact with the niche), and signaling through soluble factors such as Dpp and Gbb (BMP signaling pathway) and Upd (JAK/Stat signaling pathway). Figure from stembook (http://www.stembook.org/node/497).

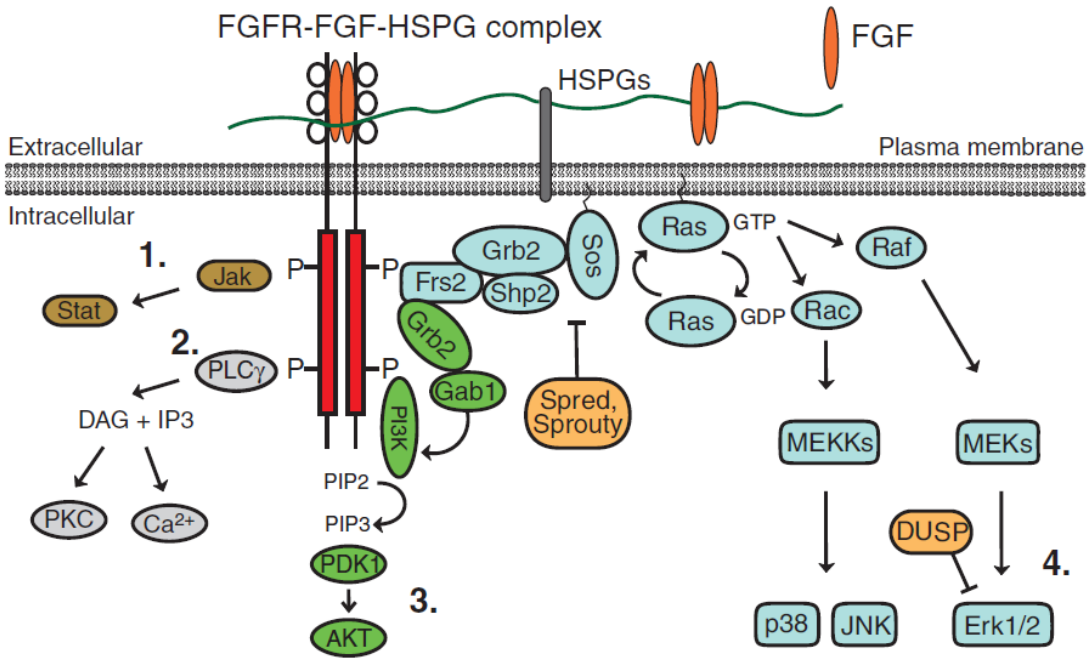

Figure I8. The FGF signaling pathway. A fibroblast growth factor ligand (FGF) interacts with the extracellular immunoglobulin-like domain of a FGF receptor (FGFR) resulting in the activation of the intracellular tyrosine kinase domain by autophosphorylation. Heparan sulfate proteoglycans (HSPGs) are co-receptors for FGFs, and can also modulate their bioavailability. The intracellular domain then signals through different downstream pathways, mainly: the Janus kinase/signal transducer and activator of transcription (Jak/Stat; 1, brown), phosphoinositide phospholipase C (PLCg; 2, gray), phosphatidylinositol 3-kinase (PI3K; 3, green) and mitogen-activated protein kinase/extracellular signal-regulated kinase (MAPK/Erk; 4, blue). Dual specificity phosphatases (DUSPs), Spred and Sprouty proteins (orange) reduce or terminate FGF signaling. Figure and legend modified from Lanner and Rossant (2010).

3.6. Methods for the identification and analysis of stem cells

Identification of stem cells within tissues is not trivial, since they are not easily distinguishable by histological methods, and most molecular markers are also shared with their immediate progeny (Morrison and Spradling 2008). In a few cases, unique molecular markers have been found for a particular stem cell population, but such markers are only rarely shared by more than one stem cell type (*e.g.* the Lgr5 R-spondin receptor, see section 3.7.3). If such markers are found, the stem cells can even be identified *in vivo* within the tissues by creating transgenic organisms with a genetic fusion of the promoter of the marker gene to fluorescent proteins, such as GFP (Rompolas, Mesa, and Greco 2013; Ritsma et al. 2014).

Stem cells have been identified and isolated from cell suspensions of diverse tissues by Fluorescence-Activated Cell Sorting (FACS), using complex combinations of different positive and negative surface markers, after which their properties and potency can be determined by *in vivo* and *in vitro* assays. This was first achieved for murine HSCs, resulting in the first prospective purification of an adult stem cell population (Spangrude, Heimfeld, and Weissman 1988), which has since been extensively refined for achieving higher stem cell purities (Bryder, Rossi, and Weissman 2006). However, it is not easy to identify such cells *in situ* using these complex marker combinations, which are appropriate for FACS but not for immunohistofluorescence methods (IHF).

At the functional level, three main strategies are used for characterizing stem cells, each with its own advantages and disadvantages (Yanger and Stanger 2011):

1) Transplantation experiments

In these experiments, purified stem cell preparations or even individual stem cells are introduced into a living organism, and their self-renewal and differentiation is measured (when individual stem cells are transplanted, clonal analysis of their output can be achieved). In order to identify the cells that are derived from the donor, these are genetically labeled (for example by using a different, identifiable donor genotype or strain). Usually, the host organism is depleted of its own stem cells (for example by lethal irradiation) in order to increase the engraftment of the donor stem cells. These assays are very powerful, but require a purified stem cell population, and typically

measure the potency of the donor stem cells under conditions that are not of normal homeostatic cell turnover. The classic example for this kind of experiments is the characterization of HSCs from bone marrow. Indeed, the existence of HSCs was originally postulated from the results of transplantation experiments into lethally irradiated hosts. Today, long-term repopulation of all main hematopoietic lineages after transplantation of a lethally irradiated host is typically used as the operational definition of HSCs.

2) *In vitro* analysis

In these experiments, stem cells are isolated and cultured *in vitro* under appropriate conditions in order to determine their self-renewal and differentiation potential. By performing clonal analysis of their proliferative output (*i.e.* by seeding cells at clonal density or by seeding individual cells into culture) the potency of individual stem cells can be determined for large numbers of such cells. However, for most stem cells determining the ideal culture conditions is not trivial, and furthermore, different culture conditions may affect their proliferative output. Finally, whether the potency of such cells *in vivo* would be the same as the one displayed *in vitro* is unknown

3) Lineage tracing of genetically labeled cells

For models that can be genetically manipulated, indelible genetic labeling of stem cells can be achieved by means of the Cre recombinase system (Jaisser 2000). In this system, a construct is introduced into the genome in which the Cre recombinase is under the control of the promoter of a stem cell-specific gene. When the Cre recombinase is expressed in the stem cells, it can permanently activate a marker gene such as GFP or GUS, which is in a different locus and is interrupted by a sequence flanked by Cre target sequences (*lox* sequences). Furthermore, temporal control of activation can be achieved by using instead a fusion of Cre to mutant versions of the estrogen receptor ligand binding domain (CreER). CreER is normally cytoplasmatic, and will only become activated by injection of synthetic estrogen analogues such as tamoxifen, resulting in the translocation of CreER to the nucleus were it can remove the inactivating sequences from the target gene. Therefore, stem cells and their progeny can be traced *in vivo* by activating CreER and analyzing the labeled cells after different time periods. By adding limiting concentrations of tamoxifen, only a small proportion of the stem cells become labeled, and clonal analysis of individual stem cells can be

performed. This is a very powerful method, since it allows the determination of the potency of individual stem cells under normal *in vivo* conditions, but only if an exclusive marker gene is known for such cells, and if the progeny of the stem cells remain in close proximity (as is usually the case for epithelial tissues). In any case, even when no such gene is known, one can search for stem cell activity within any tissue by randomly activating CreER in a small subset of all cells, and searching for long-term self-renewal and multipotent differentiation among the progeny of the activated cells. This will not give any indication, however, about the identity of such cells.

3.7. Stem cells and cell renewal mechanisms in vertebrates

Because of the obvious relevance of vertebrate stem cells for human health and medicine, they have been extensively studied, although they represent relatively difficult models given the complexity and size of vertebrate tissues. Most studies are performed in the murine model, although amphibians (*Xenopus* and several urodeles) and fish (such as zebrafish) are also important, in particular for studies of vertebrate regeneration, a process that is very limited in mammals (Tanaka and Reddien 2011).

In the following paragraphs, I will summarize current knowledge regarding selected well-studied mammalian adult tissues and for embryonic stem cells, in order to illustrate the great variety of cell renewal strategies that can be found in mammals. Within this variety, a general trend that can be found in many fast-renewing adult tissues is that they are supported under normal conditions by actively proliferating stem cells, but these are supplemented under special conditions (such as injury repair) by other cell populations that are normally quiescent (quiescent stem cells or differentiated cells).

3.7.1. Embryonic Stem Cells

In mammals, only the zygote and the early blastomeres of the embryo are totipotent (Hanna, Saha, and Jaenisch 2010). Early during mammalian development, the blastomeres divide into the trophoblast, which will contribute exclusively to the extra-embryonic placenta, and the inner cell mass (ICM), which will generate all of the tissues of the embryo and several other extra-embryonic tissues The ICM cells within the embryo are thus pluripotent, but are not self-renewing since they become quickly committed to either the epiblast (which will generate the embryonic tissues) or to extra-embryonic lineages. The epiblast cells themselves are initially pluripotent but become further committed to contribute to specific germ layers.

Murine ICM cells can be isolated and cultured *in vitro*, and can be propagated under specific conditions without losing their pluripotency (that is, they can be induced to self-renew). These cells are referred to as embryonic stem cells (ESCs) (Hanna, Saha, and Jaenisch 2010). By changing the culture conditions, they can be further induced to differentiate into specific cell types. ESCs were originally cultured in the presence of feeder cells, but later methodological refinement allowed their culture under completely defined conditions (Ying et al. 2008). Important exogenous factors that promote ESC self-renewal include signaling by Leukemia Inhibitory Factor (LIF) through Stat3 (JAK/STAT pathway) and activation of the Wnt pathway (ten Berge et al. 2011). A further important factor is the inhibition or antagonism of the ERK kinase cascade (Ying et al. 2008), which is normally activated in ESCs (as well as in the ICM) by autocrine FGF4-mediated signaling. FGF4 instructs ESCs to exit self-renewal and primes them for differentiation (Lanner and Rossant 2010).

ESCs remain pluripotent, as can be seen by *in vivo* experiments such as their contribution to the formation of tissues from all three germ layers in embryonic chimaeras, and the formation of teratomas when injected into adult hosts (Hanna, Saha, and Jaenisch 2010). They also retain several regulatory and epigenetic characteristics from the ICM cells: they express the transcription factors Oct4, Nanog and Sox2 (which form a positive feedback regulatory circuit that promotes the maintenance of pluripotency), they lack differentiation markers, and they retain both X chromosomes in a pre-inactivation state (for female-derived ESC). However, they show extensive

genome methylation, unlike the ICM cells which are hypomethylated (Hanna, Saha, and Jaenisch 2010).

Pluripotent embryonic cells can also be isolated and propagated *in vitro* from the epiblast (epiblast stem cells, EpiSCs). These cells have reduced potency as compared to ESC, since they show multi-lineage differentiation in teratomas, but are very inefficient in chimaera formation and have limited clonogenic potential (Hanna, Saha, and Jaenisch 2010). It is thought that EpiSCs are in a "primed" pluripotent state, ready to differentiate, unlike the ESCs which are in a "naïve" pluripotent state. This can be also seen at the epigenetic and gene regulatory level, since EpiSC show a reduction in the expression of Nanog and other pluripotency regulators, the activation of early lineage markers, and the inactivation of one of the X chromosomes (for female-derived EpiSCs). Furthermore, whereas FGF/ERK signaling induces the differentiation of ES cells into an EpiSC-like state, it promotes the self-renewal and proliferation of EpiSC (Hanna, Saha, and Jaenisch 2010; Lanner and Rossant 2010).

Pluripotent ESCs have also been isolated from human embryos (hESCs). Originally, however, hESC cultured under diverse conditions consistently showed characteristics similar to mouse EpiSC (that is, hESC were already in a "primed" pluripotent state) (Hanna, Saha, and Jaenisch 2010). Very recently, culture conditions have been developed that result in hESC propagation in a "naïve" state (Gafni et al. 2013), holding great therapeutic promise which is however curtailed because of the ethical implications of working with cells derived from human embryos. Importantly, pluripotent cells with similar characteristics to "naïve" ESCs can be derived from adult somatic cells by transfection with transgenes for the transcription factors Oct4, Sox-2, c-Myc and Klf-4, which promote pluripotency (induced pluripotent stem cells, iPSCs) (Takahashi and Yamanaka 2006; Rais et al. 2013), or by transfer of adult somatic nuclei into oocytes (nuclear transfer embryonic stem cells, NT-ESCs) (Tachibana et al. 2013). These strategies open the door for the generation of pluripotent cells for therapeutic applications that are independent of the use of human embryos.

3.7.2. Hematopoietic stem cells

The murine hematopoietic system was the first extensively characterized mammalian adult stem cell system, and HSCs were the first adult stem cells to be prospectively purified and characterized (Spangrude, Heimfeld, and Weissman 1988; Bryder, Rossi, and Weissman 2006). The HSC paradigm has therefore been extensively applied, for better or worse, to many other stem cell systems. Originally, the existence of HSC was proposed from the observation that cell preparations from the bone marrow of a donor could rescue hematopoiesis in lethally irradiated hosts, and limiting amounts of donor bone marrow cells were able to generate multi-lineage clonal colonies in the host spleen. The cells responsible of generating these colonies were called CFU-S (colony forming unit - spleen) and were proposed to be multipotent hematopoietic stem cells (Domen, Wagers, and Weissman 2006). Today, it is known that only a fraction of the CFU-Ss are true HSCs, whereas the rest represent multipotent progenitors with limited self-renewal capacity (Bryder, Rossi, and Weissman 2006).

HSCs are defined as long-term self-renewing cells that are able to give rise to all of the main hematopoietic lineages. Operationally, they are defined by their ability to restore and contribute for long periods to all of the hematopoietic lineages after transplantation into lethally irradiated hosts (Bryder, Rossi, and Weissman 2006). No single specific marker of HSC is known, and instead, they are recognized by flow-cytometry methods from the presence or absence of several surface lineage markers in complex combinations (Bryder, Rossi, and Weissman 2006; Seita and Weissman 2010) (Figure I9). For many of these markers, their exact function is unknown, and do not appear to play essential roles in the physiology of HSC and their progeny. Probably because of this, although there is a good degree of correlation between murine and human HSC/progeny markers, they also show many differences, such as the expression of CD34 in human HSC, which is absent in murine HSC (Seita and Weissman 2010) (Figure I9). HSC can also be recognized by flow-cytometry from their high dye efflux activity (the so-called “side-population activity”) since they exclude vital fluorescent dyes such as Hoechst 33342 (Bryder, Rossi, and Weissman 2006). From the application of ever more complex combinations of surface markers, together with *in vivo* and *in vitro* experiments for assaying the potency of isolated bone marrow cell populations, HSCs have been isolated to very high levels of purity. The HSC population represents a

very small fraction of the bone marrow (BM), probably lower than 0.01% of BM cells (Seita and Weissman 2010).

Even within this small HSC population there is evidence of heterogeneity, with different populations having biases towards specific hematopoietic lineages (Dykstra et al. 2007), and with different proliferative activities (Wilson et al. 2008). HSCs have been shown to be quiescent under normal conditions, entering the cell-cycle only infrequently, and there is strong evidence that HSC can be further divided into dormant and active populations (d-HSCs and a-HSCs, respectively) (Wilson et al. 2008). Most cell turnover under normal homeostasis comes from the infrequent proliferation of a-HSCs, and under these conditions the d-HSCs, which have a higher capacity for long-term HSC activity, remain dormant. However, under strong hematopoietic requirements (such as after elimination of proliferative cells by chemotherapy), the d-HSCs become activated and contribute to the re-population of the hematopoietic system.

HSC give rise to multipotent progenitor cells, with their own specific signatures of surface markers (Figure I9). The multipotent progenitors have increased proliferation activity and remain multipotent, but are no longer capable of long-term self-renewal, being unable to restore hematopoiesis for long periods when transplanted to lethally irradiated hosts (Bryder, Rossi, and Weissman 2006). However, it has been proposed that it is possible that under normal homeostatic conditions, the self-renewal activity of multipotent progenitors is largely sufficient to maintain cell turnover in the absence of important contributions from HSCs (Metcalf 2007).

The multipotent progenitors in turn give rise to a stereotypic branching hierarchy of progenitors with specific surface markers, that have increased proliferation capacity, but with ever smaller self-renewal capacity and which are no longer able to generate all of the hematopoietic lineages (Figure I9) (Bryder, Rossi, and Weissman 2006). The first branching divides progenitor cells into common myeloid progenitors (CMPs, which is the source of all myeloid lineages and of dendritic cells) and the common lymphoid progenitors (CLPs, which give rise to all lymphoid lineages and to dendritic cells). These progenitors further generate specialized, oligopotent progenitors, and finally these oligopotent progenitors generate unipotent, lineage restricted progenitors which eventually differentiate into mature effector cells. The effector cells are largely post-

mitotic, although there are exceptions (for example, cell proliferation is essential for the function of B-lymphocytes) (Metcalf 2007).

The stem cell niche of HSCs is difficult to study, since BM is a large and complex tissue, and HSC are scarce and difficult to identify by immunohistofluorescence methods (since a complex combination of markers must be used to identify the HSC exclusively) (Seita and Weissman 2010; Lo Celso and Scadden 2011). Two main possible locations have been proposed for the HSC stem cell niche, and it is possible that both function as niches for all HSCs or for different sub-populations of HSC: the first is located next to the osteoblasts of the endosteal bone surface, and the other is adjacent to the sinusoidal vasculature endothelium. HSCs have been associated to both locations, and both cell types secrete factors that have been shown by genetic manipulation to be important for HSC self-renewal and localization (Lo Celso and Scadden 2011). These signaling factors include among others kit ligand (also known as SCF) that activates c-kit in the HSCs; thrombopoietin, which activates the c-Mpl receptor; and SDF1, the ligand for the CXCR4 receptor (Seita and Weissman 2010). Activation by gain-of-function mutants of the Notch pathway can lead to increased proliferation and expansion of multipotent progenitors, but loss-of-function studies show that these signaling pathways are not essential for HSC/progenitor function, and their role *in vivo* is controversial (Lo Celso and Scadden 2011).

Transplantation of HSCs and progenitor cells is of wide therapeutic use, for example to treat genetic or acquired bone marrow failure, and to restore hematopoiesis after high-dose chemotherapy against diverse cancers (Domen, Wagers, and Weissman 2006). For therapeutic use, pure HSCs preparations are not practical given the very small proportion of HSCs and the complexity of their isolation. Instead, the typical grafts used are un-fractioned preparations of bone marrow cells, or $CD34^+$ enriched cell preparations (comprising HSCs, hematopoietic progenitors and diverse contaminants) from mobilized peripheral blood or umbilical cord blood (Domen, Wagers, and Weissman 2006; Seita and Weissman 2010). Furthermore, techniques for *ex vivo* expansion of HSCs are still very limited (less than 10-fold expansion under ideal conditions), since treatment with most growth factors and cytokines which are important for self-renewal *in vivo* result in proliferation accompanied of cell differentiation *in vitro* (Seita and Weissman 2010; Takizawa, Schanz, and Manz 2011).

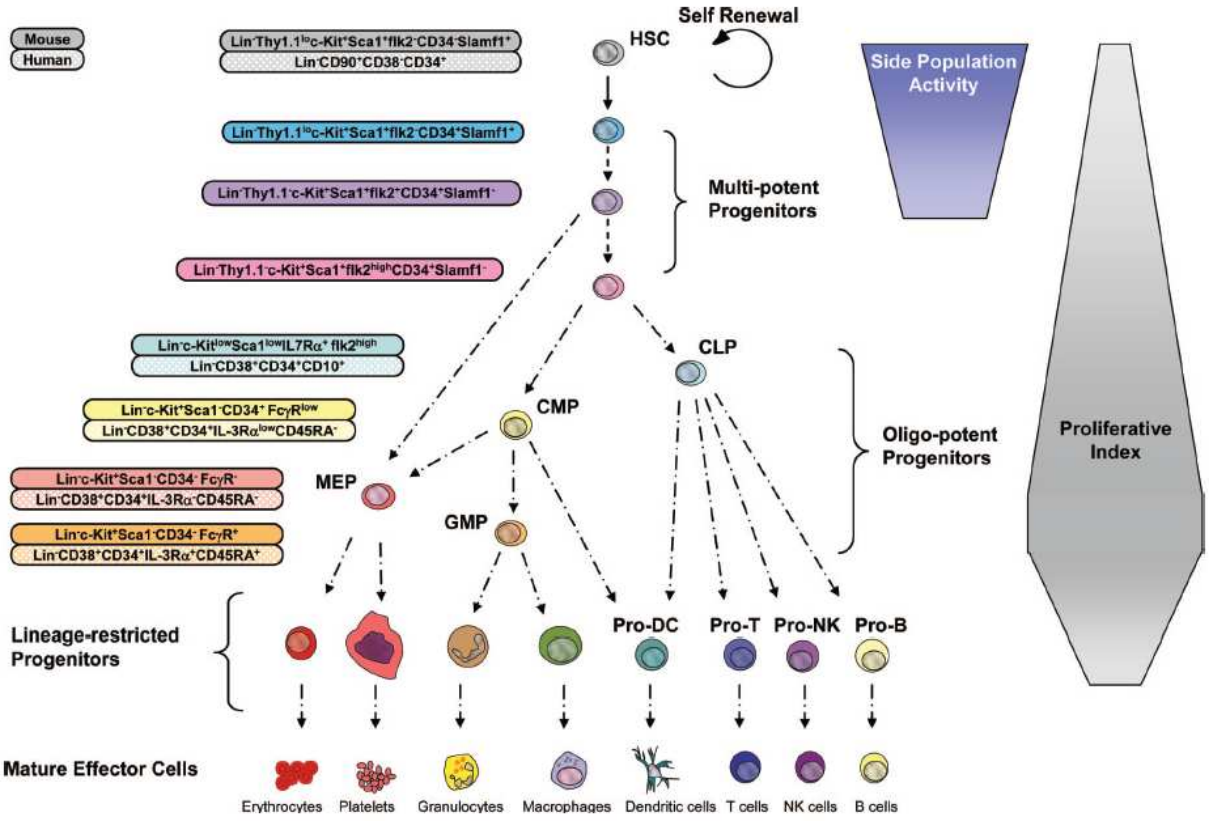

Figure I9. Model of the hematopoietic stem cell and progenitor hierarchy. Markers for murine and human hematopoietic cell populations are given on the left. See the main text for details. Figure from Bryder, Rossi, and Weissman (2006).

3.7.3. Intestinal Stem Cells

The epithelium of the small intestine is the tissue with the fastest cellular turnover in mice and other mammals (Alberts 2000). Morphologically, it is a monostratified epithelium, folded into finger-like extensions (villi) and invaginations (crypts) (Figure I10). The villi contain several terminally differentiated cell types, including the enterocytes (involved with the absorption of nutrients), goblet cells (glandular cells), endocrine cells and other quantitatively minor cell types (Alberts 2000; Stange 2013). These cells are lost by apoptosis and shedding from the tip of the villi after an average life-span of just 4 to 5 days. Cell proliferation occurs in the crypts and at the base of the villi. Newly generated cells continuously move upwards towards the surrounding villi while differentiating into mature cell types, displacing the already differentiated cells towards the tip of the villi, in a manner reminiscent of a conveyor belt (Stange 2013).

Intestinal stem cells (ISCs) are found in the crypts, and give rise to transit-amplifying cells (TA-cells) which undergo 4 to 5 divisions in the lower regions of the villi (Barker and Clevers 2010; Stange 2013). The identity of ISCs was for a long time controversial, and only recently were they identified as the undifferentiated crypt base columnar cells (CBCs), which lay at the bottom of the crypts, intercalated with the relatively long-lived Paneth cells (a type of differentiated gland cell that produces bactericidal products) (Barker et al. 2007). About 14 CBCs can be found at the bottom of each crypt, and they express a unique marker, the R-spondin receptor Lgr5 (Barker et al. 2007; Barker and Clevers 2010; Carmon et al. 2011; de Lau et al. 2011; Glinka et al. 2011). These cells are also denominated the $Lgr5^+$ ISC population. Lgr5 is not only a specific marker of the stem cell population in the intestinal epithelium, but it has also been found to be expressed by stem cells in other adult epithelial tissues (such as the pylorus region of the stomach and the regenerating liver (Barker and Clevers 2010; Barker et al. 2010; Huch, Boj, and Clevers 2013)).

Lineage tracing mediated by the CreER system conclusively showed that individual $Lgr5^+$ ISCs have the ability for long-term production of all intestinal lineages, demonstrating that they are true stem cells (Barker et al. 2007). Furthermore, isolated $Lgr5^+$ ISC have been shown to generate complete intestinal organoids *in vitro*,

with a structure similar to the normal intestinal epithelium (containing crypt and villi-like regions with various differentiated cell types) (Sato and Clevers 2013). Interestingly, these cells are not quiescent, and divide in average once every 24 hours. Furthermore, quantitative analysis of their clonal expansion *in vivo*, as well as live imaging of individual $Lgr5^+$ ISCs within the intestine, have shown that $Lgr5^+$ ISCs divide symmetrically, and the fate of their daughter cells is stochastic (Snippert et al. 2010; Ritsma et al. 2014). Cell fate (whether to remain as an ISC or to commit for differentiation) depends on the ability of each daughter cell to maintain contact with the base of the crypt, the ISC niche. ISCs therefore undergo neutral competition for limited niche space, and this limits their expansion (Snippert et al. 2010; Sato and Clevers 2013). All $Lgr5^+$ ISCs are multipotent and have the potential to remain as ISCs, but those that remain closer to the base have a competitive advantage, whereas those that become displaced to the border of the niche have a higher chance of losing the ISC identity (Ritsma et al. 2014). The $Lgr5^+$ ISCs are thus quite different from the classic paradigm of adult stem cells, since they are constantly active, and maintenance of their identity does not depend on asymmetric cell divisions. A similar mechanism of cell renewal from a pool of equivalent, actively proliferating stem cells has been proposed for the interfollicular epidermis and for spermatogenesis in the male germ line (Klein and Simons 2011).

The ISC niche is composed of the Paneth cells (which make direct contact to the $Lgr5^+$ ISC) and of the underlying intestinal mesenchyma (Sato and Clevers 2013; Takashima, Gold, and Hartenstein 2013). Paneth cells produce Notch ligands (Dll1 and Dll4), as well Wnt ligands (Wnt3 and Wnt11) and epidermal growth factor (EGF), whereas the underlying mesenchyma produces Wnt ligands and EGF (Sato and Clevers 2013). Wnt signaling in the crypt is essential for promoting ISC maintenance and proliferation, as well as TA-cell proliferation and the differentiation of Paneth cells (Clevers 2006; Sato and Clevers 2013). Interestingly, signaling of R-spondins through the Lgr5 receptor functions as a potentiator of Wnt signaling(Carmon et al. 2011; de Lau et al. 2011; Glinka et al. 2011). Notch, on the other hand not only promotes the maintenance of the undifferentiated ISC state, but also regulates the choice of the TA-cells between differentiation into the enterocyte or secretory lineages (Koch, Lehal, and Radtke 2013; Takashima, Gold, and Hartenstein 2013). Finally, EGF acts as a mitogen on the ISC and the TA-cells, acting via the ERK kinase cascade (Sato and Clevers

2013). The Wnt and EGF signaling from both sources are largely redundant, but only Paneth cells are capable of providing Notch signals since these are membrane bound and require direct cell to cell contact (Koch, Lehal, and Radtke 2013). Paneth cells are essential *in vivo* for stem cell maintenance, since the $Lgr5^+$ ISCs disappear when Paneth cells are specifically depleted (Sato et al. 2011). *In vitro*, the signals they produce can be substituted by exogenous addition of the relevant ligands to the media, but even under these conditions the addition of Paneth cells greatly improves the seeding efficiency of $Lgr5^+$ ISCs (Sato and Clevers 2013). BMP signaling, which is strong in the villi and driven by BMP-4 secretion from the villus mesenchyma, has an opposite effect to Wnt signaling and promotes ISC differentiation and quiescence (Sato and Clevers 2013). The BMP antagonist Noggin is specifically found in the crypt and counteracts this influence (Watabe and Miyazono 2009).

In addition to the recently characterized $Lgr5^+$ ISC, it has long been proposed that quiescent stem cells exist in the intestinal epithelium, in a higher position in the crypt (the so-called +4 position, by counting cells from the bottom of the crypt) (Alberts 2000). These cells were characterized as quiescent from their ability to retain labeling with the thymidine analog 5-bromo-2'-deoxyuridine (BrdU), and the loss of BrdU after tissue injury was interpreted as a re-entry of these quiescent, label-retaining cells (LRC) into the cell cycle. Although it is still possible that a separate population of quiescent stem cells exists, it has been shown that the intestinal LRC are actually undifferentiated but committed progenitors for Paneth and secretory cells. These cells are generated from the $Lgr5^+$ ISC population and normally differentiate into Paneth or secretory cells. However, when the $Lgr5^+$ ISCs are not sufficient for tissue homeostasis, such as when mitotic cells are specifically depleted, these committed progenitors have the capacity to revert to an $Lgr5^+$ ISC phenotype and therefore repopulate the crypts with ISCs (Buczacki et al. 2013). In summary, the intestinal epithelium is normally replenished by the proliferation of active $Lgr5^+$ ISCs, but after injury, committed progenitors that retain the ability to serve as “reserve stem cells” become activated. These progenitors are not in a strict sense stem cells, since they do not normally self-renew, but are constantly generated from the $Lgr5^+$ ISC pool.

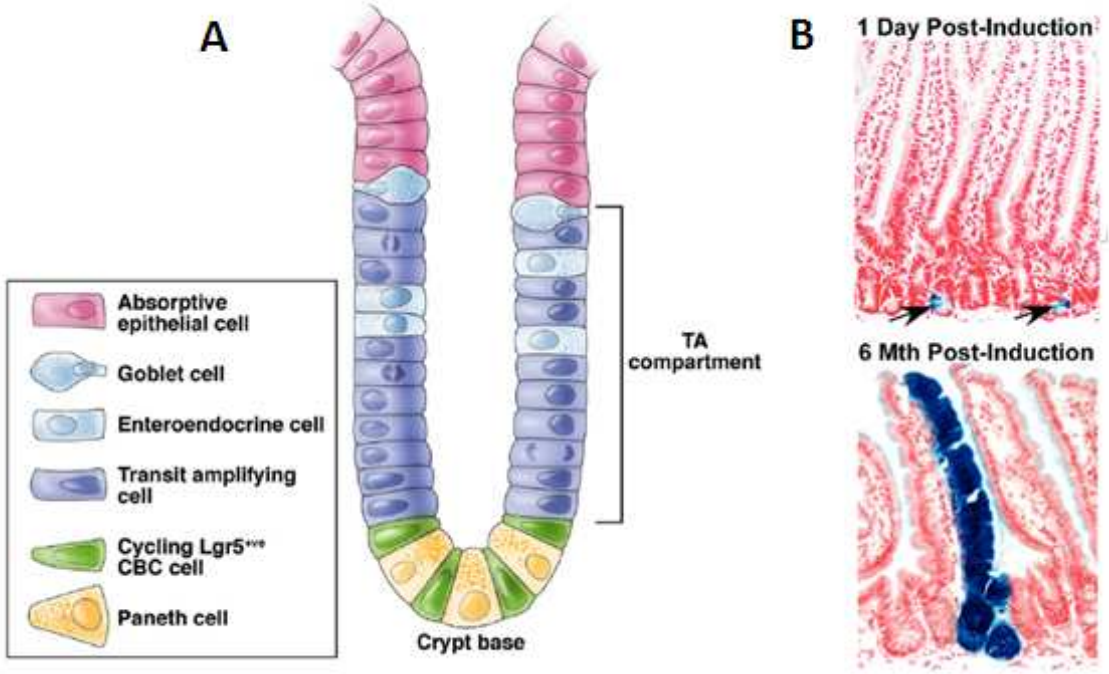

Figure I10. The Lgr5$^+$ ISCs and their niche. A. Schematic drawing showing the organization of the intestinal epithelium and the localization of the Lgr5$^+$ ISCs between the Paneth cells. **B.** Lineage tracing of Lgr5$^+$ ISCs mediated by the CreER system. Upper panel: the LacZ reporter is activated stochastically in a few Lgr5$^+$ cells at the crypt base after a low-dose tamoxifen (arrows). Lower panel: at later time points, entirely LacZ$^+$ cell strands are visible, which are thus Lgr5$^+$ ISC-derived. Figure modified from Barker and Clevers (2010).

3.7.4. Differentiated cells function as stem cells in the stomach corpus and in the alveolar epithelium of the lung

In the previous examples, stem cells contributing to tissue turnover are undifferentiated cells, which do not seem to contribute to any direct effector function in their tissue. But in other murine tissues, differentiated cells can function as stem cells under normal homeostasis or under special conditions. For example, in the epithelium of the stomach corpus region, chief cells are long-lived secretory cells that produce digestive enzymes. It was recently discovered that a sub-population of chief cells, which express the Troy receptor, has the ability to proliferate and of long-term clonal expansion, giving rise to all differentiated cell types of the stomach gland epithelium (Stange et al. 2013). These cells also express the Lgr5 receptor, and can form long-lived organoids when cultured *in vitro*. $Troy^+$ chief cells normally show low proliferative activity, and it is thought that their contribution for normal cellular turnover is very small. Instead, they function as "reserve stem cells", and become activated after depletion of proliferating cells in the stomach.

Similarly, in the alveolar sacs of the lungs two main epithelial cell types are present: the type 1 (AEC1) cells are squamous cells that mediate gas exchange, and type 2 (AEC2) cells are cuboidal cells that secrete surfactant that prevents alveolar collapse. During embryonic development, both cell types originate from a bipotent progenitor (Desai, Brownfield, and Krasnow 2014). In the adult, the alveolar sac epithelium has a low rate of cellular turnover, which is provided by proliferation of the long lived AEC2 cells. AEC2 cells can self-renew to give rise to more AEC2 cells, and they can also generate AEC1 cells (Barkauskas et al. 2013; Desai, Brownfield, and Krasnow 2014) (Figure I11). This occurs at a low rate during normal homeostasis, but the AEC2 cells can also respond to injury of the alveoli and increase their proliferative output. In summary, adult AEC2 cells function as stem cells while at the same time performing an essential effector function in the alveoli.

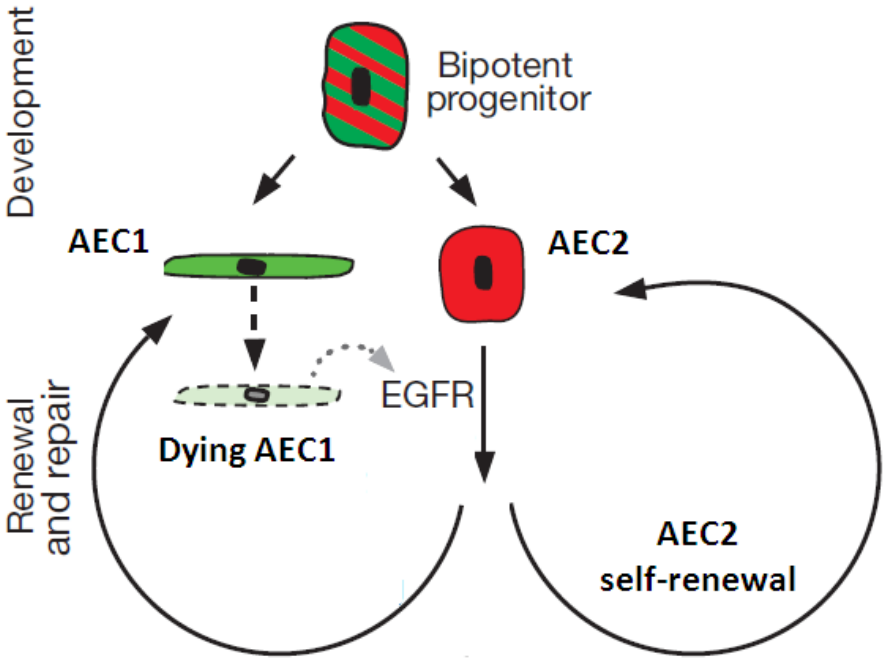

Figure I11. Developmental origin and turnover of murine alveolar epithelial cells. Bipotent progenitors differentiate into AEC1 or AEC2 cells during development. Mature AEC2 cells function as stem cells in the adult and are activated for alveolar renewal and repair (with a very slow turnover). Dying AEC1 cells are proposed to produce a signal that is transduced by epidermal growth factor receptor (EGFR), activating the division of a nearby AEC2 cell. Figure modified from Desai et al. (2014).

3.7.5. Differentiated cells self-duplicate in the liver and in the pancreas

In tissues with slow turnover, it is not rare for new cells to originate from self-duplication of existing differentiated cells (which are unipotent, and only give rise to more cells of the same type).

During normal tissue homeostasis in the liver, and during compensatory growth after partial hepatectomy (PHx), mature hepatocytes proliferate to generate new hepatocytes. This occurs at a very low rate under normal conditions, but hepatocytes are able to respond to PHx by entering the cell-cycle in a coordinated manner (Fausto and Campbell 2003; Yanger and Stanger 2011). Most hepatocytes participate of compensatory growth, and after a few rounds of cell-division, liver mass is restored to its original value. The hepatocytes have a huge potential for self-renewal, as can be seen in experiments of sequential PHx and in experiments of serial liver transplantations (Yanger and Stanger 2011). Similarly, in many models of regeneration the liver duct cells self-renew without any input from stem cells. However, in specific liver injuries mediated by chemicals, the hepatocytes are unable to proliferate, and new cells are originated from a population of undifferentiated stem cells, the so-called oval cells, which are believed to differentiate into hepatocytes and duct cells (and are thus bipotential) (Fausto and Campbell 2003; Dorrell et al. 2011; Yanger and Stanger 2011). So far, no specific marker of the oval cells has been found. They are thought to be facultative stem cells that arise by de-differentiation of cells from the biliary ducts, but the precise source of these cells is controversial. Recently, the Lgr5 receptor was shown to be specifically expressed by a population of small cells near the bile duct, but only after liver injury (Huch, Boj, and Clevers 2013). The $Lgr5^{+}$ cells were shown by Cre-mediated lineage tracing to give rise to hepatocytes after injury, and were able *in vitro* to generate organoids and to differentiate into hepatocytes and duct cells.

Another well studied example of self-renewing differentiated cells are the insulin-producing beta cells from the Langerhans islets of the pancreas. Lineage tracing by Cre-mediated recombination has shown that new beta cells originate from pre-existing, insulin producing (i.e. differentiated) beta cells (Dor et al. 2004). Furthermore, all beta cells seem to contribute similarly to the production of new beta cells during islet growth and maintenance (Brennand, Huangfu, and Melton 2007). An external source of

beta cells has only been documented under conditions of extreme beta cell loss. Under these conditions, new beta cells have been shown to originate by trans-differentiation of mature glucagon-producing alpha cells (Thorel et al. 2010).

3.8. Pluripotent and multipotent stem cells in invertebrate models

Drosophila and *Caenorhabditis* are the most common and powerful invertebrate models for developmental biology, and it is precisely in these models that the first extensive characterization of stem cell niches and their signals were performed. However, they are not very representative systems for the diversity of mechanisms of cell turnover found in adult metazoans, since adult *Drosophila* and *Caenorhabditis* have short life-spans, most (*Drosophila*) or all (*Caenorhabditis*) of their adult somatic tissues are no longer proliferative, and have very limited regenerative abilities. Finally, both of these models specify the germ line during early embryonic development, *via* the inheritance by specific blastomeres of cytoplasmic determinants (germ plasm) that were maternally synthezised and deposited in the egg ("preformation"). In contrast, most metazoans specify the germ line later in development, as a result of inductive signals from surrounding tissues ("epigenesis") (Extavour and Akam 2003).

Those tissues that show strong proliferation in adult *Drosophila*, such as the germ line and the midgut, are supported by tissue- or cell-specific stem cells (Losick et al. 2011; Takashima, Gold, and Hartenstein 2013). In contrast, there is good evidence in other invertebrate models for the existence of pluripotent or multipotent somatic stem cells in larvae and in adults. Examples of these organisms are found in most metazoan lineages, including pre-bilaterian metazoans (e.g. poriferans, cnidarians), deuterostomes (e.g. echinoderms) and lophotrochozoans (e.g. annelids, mollusks, and platyhelminthes) (Juliano, Swartz, and Wessel 2010; Solana 2013). Usually, these organisms specify their germ line by epigenesis, and may have a fluid limit between the soma and the germ line (multipotent somatic stem cells may contribute to the germ line in the adult, for example during regeneration).

These multipotent somatic stem cells have a conserved set of markers, which is shared with the germ line (Ewen-Campen, Schwager, and Extavour 2010; Juliano, Swartz, and Wessel 2010). The germ line stem cells (GSCs), although immediately unipotent (since they only give rise to gametes), conserves a "hidden" potential for pluripotency which is revealed after fertilization. Their pluripotency is also evidenced *in vitro*, as cultured germ line stem cells can generate chimeras when injected into host blastocysts and teratomas when injected into adult hosts, similarly to ESCs (Hanna,

Saha, and Jaenisch 2010). This set of shared expressed genes has therefore been denominated the "Germline Multipotency Program" (GMP) (Juliano, Swartz, and Wessel 2010). The gene products of the GMP components are associated with mRNA metabolism and the post-transcriptional regulation of gene expression. Furthermore, many are components of germ granules, which are cytoplasmic ribonucleoprotein (RNP) granules usually found in the cells of the germ line (Extavour and Akam 2003). The germ granules are part of the germ plasm in metazoans with preformation mechanisms of germ line segregation. Germ granules are therefore thought to be centers for post-transcriptional regulation of mRNA, and to carry essential determinants for germ line specification. Multipotent somatic stem cells of invertebrates may also have similar RNP granules with GMP components, and these granules receive different names in different species (e.g. chromatoid bodies, *nuage*, etc.) (Ewen-Campen, Schwager, and Extavour 2010).

Among the proteins of the proposed GMP, most have RNA binding activity, and many are translational repressors, such as Bruno, Nanos and Pumilio. Nanos proteins have two zinc-finger motifs with sequence-unspecific RNA binding activity (Curtis et al. 1997), whereas Pumilio is a member of the PUF family of sequence-specific RNA binding proteins (Wickens et al. 2002). Nanos and Pumilio interact with each other in *Drosophila*, *Caenorhabditis* and humans, and work in many cases together by binding to the 3′ UTR of target mRNAs and promoting their translational repression, deadenylation and degradation (Parisi and Lin 2000; Jaruzelska et al. 2003). They are required for maintaining the identity and quiescence of the primordial germ cells in *Drosophila*, as well as regulating proliferation and maintenance of germ cell identity in *Drosophila* and *Caenorhabditis* (Subramaniam and Seydoux 1999; Crittenden et al. 2003; Kadyrova et al. 2007; Ariz, Mainpal, and Subramaniam 2009). Other well conserved GMP proteins are Vasa, a DEAD-box ATP-dependent RNA helicase which is widely used as a marker for the germ line in many metazoans (Rebscher et al. 2007; Juliano, Swartz, and Wessel 2010; Lasko 2013), and Piwi, a member of the Argonaute family of proteins. Argonaute proteins are involved in gene silencing through small RNAs such as microRNAs (miRNAs) and small interfering RNAs (siRNAs) (Lasko 2013). Piwi proteins are associated with a specific class of small RNAs (Piwi-associated RNAs, or piRNAs) that are characteristically longer (26-31 nucleotides) than miRNAs and siRNAs, and unlike these, piRNAs are generated in a pathway that is independent

of the endoribonuclease Dicer (Juliano, Wang, and Lin 2011). Piwi and piRNAs affect gene regulation at the epigenetic level (through heterochromatin formation and DNA methylation) and by post-transcriptional regulation of RNA stability. The best characterized role of Piwi proteins and piRNAs is in the silencing of transposable elements, thus preventing their deleterious expansion in the genome of the germ line (Juliano, Wang, and Lin 2011; Skinner et al. 2014). It is clear however that other genes are also regulated by Piwi (Juliano, Wang, and Lin 2011; Peng and Lin 2013; Ross, Weiner, and Lin 2014), both in and outside the germ line, affecting aspects of germline specification, gametogenesis and stem cell maintenance in diverse organisms.

3.9. The planarian neoblasts

As previously mentioned, it is believed that in the Platyhelminthes all differentiated cells are post-mitotic, and a separate population of undifferentiated stem cells (the neoblasts) is the single source of new cells for normal tissue turnover, growth and regeneration (Peter et al. 2004; Reuter and Kreshchenko 2004). This has been studied in detail for free-living flatworms, especially for planarians, which are well known for their extensive regenerative capabilities (order Tricladida, in particular the species *Schmidtea mediterranea* and *Dugesia japonica*) (Reddien and Sanchez Alvarado 2004; Rossi et al. 2008; Rink 2013). Other free-living flatworm lineages that have been studied include the more basal groups Macrostomida (genera *Macrostomum* and *Microstomum*) (Palmberg 1990; Ladurner, Rieger, and Baguna 2000; Peter et al. 2004; Bode et al. 2006; Pfister et al. 2008; De Mulder et al. 2009b) and Catenulida (Moraczewski 1977; Dirks et al. 2012a; Dirks et al. 2012b). Recently, the development of technical advances such as RNA interference (RNAi), FACS analysis and isolation of neoblasts, and high throughput RNA sequencing have revolutionized the study of planarian regeneration and neoblast biology, placing planarians as one of the most important models for the study of regeneration at the cellular and molecular levels (Newmark and Sanchez Alvarado 2002; Rink 2013). However, some key techniques such as transgenesis and *in vitro* cell culture are still in their infancy (Schürmann and Peter 2001; Peter et al. 2004; Baguna 2012).

Planarians are able to regenerate a complete organism from almost any region of the body (Reddien and Sanchez Alvarado 2004). Furthermore, they constantly renew all of their somatic tissues at a very high rate (Rink 2013). The main tissues and organs of planarians, including the epidermis, digestive system, excretory system and nervous system lack any residing proliferating cells, and are instead supported by the integration of proliferating neoblasts that reside in the mesodermal parenchyma that surrounds the organs (Figure I12) (Rossi et al. 2008; Rink 2013). Neoblasts can be found throughout the planarian body except in the anterior-most region (in front of the photoreceptors) and in the pharynx, and these are precisely the only regions that are unable to regenerate after excision (Newmark and Sanchez Alvarado 2000; Reddien and Sanchez Alvarado 2004; Rink 2013). During regeneration, proliferating neoblasts accumulate close to the

wound site. As they enter diverse differentiation pathways they form a mass of undifferentiated and differentiating cells at the wound site (the regeneration blastema). The blastema is already post-mitotic, and the proliferating neoblasts are situated immediately adjacent to it (in the post-blastema) (Reddien and Sanchez Alvarado 2004; Eisenhoffer, Kang, and Sanchez Alvarado 2008).

Planarian neoblasts are small and basophilic undifferentiated cells, with a large nucleus and nucleolus and scant cytoplasm (Baguñà and Romero 1981; Peter et al. 2004; Rossi et al. 2008). At the ultrastructural level, they show abundant free ribosomes and mitochondria, and lack discernible rough endoplasmic reticulum and Golgi cisternae (Morita, Best, and Noel 1969; Hay and Coward 1975). Importantly, they show perinuclear RNP granules denominated "chromatoid bodies", which are molecularly and morphologically similar to the germ granules present in the germ cells of many animals (Morita, Best, and Noel 1969; Hay and Coward 1975; Auladell, Garcia-Valero, and Baguña 1993; Yoshida-Kashikawa et al. 2007; Rossi et al. 2008) (Figure I12). Because neoblasts are the only proliferating cells, they are specifically sensitive to ionizing irradiation, making this a very useful technique for depleting tissues of neoblasts for diverse experimental purposes (Hayashi et al. 2006; Rossi et al. 2007; Eisenhoffer, Kang, and Sanchez Alvarado 2008; Salvetti et al. 2009; Solana et al. 2012).

Molecular markers of the neoblast population were found originally by analysis of candidate genes, and later from transcriptomic analyses of neoblast-depleted planarians and of FACS-isolated neoblasts (Shibata et al. 1999; Salvetti et al. 2000; Orii, Sakurai, and Watanabe 2005; Reddien et al. 2005; Salvetti et al. 2005; Guo, Peters, and Newmark 2006; Rossi et al. 2007; Eisenhoffer, Kang, and Sanchez Alvarado 2008; Rossi et al. 2008; Rouhana et al. 2010; Labbe et al. 2012; Onal et al. 2012; Rink 2013). These studies have consistently shown that neoblasts specifically express several components of the GMP, and more generally, of many proteins related to post-transcriptional regulation of gene expression (Juliano, Swartz, and Wessel 2010; Rouhana et al. 2010). Many of these genes have been show by RNAi to have an important function in neoblast maintenance or differentiation, including orthologs of *vasa* and *piwi* (Reddien et al. 2005; Wagner, Ho, and Reddien 2012). Several *piwi* genes are expressed in planarian neoblasts, and in particular *smedwi-1* from *Schmidtea mediterranea* and its orthologs in other planarian species are the most widely used neoblast markers (Reddien et al. 2005; Palakodeti et al. 2008) (Figure I12). Although no

clear phenotype was observed from *smedwi-1* RNAi, other *piwi* genes such as *smedwi-2* and *smedwi-3* have been shown by RNAi to be important for neoblast differentiation and self-renewal. Other gene categories with an enriched expression in neoblasts include epigenetic regulators and transcription factors, as well as components of particular signaling pathways, including FGF receptors (Ogawa et al. 2002; Onal et al. 2012; Wagner, Ho, and Reddien 2012; Rink 2013). Recently, it was shown that although no clear-cut orthologs of the mammalian ESC regulators Oct4, Sox2 or Nanog can be found in planarians, the transcriptomes of neoblasts and mammalian ESC are highly correlated, indicating a broad conservation of pluripotency regulators between both models, and by extension, across metazoans (Onal et al. 2012).

Traditionally, neoblasts were considered to be a homogeneous population of pluripotent cells. Originally, neoblasts were shown at the whole-population level to be pluripotent and essential for regeneration, since only neoblast-enriched cell preparations were able to rescue lethally irradiated hosts after transplantation, whereas transplants of differentiated cells were unable to do so (Baguñà, Saló, and Auladell 1989). However, these experiments left open the possibility that several neoblast lineages with restricted potencies exist which can rescue and repopulate the irradiated host. Recently, it was shown through impressive single-cell transplantation experiments that at least a proportion of neoblasts (clonogenic neoblasts, or cNeoblasts) are truly pluripotent, being able to completely repopulate and replace all of the tissues of an allogeneic host. cNeoblasts were shown to be at least 5% of all neoblasts (which is the percentage of irradiated hosts that were rescued by the transplants), and is likely to be higher given the technically challenging method employed (Wagner, Wang, and Reddien 2011). However, it is not known whether all neoblasts are cNeoblasts, and there is evidence from gene expression studies showing that neoblasts are actually heterogeneous, since several markers are only expressed in sub-populations of the neoblasts. For example, the planarian *nanos* homolog is specifically expressed in the germ line stem cells (GSC), which are morphologically undistinguishable from somatic neoblasts and express other common neoblast markers (Sato et al. 2006; Handberg-Thorsager and Salo 2007; Wang et al. 2007). *nanos*$^{+}$ GSC are regenerated from *nanos*$^{-}$ somatic neoblasts (Sato et al. 2006), and the germ line can contribute to somatic tissues during regeneration (Reddien and Sanchez Alvarado 2004), demonstrating that the soma – germ line is fluid in planarians and that these neoblast sub-populations can interconvert

between each other. Furthermore, some proliferating neoblasts (expressing *smedwi-1* and proliferation markers, and X-ray sensitive) show co-expression of specific lineage markers during regeneration of the eyes and of the excretory system (Reddien 2013). This suggests the existence of populations of committed, lineage-specific neoblasts as well. Finally, it has been shown that some cells with neoblast-like morphology, or with intermediate morphologies between neoblasts and differentiated cells, are already post-mitotic and express different combinations of markers that represent different stages or different lineages of neoblast differentiation (Higuchi et al. 2007; Shibata, Rouhana, and Agata 2010).

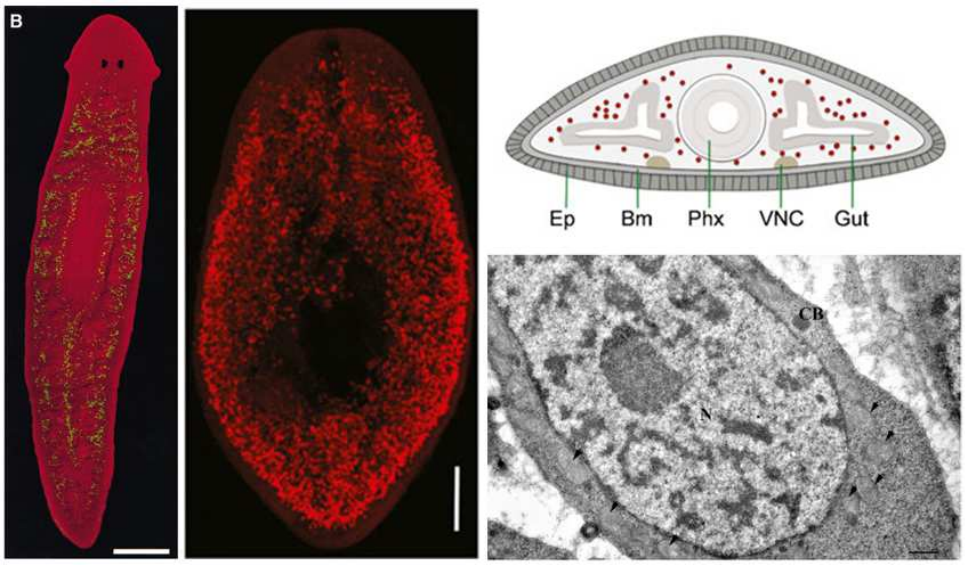

Figure I12. The planarian neoblasts. A. Distribution of proliferative cells as determined by BrdU incorporation (green) in the planarian *Girardia dorotocephala*. Bar represents 450 μm. From Newmark and Sanchez Alvarado, 2000. **B.** Distribution of *smedwi-1*$^{+}$ cells (red) in the planarian *Schmidtea mediterranea*. Bar represents 200 μm. From Rink, 2013. **C.** Schematic illustration of the distribution of neoblasts in the parenchyma, in a transverse section at the level of the pharynx. From Rink, 2013. **D.** Transmission electron microscopy image of a neoblast, showing a chromatoid body (CB) and mitochondria (arrowheads). Bar represents 100 nm. From Rossi et al., 2012. Abbreviations: Bm, basal membrane; Ep, epidermis; Phr, photoreceptor; Phx, pharynx; VNC, ventral nerve cords.

3.10. The cestode germinative cells [1]

In cestodes, undifferentiated proliferating cells (equivalent to the planarian neoblasts) are usually denominated as "germinative cells" (Gustafsson 1990; Reuter and Kreshchenko 2004; Koziol and Castillo 2011). By classic histological techniques, germinative cells have been characterized as round or oval cells with a strongly basophilic cytoplasm (due to the abundance of rRNA), few cytoplasmic extensions, a large nucleus and a large and prominent nucleolus (Douglas 1961; Bolla and Roberts 1971; Wikgren and Gustafsson 1971; Sulgostowska 1972; Gustafsson 1976b; Loehr and Mead 1979; Koziol et al. 2010) (Figure I13). More than one lineage of morphologically similar germinative cells may actually exist, and in some models, several sub-types of germinative cells have been proposed based on their nucleo-cytoplasmic ratio, absolute size and staining characteristics (Douglas 1961; Sulgostowska 1972). At the ultrastructural level, germinative cells have been described in oncospheres, metacestodes and adult cestodes (Collin 1969; Sakamoto and Sugimura 1970; Bolla and Roberts 1971; Wikgren and Gustafsson 1971; Swiderski 1983; Jabbar et al. 2010). These cells have a high nucleo-cytoplasmic ratio, nuclei with little heterochromatin, an electron-dense cytoplasm with abundant free ribosomes, and absent or scarce endoplasmic reticulum and Golgi apparatus. Their morphology is thus very similar to neoblasts from planarians, except that chromatoid bodies have never been described in cestodes (Figure I13).

In adult cestodes and during the early stages of segmentation, a conserved pattern has been described for the distribution of proliferating germinative cells within the neck region of several species (the generative region from which new segments are formed). Proliferative cells are found mainly or exclusively in the external region of the medullar parenchyma, close to the inner muscle layer in *Diphyllobothrium* spp. (Wikgren and Gustafsson 1971), *Cylindrotaenia diana* (Douglas 1961), *Hymenolepis diminuta* and *Hymenolepis nana* (Bolla and Roberts 1971; Henderson and Hanna 1988),

[1] This section is largely based on a previous review written by myself and Dr. E. Castillo: Koziol, U., and E. Castillo. 2011. Cell proliferation and differentiation in cestodes. Pp. 121-138 *in* A. Esteves, ed. Research in Helminths. Transworld Research Network, Kervala, India.

Taenia solium (Willms et al. 2001) and *Mesocestoides corti* (Koziol et al. 2010) (Figure I14). Proliferation in the cortical parenchyma is absent or restricted to the innermost regions. The conservation of this close apposition between the germinative cells and the inner muscle layer suggests that the muscle cells and/or the closely positioned nerve cords could provide signals for the germinative cells. In contrast, in the metacestode stages of *Hymenolepis diminuta* and *Taenia solium*, proliferating germinative cells are not restricted to the medullar parenchyma, suggesting that greater variability exists in larval stages (Bolla and Roberts 1971; Merchant, Corella, and Willms 1997).

In *Echinococcus* spp., studies on stem cells have focused in the oncosphere, where 10 germinative cells were described (Swiderski 1983) (Figure I15), and in the metacestode stage. During early metacestode development in *E. multilocularis*, two types of undifferentiated cells were described at the ultrastructural level: "light stained undifferentiated cells" (LS-cells) and "dark-stained undifferentiated cells" (DS-cells), both of which were found in mitosis (Sakamoto and Sugimura 1970). LS-cells were only found during the earliest stages of the oncosphere to metacestode metamorphosis, and were proposed to give rise to the DS-cells. DS-cells accumulate during the formation of brood capsules and protoscoleces, and it was proposed that DS-cells differentiate into several cell types such as tegumental cells, muscle cells and glycogen storing cells (Figure I16). Ultrastructural studies of *E. granulosus* metacestodes also described other differentiated cell types, such as calcareous corpuscle cells and excretory cells (cells of the excretory tubules and flame cells) (Lascano, Coltorti, and Varela-Diaz 1975; Smith and Richards 1993). In the metacestode of *E. granulosus*, proliferating cells incorporating ^{3}H-thymidine (^{3}H-T) are found dispersed throughout the germinal layer, accumulating during the development of protoscoleces (Galindo et al. 2003). At later stages of development and in fully differentiated protoscoleces, the number of cells incorporating ^{3}H-T decreased to very low levels, suggesting that the protoscoleces entered a quiescent state.

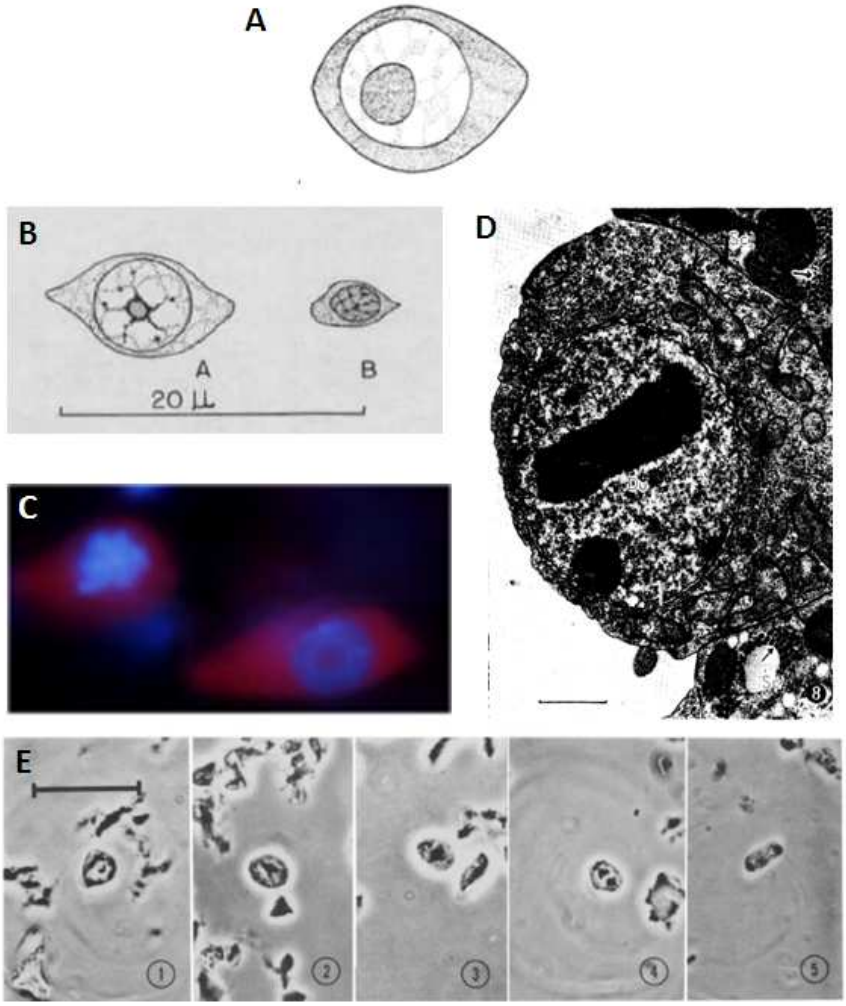

Figure I13. The germinative cells of cestodes. **A.** Schematic drawing of a germinative cell from the neck region of segmenting *Diphyllobothrium dendriticum*. Modified from Gustafsson, 1976. **B.** Schematic drawings of germinative cells (of two different proposed sub-types) from the developing proglottids of *Cylindrotaenia diana* (syn. *Baerietta diana*). Modified from Douglas, 1961. **C.** Germinative cells from the neck region of segmenting *Mesocestoides corti* (syn. *Mesocestoides vogae*) stained with DAPI (DNA) and ethidium bromide (all nucleic acids). The cell on the left is in mitosis. Bar represents 10 µm. Modified from Koziol et al., 2010. D. Transmission electron microscopy image of a germinative cell (referred to as "dark undifferentiated cell") from the developing metacestode of *E. multilocularis*. Bar represents 1 µm. Modified from Sakamoto and Sugimura (1970). **E.** Germinative cells from the neck region of adult *Hymenolepis citelli* in interphase (1) and in diverse stages of mitosis (2 to 4: prophase, metaphase, anaphase and telophase, respectively) as seen in cell macerates. Bar represents 20 µm. Modified from Loehr and Mead, 1979.

3. Introduction

Nothing was known before this work regarding specific gene expression in cestode germinative cells, but analysis of the genome sequences of cestodes and trematodes has shown that important components of the GMP, such as orthologs of *piwi, vasa* and group 9 *tudor* genes have been lost in these lineages (Tsai et al. 2013). This, combined with the lack of chromatoid bodies in cestode germinative cells, implicates the existence of important differences with planarian neoblasts (Skinner et al. 2014). It is possible that in the stem cells of cestodes and trematodes other gene paralogs of the Argonaute, DEAD box helicase and Tudor protein families could be performing similar functions as *piwi*, *vasa* and group 9 *tudor* genes, respectively. Recently, the existence of neoblast-like cells in the parenchyma of the adult and larval stages of the trematode *Schistosoma mansoni* has been demonstrated. In *S. mansoni*, paralogs of *piwi* (*sm-ago2-1*) and *vasa* (*sm-vlg-3*) are specifically expressed in the neoblast-like stem cells and have important roles in their maintenance, which is consistent with that hypothesis (Collins et al. 2013; Wang, Collins, and Newmark 2013). Furthermore, at least one FGF receptor is specifically expressed in the *S. mansoni* neoblast-like cells and is essential for their maintenance, indicating further commonalities between the planarian and *S. mansoni* stem cell systems (Collins et al. 2013).

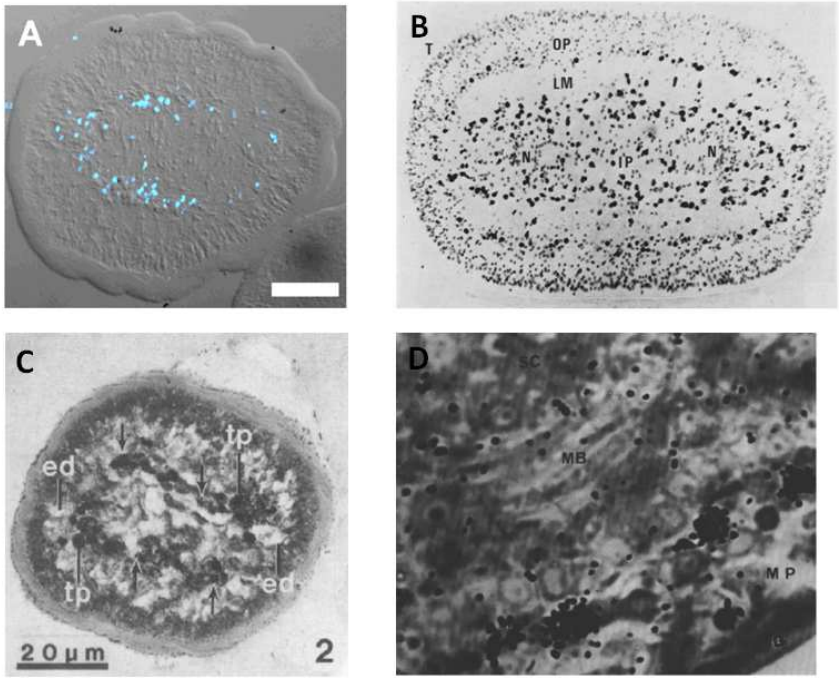

Figure I14. Distribution of proliferating cells close to the inner muscle layer in segmenting cestodes. A. BrdU incorporation in cells close to the inner muscle layer (thus seen as a ring of $BrdU^+$ cells in cross-sections) in *M. corti*. Bar represents 50 µm. Modified from Koziol *et al*., 2010. **B.** ^{3}H-thymidine incorporation in *D. dendriticum*. IP, inner parenchyma; LM, inner longitudinal muscle layer; N, nerve cords; OP, outer parenchyma. Modified from Gustafsson, 1976. **C.** ^{3}H-thymidine incorporation in *Hymenolepis nana* in cells close to the inner muscle layer (arrows). Modified from Henderson and Hanna, 1988. **D.** Detail of ^{3}H-thymidine incorporation in *Hymenolepis diminuta* in germinative cells in the border of the inner parenchyma (MP) just internal to the inner muscle layer (MB). Modified from Bolla and Roberts, 1971.

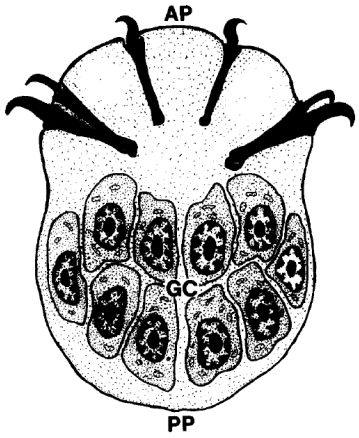

Figure I15. Distribution of the five pairs of germinative cells present in the oncospheres of *E. granulosus.* The distribution was reconstructed from electron microscopical studies. From Swiderski, 1983.

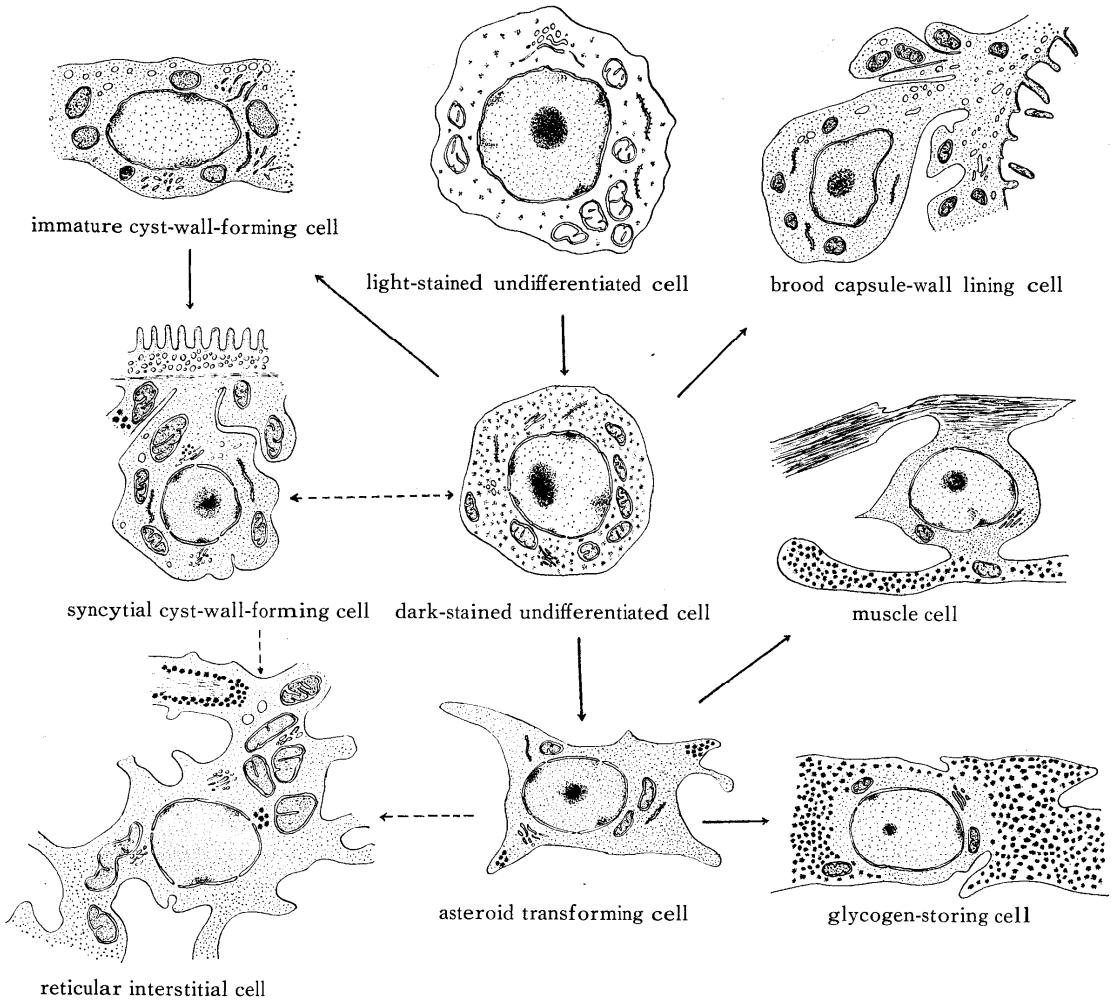

Figure I16. Cell types during early development of *E. multilocularis* metacestodes. Differentiated cell types proposed to originate from undifferentiated cells (germinative cells) from ultrastructural studies. From Sakamoto and Sugimura, 1970.

4. Hypothesis and Objectives

The **hypothesis** behind this work is that germinative cells are the only stem cells / progenitor cells of *Echinococcus multilocularis*, and that they may express conserved regulators and signaling cascades found in stem cells of other metazoans, including other flatworms.

The **general objective** of this work is to characterize the germinative cells of *Echinococcus multilocularis* metacestodes.

The **specific objectives** of this work are:

1) To characterize the germinative cells of the metacestode stage of *E. multilocularis* at the morphological level

2) To demonstrate that only the germinative cells proliferate in *E. multilocularis* metacestodes, and give rise to differentiated cell types.

3) To discover genes that are expressed in the germinative cells, including specific molecular markers for this population (or sub-populations).

4) To determine if the previously described insulin and FGF signaling cascades of *E. multilocularis* (Förster 2012; Hemer et al. 2014) are expressed and/or active in the germinative cells.

5) To discover molecular markers for differentiated cell types that would allow to trace their differentiation and to describe the development of the metacestode.

5. Results

5.1. CHAPTER 1: "The unique stem cell system of the immortal larva of the human parasite *Echinococcus multilocularis*"

Originally published as Koziol *et al*. (2014), EvoDevo 5:10

Author contributions

General study design:

Klaus Brehm and Uriel Koziol

Experimental design and work:

Uriel Koziol designed, performed or participated in all the experiments. Theresa Rauschendörfer performed RT-PCR, cloning, and part of the histochemical analyses of alkaline phosphatase genes under the direct supervision of Uriel Koziol. Luis Zanón Rodríguez performed long-range PCR, part of the RT-PCR, cloning, and confirmatory WMISH experiments of argonaute genes under the direct supervision of Uriel Koziol. Georg Krohne designed, supervised and interpreted the results of electron microscopy experiments.

Analysis of the results:

Uriel Koziol, Klaus Brehm, Georg Krohne

Writing of the manuscript:

Uriel Koziol wrote the first manuscript draft, which was corrected by Klaus Brehm and accepted by all the authors

The unique stem cell system of the immortal larva of the human parasite *Echinococcus multilocularis*

Uriel Koziol[1,3], Theresa Rauschendorfer[1], Luis Zanon Rodríguez[1], Georg Krohne[2], Klaus Brehm[1,*]

[1] University of Würzburg, Institute of Hygiene and Microbiology, Josef-Schneider-Strasse 2, D-97080 Würzburg, Germany

[2] University of Würzburg, Department of Electron Microscopy, Biocenter, D-97078 Würzburg, Germany

[3] Universidad de la República, Facultad de Ciencias, Sección Bioquímica y Biología Molecular, Iguá 4225, CP 11400, Montevideo, Uruguay.

* Corresponding Author

Abstract

Background

It is believed that in tapeworms a separate population of undifferentiated cells, the germinative cells, is the only source of cell proliferation throughout the life cycle (similarly to the neoblasts of free living flatworms). In *Echinococcus multilocularis*, the metacestode larval stage has a unique development, growing continuously like a mass of vesicles that infiltrate the tissues of the intermediate host, generating multiple protoscoleces by asexual budding. This unique proliferation potential indicates the existence of stem cells that are totipotent and have the ability for extensive self renewal.

Results

We show that only the germinative cells proliferate in the larval vesicles and in primary cell cultures that undergo complete vesicle regeneration, by using a combination of morphological criteria and by developing molecular markers of differentiated cell types. The germinative cells are homogeneous in morphology but heterogeneous at the molecular level, since only sub-populations express homologs of the post-transcriptional regulators *nanos* and *argonaute*. Important differences are observed between the expression patterns of selected neoblast marker genes of other flatworms and the *E. multilocularis* germinative cells, including widespread expression in *E. multilocularis* of some genes that are neoblast-specific in planarians. Hydroxyurea treatment results in the depletion of germinative cells in larval vesicles, and after recovery of hydroxyurea treatment, surviving proliferating cells grow as patches that suggest extensive self-renewal potential for individual germinative cells.

Conclusions

In *E. multilocularis* metacestodes, the germinative cells are the only proliferating cells, presumably driving the continuous growth of the larval vesicles. However, the existence of sub-populations of the germinative cells is strongly supported by our data. Although the germinative cells are very similar to the neoblasts of other flatworms in

function and in undifferentiated morphology, their unique gene expression pattern and the evolutionary loss of conserved stem cells regulators suggest that important differences in their physiology exist, which could be related to the unique biology of *E. multilocularis* larvae.

Keywords: cestoda, *Echinococcus*, neoblast, germinative cell, stem cell, nanos, argonaute, mucin, alkaline phosphatase.

Background

The Platyhelminthes (flatworms) comprise a highly diverse phylum in terms of morphology, embryology, life-cycle complexity and capacity for regeneration and asexual reproduction (Hyman 1951; Ax 1996; Egger, Gschwentner, and Rieger 2007; Martin-Duran and Egger 2013). However, they are united by having a unique population of undifferentiated stem cells, commonly known as 'neoblasts' (Reuter and Kreshchenko 2004; Koziol and Castillo 2011). It is thought that neoblasts represent the only proliferative cell population, and are therefore the source of new cells for normal tissue turnover, growth and regeneration.

The characterization of neoblasts has been most extensive for free living flatworms, especially for planarians. Planarian neoblasts have been shown to be truly pluripotent (Wagner, Wang, and Reddien 2011), and are essential for planarian regeneration (Baguñà, Saló, and Auladell 1989). Classical ultrastructural studies in planarians described the neoblasts as small, round cells with a large nucleus containing little heterochromatin and a large nucleolus, with scant cytoplasm containing mitochondria, abundant free ribosomes and few other organelles (Rossi et al. 2008; Rink 2013). Furthermore, they possess cytoplasmic electron-dense ribonucleoprotein (RNP) granules called chromatoid bodies, which are molecularly and morphologically similar to the well known germ granules present in the germ cells of many animals. Germ granules are thought to function as centers for post-transcriptional regulation of mRNA, similar to other RNP bodies in somatic cells (Extavour and Akam 2003; Ewen-Campen, Schwager, and Extavour 2010). Many studies have shown that genes involved in post-transcriptional regulation and chromatin modification are highly upregulated in neoblasts (Rossi et al. 2007; Eisenhoffer, Kang, and Sanchez Alvarado 2008; Rouhana et al. 2010; Labbe et al. 2012; Onal et al. 2012; Wagner, Ho, and Reddien 2012). These include genes that are typically considered markers of germ cells in other model animals, such as the DEAD box RNA helicase *vasa* and the Argonaute family gene *piwi* (Ewen-Campen, Schwager, and Extavour 2010). This expression of germ line markers in somatic multipotent stem cells has also been found in other animal lineages, and has been interpreted as part of a multipotency program conserved between the germ line and

multipotent somatic stem cells (Juliano, Swartz, and Wessel 2010). The development of molecular markers has further shown that the neoblasts are actually heterogeneous at the molecular level (Rossi et al. 2008; Rink 2013).

The main groups of parasitic flatworms, including cestodes, trematodes and monogeneans, form the monophyletic clade Neodermata (Ax 1996; Baguñà and Riutort 2004). In cestodes, classical studies have evidenced a population of undifferentiated stem cell similar to the neoblasts, which are denominated the germinative cells (Douglas 1961; Sakamoto and Sugimura 1970; Bolla and Roberts 1971; Wikgren and Gustafsson 1971; Sulgostowska 1972; Gustafsson 1976b; Mead 1982; Koziol et al. 2010). However, unlike for planarian neoblasts, chromatoid bodies have never been described for the germinative cells. Germinative cells are thought to drive the development throughout the cestode life cycle. In the 'typical' cestode life cycle, the oncosphere (first larval stage) is a highly reduced organism that has a small population of set-aside germinative cells. Once the oncosphere infects the intermediate host, it develops into the metacestode (second larval stage), and it is thought that only the germinative cells contribute to this metamorphosis (Rybicka 1966). Usually, the metacestode is similar to a 'juvenile' tapeworm, containing the scolex (head) with the attachment organs, but lacking the reproductive systems. Finally, the intermediate host containing the metacestode is ingested by the definitive host, and the metacestode develops into an adult in the intestine. New segments, each containing a complete set of male and female reproductive systems, are generated continuously from the proliferative region of the neck, behind the scolex, and produce oncospheres by sexual reproduction. In the neck region of segmenting cestodes, the proliferating germinative cells are localized close to the inner muscle layer, and have been shown to be the only proliferating cell type (Douglas 1961; Bolla and Roberts 1971; Gustafsson 1976b; Henderson and Hanna 1988; Koziol et al. 2010).

The metacestode stage of *Echinococcus multilocularis* is atypical in its development and morphology (Eckert, Thompson, and Mehlhorn 1983; Mehlhorn, Eckert, and Thompson 1983; Eckert and Deplazes 2004). After the oncosphere is ingested by the intermediate host (diverse rodents, but also accidentally humans) it develops in the liver as a labyrinth of vesicles, which grow cancer-like and infiltrate the tissue of the host, forming new vesicles and even metastases. The metacestode growth

causes the disease alveolar echinococcosis, one of the most dangerous zoonoses of the Northern Hemisphere (Eckert and Deplazes 2004). The metacestode vesicles comprise a thin layer of tissue (the germinal layer) covered by a syncitial tegument that secretes an acellular, carbohydrate-rich external layer (the laminated layer) (Figure 1). The remaining volume of the vesicles is filled with fluid (hydatid fluid). Within the germinal layer, thickenings (buds) occur that invaginate into the vesicle, resulting in the formation of brood capsules (Figure 1A). Within the brood capsules, a new budding process occurs, that results in the formation of protoscoleces, the infective form for the definitive host (Figure 1B-C). The protoscolex already resembles the anterior region of the adult form, with a scolex that lays invaginated within a small posterior body (Figure 1D). After ingestion of the protoscolex by the definitive host (canids), it evaginates its scolex, attaches to the intestine and develops into the adult tapeworm (Eckert and Deplazes 2004).

The metacestode tissue can be maintained and will grow indefinitely in intermediate hosts by serial passage, and is in this sense ´immortal´ (Norman and Kagan 1961; Spiliotis and Brehm 2009). Recently, we have developed methods for the axenic *in vitro* maintenance of metacestode vesicles, and for primary cell cultures that result in complete regeneration of metacestode vesicles (Spiliotis et al. 2008). These methods allow for *in vitro* analysis of development in *Echinococcus* metacestodes, and show that at least at a population level, the primary cell preparations are multipotent. Classical ultrastructural studies in *E. multilocularis* and the related *Echinococcus granulosus* demonstrated the existence of germinative cells in the germinal layer, which proliferate and accumulate during brood capsule and protoscolex development (Sakamoto and Sugimura 1970). This accumulation of proliferating cells in the developing protoscolex was confirmed by labeling with radioactive thymidine (Galindo et al. 2003). Nothing is known to this date about gene expression in cestode germinative cells, but the genome sequencing project of *E. multilocularis* demonstrated the lack of *vasa* and *piwi* orthologs, suggesting fundamental differences between germinative cells and planarian neoblasts (Tsai et al. 2103). Differentiated cell types have also been described in the germinal layer, including tegumental cells (the cell bodies of the tegumental syncitium, which are connected to the overlying syncitial tegument by cytoplasmatic bridges), muscle cells, glycogen/lipid storing cells, and recently nerve cells (Sakamoto and

Sugimura 1970; Lascano, Coltorti, and Varela-Diaz 1975; Koziol, Krohne, and Brehm 2013).

In this work, we characterize the germinative cells in the metacestodes and in primary cell cultures as the only proliferating cells, driving metacestode growth and regeneration. By developing methods for analyzing gene expression with cellular resolution in *E. multilocularis*, we show that differentiated cell types do not proliferate, and that the germinative cells are heterogeneous at the molecular level, showing in addition several differences with the neoblasts from other flatworms. Finally, by analyzing the response of the metacestodes after partial germinative cell depletion, we provide evidence that indicates extensive self renewal capabilities for individual germinative cells.

Results

Cell proliferation in *E. multilocularis* larval development

In order to detect proliferating cells, we incubated metacestode vesicles from *in vitro* culture with the thymidine analog 5-ethynyl-2′-deoxyuridine (EdU) (Salic and Mitchison 2008), which is incorporated into DNA during its synthesis in the S-phase of the cell cycle, and later performed the fluorescent detection reaction on metacestode whole-mounts and sections. A relatively long time (2 hours) and high concentration of EdU (10 μM) was required for any labeling to be detected, probably because of slow equilibration between the EdU concentration in the medium and in the large amount of hydatid fluid within the vesicles. For typical labeling experiments, we used a 5 hour incubation time and 50 μM EdU. EdU positive (EdU+) cells can be detected throughout the germinal layer, and are in average 5.9% of all the cells (n=6 independent labeling experiments, with > 200 cells per experiment; range =2.4%-10.9%) (Figure 2A). The vast majority of the labeled cells were in interphase, but a few cases of mitotic cells with low levels of labeling were observed, suggesting that during the 5 hour pulse they were labeled just at the end of the S-phase and transited through G2 / mitosis (Additional File 1).

There is a strong accumulation of EdU+ cells in the brood capsule buds and in the protoscolex buds (Figures 2A and 2B). During early development, most EdU+ cells do not reach the periphery of the bud (Figure 2B). This pattern becomes more distinct as development progresses, and when the main nervous commissure becomes evident by FMRFamide immunoreactivity (Koziol, Krohne, and Brehm 2013) most EdU+ cells are located posterior to it (Figure 2C). In the last stages of protoscolex development, there are some EdU+ cells in the posterior body, while in the scolex EdU+ cells accumulate massively at the base of the developing suckers, but not in the rest of the sucker tissue (Figure 2D). Finally, cell proliferation becomes very low when protoscolex development is complete and the scolex is invaginated (Figures 2A and 2B). Identical results were obtained when metacestodes that had been cultured *in vivo* in gerbils were incubated with EdU *ex vivo* immediately after removing the material from the host (Additional File 2), and similar patterns of cell proliferation have been described for protoscolex development in *E. granulosus* (Galindo et al. 2003).

5. Results

EdU incorporation remains very low for the first hours after protoscoleces are isolated from the metacestode material. However, when we activated protoscoleces by artificially mimicking the ingestion by the definitive host, the number of EdU+ cells increased dramatically. Furthermore, prolonged *in vitro* culture of protoscoleces in the absence of activation factors also resulted in an increase of cell proliferation in many of them (Additional File 3). This indicates that in the developed protoscolex there is a large population of cells capable of proliferation, but they remain in a quiescent state or with slow cell-cycle kinetics for as long as the protoscolex remains resting within the metacestode.

As a complementary approach, we analyzed the distribution of mitotic cells by immunohistochemistry against histone H3 phosphorylated in Serine 10 (H3S10-P, (Hendzel et al. 1997)) after allowing the mitotic figures to accumulate by *in vitro* incubation with colchicine (Wikgren and Gustafsson 1971; Koziol et al. 2010). The distribution of H3S10-P+ cells was identical to the distribution of EdU+ cells, confirming the previous results (Figure 2A). The percentage of H3S10-P+ cells in the germinal layer was low in the absence of colchicine incubation (<0.5% of all cells), which suggests a fast transition through mitosis, as has been described in other cestodes (Wikgren and Gustafsson 1967; Bolla and Roberts 1971).

Identification of germinative cells as the only proliferating cells

Because of the small size of *Echinococcus* cells and the loose organization of the germinal layer, it is very difficult to identify cell types *in situ* by morphology except by means of electron microscopy (Sakamoto and Sugimura 1970; Gustafsson 1976c). In order to identify the EdU+ cells, we performed a tissue maceration procedure that results in a suspension of cells that retain their original morphology (David 1973; Loehr and Mead 1979; Baguñà and Romero 1981; Newmark and Sanchez Alvarado 2000). We then stained these suspensions with 4',6-diamidino-2-phenylindole (DAPI, that stains specifically DNA) combined with propidium iodide (PI) or the Thermo Scientific™ Cellomics Whole Cell Stain (WCS), that stain all nucleic acids and are therefore analogous to the traditional Pyronin Y staining for basophilic, RNA rich cells (Wikgren and Gustafsson 1971). In parallel, we performed staining of cell suspensions for lipids using Nile Red (NR) combined with DAPI (Figure 3).

With this method, we consistently identified the germinative cells as small (5 to 12 μm across the longest axis), pear-shaped to fusiform cells that are strongly stained with PI and WCS, and that can sometimes have thin cytoplasmic extensions protruding from the poles. The nucleus is round and very large, with one to three very prominent nucleoli and with finely granular chromatin, giving a very bright staining with DAPI. Cytoplasmic lipid droplets were rare.

The germinative cells were the only cells that incorporated EdU after 2 to 6 hours of incubation *in vitro* (n=5 independent labeling experiments): after 5 hours of labeling, an average of 24% ± 6.7% (standard deviation) of the germinative cells were EdU+. Germinative cells were also the only cells observed in mitosis. Size differences were observed between these cells, and smaller germinative cells were less likely to incorporate EdU (Additional File 4), suggesting that cell size may be related in part to different cell-cycle phases. In small metacestode vesicles, the germinative cells were on average 21% of all the cells. We observed that in larger vesicles, the apparent abundance of the germinative cells was higher, up to ca. 50% of all cells. However, in these vesicles the tissue maceration was incomplete, and we believe that the germinative cells were overrepresented in the cell suspensions. Indeed, taking into account that in whole-mounts of these vesicles an average of 5.9% of all cells were EdU+, and that 24% of all germinative cells are EdU+ in the cell suspensions, by assuming that all EdU+ are germinative cells (see above) one can approximately estimate the fraction of germinative cells as 25% of all cells. In activated protoscoleces, although the tissue maceration was also incomplete, we observed germinative cells as the only EdU+ cells after a 5 hour pulse as well (Additional File 5).

All morphologically differentiated cells were consistently EdU-, indicating that they are generated by differentiation of the proliferating germinative cells. Among the differentiated cells, we could recognize several types by comparison with ultrastructural descriptions from *E. multilocularis* metacestodes and classic histological studies in other cestodes (Sakamoto and Sugimura 1970; Lascano, Coltorti, and Varela-Diaz 1975; Gustafsson 1976b; Loehr and Mead 1979) (Figure 3). These included: 1) the tegumental cells, with abundant cytoplasm strongly stained with PI/WCS, uniformly stained by NR, and with an irregularly shaped border. The nucleus can be slightly irregularly shaped and shows chromatin clumps in the periphery; 2) the glycogen/lipid

storage cells. These cells have large and smooth cytoplasmic lobes, show very low staining with PI/WCS, and have lipid droplets as seen by NR staining; 3) the calcareous corpuscle forming cells, with a small and eccentric nucleus and a large round cytoplasm that shows little staining for PI, WCS or NR; 4) several small cell types with a small, heterochromatin-rich nucleus. It is likely that muscle cells and nerve cells are found in this category after losing their cytoplasmic extensions during the maceration procedure.

In order to confirm that the differentiated cell types are generated from the pool of proliferating germinative cells, we performed EdU pulse-chase assays, in which we incubated the vesicles for 2 hours with 50 μM to 100 μM EdU, followed by washing and incubation in EdU free medium for up to 7 days. Unfortunately, we observed that the EdU signal was stronger after a 3 day chase period than directly after the pulse (data not shown), indicating that EdU remains in the hydatid fluid after washing. As a complementary approach, we performed continuous EdU labeling experiments with 1 μM to 10 μM EdU for up to 14 days. In this setting we observed that the higher concentrations (10 μM) showed some toxicity in this setup, whereas lower concentrations (0.5 μM) did not yield cells with enough labeling for detection. In both pulse-chase and continuous labeling experiments, we observed EdU+ tegumental and glycogen/lipid storing cells after 7 days (Figure 3 and data not shown), suggesting differentiation of germinative cells into these cell types. In summary, we identified the germinative cells as the only proliferating cell population, and the evidence suggests that differentiated cell types are generated from the germinative cells.

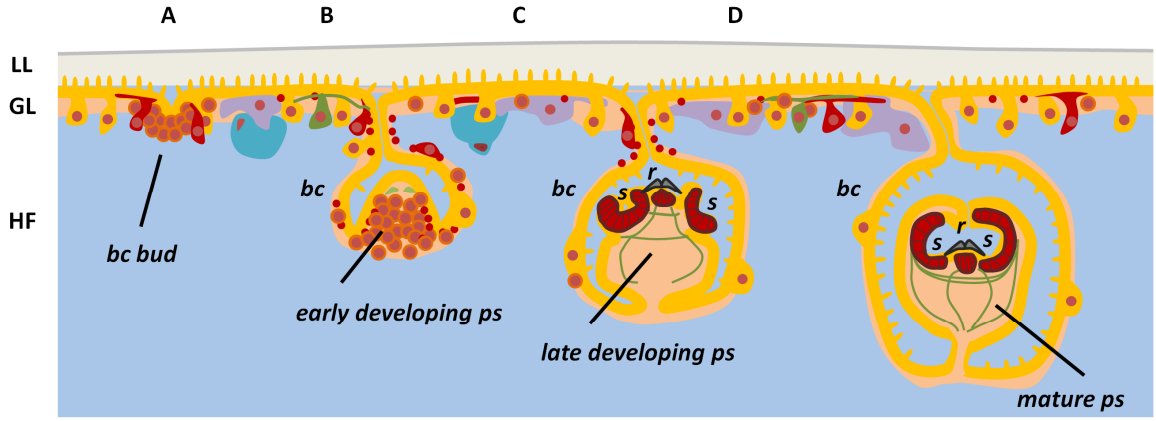

Figure 1. Schematic drawing showing the general organization and development of *E. multilocularis* metacestodes. A. Early brood capsule bud. B. Brood capsule with protoscolex bud. C. Brood capsule with protoscolex in late development. D. Brood capsule with invaginated protoscolex. The syncitial tegument is shown in orange, the germinative cells in brown, glycogen/lipid storage cells in violet, calcareous corpuscle cells in light blue, nerve cells in green and muscle cells and fibers in red. bc, brood capsule; GL, germinal layer; HF, hydatid fluid, LL, laminated layer; ps, protoscolex; r, rostellum; s, sucker.

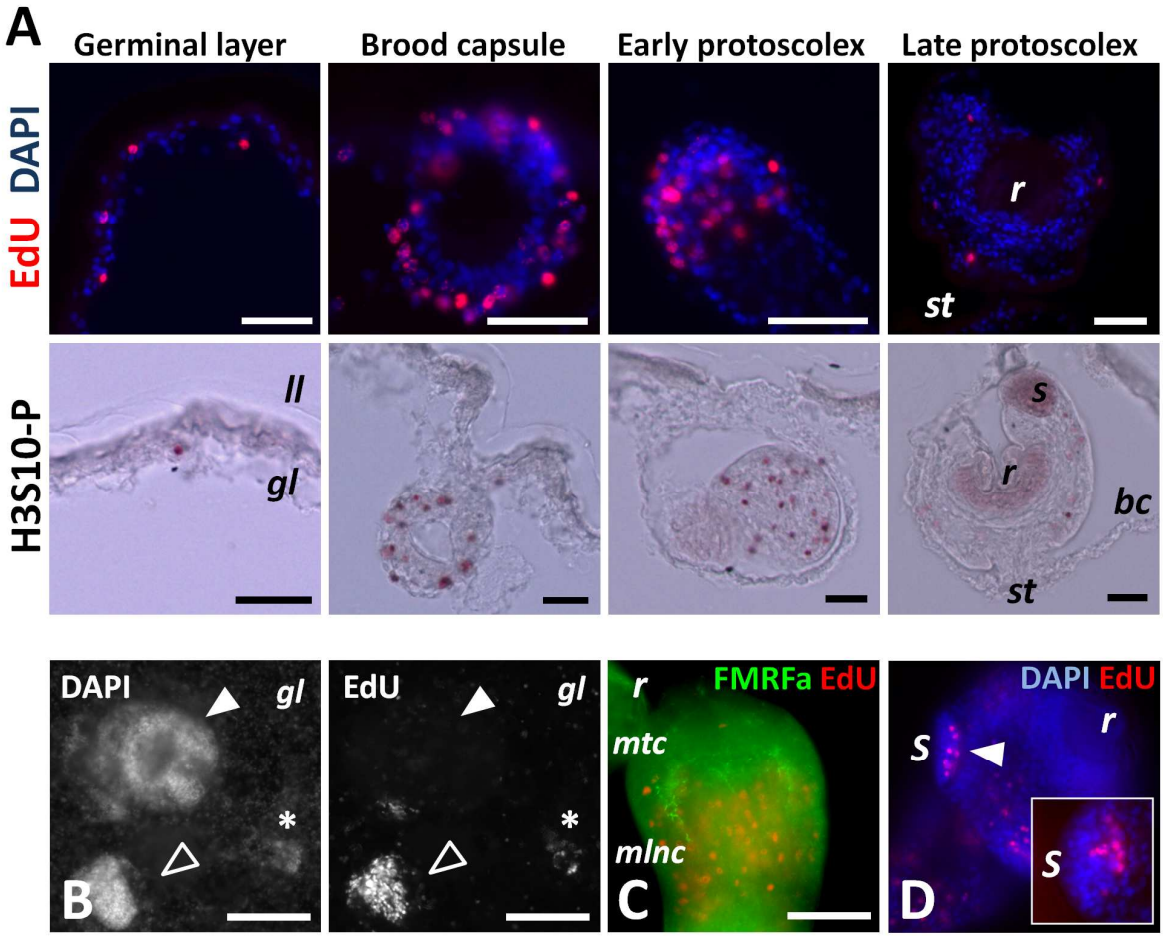

Figure 2. Cell proliferation in *E. multilocularis* metacestodes. A. Detection of EdU incorporation and of H3S10-P in paraplast sections of different stages of development (some unspecific staining is seen in suckers and rostellum of protoscoleces for H3S10-P staining). B. Whole-mount detection of EdU incorporation in a larval vesicle. The asterisk indicates an early brood capsule bud, the open arrowhead a brood capsule with a protoscolex bud, and the filled arrowhead an invaginated protoscolex. Notice also the dispersed EdU+ cells in the germinal layer. C. Whole-mount EdU detection (red) and FMRFamide immunofluorescence (green) during early protoscolex development. Most EdU+ cells are located behind the main transverse commissure. D. Whole-mount detection of EdU incorporation (red) during late protoscolex development. The arrowhead indicates the accumulation of EdU+ cells at the base of the sucker. The inset shows EdU+ cells in the base of a developing sucker as seen in a paraplast section. Abbreviations: bc, brood capsule; gl, germinal layer; ll, laminated layer; mlnc, main lateral nerve cord; mtc, main transverse commissure; r, rostellum or developing rostellum; s, sucker; st, stalk. Bars represent 30 µm except for B, 100 µm.

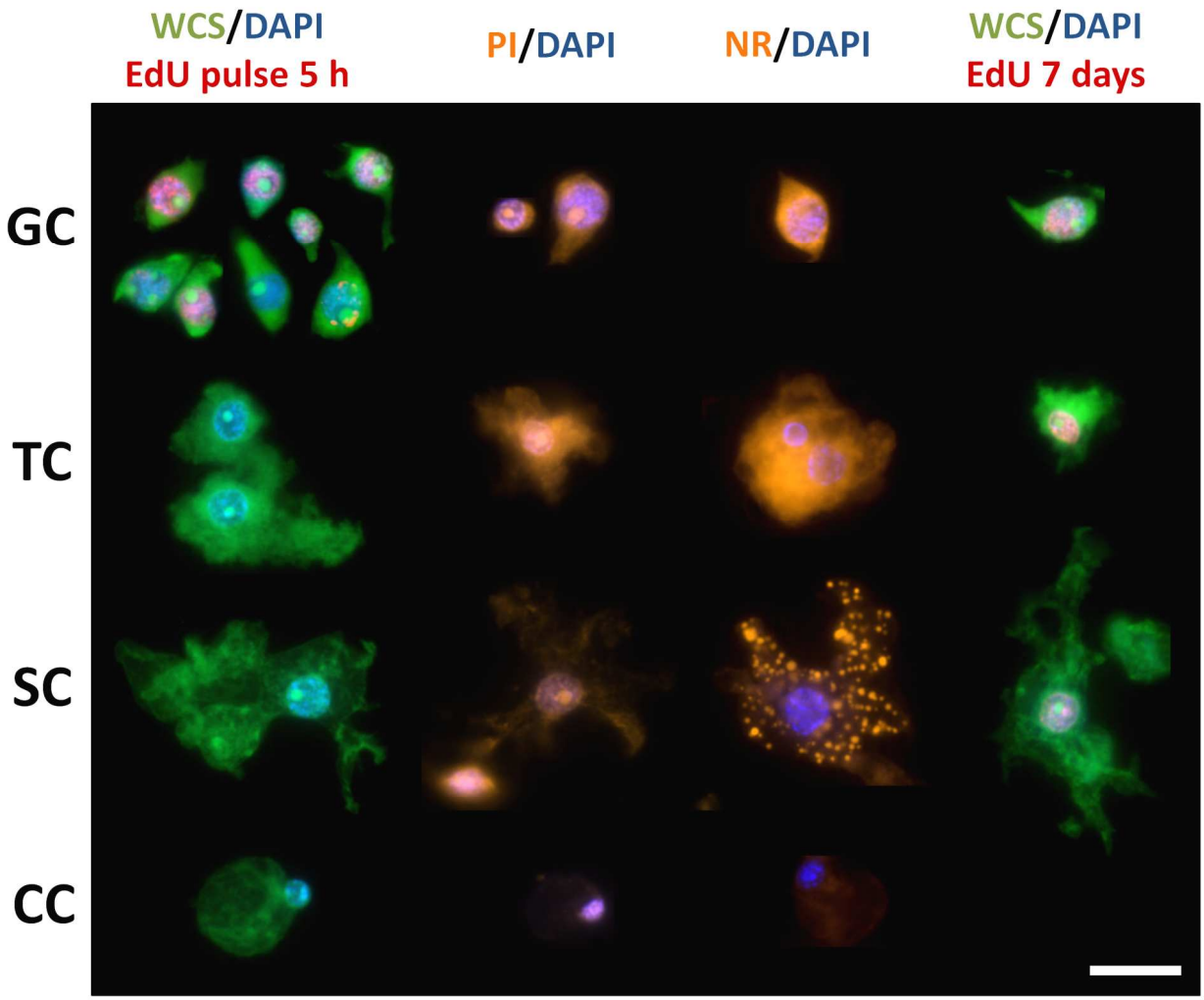

Figure 3. Cell suspensions of *Echinococcus multilocularis*. This is a montage of images of different cell types as observed in cell suspensions after different staining procedures. Cell types are indicated on the left (GC: germinative cells; TC, tegumental cells; SC, glycogen/lipid storage cells; CC, calcareous corpuscle cells) and staining procedures are indicated on top (NR, Nile Red, shown in orange; PI, propidium iodide, shown in orange; WCS, whole cell staining, shown in green), including the detection of EdU (shown in red) after two different labeling treatments, 50 µM for 5 hours and 1-10 µM for 7 days (see the main text for details). The bar represents 10 µm.

5. Results

Gene expression patterns in the germinative cells

To identify genes that are specifically expressed in the germinative cells, we analyzed the expression of several candidate genes among planarian neoblast markers by whole-mount *in situ* hybridization (WMISH).

em-h2b. As a possible general marker of all proliferating germinative cells, we analyzed the expression of histone H2B homologs, since canonical histones are synthesized in a cell-cycle dependent manner: histone transcripts only accumulate during the S-phase, when new histones are needed to accompany the synthesis of DNA (Jaeger et al. 2005). Furthermore, H2B genes have been found to be specifically expressed in proliferating planarian neoblasts and in the neoblast-like cells of the trematode *Schistosoma mansoni* (Solana et al. 2012; Collins et al. 2013).

Several canonical H2B genes are present in the *E. multilocularis* genome. Most of them are almost identical to each other (>95% nucleotide identity), which we denominate the *em-h2b-1* group. Another gene, *em-h2b-2*, also shows high amino acid identity (97%) but lower nucleotide identity (85%) to *em-h2b-1*. Using probes for *em-h2b-1* and *em-h2b-2* gave identical results, which were indistinguishable from the EdU labeling pattern in the germinal layer and throughout the development of brood capsules and protoscoleces (Figure 4). This is particularly striking during late protoscolex development, where a massive accumulation of *em-h2b*+ cells is found at the base of the suckers but no expression is seen in the remaining sucker tissue (Figure 4E).

The WMISH signal labeled the cytoplasm of cells with the typical germinative cell morphology (Figure 4B). Furthermore, when combining WMISH with EdU detection after a 5 hour pulse, 78% of all *em-h2b*+ cells were also EdU+ (n=197 *h2b*+ cells), and conversely, 87% of all EdU+ cells were also *em-h2b*+(n=176 EdU+ cells) (Figure 4F). Because only germinative cells proliferate (see above), *em-h2b* is therefore a *bona fide* marker of S-phase germinative cells, but would not detect resting or G1 and G2/M germinative cells. The smaller proportion of EdU- *h2b*+ cells had probably already entered S-phase but were fixed before enough EdU was incorporated for detection, while the EdU+ *h2b*- cells were probably fixed after they had already incorporated EdU but exited the S-phase during the incubation time.

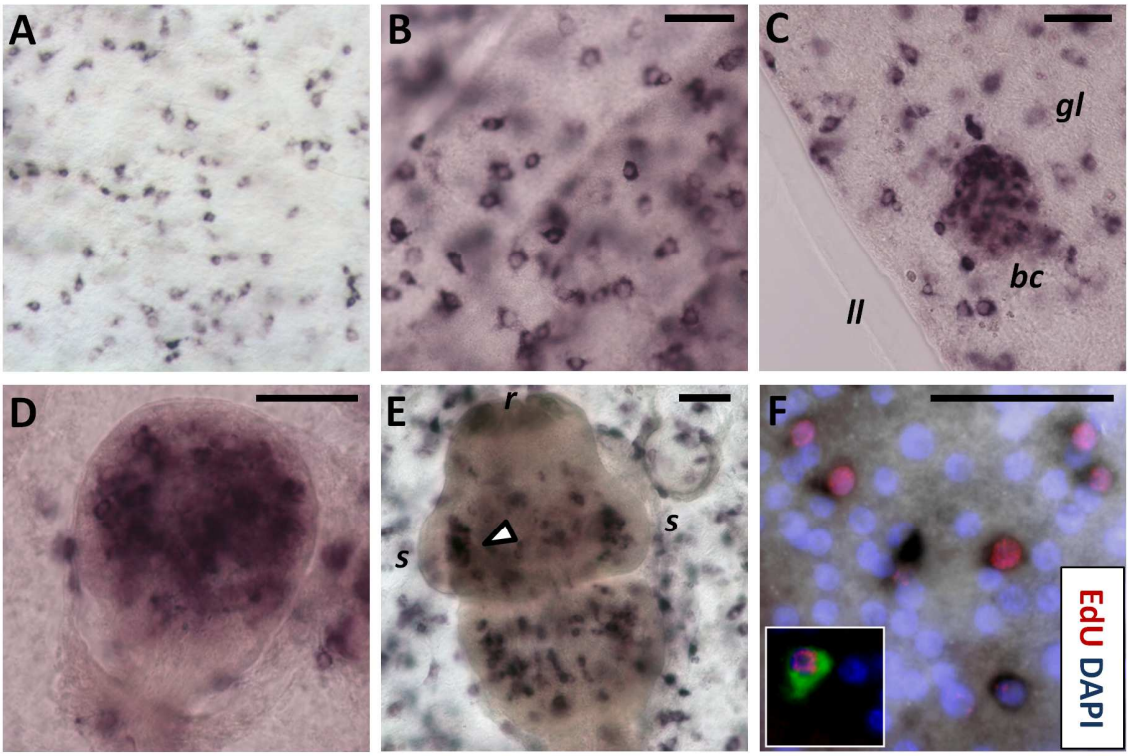

Figure 4. WMISH detection of *em-h2b*. A. General view of the germinal layer. B. Detail of the germinal layer; showing the germinative cell morphology of the positive cells. C. Early brood capsule bud. D. Protoscolex bud. E. Late protoscolex development. The arrowhead indicates the accumulation of positive cells at the base of the sucker. F. Co-localization of *em-h2b* (dark precipitate) and EdU detection (red) after a 50 µM, 5 h pulse. The inset shows an example in which the *em-h2b* signal was inverted and pseudo-coloured in green to facilitate the visualization of the co-labeling. Abbreviations are as in Figure 2. Bars represent 25 µm.

***em-nos-1* and *em-nos-2*.** We then turned to possible post-transcriptional regulators of the germinative cells. *nanos* genes are molecular markers of the germ line in many classical models, but are also expressed in multipotent stem cells in various basal metazoan lineages (Mochizuki et al. 2000; Rebscher et al. 2007; Ewen-Campen, Schwager, and Extavour 2010; Juliano, Swartz, and Wessel 2010). Two *nanos* genes are present in *E. multilocularis* (*em-nos-1* and *em-nos-2*). Both genes were expressed in few cells with a patchy distribution in the germinal layer (Figures 5A and D), and with the morphology of large germinative cells (<1.6% of all cells for both *em-nos-1* and *em-nos-2*, n=4632 cells and n=7475 cells, respectively; Figures 5B and E). Furthermore, *em-nos-1* and *em-nos-2* cells can incorporate EdU (19% of *em-nos1*+ cells are EdU+ after a 5 hour pulse, n=96), although the vast majority of EdU+ cells do not express either gene (<5% of all EdU+ cells express either *nanos* gene, Figures 5C and F). Altogether, these data show that a small subpopulation of the germinative cells in the germinal layer express *em-nos-1* and *em-nos-2*, although it is not clear if both genes are co-expressed in the same cells.

During brood capsule and protoscolex development, *em-nos1* expression was not detected. Expression of *em-nos2* was sometimes seen around brood capsule buds, and later during early protoscolex development as a small population of cells at the base of the protoscolex bud (Figures 5G and H). Finally, *em-nos-2* is expressed in a few cells associated with the developing nervous system, in the region of the developing lateral ganglia and the main commissure (Figure 5I). These results show that most proliferating cells do not express *nanos* genes in the developing protoscolex, and suggest a role for *em-nos-2* during nervous system development.

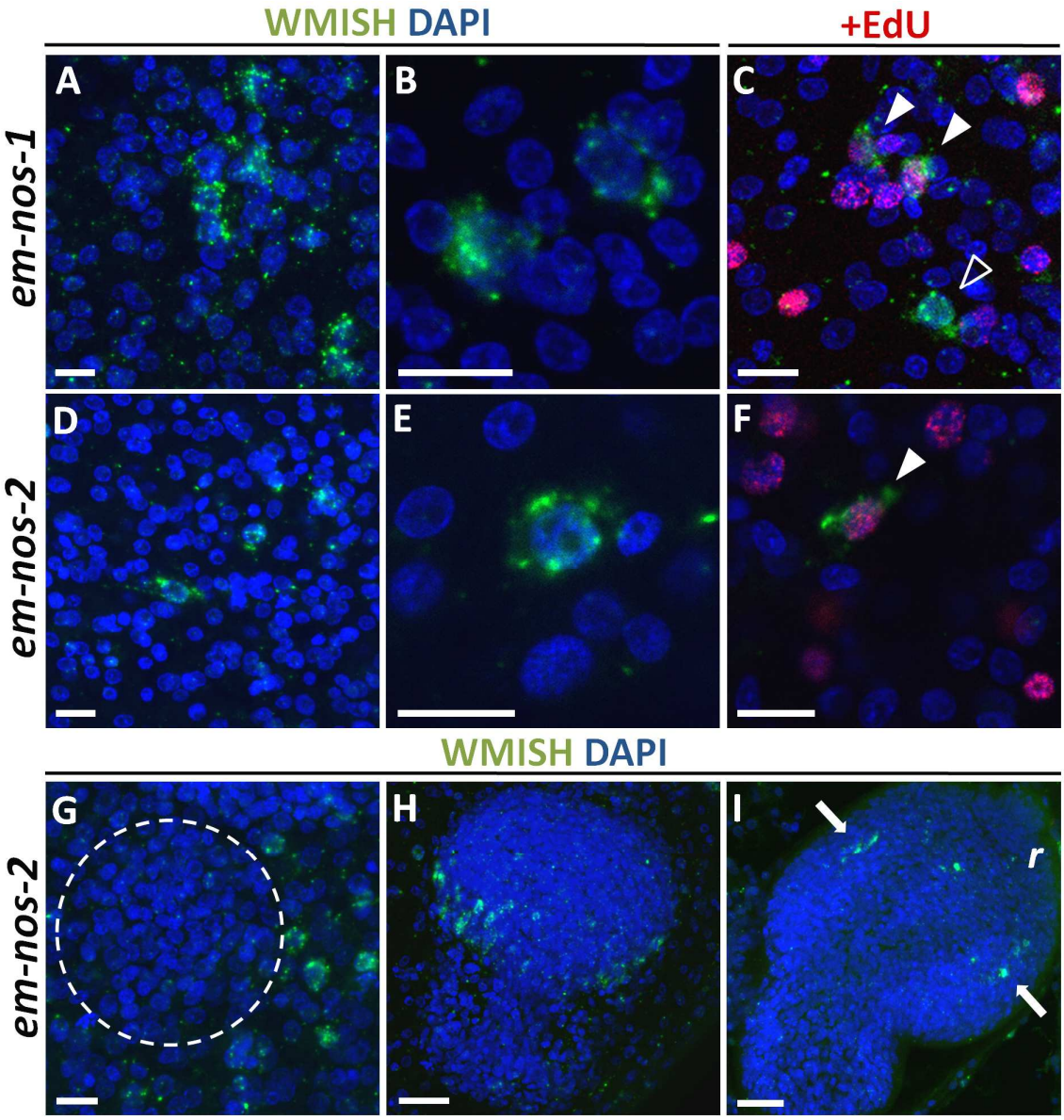

Figure 5. WMISH detection of *em-nos-1* (A-C) and *em-nos-2* (D-I). A and D, general view and B and E, detail of the positive cells in the germinal layer. C and F, co-localization in the germinal layer of *em-nos-1* and *em-nos-2* (green) with EdU incorporation (red) after a 5 h 50 µM pulse. Double positive cells are indicated with a filled arrowhead, whereas cells expressing a *nanos* gene but EdU- are indicated with an open arrowhead. G. Expression of *em-nos-2* in cells surrounding a brood capsule bud (dashed circle). H. Protoscolex bud. I. Later protoscolex development. Arrows indicate *em-nos-2*+ cells in the position of the developing lateral ganglia. Abbreviations are as in Figure 2. Bars represent 10 µm except for H, 20 µm.

em-ago2. Although *piwi* genes are not present in *E. multilocularis*, there are other argonaute proteins encoded by the genome: an ortholog of human Ago-1-4 proteins which is likely involved in RNA interference (EmAgo1 (Spiliotis et al. 2010)) and three copies of an argonaute gene family that is specific for cestodes and trematodes (Tsai et al. 2013), which we dubbed *em-ago2-A* to *em-ago2-C*. We further identified a pseudogene, *em-ago2-Ψ* (Additional File 6). These copies have resulted from a recent duplication that occurred after the divergence of *Hymenolepis* and [*Echinococcus* + *Taenia*] (see the phylogenetic analyses in Tsai et al. (2013)), with 88 to 99% nucleotide sequence identity between copies (depending of the copies and the specific regions compared). Moreover, they are organized as two couples of tandemly arranged copies in close proximity to a copy of a Sec61 homolog (Additional File 6). This conservation of synteny suggests that one first duplication occurred which resulted in two adjacent copies of an original *em-ago2* gene located next to a Sec61 gene, followed by the duplication of the whole region. Long-range PCR with genomic DNA confirmed the organization of these genomic regions (Additional File 6), while sequencing of smaller PCR fragments confirmed the existence of all four copies, demonstrating that they are not an artifact of genome assembly. By RT-PCR only *em-ago2-A*, *em-ago2-B* and *em-ago2-Ψ* mRNA could be detected, whereas *ago-2-C* was absent or barely detected in all of the larval stages and in primary cell cultures.

We performed WMISH using two different probes for *em-ago2-A*. These probes would probably cross-react with all other *em-ago2* copies, and we refer to the expression pattern of all these genes by the collective name *em-ago2*. *em-ago2* expression was similar to the pattern of EdU incorporation in the germinal layer, and cells strongly expressing *em-ago2* accumulate in the brood capsules and protoscolex buds (Figures 6A to 6C). The distribution of the *em-ago2* signal within cells is very distinct since it is only observed close to or within the nucleus (Figure 6A). Strongly positive *em-ago2*+ cells account for approximately 30% of all cells in the germinal layer, but notably, some expression of *em-ago2* was observed in more than 50% of all cells, indicating that it is not exclusive of the germinative cell population.

There is no clear-cut correlation between the level of *em-ago2* expression and proliferation, since approximately 50% of EdU+ cells show low or no expression of *em-ago2* (Figure 6A). Conversely, during early protoscolex development, it is clear that

although *em-ago2* expression is present in most cells, the cells with the strongest *em-ago2* signal are almost invariably EdU- (Figure 6C). During late protoscolex development, some *em-ago2* signal is observed in most cells (Figures 6D and E), and is not restricted to the base in the suckers (where cell proliferation occurs). It is therefore clear that the expression of *em-ago2* is not restricted to proliferating cells. Moreover, the expression of *em-nos-1*, *em-nos-2* and *em-ago2* point to extensive heterogeneity at the molecular level among the proliferating germinative cells.

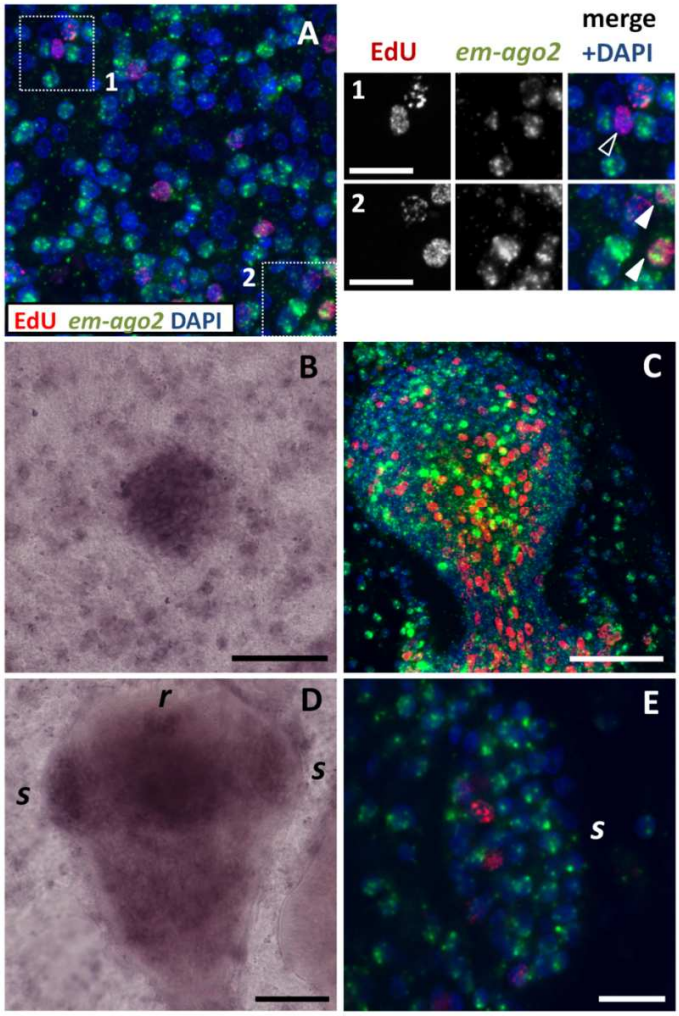

Figure 6. WMISH detection of *em-ago2*. A. General view of the germinal layer. The insets show details of EdU+ *em-ago2*- cells (open arrowheads) and EdU+ *em-ago2*+ cells (filled arrowheads) after a 5 h, 50 µM EdU pulse. B. Early brood capsule bud. C. Protoscolex bud; colors are coded as in Figure 5A. D. Late protoscolex development. E. Detail of a sucker from a protoscolex in late development, showing that *em-ago2* expression is not restricted to the base; colors are coded as in Figure 5A. Abbreviations are as in Figure 2. Bars represent 10 µm in A1 and A2, and 40 µm in all other panels.

em-hdac1* and *em-phb1. The histone deacetylase HDAC1 is one of many chromatin modifying proteins that are specifically expressed in planarian neoblasts (Eisenhoffer, Kang, and Sanchez Alvarado 2008; Zhu and Pearson 2013). Neoblast specific expression has also been shown for the mRNA of homologs of prohibitin-1 and prohibitin-2 (Rossi et al. 2007; Eisenhoffer, Kang, and Sanchez Alvarado 2008). In mammalian cells, prohibitins form complexes in the inner mitochondrial membrane with unclear biochemical function, and have been linked to mitochondrial biogenesis and cell proliferation (Merkwirth and Langer 2009).

We found single-copy orthologs of HDAC1 (*em-hdac1*) and prohibitin-1 (*em-phb1*) in the *E. multilocularis* genome, and both genes showed widespread expression in the germinal layer and during protoscolex development (Additional Files 7 and 8). We also determined the distribution of the Em-PHB1 protein by immunohistochemistry, and compared this to the distribution in planarian tissues, using a commercial antibody that recognizes a conserved region in all PHB1 proteins. In planarians, although low levels of PHB1 are seen in post-mitotic tissues such as the pharynx, the highest signal is observed in neoblast-like cells in the mesenchyma (Additional File 9). In contrast, *E. multilocularis* Em-PHB1 is observed throughout the germinal layer, brood capsules and developing protoscoleces (Additional File 10). In summary, neither gene has a germinative cell specific expression in *E. multilocularis* metacestodes.

Identification of molecular markers for differentiated cell types.

The identification of differentiated cell types in the germinal layer is difficult, and unlike the situation in adult cestodes, trematodes and planarians, the lack of spatial segregation of any post-mitotic cell types makes it impossible to trace the differentiation of germinative cells *in situ.* Therefore, we set out to find molecular markers of differentiated cell types in *Echinococcus*.

***em-muc-1* and *em-alp-2* as tegumental cell markers**. Since the laminated layer is synthesized by the tegumental syncitium, genes coding for laminated layer components should be expressed by the tegumental cells (Diaz et al. 2011). We analyzed the expression of *em-muc-1*, a member of an *Echinococcus*-specific, highly expressed apomucin gene family that has been proposed to be a main component of the laminated layer (Diaz et al. 2011; Parkinson et al. 2012; Tsai et al. 2013). Because all

members are very similar (with regions with over 90% identity at the nucleotide level) it is likely that the *em-muc-1* probe recognizes most genes of this gene family.

em-muc-1 is strongly expressed in the germinal layer but not in protoscoleces, as is expected for a component of the laminated layer (Figure 7A). *em-muc-1* was expressed in cells with abundant cytoplasm that fuse or interdigitate with each other, and which constitute 27 to 37% of all cells in the germinal layer (two independent WMISH experiments; n=3440 and 780 cells, respectively; Figure 7B). In stark contrast, no expression is observed in early brood capsule buds or in developing protoscoleces. To our surprise, however, we could detect low levels of *em-muc-1* in late brood capsules, which suggests that the glycocalix of the brood capsule may also contain the product of *em-muc-1*, although the laminated layer does not line the brood capsule cavity (Diaz et al. 2011) (Figure 7D). By combining WMISH with EdU detection, we observed the absence of EdU+ cells among the *em-muc-1*+ cell population (n=1454 *em-muc-1*+ cells from two independent WMISH experiments; Figure 7C). We conclude that *em-muc-1* is a robust marker for tegumental cells in the germinal layer, and confirm that the tegumental cell population does not proliferate.

While searching for possible histochemical markers, we observed that alkaline phosphatase activity in the metacestode is very high (strong reaction in less than 5 minutes) and restricted to the distal syncitial tegument of the germinal layer (Figure 8A; see also (del Cacho et al. 1996)), but is not found in brood capsules (Additional File 11). This indicated that one or more alkaline phosphatase genes must be expressed in the tegumental cells. In protoscoleces, alkaline phosphatase was detected only after several hours, and only in the excretory system (Figure 8 B), similarly to what has been described in the developing adult (Arsac et al. 1997). This activity increased after protoscolex activation (Additional File 11). Four genes encoding alkaline phosphatases (*em-alp-1* to *em-alp-4*) were found in the *E. multilocularis* genome. By RT-PCR, *em-alp-1* and *em-alp-2* were found to be specifically expressed in the germinal layer, while *em-alp-3* was only detected in protoscoleces, with a strong up-regulation after protoscolex activation (Figure 8C). *em-alp-4* has substitutions of conserved catalytic amino acid residues, and no expression was detected by RT-PCR in the germinal layer or in protoscoleces, suggesting that it is a pseudogene, although expression was observed in high throughput RNA sequencing data of adult worms (Tsai et al. 2013).

Altogether, the data suggested that *em-alp-1* and *em-alp-2* were expressed in the tegumental cells of the germinal layer, while *em-alp-3* was expressed in the protoscolex excretory system, and is to the best of our knowledge the first gene shown to be up-regulated after protoscolex activation. We therefore analyzed the expression pattern of *em-alp-2* by WMISH, and found it to be identical to that of *em-muc-1* in the germinal layer, with no expression in the brood capsule buds or in the developing protoscoleces (Figure 8D). In conclusion, *em-alp-2* is another marker for the tegumental cells in the germinal layer.

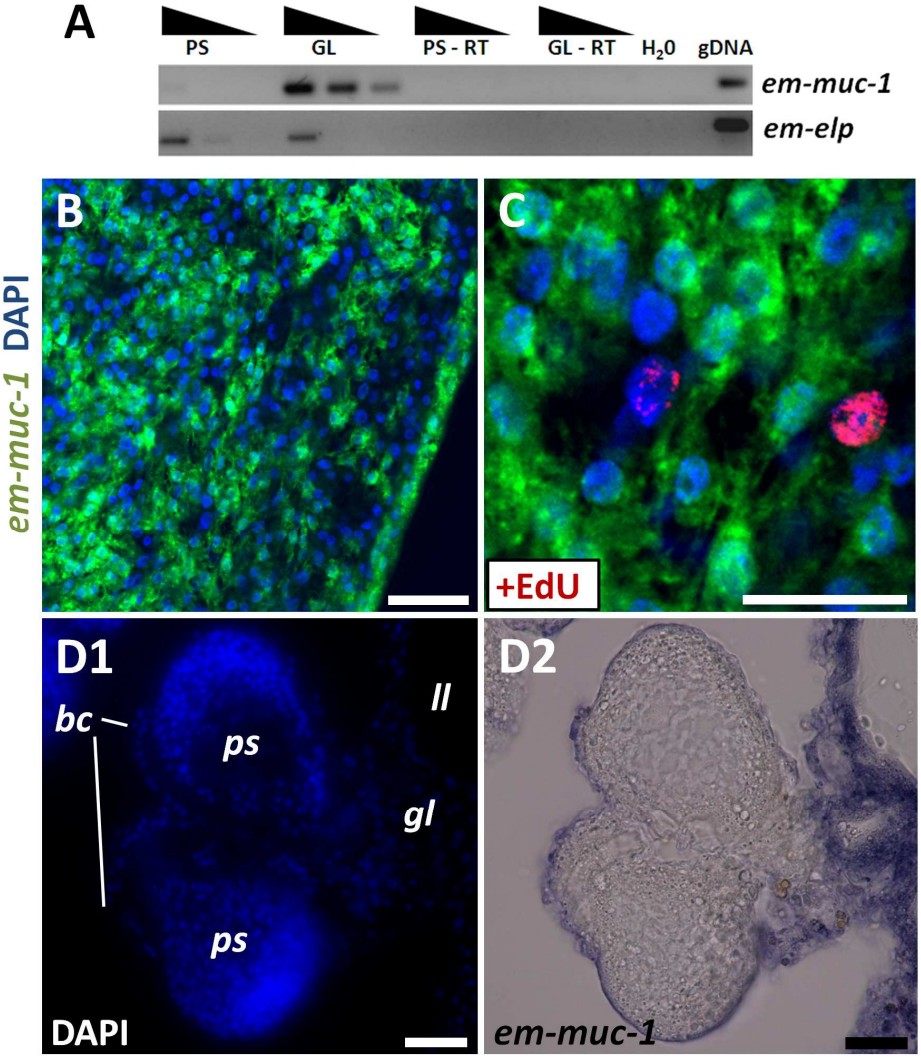

Figure 7. Expression of *em-muc-1*. A. Semi-quantitative RT-PCR with serial ten-fold dilutions of cDNA from protoscoleces (PS) and germinal layer (GL). Controls without reverse transcriptase (-RT) and without template (H_20) are included. B-D. WMISH of *em-muc-1*. B. General view of the germinal layer. C. Double detection of WMISH (green) and EdU incorporation after a 5 h, 50 µM EdU pulse (red); note the lack of EdU labeling among the *em-muc-1*+ cells. D1 and D2.Section of metacestode processed for WMISH, showing the lack of expression in the developing protoscoleces, strong expression in the germinal layer, and expression in the brood capsule wall. Abbreviations are as in Figure 2. Bars represent 20 µm except for B, 10 µm.

5. Results

Acetylated tubulin α as a marker of nerve cells. We have recently shown that a net of nerve cells in the germinal layer can be detected by immunohistofluorescence against acetylated tubulin α (AcTub+ cells, (Koziol, Krohne, and Brehm 2013)). Here, we show that the nerve cells do not proliferate, since they are EdU- after a 5 hour, 50 μM EdU pulse (n = 874 AcTub+ cells from three independent experiments; Additional File 12). Similarly, in activated protoscoleces all AcTub+ cells (including in this case both nerve cells and flame cells (Koziol, Krohne, and Brehm 2013)) were EdU- (data not shown).

We performed a quantitative analysis of the formation of new AcTub+ cells by determining the percentage of EdU+ AcTub+ cells during continuous EdU labeling. No double labeled cells were observed after 7 days, but the percentage increased to 13.3% after 14 days (Additional File 12). Because no EdU incorporation was observed in nerve cells even after 7 days of continuous exposure, this strongly indicates that all EdU+ nerve cells must originate from the differentiation of proliferating germinative cells, which would require more than 7 days after exiting the cell cycle to become AcTub+. Higher concentrations of EdU (10 μM) apparently had a toxic effect, and only 2.8% of the AcTub+ cells were EdU+ after 14 days (Additional File 12).

***em-tpm-1.hmw* as a marker for muscle cells during protoscolex development**. Using a specific antibody that recognizes the high molecular weight (HMW) isoforms of two tropomyosin genes from cestodes (*tpm-1* and *tpm-2*), HMW tropomyosins have been shown to be present exclusively in the muscle fibers in the cestode *Mesocestoides corti*, and are strongly expressed in the suckers of *E. granulosus* protoscoleces (Alvite and Esteves 2009; Koziol et al. 2011). Using this antibody, we confirmed that HMW tropomyosin isoforms can be found in the muscle fibers in the germinal layer, accumulating in the interior of brood capsules, and in the muscle layers during protoscolex development in *E. multilocularis* (Additional File 13), in perfect correlation to the description of muscle fibers as determined by phalloidin labeling (Koziol, Krohne, and Brehm 2013).

Because in cestodes the nucleus of muscle cells is located in a non-contractile cell body, connected by thin cytoplasmic bridges to the contractile myofibers (Halton and Maule 2003; Smyth and McManus 2007), it is not possible to identify the cell

bodies by immunodetection of HMW-Tropomyosins. Instead, we analyzed the expression of the HMW isoform of *em-tpm-1* by WMISH using a specific probe. Surprisingly, no expression was observed in the germinal layer, suggesting that muscle cells in this tissue express other tropomyosin isoforms (i.e. from *em-tpm-2*). Instead, *em-tpm-1.hmw* was detected in individual cells in the center of invaginating brood capsules (Figure 9A), in close proximity to the location of muscle fibers (Koziol, Krohne, and Brehm 2013). During early protoscolex development, when muscle development is already underway (Koziol, Krohne, and Brehm 2013), *em-tpm-1.hmw* is expressed in two symmetrical bands of superficial cells and one internal medial band (Figure 9B). Because of their distribution, these are likely to be the subtegumental circular muscle cells and the inner longitudinal muscle cells. Finally, strong expression was observed in the muscular suckers and rostellum and in individual cells in the body of the developed protoscolex (Figure 9C). In summary, *em-tpm-1.hmw* can be used as a molecular marker for the development of muscle cells during brood capsule and protoscolex development, but not in the germinal layer.

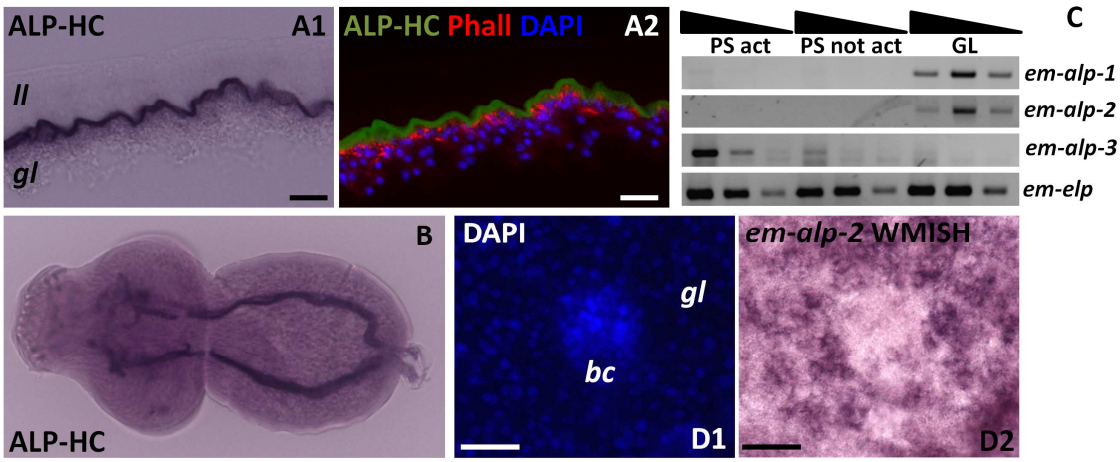

Figure 8. Alkaline phosphatase activity and gene expression. A1. Alkaline phosphatase histochemistry in the germinal layer, showing strong activity in the syncitial tegument. A2. The signal in A1 was inverted and pseudo-colored in green, and combined with DAPI (blue) and phalloidin (red) staining to show the distribution of the nuclei and muscle fibers, respectively. B. Alkaline phosphatase histochemistry in an activated protoscolex, showing activity in the excretory system. C. Semi-quantitative RT-PCR with serial ten-fold dilutions of cDNA from activated protoscoleces (PS act), non-activated protoscoleces (PS not act) and germinal layer (GL). The experiment was repeated three times with similar results. D. WMISH of *em-alp-2,* showing strong expression in the germinal layer but not in the brood capsule bud. Abbreviations are as in Figure 2. Bars represent 20 μm.

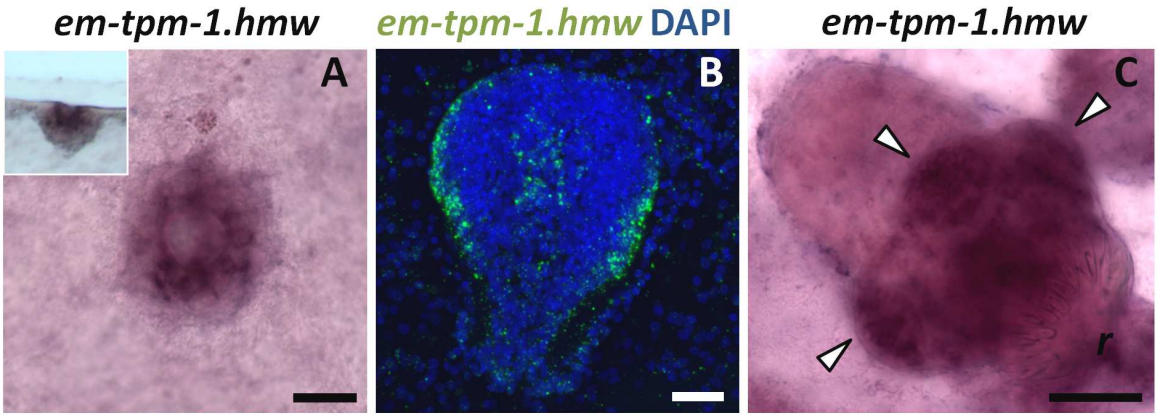

Figure 9. WMISH detection of *em-tpm-1.hmw*. A. Early brood capsule bud as seen from above. The inset shows a lateral view. B. Protoscolex bud. C. Developed protoscolex. The arrowheads point to the suckers. Abbreviations are as in Figure 2. Bars represent 20 μm (A, B) or 40 μm (C).

5. Results

Partial depletion of germinative cells by irradiation and hydroxyurea treatments

Total and partial elimination of neoblasts by irradiation has been a powerful tool for studying neoblast gene expression and physiology in many flatworms (Pfister et al. 2007; Rossi et al. 2007; Eisenhoffer, Kang, and Sanchez Alvarado 2008; Pfister et al. 2008; Wagner, Wang, and Reddien 2011; Wagner, Ho, and Reddien 2012; Collins et al. 2013). In *E. multilocularis*, comparable doses of ionizing radiation (50-100 Gy) were found to only retard growth of metacestodes, and did not eliminate the germinative cells (Pohle et al. 2011). We performed similar experiments with a single X-ray irradiation dose of 150 Gy on metacestode vesicles (lacking brood capsules and protoscoleces). At 48 hours post-irradiation, we observed that the number of cells incorporating EdU per area of germinal layer decreased in average to 22% of unirradiated controls, showing that very high dosages of X-ray irradiation decrease but are unable to eliminate all proliferating cells (Figure 10A). Interestingly, we observed no significant increase in the number of EdU incorporating cells for up to 48 days post-irradiation, and the number of EdU+ cells per area was still in average only 28% that of unirradiated controls (Figure 10A). Despite this long-term decrease in cell proliferation, no difference in survival was observed between irradiated and unirradiated metacestodes after 48 days (82% versus 86%, p=0.49, Chi-Square test).

As an alternative approach, we used hydroxyurea (HU), an inhibitor of ribonucleotide reductase (RRM) that is specifically toxic to cells undergoing DNA synthesis during cell proliferation (Sinclair 1965; Krakoff, Brown, and Reichard 1968; Farber and Baserga 1969), and which has also been used in other invertebrates to eliminate stem cells (Salo and Baguna 1984; Pfister et al. 2007; De Mulder et al. 2009a). The mechanism of toxicity is based on the depletion of dNTPs that results from RRM inhibition, provoking the cessation of DNA replication, thus leading to stalled replication forks and eventually to chromosomal DNA damage (Petermann et al. 2010). In order to confirm a similar effect of HU on *E. multilocularis* cells, we incubated primary cell cultures with different HU concentrations. Indeed, incorporation of the thymidine analog 5-bromo-2'-deoxyuridine (BrdU) was reduced by approximately 50% and 90% in the presence of 10 mM and 40 mM HU, respectively. Furthermore, the regeneration of metacestode vesicles from primary cells was strongly decreased by 10 mM HU and abolished by 40 mM HU (Additional File 14).

We therefore incubated metacestode vesicles (lacking brood capsules and protoscoleces) with 40 mM HU for 7 days, and allowed them to recover in HU free media for 24 hours. This resulted on average in a 90% reduction in the number of cells incorporating EdU per area of germinal layer (Figure 10B). Furthermore, the experimental results could be divided into two groups: Group 1, from experiments performed on larger and older vesicles, resulted in a decrease of only 66% to 93% in the number of EdU+ cells (similar to the results observed after X-ray irradiation), whereas Group 2, performed in smaller and younger vesicles, resulted in a stronger decrease of 97.7% to 99.8% of EdU+ cells with respect to the non-treated controls.

We analyzed in detail the effect of HU on the metacestode vesicles. Quantification of germinative cells in tissue macerates showed that the loss of EdU+ cells was paralleled by a decrease in germinative cells, from 20-22% to 3-5% of all cells (two independent experiments, $p \leq 0.001$ for both, Chi-Square test). However, differentiated cells did not seem to be affected by the HU treatment: nerve cell numbers per area of germinal layer were not significantly reduced, as determined by AcTub immunohistofluorescence (Figure 10C) and the tegumental cell marker *em-muc-1* showed a qualitatively similar expression pattern in both conditions (Figure 10D). We conclude that HU treatment for 7 days specifically depletes the germinative cell population, with little effect on the number of differentiated cells.

Prolonged times of recovery of vesicles from Group 1 in HU free media did not result in a significant increase of EdU+ cells after up to 22 days, similar to the results obtained after X-ray irradiation. However, in Group 2, we could observe highly localized, time-dependent increments in the number of EdU+ cells, strongly suggestive of clonal growth from surviving proliferating cells (Figure 11). In most experiments only isolated EdU+ cells could be found after 1 day of recovery. As recovery time increased, patches of 2 EdU+ cells (after 1 to 4 days of recovery), 3 to 4 EdU+ cells (after 4 to 9 days of recovery) and of more than 30 EdU+ cells (after 9 days of recovery) could be found in some of the metacestode vesicles. This strongly indicates the existence of cells in the metacestode (presumably germinative cells) that can respond to the strong depletion of proliferating cells by undergoing self-renewing divisions into proliferation-competent cells.

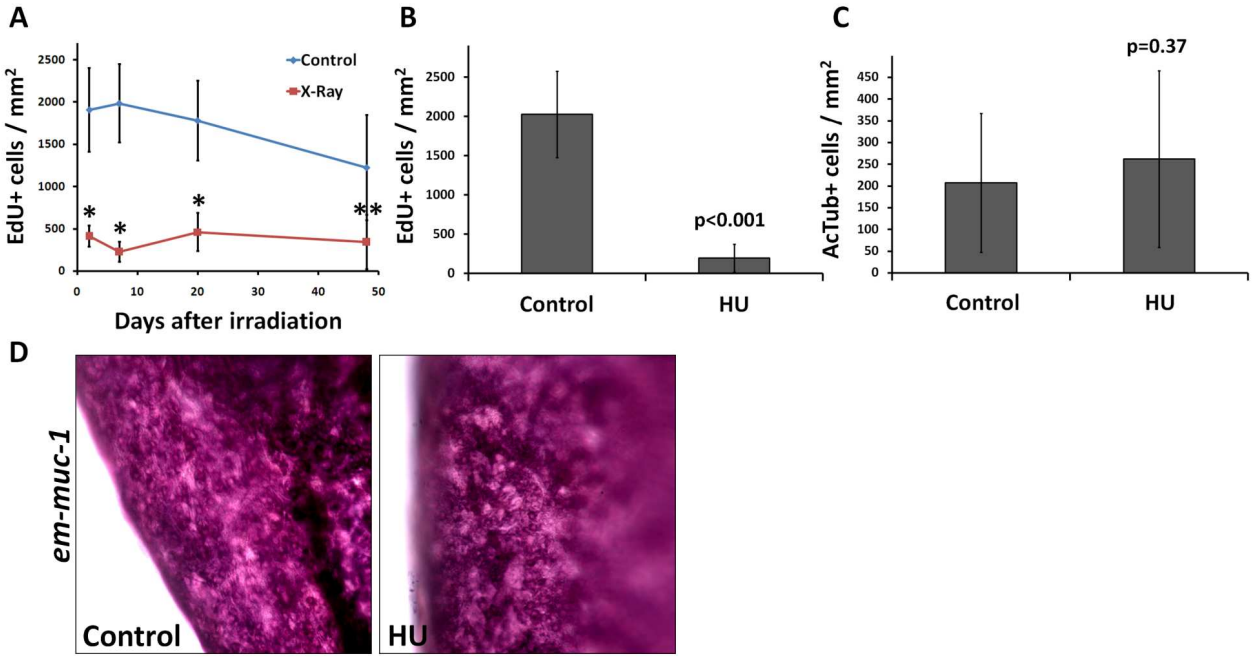

Figure 10. Effect of X-Ray irradiation and HU treatment. A. Number of EdU+ cells per area at different times after X-Ray irradiation (150 Gy) and in non-irradiated controls, after a 5 h 50 µm EdU pulse (average and standard deviations of 7 to 14 vesicles per time point). B. Number of EdU+ cells per area in vesicles treated with HU (40 mM for 7 days) and in non-treated controls (all vesicles were allowed to recover for 24 hours in HU free medium, followed by a 5 h 50 µm EdU pulse; average and standard deviation of 7 independent experiments). C. Number of AcTub+ cells per area in vesicles treated with HU (40 mM for 7 days) and in non-treated controls (average and standard deviation of 9 to 11 vesicles pooled from 3 independent experiments). D. WMISH of *em-muc-1* in a vesicle treated with HU (40 mM for 7 days) and in a non-treated control. * $p<0.001$,**$p<0.01$. The Mann-Whitney U-Test was used for A-C.

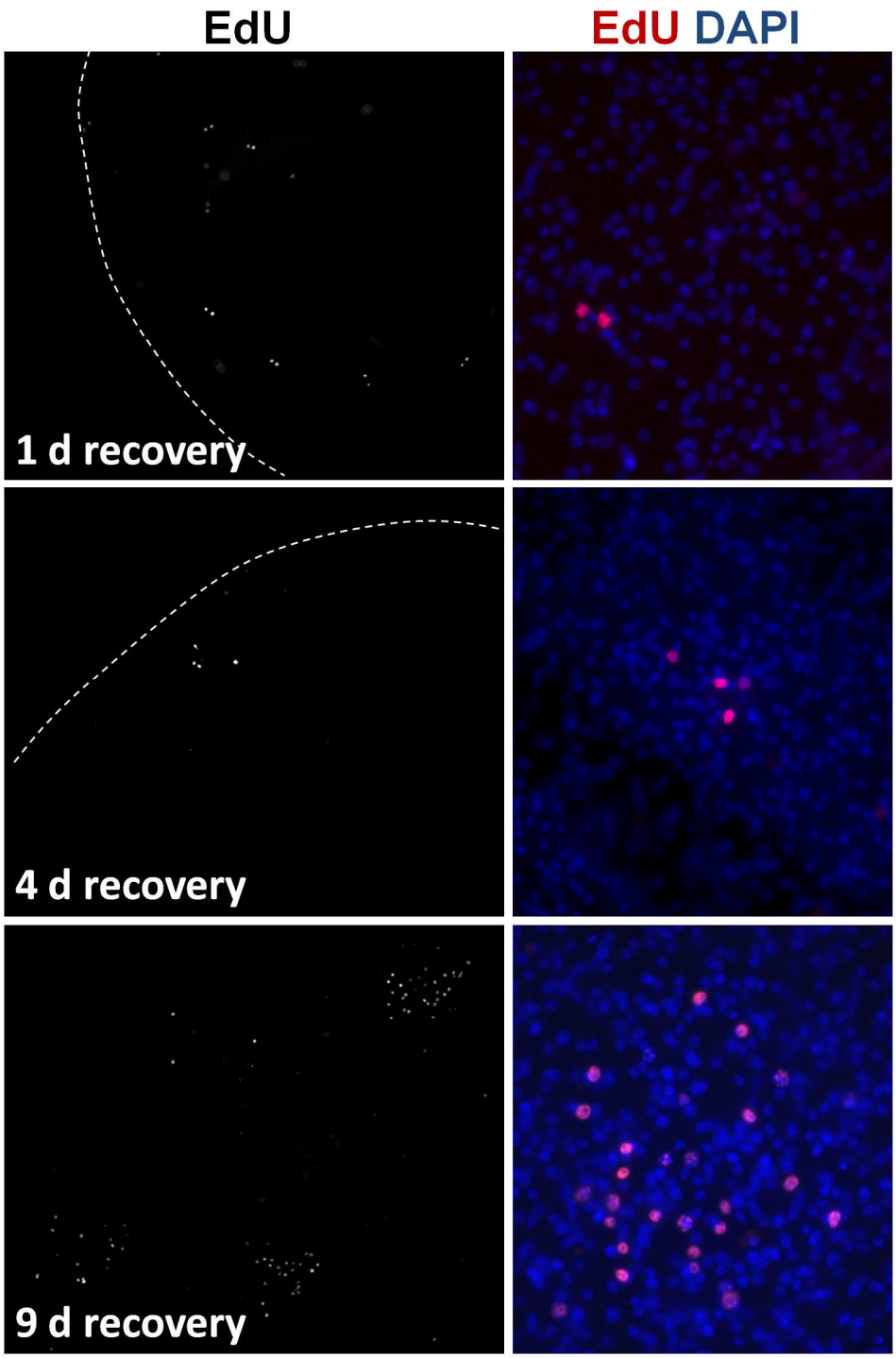

Figure 11. Growing patches of EdU+ cells during recovery from HU treatment. Vesicles were treated for 7 days with 40 mM HU, transferred to HU-free medium and samples were taken for EdU labeling (5 h with 50 µM EdU) and detection at the indicated times of recovery.

5. Results

Germinative cells proliferate and are enriched in primary cell preparations.

In the previously described primary cell regeneration system (Spiliotis et al. 2008), primary cells obtained from *E. multilocularis* metacestodes initially form small aggregates that grow and fuse to each other. Within these aggregates fluid-filled cavities are formed, and eventually new metacestode vesicles are generated by a still incompletely understood process. We analyzed cell proliferation within the early aggregates (after 2 days of culture) by EdU labeling. We observed extensive cell proliferation in a layer within the aggregates, but the innermost cells did not incorporate EdU, suggesting that they have exited the cell cycle, which may be related to the initial formation of internal cavities (typically observed after 4 days of culture) (Figure 12A). In order to morphologically identify the proliferating cells during regeneration, we prepared cell suspensions by the tissue maceration procedure, and based the identification of cell types on the previously described morphological criteria. As found in metacestodes, germinative cells were the only cell type labeled by EdU in primary cell preparations (Figures 12C and D). Furthermore, germinative cells were enriched in two day-old aggregates, comprising 62% to 83% of all cells, as compared to 32% to 55% in the metacestodes that were used to generate the primary cell preparations (3 independent primary cell preparations, $p<0.02$ for all preparations, Chi-square test; furthermore, note that the percentage of germinative cells is likely overestimated for the metacestodes since large vesicles were used). Among the differentiated cells, tegumental and glycogen/lipid storage cells were conspicuously few, and an increase in cells with degenerating morphology was noted. Further confirmation of the strong depletion of tegumental cells was obtained by analyzing the expression of the tegumental cell markers *em-muc-1*, *em-alp-2* and of *em-alp-1*. Preliminary high throughput RNA sequencing data indicated low expression levels for all three genes in primary cells (2%, 7% and 0% of the levels found in the germinal layer, respectively), that was confirmed by semi-quantitative RT-PCR for *em-alp-1 and em-alp-2* (Figure 12B).

To confirm the enrichment of germinative cells and to determine which other cell types are present in early primary cell aggregates, we performed transmission electron microscopical studies of two day-old primary cell aggregates. Abundant germinative cells could be found in the aggregates, surrounded by an external layer of

cells showing signs of degeneration (necrosis) (Figure 12E and Additional File 15). Also, many muscle fibers and some muscle cells could be identified (Figure 12F). In cryosections of primary cells after three days of culture, muscle fibers were also found by phalloidin staining, and nerve cells were identified by AcTub immunohistofluorescence (Additional File 16). In summary, early primary cell preparations are enriched in proliferating germinative cells, but other cell types such as muscle cells and nerve cells are also present.

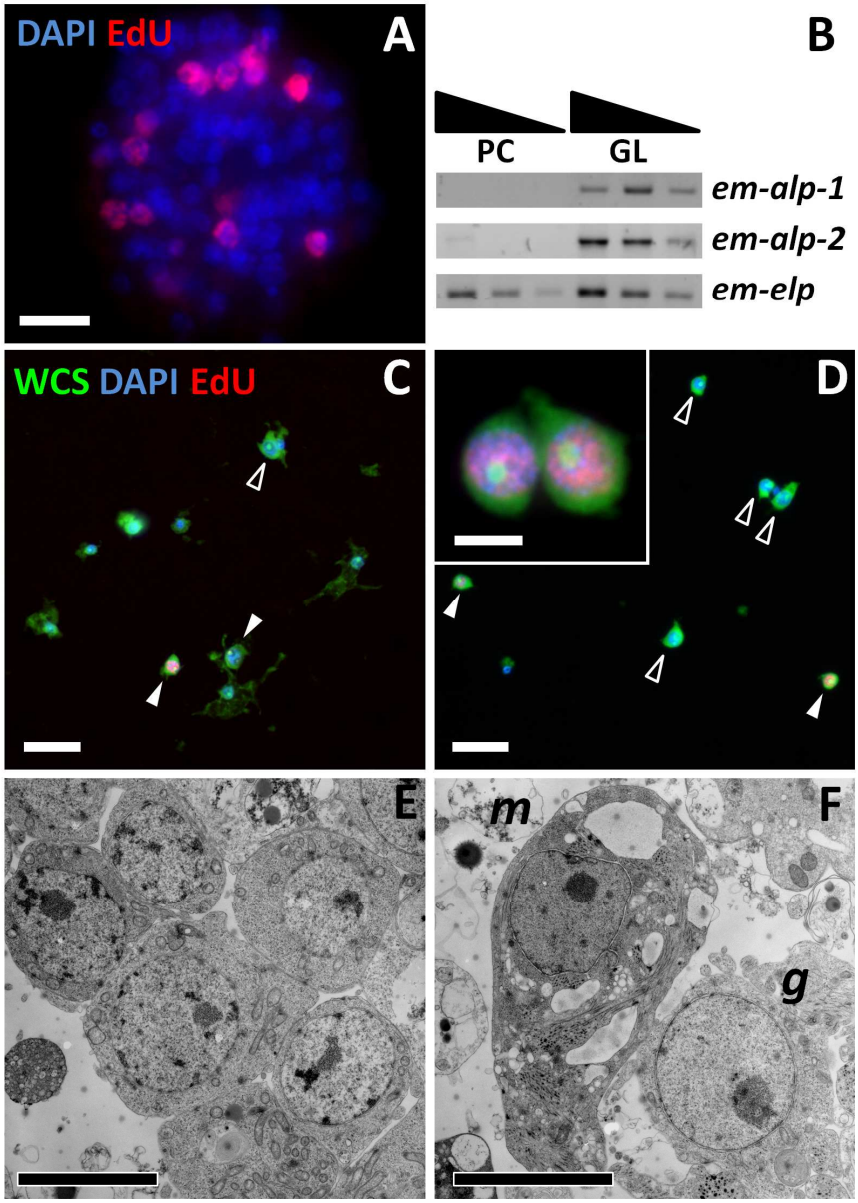

Figure 12. Characterization of early primary cell preparations. A. EdU incorporation after a 50 µM 5 h pulse of primary cell aggregates (2 days-old). B. Semi-quantitative RT-PCR of *em-alp-1* and *em-alp-2* genes with serial ten-fold dilutions of cDNA from primary cells (PC) and germinal layer (GL). The experiment was repeated three times with similar results. C and D. Representative microscopy fields of cell suspensions obtained from the germinal layer (C) and from primary cells (D). EdU+ and EdU- germinative cells are indicated by filled and open arrowheads, respectively. The inset in D shows a close-up of two EdU+ germinative cells in the primary cell preparations. E and F. TEM of primary cell aggregates (2 days-old). E. Accumulation of germinative cells. F. A muscle cell (m), containing myofibers and extensive smooth endoplasmic reticulum, and a germinative cell (g) in the periphery of an aggregate. Notice also cell debris surrounding the cells. Bars represent 4 µm (A, E, F and inset in D) and 20 µm (C and D).

Discussion

Germinative cells are the only proliferating cells in *Echinococcus multilocularis* larvae

The germinative cells in *E. multilocularis* constitute a morphologically homogeneous population, similar to descriptions in other cestode species and life stages (Douglas 1961; Bolla and Roberts 1971; Sulgostowska 1972; Gustafsson 1976b; Koziol et al. 2010), and generally similar to the neoblasts in free living flatworms and the neoblast-like cells of the trematode *Schistosoma mansoni* (Reuter and Kreshchenko 2004; Collins et al. 2013). The main differences observed within the germinative cells in *E. multilocularis* were related to the number of nucleoli, size, and the presence or absence of thin cytoplasmic projections. All of these differences could be related in part to normal changes during the cell cycle and cell migration (Wachtler and Stahl 1993; Alberts 2000), although other authors have sub-divided the germinative cells into different types based on size and histological details (Douglas 1961; Sulgostowska 1972). Germinative cells were identified as the only proliferating cell type during metacestode growth and regeneration, indicating that all new cells must originate from this population. However, the existence of de-differentiation and trans-differentiation processes in differentiated cells cannot completely be ruled out at this point. Unambiguous lineage tracing will require analyses mediated by stable genetic markers, and current efforts in our laboratory are being made towards transgenic modification of *Echinococcus* germinative cells. Furthermore, the markers for differentiated cell types developed in this work will be an important tool for tracing the differentiation pathways of germinative cells.

Unfortunately, we have been unable to find a universal molecular marker for the germinative cells so far. However, H3S10-P and *em-h2B* are useful endogenous markers to identify the proliferating germinative cells in metacestode tissues, and open the possibility to identify such cells in *in vivo* material (in the absence of labeling with thymidine analogs). Despite the morphological uniformity of germinative cells, gene expression analyses have clearly shown that the germinative cells are heterogeneous at the molecular level: *em-ago-2*, *em-nos-1* and *em-nos-2* genes are only expressed in subpopulations of the proliferating germinative cells. Because argonaute and nanos

proteins are well known post-transcriptional regulators with important roles in stem cell and germ cell biology (Carmell et al. 2002; Ewen-Campen, Schwager, and Extavour 2010; Juliano, Swartz, and Wessel 2010), this points to the existence of different sub-populations of germinative cells, perhaps with different self-renewal or differentiation potencies.

The capacity for self renewal of at least some of the germinative cells is strongly suggested by the HU-mediated depletion experiments, and is expected given the ability of metacestode tissue to be indefinitely passaged *in vivo* (Norman and Kagan 1961; Spiliotis and Brehm 2009). It is interesting that no proliferation response was observed after milder depletions, and the metacestode vesicles were able to survive for long periods under these conditions. This suggests that the control of cell proliferation is relatively lax in *E. multilocularis* metacestodes. It is possible that a relatively low number of proliferating germinative cells are enough for basal tissue turnover, but that a larger number is required for actively growing vesicles. Similarly, large differences in the number of EdU incorporating cells can be observed in vesicles incubated *ex vivo* from a single infected rodent (Koziol and Brehm, unpublished data).

Could cells expressing *nanos* in *Echinococcus* metacestodes represent the germ line?

In many free living flatworms, it is traditionally thought that the germ line is segregated by epigenesis in the juveniles or adults (Extavour and Akam 2003). In fact, the limit between the somatic stem cells and the germ line is fluid in planarians and *Macrostomum*, since the somatic neoblasts are able to contribute to the germ line during regeneration (Sato et al. 2006; Handberg-Thorsager and Salo 2007; Pfister et al. 2008). However, recent studies using molecular markers have allowed the identification of germ cells already at the time of hatching, suggesting that in these flatworms the germ line may be segregated earlier than was previously thought (Handberg-Thorsager and Salo 2007; Pfister et al. 2008). For example *nanos*, another classical germ line marker, has been shown to be expressed only in the planarian germ line stem cells, but not in the morphologically indistinguishable somatic neoblasts (Sato et al. 2006; Handberg-Thorsager and Salo 2007; Wang et al. 2007).

In cestodes, it is assumed that the germ line is originated by epigenesis, from the germinative cells in the neck region of the developing adult (Sulgostowska 1972; Gustafsson 1990; Extavour and Akam 2003). It is conceivable, however, that a subpopulation of the germinative cells could be segregated into the germ line earlier in development, particularly since lineage tracing has never been achieved in cestode embryos (Rybicka 1966). In the case of *E. multilocularis*, the extensive asexual reproduction and growth in the intermediate host makes an epigenetic mechanism very likely, since early segregation of the germ line by preformation would require incorporation of cells from a segregated germ line within every new vesicle and protoscolex that is asexually generated. Our data suggests that the germinative cell subpopulation expressing *nanos* homologues are not germ line cells: no expression was observed of *em-nos-1* during brood capsule and protoscolex development, and *em-nos-2* was not consistently observed in brood capsule buds. Moreover, *em-nos-2* expression in late protoscolex development suggests a role in the formation of the nervous system. Relatedly, specific *nanos* paralogs are expressed in the nervous system in many metazoans (Haraguchi et al. 2003; Ye et al. 2004; Aoki et al. 2009; Kanska and Frank 2013).

Echinococcus primary cells as an experimental model for stem cell research

A great advantage of the *E. multilocularis* model is the possibility of long term *in vitro* culture for primary cell preparations, resulting in complete vesicle regeneration (Spiliotis et al. 2008). Here, we show that primary cell cultures are enriched for germinative cells, which actively proliferate from the earliest stages of development. Genes enriched in transcriptomic studies of early primary cells and depleted in HU-treated metacestodes could therefore be mined to search for germinative cell-specific expression.

The mechanism for enrichment is not clear, and could involve differential extraction of the germinative cells from the metacestode tissues, differential survival and aggregation of the germinative cells during culture, and the accumulation of germinative cells from self-renewing divisions. There is indirect evidence supporting all of these mechanisms, since: 1) it has been shown previously that 30% of all cells in fresh primary cell preparations are in S and G2/M, making the total percentage of

proliferating cells very large before they are set into culture (Spiliotis et al. 2008), 2) there is evidence of abundant cell death in electron microscopical studies and cell suspensions, and 3) germinative cells actively proliferate in the early aggregates. Besides the germinative cells, differentiated cells such as nerve cells and muscle cells are present in the aggregates. Their role in regeneration, if any, is unknown, but the neuromuscular system has been suggested to influence cell proliferation, differentiation and pattern formation in free living flatworms (Reuter and Gustafsson 1996; Rossi, Iacopetti, and Salvetti 2012; Witchley et al. 2013).

Differences between the *Echinococcus* germinative cells and the neoblasts in other flatworms

The lack of chromatoid bodies and the absence of *vasa* and *piwi* orthologs imply important differences between the germinative cells of cestodes and the neoblasts of planarians. Furthermore, genes that are neoblast-specific in planarians, such as *hdac1* and *phb1*, are widely expressed in *E. multilocularis*. Homologs of these genes have been shown to be important for stem cell biology and cell proliferation in other organisms, but they do not have a stem cell or even a proliferating cell-specific expression in these models (MacDonald and Roskams 2008; Brunmeir, Lagger, and Seiser 2009; Merkwirth and Langer 2009; Murko et al. 2010). It is therefore possible that the specific expression of these genes in neoblasts is a planarian novelty, which may not be shared with other flatworms. At the functional level, the response of *E. multilocularis* to partial germinative cell depletion is also different to that described in free living flatworms, since in planarians and in *Macrostomum* there is always a quick response by which the neoblast population is restored to normal levels within narrow margins, even when relatively large numbers of neoblasts remain in the tissues (Salvetti et al. 2009; De Mulder et al. 2010).

Recently, Newmark and colleagues demonstrated the existence of neoblast-like cells in the trematode *Schistosoma mansoni*, and in this organism, which also lacks *vasa* and *piwi* orthologs, paralogs of these genes are specifically expressed in the neoblast-like stem cells and have important roles in their maintenance (Collins et al. 2013; Wang, Collins, and Newmark 2013). In *Schistosoma mansoni* sporocysts the *ago2-1* gene (an ortholog of the *em-ago-2* genes) is expressed in all neoblast-like cells, and *nanos-2* is

expressed in a large subpopulation of neoblast-like cells. In adults, both genes are expressed in many, if not all, somatic stem cells. Therefore, differences can also be observed in the gene expression repertoire between *E. multilocularis* germinative cells and the *Schistosoma* neoblast-like cells, making the *E. multilocularis* stem cell system unique among flatworms. Further gene expression studies will depict a clearer picture of their similarities and differences, including the analysis of *vasa*-like genes (paralogs of *vasa* such as *PL-10*) which are expressed in planarian and schistosome stem cells (Rouhana et al. 2010; Wagner, Ho, and Reddien 2012; Wang, Collins, and Newmark 2013).

The *E. multilocularis* metacestode, with its ability to grow infiltratively like a tumor into the tissues of the host, is a relatively recent evolutionary novelty and is derived from the more typical cysterci larvae found in other taeniid cestodes (Freeman 1973; Slais 1973). Although rare in most cestodes, asexual reproduction by the formation of new scoleces is found in many taeniids (Slais 1973; Moore and Brooks 1987; Toledo et al. 1997; Loos-Frank 2000) and it is possible that the huge proliferative potential of *E. multilocularis* germinative cells and larvae was adapted from an already increased potential found in a common taeniid ancestor. The germinative cells in *E. multilocularis*, although similar in morphology and functionally analogous to the neoblasts in other flatworms, show important differences at the level of gene expression, which could be related to this recent evolutionary change in their developmental biology. At this point, nothing is known about gene expression in the germinative cells of adult cestodes. Because of the biological hazard related to working with *E. multilocularis* adults, comparative studies in related cestode models such as *Hymenolepis microstoma* (Cunningham and Olson 2010) and *Mesocestoides corti* (Specht and Voge 1965; Koziol et al. 2010) would be of great importance to delineate which characteristics of the germinative cells of *E. multilocularis* metacestodes are unique to this species and larval form, and which are a general feature of cestode germinative cells.

Conclusions

E. multilocularis is an important model for the study of parasite development and host-parasite interactions, and is the only flatworm model with a robust cell culture system (Brehm 2010b). Growth and regeneration of *E. multilocularis* larvae is driven by the germinative cells, which are morphologically and functionally similar to the neoblasts of free living flatworms, but which show important differences in their gene expression patterns and in the loss of conserved stem cell regulators. This work represent the first description of the germinative cells at the molecular level, giving the first evidence of the existence of sub-populations of germinative cells with different gene expression patterns, and provides molecular markers for identifying differentiated cell types *in situ.* Some differences between the germinative cells and the neoblasts of other flatworms could have arisen as specific adaptations of the stem cell system for the unique asexual development of *E. multilocularis*. The novel development of *E. multilocularis* and other taeniids is therefore an excellent model for the study of the evolutionary origins of asexual reproduction and its effect on stem cell systems.

Methods

Parasite material, culture and primary cell preparation

Parasite isolates were maintained by serial intraperitoneal passage in *Meriones unguiculatus* as previously described (Spiliotis and Brehm 2009). Unless otherwise stated, all experiments were performed on *in vitro* cultured metacestodes. Standard *in vitro* culture of metacestodes was done in co-culture with rat Reuber hepatoma feeder cells, and primary cell preparations were performed and cultured in cDMEM-A pre-conditioned medium essentially as previously described (Spiliotis and Brehm 2009), with the following modifications: 1) cells were detached from the metacestode tissue with a single treatment of 20 minutes with trypsin/ethylenediaminetetraacetic acid (EDTA) and 2) primary cells were cultured in cDMEM-A instead of hydatid fluid.

For primary cell cultures, isolate H95 (Jura et al. 1996), which has been passaged for 18 years and has developed a strong defect in protoscolex formation was used. For other experiments, more recent isolates were used, obtained from accidental infections of Old World Monkeys in a breeding exclosure (Tappe et al. 2007). *Dugesia tahitiensis* ((Peter, Ladurner, and Rieger 2001), obtained from Bernhard Egger) was the planarian species used for immunohistofluorescence.

Ethical approval

All experiments were carried out in accordance with European and German regulations on the protection of animals (*Tierschutzgesetz*). Ethical approval of the study was obtained from the local ethics committee of the government of Lower Franconia (55.2-2531.01-31/10).

EdU labeling and detection

For short term labeling, 50 µM of 5-ethynyl-2′-deoxyuridine (EdU, Life Technologies) was added to the media and the material was incubated for 5 hours. For continuous labeling, 1 µM EdU was used for up to 14 days. The length of incubation and the EdU concentrations were determined after varying the parameters in preliminary experiments (see the main text). Before fixation, metacestode vesicles were gently opened using a syringe tip in order to allow the entry of the fixative and other reagents during detection procedures. Samples were fixed in 4% paraformaldehyde prepared in phosphate buffer saline (PFA-PBS) for 1 hour at room temperature, and

processed for detection of EdU in paraplast sections. Detection was performed with the Click-iT® EdU Alexa Fluor® 555 Imaging Kit as described by the manufacturer for sections. Whole-mount detection was performed by a modified protocol in which all steps were doubled in length and the washes were increased in number. For double labeling, EdU detection was always performed after the immunohistofluorescence or *in situ* hybridization protocols.

Tissue maceration and staining of cell suspensions

Cell suspensions were prepared by a modification of the method of David (David 1973). Metacestode vesicles were opened and washed in phosphate buffer saline (PBS), and placed in maceration solution (13:1:1 distilled water : glacial acetic acid : glycerol, 100 µl of solution per vesicle). Primary cell aggregates (from one well of a six-well plate, after two days of culture) were washed in PBS, allowed to settle and placed in 500 µl of maceration solution. Both kinds of samples were pipetted up and down with a p1000 pipette, and placed overnight at 4 ºC. The next day they were once again disaggregated by pipetting, diluted to 1:10 with maceration solution, and 10 µl were spotted on SuperFrost slides (Thermo Scientific). The slides were dried overnight at room temperature and stained by either of these procedures:

A) Propidium iodide (PI) plus 4',6-diamidino-2-phenylindole (DAPI) : after washing the slides with PBS plus 0.05% Triton X.100, the slides were stained successively with DAPI (1 µg/ml in PBS) and PI (2.5 µg/ml in PBS), washed twice with PBS and mounted with Fluoprep (bioMérieux).

B) Whole Cell Stain (WCS) plus DAPI: the Cellomics WCS Green (Thermo Scientific) was used as instructed by the manufacturer, followed by DAPI staining, washing and Fluoprep mounting. When done in combination, EdU detection was performed first, followed by WCS plus DAPI staining.

C) Nile Red plus DAPI: after washing with PBS, the slides were stained with Nile Red (Greenspan, Mayer, and Fowler 1985) (Sigma-Aldrich, 100 ng/ml in PBS from a 4.2 mg/ml stock in acetone) followed by DAPI staining, washing, and Fluoprep Mounting. Imaging was performed with the rhodamine channel of the Zeiss Axio Imager.Z1 microscope.

Hydroxyurea treatment and X-ray irradiation

Metacestode vesicles were cultured in axenic, pre-conditioned cDMEM-A medium (Spiliotis and Brehm 2009) with a nitrogen gas phase (40 vesicles in 5 ml of medium in 25 cm² cell culture flasks, vertically positioned). Hydroxyurea (HU) was added to a final concentration of 40 mM from a 2 M stock (dissolved in medium), whereas only medium was added to controls. HU was added daily to the medium since it is not stable in solution at temperatures circa 37 ºC (Heeney et al. 2004), and the medium was replaced every two days. After 7 days of treatment the vesicles were washed extensively and transferred to HU-free medium. Some vesicles were fixed immediately for immunohistofluorescence and whole-mount *in situ* hybridization. The remaining vesicles were kept in HU free medium, taking samples for EdU labeling after 1, 4, 9 and 22 days.

Determination of BrdU incorporation in primary cells after HU treatment was done with the Cell Proliferation Elisa, BrdU (Colorimetric) Kit (Roche). Briefly, primary cells were cultured in the presence of 0, 10 or 40 mM HU for 40 hours, after which half of the medium was replaced with fresh medium containing HU and BrdU (10 μM, final concentration). The cells were cultured for 4 hours and processed for detection as indicated by the manufacturer. For studying the effect of HU on regeneration, primary cells were cultured with 0, 10 or 40 mM HU, changing medium and HU every 48 to 72 h. After three weeks the number of newly formed vesicles was counted.

For X-ray irradiation, a 150 Gy dose was applied to metacestodes with a Faxitron CP160 source. Vesicles were then set back into axenic culture, taking samples for EdU labeling after 2, 7, 20 and 48 days. Surviving metacestodes were defined as vesicles being able to maintain turgency and with an apparently intact germinal layer as seen under a dissecting microscope.

PCR, RT-PCR and molecular cloning

For RT-PCR, RNA was extracted with Tri-Reagent (5 PRIME) and 700 ng of total RNA were used for cDNA synthesis using PrimeScript reverse transcriptase (Takara). For the analysis of genes lacking introns, RNA was previously treated with

RQ1 DNase (Promega, 2 units / µg for one hour) and mock controls with no reverse transcriptase were done in parallel to ensure that no amplification was obtained from contaminating genomic DNA. For genes with introns, primers were always designed in two separate exons. A list of primers and annealing temperatures, together with the *E. multilocularis* GeneDB codes (http://www.genedb.org/Homepage/Emultilocularis), is included as supplementary material for all genes (Additional File 17).

For semi-quantitative RT-PCR, 10-fold serial dilutions of each cDNA were used for PCR with Taq polymerase (New England Biolabs), and the amplification was limited to 28 to 30 cycles. For normalization, RT-PCR with the constitutive gene *em-elp* (Brehm et al. 2003) was performed.

For the cloning of gene fragments for whole-mount *in situ* hybridization, to confirm the complete coding domain sequences (CDS) of genes and for long-range PCR with genomic DNA, KOD Hot Start polymerase (Millipore) was used following the manufacturer´s instructions. In the case of *em-ago2-A*, the 5´region of the gene is interrupted by the end of the genomic scaffold. We obtained most of the 5´region of the CDS by taking advantage of the high similarity between the *em-ago2* genes, using a combination of a specific *em-ago2-A* primer with a primer for the 5´end of *em-ago2-B*. PCR products for sequencing and probe synthesis were cloned into pDrive (Qiagen) or pJet1.2 (Thermo-Scientific).

Alkaline Phosphatase Histochemistry

Alkaline Phosphatase Histochemistry was done in cryosections and whole-mounts with Nitro blue tetrazolium chloride and 5-Bromo-4-chloro-3-indolyl phosphate (NBT/BCIP) as described by Cox and Singer (Cox and Singer 1999).

Immunohistochemistry and Immunohistofluorescence

Immunohistochemistry and immunohistofluorescence in paraplast sections and cryosections, and whole mount immunohistofluorescence were performed as previously described (Koziol et al. 2011; Koziol, Krohne, and Brehm 2013). For anti-PHB1 and anti-H3S10-P, a step of heat induced epitope retrieval was included after re-hydration, by boiling the slides for 20 minutes in a microwave in a solution of 10 mM sodium citrate, pH 6.0 with 0.1% Triton X-100.

Primary antibodies used were Anti-PHB1 (rabbit polyclonal, Sigma-Aldrich HPA003280, 1:100 dilution), anti-Phospho-Histone H3 (Ser10) (rabbit polyclonal, Cell Signaling Technology 9701, 1:100 dilution), anti-FMRFamide (Immunostar, 20091), anti-HMW-Tropomyosin ((Alvite and Esteves 2009; Koziol et al. 2011) ,1:500 dilution) and anti-acetylated tubulin (mouse monoclonal, clone 6-11B-1, Santa Cruz Biotechnology, 1:100 dilution). In the case of anti-PHB1, we also performed a Western Blot analysis with protein extracts of *E. multilocularis* metacestodes that confirmed that the antibody recognized a protein of the expected size. Secondary antibodies used were anti-mouse conjugated to FITC, anti-rabbit conjugated to FITC and anti-rabbit conjugated to peroxidase (Jackson ImmunoResearch).

Whole-Mount *in situ* hybridization (WMISH)

Digoxigenin-labeled probes were synthesized by *in vitro* transcription with T7 or SP6 polymerases (New England Biolabs), using the DIG RNA labeling mix (Roche) as described by the manufacturer, from a fragment of the relevant gene cloned into pDrive or pJet1.2 (previously linearized by digestion after the gene fragment with the appropriate restriction enzyme). A list of the probes used and their lengths is described for each gene in Additional File 17. The probes were then purified with the RNeasy Mini Kit (Qiagen), checked by agarose gel electrophoresis and quantified by comparison of serial dilutions in a dot blot with the DIG-labeled Control RNA (Roche).

The WMISH protocol was adapted from the one used in the laboratory of Pete Olson (http://www.olsonlab.com/). All solutions used up to the hybridization step were RNAse free by treatment with DEPC. The metacestode vesicles (with or without developing protoscoleces) were opened with a syringe tip and fixed in PFA-PBS overnight at 4 º C. The next day, the samples were washed twice in 100% methanol, and kept at -20 ºC in methanol until further use. The vesicles were then transferred to 100% ethanol, rehydrated by successive steps in 75% and 50% ethanol in PBS, and washed extensively with PBS plus 0.1% Tween-20 (PBS-T). The tissue was then permeabilized with 15 µg/ml Proteinase K (Fermentas) in PBS-T for 10 minutes, rinsed twice for 5 minutes in 0.1 M triethanolamine (TEA), pH 8, and treated twice with 0.25% v/v acetic anhydride in TEA buffer for 5 minutes. After washing twice for 5 minutes with PBS-T,

the samples were re-fixed for 20 minutes in PFA-PBS at room temperature and washed extensively with PBS-T.

Samples were then transferred to pre-hybridization buffer (50% formamide, 5 X SSC buffer (Sambrook, Fritsch, and Maniatis 1989), 1 mg/ml *Torula* yeast RNA, 100 µg/ml heparin, 1 X Denhardt´s solution, 0.1% Tween-20, and 0.1% CHAPS; all components were obtained from Sigma-Aldrich). The buffer was changed twice before pre-hybridizing for 6 to 24 hours at 60 ºC. Probes were then denatured by heating at 80 º C for three minutes and placing directly on ice for 3 minutes, and added to the specimens at a concentration of 0.2 to 2 ng/µl. Hybridization was performed at 53-54 ºC (for the shorter probes for *em-muc-1* and *em-h2b* of circa 200 bp) or at 57-58 º C (for other probes) for 16 to 24 hours with constant shaking.

After hybridization, the samples were washed twice with the pre-hybridization buffer for 10 minutes at 57 ºC, three times in SSC 2X plus 0.1% Tween-20 for 20 minutes at 57 ºC, and three times with SSC 0.2X plus 0.1% Tween-20 at 57 ºC. Samples were then transferred to room temperature, washed twice with maleic acid buffer (MAB-T : 100 mM maleic acid, 150 mM NaCl, 0.1% Tween-20) and blocked for two hours at room temperature with blocking buffer (MAB-T plus 1% w/v blocking reagent for nucleic acid hybridization and detection, Roche, and 5% v/v heat-inactivated sheep serum, Sigma Aldrich). Then they were incubated overnight with shaking at 4 ºC with anti-digoxigenin antibodies conjugated to either alkaline phosphatase or to peroxidase (Roche) in blocking buffer without sheep serum.

Finally, samples were extensively washed with MAB-T and development was performed with NBT/BCIP for alkaline phosphatase conjugated antibodies (conventional WMISH), or with Fluorescein-Tyramide for peroxidase antibodies, prepared and used as described by Hopman et al. (Hopman, Ramaekers, and Speel 1998) (fluorescent WMISH). Control sense probes were also used for all genes except *em-tpm-1.hmw*, and at least one control sense probe was included in all WMISH experiments, with no resulting signal (examples are included in Additional File 18).

Fluorescence Microscopy

Samples were analyzed by confocal microscopy (Leica TCS SP5) and by epifluorescence microscopy (Zeiss Axio Imager.Z1 and Keyence BZ9000). For the quantification of EdU+ and AcTub+ cells, at least 4 random microscopic fields were captured for each whole-mount metacestode vesicle, from which the positive cells were manually counted and averaged.

Transmission Electron Microscopy (TEM)

Protocols for TEM were performed as previously described (Spiliotis et al. 2008).

Abbreviations

ALP-HC: alkaline phosphatase histochemistry; AcTub: acetylated tubulin alpha; BC: brood capsule; BrdU: 5-bromo-2'-deoxyuridine; CHAPS: 3-[(3-Cholamidopropyl)dimethylammonio]-1-propanesulfonate; cDNA: complimentary DNA; CDS: coding domain sequence; DAPI, 4',6-diamidino-2-phenylindole; EDTA: Ethylenediaminetetraacetic acid, EdU: 5-Ethynyl-2'-deoxyuridine; ELISA: enzyme-linked immunosorbent assay; FITC: Fluorescein isothiocyanate; GL: germinal layer; H3S10-P: Histone H3 phosphorylated in Serine 10; HF: hydatid fluid; HMW: high molecular weight; HU: hydroxyurea; LL: laminated layer; MAB: maleic acid buffer; NBT/BCIP: Nitro blue tetrazolium chloride and 5-Bromo-4-chloro-3-indolyl phosphate; NR: Nile red; PBS: phosphate buffer saline; PCR: polymerase chain reaction; PFA: paraformaldehyde; PI, propidium iodide; PS: protoscolex; RNP: ribonucleoprotein particle; RRM: ribonucleotide reductase; RT-PCR: reverse transcription polymerase chain reaction; SSC: saline-sodium citrate buffer; TEA: triethanolamine; TEM: transmission electron microscopy; WCS: whole cell stain; WMISH: whole mount *in situ* hybridization.

Competing interests

The authors declare that they have no competing interests.

Author´s contributions

UK carried out or participated in all experiments and drafted the manuscript. UK and KB designed the study, as well as analyzed and interpreted the data. GK designed and interpreted the results of TEM experiments. TR and LZ participated in the characterization of the *em-alp* and *em-ago2* gene families, respectively. All authors read and approved the final manuscript.

Acknowledgements

This work was supported by grants from the Deutsche Forschungsgemeinschaft (DFG; BR 2045/4-1) and the Wellhöfer Foundation (all to KB). UK was supported by a grant of the German *Excellence Initiative* to the Graduate School of Life Sciences, University of Würzburg. The authors wish to thank Monika Bergmann and Dirk Radloff for excellent technical assistance, Dr. Thomas Kerkau of the Institut für Virologie und Immunobiologie, Würzburg, for his assistance with the X-Ray irradiation equipment, and Hilde Merkert, of the Institute for Molecular Infection Biology, Würzburg, for her assistance with confocal microscopy. This publication was funded by the German Research Foundation (DFG) and the University of Würzburg in the funding programme Open Access Publishing.

Additional Files

Additional File 1 - Supplementary figure (.tif format). Example of a rare mitotic EdU+ cell after a 50 μM 5 h pulse. DAPI staining is shown in blue, EdU detection in red, and tubulin immunohistofluorescence in green. The bar represents 5 μm.

Additional File 2 - Supplementary figure (.tif format). EdU incorporation in *ex-vivo* cultured metacestode material. Abbreviations: bc, brood capsule; dev ps, developing protoscoleces; gl, germinal layer; inv ps, invaginated protoscolex; host, host tissue. Bars represent 200 μm.

Additional File 3 - Supplementary figure (.tif format). EdU incorporation after protoscolex isolation and activation. The protocol and representative images of EdU incorporation are shown for each condition. The experiment was repeated twice with similar results.

Additional File 4 - Supplementary figure (.tif format). Histogram of cell areas as seen in cell suspensions (used as a proxy for cell size) for all germinative cells and for EdU+ germinative cells in the germinal layer and in primary cell preparations. Smaller cells are less likely to incorporate EdU, and EdU+ cells are overrepresented at intermediate sizes. This is compatible with smaller cells being in G1/G0-phase, cells of intermediate size in S-phase and the larger cells in G2-phase. However, it is possible that other factors (such as different germinative cell sub-populations) also affect germinative cell size.

Additional File 5 - Supplementary figure (.tif format). Example of a EdU+ germinative cell in a cell suspension prepared from protoscoleces (previously incubated for 5 h in 50 μM EdU). WCS is shown in green, EdU in red and DAPI in blue.

Additional File 6 - Supplementary figure (.tif format). Genomic organization of *em-ago2* genes. A. Graphical representation of the end of scaffold 7767 and the beginning of scaffold 7771, showing the position of primers used for PCR with genomic DNA.

Both DNA strands and all six reading frames are shown, together with the position of genes and their exons and the *em-ago2-ψ* pseudogene. B. PCR with genomic DNA to confirm the structure of both scaffolds. Lanes 1, 2 and 3 in each gel indicate primer sets 1F/R, 2F/R, 3F/R for scaffolds 7767 and 7771, and lane 4 indicates primer set 4F/R for scaffold 7771. Bands of the expected size are observed in all cases (indicated by red dots) except for the primer combination 7767-3F/R. It is possible that a difference occurs in the analyzed isolate (MP1) as compared to the reference genome in this particular region.

Additional File 7 - Supplementary figure (.tif format). Fluorescent WMISH of *em-hdac1* on metacestode vesicles. Bars represent 40 μm.

Additional File 8 - Supplementary figure (.tif format). WMISH of *em-phb1* on metacestode vesicles, on the germinal layer (upper panel), brood capsules (middle panel) and protoscolex buds (lower panel).

Additional File 9 - Supplementary figure (.tif format). Immunohistofluorescence of PHB1 in sections of *Dugesia tahitiensis*. A. General view of a cross section at the level of the pharynx (DAPI stained). A1 and A2. Detail of the region of the pharynx (f) and the nerve cords (Figure A1) and of the mesenchyme surrounding the intestine (i) (Figure A2), as seen with DAPI and PHB1 immunoreactivity. Because of strong auto-fluorescence seen in the region of the gut and epidermis in all fluorescence channels, we also provide the signal in the rhodamine channel for comparison (autofluorescence thus appears yellow in the merged image). PHB1 is most strongly expressed in small neoblast-like cells in the mesenchyme and around the nerve cords. B. Negative control (no primary antibody). Bars represent 50 μm in A1, A2 and B, and 20 μm in the detailed views.

Additional File 10 - Supplementary figure (.tif format). Em-PHB1 immunodetection in *E. multilocularis*. Top, immunohistochemistry (IHC) of PHB1 in sections of a vesicle with brood capsules and protoscoleces. Bottom, control IHC without any primary antibody. Bars represent 20 μm.

Additional File 11 - Supplementary figure (.tif format). Details of alkaline phosphatase activity in *E. multilocularis*. A. Lack of alkaline phosphatase activity in the tegument of the brood capsule. B. Qualitative assessment of whole-mount alkaline phosphatase activity in the excretory system of activated and non-activated protoscoleces. 150 protoscoleces were examined and their signal classified as either strong (strong signal in scolex and body), moderate (moderate signal only in scolex or body), weak (barely detectable signal) or not stained (no signal observed).

Additional File 12 - Supplementary figure (.tif format). Differentiation of nerve cells in EdU continuous labeling experiments. A. Double detection of AcTub immunohistofluorescence and EdU incorporation after a 5 h 50 µM pulse. No double positive cells can be detected. B. Example of a double positive cell after 14 days of incubation in 10 µM EdU. C. Percentage of AcTub+EdU+ double positive cells over all AcTub+ cells after 5 h, 7 days and 14 days of incubation in medium containing 1 µM or 10 µM EdU (average and standard deviation of 2 to 3 metacestode vesicles per time point and condition). Bars represent 20 µm.

Additional File 13 - Supplementary figure (.tif format). Immunohistofluorescence with anti-HMW-Tropomyosin in metacestode sections. A. Germinal layer. B. Brood capsule. C. Brood capsule with a protoscolex bud. D. Invaginated protoscolex. Arrowheads point to the subtegumental muscle layer, which is greatly thickened in brood capsules as compared to the germinal layer. Bars represent 20 µm.

Additional File 14 - Supplementary figure (.tif format). Effect of hydroxyurea (HU) on primary cells. A. Effect on proliferation as assayed by BrdU incorporation and ELISA detection. The BrdU incorporation levels in non-treated controls was set as 100% and relative values are shown for 10 mM and 40 mM HU, as well as for the control without BrdU (average and standard deviation of 4 independent experiments). B. Effect on new vesicle of regeneration from primary cells after 3 weeks of culture (average and standard deviation of two independent experiments).

Additional File 15 - Supplementary figure (.tif format). Example of degenerating cell in TEM analysis of early (two days of culture) primary cell preparations.

Additional File 16 - Supplementary figure (.tif format). AcTub immunohistofluorescence and phalloidin staining of primary cell aggregates after 3 days of culture. Bars represent 20 μm.

Additional File 17 - Supplementary table (.xls format). List of GeneDB gene codes, primers and probes from this work.

Additional File 18 - Supplementary figure (.tif format). Representative examples of WMISH experiments and the respective controls performed with sense probes, for genes with different levels of expression.

5.2. CHAPTER 2: "A novel terminal-repeat transposon in miniature (TRIM) is massively expressed in *Echinococcus multilocularis* stem cells."

To be submitted as Koziol *et al*. to Molecular Biology and Evolution

Author contributions

General study design:

Uriel Koziol, Klaus Brehm, Cecilia Fernández

Experimental design and work:

Uriel Koziol designed, performed or participated in all the experiments and in bioinformatic/phylogenetic analyses related to *E. multilocularis* and *Taenia* spp. Santiago Radio and Pablo Smircich performed the bioinformatic analyses in *E. granulosus*, as well as gene ontology and RNA secondary structure analyses. Magdalena Zarowiecki performed RNAseq analysis, tRNA identification, and mapping of TRIM elements on the *E. multilocularis* chromosomes.

Analysis of the results:

Uriel Koziol, Santiago Radio, Magdalena Zarowiecki, Pablo Smircich, Klaus Brehm,

Writing of the manuscript:

Uriel Koziol wrote the first manuscript draft, which was corrected and accepted by all the authors

A novel terminal-repeat retrotransposon in miniature (TRIM) is massively expressed in *Echinococcus multilocularis* stem cells.

Koziol, U.[1,2]., Radio, S.[3], Smircich, P.[3], Zarowiecki, M.[4], Fernández, C.[5], Brehm, K.[1,*]

[1]University of Würzburg, Institute of Hygiene and Microbiology, Josef-Schneider-Strasse 2, D-97080 Würzburg, Germany

[2]Universidad de la República, Facultad de Ciencias, Sección Bioquímica y Biología Molecular, Iguá 4225, CP 11400, Montevideo, Uruguay

[3]Universidad de la República, Facultad de Ciencias, Laboratorio de Interacciones Moleculares, CP 11400, Montevideo, Uruguay

[4]Parasite Genomics, Wellcome Trust Sanger Institute, Wellcome Trust Genome Campus, Hinxton, Cambridge CB10 1SA, UK

[5]Cátedra de Inmunología, Facultad de Química, Universidad de la República, Avenida Alfredo Navarro 3051, piso 2, Montevideo, CP11600, Uruguay

* Corresponding Author

Abstract

Taeniid cestodes (including the human parasites *Echinococcus* spp. and *Taenia solium*) have a very low number of mobile genetic elements (MGEs) in their genome, despite lacking a canonical ortholog of Piwi. The MGEs of these parasites are virtually unexplored, and nothing is known about their expression and silencing. In this work, we report the discovery of *ta-TRIM,* a novel family of small non-autonomous retrotransposons (Terminal Repeat Retroransposons in Miniature, TRIMs). *ta-TRIM*s are only the second TRIM elements discovered in animals, and are likely the result of convergent reductive evolution in different taxonomic groups. These elements originated at the base of the taeniid tree and have expanded during taeniid diversification, including after the divergence of closely related species such as *Echinococcus multilocularis* and *Echinococcus granulosus*. They are massively expressed in larval stages, from full length copies and from isolated terminal repeats that show transcriptional read-through into downstream regions, generating novel non-coding RNAs and transcriptional fusions to coding genes. Despite their high expression, it is likely that they are no longer mobile in *E. multilocularis*, perhaps due to the extinction of their autonomous retrotransposons partner. In *E. multilocularis*, *ta-TRIM*s are specifically expressed in the germinative cells (the somatic stem cells) during asexual reproduction of metacestode larvae. This would provide a developmental mechanism for insertion of *ta-TRIM*s into cells that will eventually generate the adult germ line. Future studies of *ta-TRIM*s in comparison with other MGEs could give the first clues on MGE silencing mechanisms in cestodes.

Introduction

Mobile genetic elements (MGEs) have the capacity to replicate within the genome of their host. This gives them a selective advantage over other genetic elements, resulting in their ability to increase their frequency in natural populations, even though their expansion can usually be detrimental to the host (Kidwell and Lisch 2001; Werren 2011). In this sense, they act as "selfish" genetic elements, and can accumulate to very large numbers, making a sizeable portion of the genomes of most eukaryotes (Lander et al. 2001; Feschotte, Jiang, and Wessler 2002; Wicker et al. 2007; Werren 2011). However, like all genetic elements they are a substrate for natural selection and can be an important source of variation and novelty for the evolution of genomes (Kidwell and Lisch 2001; Werren 2011).

Long terminal repeat retrotransposons (LTR-RTns) are a large group of MGEs present in almost all eukaryotes, including animals (metazoans) (Boeke and Stoye 1997; Havecker, Gao, and Voytas 2004; Wicker et al. 2007). These elements consist of two identical direct repeats (long terminal repeats; LTRs) that flank sequences coding for structural components (Gag) and enzymatic components (protease (PR), reverse transcriptase (RT), RNAse H (RH) and integrase (IN)) which are required for the retrotransposition cycle. PR, RT, RH and IN are encoded in a polyprotein (Pol) that is later processed into individual polypeptides by PR. The 5´LTR functions as an RNApol II promoter for the transcription of the retrotransposon RNA (rtnRNA). Although it has an identical sequence, the 3´LTR is instead the site of 3´end processing of the retrotransposon transcript, which is cleaved and polyadenylated by the cellular machinery. In the related retroviruses of vertebrates, different strategies result in the specific induction of promoter activity and the suppression of 3´end processing at the 5´LTR, and conversely in weak promoter activity and strong 3´ end processing at the 3´LTR (Klaver and Berkhout 1994; Schrom et al. 2013).

The rtnRNA, which therefore lacks the 5´most region of the 5´LTR (U3 region) and the 3´most region of the 3´LTR (U5 region), is exported to the cytoplasm where it is translated. In the cytoplasm, the rtnRNA associates with Gag to form viral-like particles (VLPs) where reverse transcription takes place (Telesnitsky and Goff 1997; Havecker,

Gao, and Voytas 2004). Reverse transcription is a complex mechanism that results in the formation of double stranded retrotransposon cDNA (rtnDNA) with complete LTRs (Telesnitsky and Goff 1997). For reverse transcription, two other sequence elements are crucial. The first is the primer binding site (PBS), located immediately downstream of the 5´LTR, where binding of a tRNA to a sequence of 8 to 18 bases complementary to its 3´end serves as the primer for the synthesis of the (-)rtnDNA strand (Mak and Kleiman 1997). The other is the polypurine tract (PPT), located immediately upstream of the 3´LTR, from which the synthesis of the (+) rtnDNA strand begins (Telesnitsky and Goff 1997). The rtnDNA is imported into the nucleus, where it is integrated into the genome by IN. For this, IN recognizes sequences in the ends of the LTRs (around 8 to 20 bases), of which the most crucial part are the invariable 5´-CA-3´-OH ends (Hindmarsh and Leis 1999; Zhou et al. 2001). IN catalyzes the joining of the ends of the rtnDNA to a staggered double stranded cut in the genomic DNA. The single stranded gaps between the rtnDNA and the genomic DNA are repaired by the cell, resulting in the duplication of the cut target sequence, as direct repeats flanking the integrated retrotransposon (target site duplications; TSD; (Hindmarsh and Leis 1999; Ballandras-Colas et al. 2013)).

In addition to these functional retrotransposons, other elements have been described that lack most or all of the coding sequences, but which are still mobilized by the machinery of functional (autonomous) elements (Havecker, Gao, and Voytas 2004; Wicker et al. 2007; Schulman 2012). This non-autonomous elements (NA-elements) only have the non-coding sequences that are essential for the retrotransposition cycle, such as the LTRs, PBS and PPT. NA-elements include large retrotransposon derivatives (LARDs, > 4 kb), and terminal-repeat retrotransposons in miniature (TRIMs, <4 kb, typically around 0.5 to 1 kb in length) (Witte et al. 2001; Jiang, Jordan, and Wessler 2002; Havecker, Gao, and Voytas 2004; Wicker et al. 2007; Schulman 2012). LARDs and TRIMs were originally described in plants (Witte et al. 2001; Jiang, Jordan, and Wessler 2002; Kalendar et al. 2008), and only recently was the first example of a group of TRIMs described in a metazoan (the red harvester ant, *Pogonomyrmex barbatus*; (Zhou and Cahan 2012)). TRIMs of plants and ants are presumed to be the result of convergent reductive evolution from autonomous elements, retaining only the minimal sequences required to efficiently complete the retrotranspotion cycle (Schulman 2012).

5. Results

Because of the deleterious effect of MGEs, the hosts have developed effective mechanisms to suppress their expression and expansion. This is particularly important in the germ line of animals, since replication of MGEs in these cells would lead to their accumulation in the next generation. The Piwi pathway is a conserved metazoan mechanism that silences MGEs in the germ line (Juliano, Wang, and Lin 2011). Piwi is a member of the Argonaute family of proteins, which are involved in gene silencing through small RNAs (Hock and Meister 2008). Piwi proteins are associated with a specific class of small RNAs (Piwi-associated RNAs, or piRNAs), and the Piwi / piRNA complex can silence the MGEs at the epigenetic level and by post-transcriptional regulation of RNA stability (the specific mechanisms vary in different animal models, (Juliano, Wang, and Lin 2011)).

Piwi proteins are highly expressed in the germ line of many metazoans, and the pathway has been shown to be crucial for repressing MGE activity in diverse animal models (Juliano, Wang, and Lin 2011). Many invertebrates have a discontinuous germ line, which is generated from multipotent stem cells by inductive mechanisms after embryonic development (Extavour and Akam 2003; Juliano, Swartz, and Wessel 2010). In planarians and other free-living flatworms (phylum Platyhelminthes), these adult multipotent somatic stem cells are denominated neoblasts, and are the cellular basis for their regenerative capabilities, including the ability for *de novo* formation of the germ line (Sato et al. 2006; Handberg-Thorsager and Salo 2007; Wang et al. 2007; Rossi et al. 2008; Juliano, Wang, and Lin 2011; Rink 2013) . Free-living flatworms have been shown to specifically express *piwi* homologs in their neoblasts (Reddien et al. 2005; Palakodeti et al. 2008), and it has been suggested that these *piwi* genes could play a role in the protection of the genome of the neoblasts from MGEs (Rink 2013). In contrast, *piwi* orthologs have been lost from the main group of parasitic flatworms (the monophyletic clade Neodermata, including the flukes [Digenea] and tapeworms [Cestoda] (Tsai et al. 2013; Skinner et al. 2014)). In the digenean *Schistosoma mansoni*, a member of a divergent group of neodermatan-specific *argonaute* genes (*sm-ago2-1*) is highly expressed in neoblast-like stem cells, and it has been proposed that this gene could be performing similar functions to those of *piwi* in other organisms (Collins et al. 2013; Wang, Collins, and Newmark 2013). We have recently characterized the neoblast-like cells of the asexually proliferating metacestode larva of the human parasite

Echinococcus multilocularis (Cestoda: Taeniidae) (Koziol et al. 2014). In cestodes, such cells are typically denominated "germinative cells" (Reuter and Kreshchenko 2004; Koziol and Castillo 2011). In contrast to *S. mansoni*, only a fraction of the *E. multilocularis* germinative cells express *em-ago2-A-C* (orthologs of *sm-ago2-1*), and expression is also seen in post-mitotic, differentiated cells, so it is unclear if the functions of these *argonaute* genes are shared between cestodes and trematodes (Koziol et al. 2014). However, the burden of MGEs in *E. multilocularis* is very low (*circa* 2% of the genome), as is for other related cestodes, indicating that a highly effective mechanism of MGE suppression must be at play (Tsai et al. 2013; Skinner et al. 2014).

In this work, we report the discovery of a novel group of TRIM elements that is specific for *E. multilocularis* and related taeniid cestodes. TRIMs have somehow escaped silencing and are massively expressed in the *E. multilocularis* germinative cells, constituting their best molecular marker to date. These TRIMs have expanded during the evolution and divergence of taeniids, and may still be active in some species. In *E. multilocularis*, these elements may now be inactive for retrotransposition, but have left on their wake a substantial re-shaping of the host´s transcriptome, as they are the source of TRIM transcripts and of fusion transcripts to coding genes and novel non-coding RNAs.

Results

Discovery of TRIM elements in taeniid cestodes

In *Echinococcus* spp., the metacestode larvae develop as fluid-filled cysts in which numerous protoscoleces, the infective form for the definitive host, are developed from the cyst wall by asexual budding. Previously, a long non-coding RNA (lncRNA) of *ca.* 900 bases with similarity to the *Echinococcus granulosus* repeat element EgRep (Marin et al. 1993) was described to be highly expressed in the cyst wall and protoscoleces of *Echinococcus granulosus*, and similar lncRNAs were reported to be found among ESTs of *Echinococcus multilocularis* (Parkinson et al. 2012). By mapping ESTs of *E. multilocularis* and *E. granulosus* to their recently published genomic sequences, we have found that these lncRNAs are transcribed from many loci that have all of the characteristics of short non-autonomous retrotransposons (TRIMs), and which we have denominated *ta-TRIMs* (taeniid TRIMs). This includes: 1) two LTRs of *ca*. 198 bp, starting with 5′-TG-′3 and finishing with 5′-CA-3′ (*i.e*. with 5′-CA-3′at both 3′ends); 2) a primer binding site (PBS) with 9 bases of complementarity to the 3′ end of an *Echinococcus* ^{Leu}tRNA, positioned at 4 bases from the end of the 5′LTR; and 3) a polypurine tract (PPT) of 15 bases, located 3 bases upstream of the 3′LTR (Figure 1 and Figure 3A). Between both LTRs, there are approximately 590 bp that lack any open reading frames longer than 120 codons, and show no similarity by blastx to any known proteins, but which have a strong secondary structure which is conserved between different copies. This region may contain the packaging signal (PSI), a region of secondary structure which is not conserved at the level of primary sequence, but which is of importance for the packaging of retroviral RNAs with Gag proteins (Wicker et al. 2007). Flanking the LTRs, short (4 to 5 bp) target duplication sites can be found in many of the elements, as is characteristic of retrotransposons and retroviruses after integration. All of these characteristics strongly indicate that *ta-TRIM*s are NA-retrotransposons that must be mobilized from an autonomous element *in trans.*

From complete ESTs and RNAseq data of both species, and from 3′ RACE experiments in *E. multilocularis*, the initiation of transcription and the site of polyadenylation could clearly be identified within the 5′ LTR and the 3′ LTR,

respectively (Figure 1, and Figure 3A). Polyadenylation of different TRIM loci occurred within a 6 bp window in the 3´LTR, upstream of which no canonical polyadenylation signal (AATAAA) could be found. Instead, there is an A/T rich region, containing in most cases an alternative polyadenylation signal previously proposed for *Echinococcus* spp., AATATA (Konrad et al. 2003; Koziol et al. 2009) located 12 to 15 bp upstream of the cleavage and polyadenylation site. Therefore, the LTRs could be unambiguously divided into U3, R and U5 regions (Figure 1).

We searched for *ta-TRIM*s in the draft genomes of other taeniid cestodes (*Taenia solium* (Tsai et al. 2013), *Taenia asiatica* and *Taenia taeniaeformis* (50 helminth genomes initiative, at the Wellcome Trust Sanger Institute)), as well as non-taeniid cestodes and other flatworms (*Hymenolepis microstoma* (Tsai et al. 2013), *Mesocestoides corti* and *Diphyllobothrium latum* (50 helminth genomes initiative), *Schistosoma mansoni* (Berriman et al. 2009) and the planarian *Schmidtea mediterranea* (Robb, Ross, and Sanchez Alvarado 2008)). We could clearly find related *ta-TRIM* sequences in all *Taenia* spp., which were approximately 50% identical after alignment to the *Echinococcus ta-TRIM*s. This comprised the conserved LTRs and also parts of the region between LTRs, including the crucial PBS and PPT (Supplementary data 1). Furthermore, TSD sequences could usually be found flanking the LTRs of the complete *ta-TRIM*s in these species (Supplementary data 2). In contrast, no similar sequences could be detected in other flatworms, or in GenBank. Because the analyzed species of *Taenia* and *Echinococcus* cover all of the major lineages of taeniid cestodes (Knapp et al. 2011; Nakao et al. 2013), this indicates that *ta-TRIM*s originated at the base of the taeniid tree and are specific for this family.

We classified the *ta-TRIM* elements of *E. multilocularis*, by searching for them by blastn and dividing them into complete/near-complete elements (lacking only a few bases), or into partial elements (lacking at least 20 nucleotides from either LTR). At least 8 almost-complete elements can be found in *E. multilocularis*, but many have substitutions in presumably important positions such as the 5´-CA-3´ motif at the LTRs, or within the PBS and PPT, resulting in only two “perfect” elements (loci 36 and 39 of Supplementary Data 3). In addition, 41 more elements could be found that comprised at least 80% of the length of *ta-TRIM*, and a total of 1058 loci in the genome show significant similarity by blastn to the identified perfect elements of *E. multilocularis*

(threshold = e-10, with hits located less than 2 kb apart counted as single hits). Pairwise divergence between copies that were at least 80% complete was between 1.2% and 22.3%, not taking into account two linked copies (15 kb distance) in chromosome 3 with 0.1% divergence. These numbers may change as newer versions of the *E. multilocularis* assembly are released, but are likely to be close to the real numbers given the high quality of the current one (Tsai et al., 2013). The *ta-TRIM*s of *E. multilocularis* were found dispersed in all chromosomes, and in unplaced contigs (Supplementary Data 4). Among the partial *ta-TRIM* sequences, many consisted of "solo-LTRs", that is, isolated LTR elements. Solo-LTRs are a common derivative of LTR-retrotransposons, and are thought to be originated from unequal crossing-over between LTRs of a single element. Consistent with this origin, many of the solo-LTRs are flanked by TSDs (see below).

Similar results were found in the *E. granulosus* draft genomic assembly. In contrast, in *Taenia solium* at least 14 different "perfect" *ta-TRIMs* can be found, with pairwise divergence between copies of 1.1% to 15.8%. The total number of copies is difficult to assess given the fragmentary nature of the *T. solium* genomic assembly, but 611 loci show significant similarity by blastn to the perfect elements (using the same criteria as for *E. multilocularis*). Only a superficial analysis of the number of *ta-TRIM*s was performed for the unpublished provisional drafts of *T. asiatica* and *T. taeniaeformis*. Results in *T. asiatica* were similar to *T. solium*, and at least 3 perfect *ta-TRIM* elements could be found. In contrast, in *T. taeniaeformis*, although some almost complete *ta-TRIMs* could be found, they were divergent and had substitutions in key positions, suggesting that they are pseudo-elements.

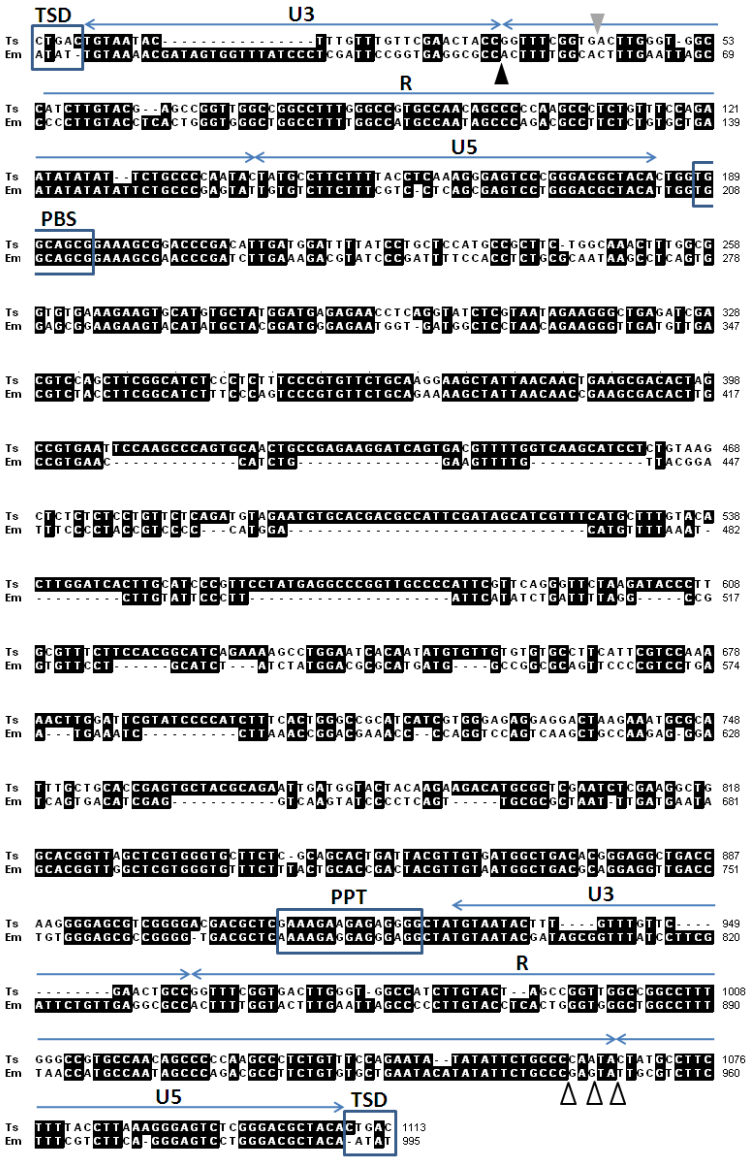

Figure 1. Alignment of *ta-TRIM*s from *Echinococcus multilocularis* (Em) and *Taenia solium* (Ts). The limits of the U3, R and U5 regions of the LTRs are indicated above for Em. The arrowheads in the 5´LTR show the beginning of transcription in Em elements (black), and Ts (grey), as determined from full length ESTs. White arrowheads in the 3´LTR show the 3´end of *ta-TRIM* transcripts in Em, as determined from full length ESTs and 3´ RACE experiments. PBS, primer binding site; PPT, polypurine site; TSD, target site duplications.

Evolution and retrotransposition events of *ta-TRIM*s

Strikingly, *ta-TRIM*s showed high similarity between *E. granulosus* and *E. multilocularis*, as well as between *T. solium* and *T. asiatica* (>90 % for the most similar copies), but had much lower similarity when comparing other species pairs (*ca*. 50 %). Phylogenetic analysis of *ta-TRIM*s from all the analyzed species show that the elements of *Echinococcus* spp. form a well supported clade, as do those of *T. asiatica* plus *T. solium*, and those of *T. taeniaeformis* (Figure 2A). Furthermore, most *T. asiatica* elements form a monophyletic clade. This topology suggests that massive independent expansions of *ta-TRIM* elements occurred in each of the main taeniid lineages, as well as in *T. asiatica*. Alternatively, the reciprocal monophyly between the elements of each species could be the consequence of extensive gene conversion between all of the copies of each genome. We searched for evidence of ongoing gene conversion between copies of *ta-TRIM*s in each species using the program GENECONV (Sawyer 1989; Sawyer 1999). No evidence was found in *E. multilocularis*, *E. granulosus*, *T. asiatica* or *T. taeniaeformis*, but in *T. solium* 4 examples were found that showed statistically significant evidence of gene conversion (global p-values < 0.05). The low levels of gene conversion suggest that the first hypothesis is correct. However, we cannot discard the possibility that gene conversion was more extensive in the past, during the early expansion of *ta-TRIM*s.

We searched for evidence of the occurrence of *ta-TRIM* integration events after the splitting of *E. multilocularis and E. granulosus,* a relatively recent event that was estimated to have occurred between 2.5 and 9.2 million years ago (Knapp et al. 2011). For this, we compared the flanking sequences of complete/almost-complete elements from *E. multilocularis* (at least 2 kb upstream and downstream of each *ta-TRIM*) with the homologous regions of *E. granulosus* (Figure 2B). In three out of seven comparisons, strong evidence of integration could be found, since the *ta-TRIM* is precisely lacking in the equivalent region in *E. granulosus*, and at that position a sequence can be found that is identical or has only one mismatch to the flanking TSD of the *E. multilocularis ta-TRIM* (Figure 2B and Supplementary Data 5). With the same strategy, we searched for integration events after the splitting of *T. solium* and *T. asiatica*, and from five regions that could be compared between these assemblies, three examples showed strong evidence of integration after the splitting of these species.

5. Results

As a result of the particular mechanism of reverse transcription of LTR retrotransposons, both LTRs of each element are initially identical at the time of insertion (Telesnitsky and Goff 1997). Therefore, nucleotide identity between the 5´ and 3´ LTR of each *ta-TRIM* can be used to estimate the time of integration (Kijima and Innan 2010), if the rate of neutral nucleotide substitution is known (calibrated from the fossil record, or from biogeographic vicariance estimates). An important assumption for this method is that gene conversion must not occur between the LTRs (Kijima and Innan 2010). The size of the LTRs of *ta-TRIM*s is around or below the limit for efficient gene conversion in other systems (around 200 bp in mice, and *ca*. 300-500 bp in humans (Chen et al. 2007)). Furthermore, it has been shown in other models that gene conversion is very low when LTRs are very close (< 4 kb distance (Kijima and Innan 2010)). Therefore, this assumption seems to be reasonable in our case. Any gene conversion events between LTRs of different *ta-TRIM*s would be expected to increase their observed divergence values, increasing their estimated insertion date. Thus, any estimates obtained would be a conservative maximum date.

We thus analyzed the divergence between 5' and 3' LTRs for complete/almost-complete *ta-TRIM*s, for one representative of each main taeniid lineage (*E. multilocularis*, *T. solium* and *T. taeniaeformis*; Figure 2C). In *E. multilocularis*, divergence values between LTRs were between 6.1% and 22.9% (n = 21), whereas in *T. solium* they were between 2.2% and 14.9% (n = 25), and in *T. taeniaeformis* between 19% and 27% (n = 3). The distribution of the divergence values of LTRs was significantly different between all species pairs (Mann Whitney Wilcoxon U-Test, Bonferroni correction, $p<0.02$). Assuming equal substitution rates for all lineages, this implies that the waves of retrotransposition occurred at different time points for each lineage, and the relatively large divergence in *E. multilocularis* and *T. taeniaeformis* LTRs further suggests that in these elements *ta-TRIM*s may be no longer active.

There is no fossil record for taeniids, but the neotropical sister species *Echinococcus vogeli* and *Echinococcus oligarthrus* were proposed to have split during the great american biotic interchange, 3 million years ago (Knapp et al. 2011). Unfortunately, there is only very limited sequence information for these taxa. Given the low number of synonymous substitution sites available for analysis, and since we were interested in calibrating non-coding sequences (which can have different rates of neutral

substitution to coding sequences, (Subramanian and Kumar 2003; Hoffman and Birney 2007)), we obtained instead an estimate for the divergence of neutral intronic sequences (Hoffman and Birney 2007) in two available genes. The estimated neutral substitution rate for introns in these species was 7.1×10^{-9} substitutions per site per year, which is well within the margin of rates described for neutral substitutions in other metazoans (Bowen and McDonald 2001; Gillooly et al. 2005; Hoffman and Birney 2007). By applying the substitution rate found for introns on the substitution values of LTRs (corrected using the K2P+G model), we estimated that the most recent *ta-TRIM* insertion occurred 0.84×10^6, 4.76×10^6, and 13.3×10^6 years ago for *T. solium*, *E. multilocularis*, and *T. taeniaeformis*, respectively. Furthermore, by directly comparing the divergence values of LTRs with the divergence values found for introns between *E. multilocularis* and *T. solium* (30.3 ± 3.1 %, n = 7 genes), it is apparent that most insertions must have occurred after the divergence of both lineages. In contrast, divergence in introns between *E. multilocularis* and *E. granulosus* (3.9 ± 0.76 %, n = 8 genes) is of the same magnitude as between the most similar LTRs in *E. multilocularis*, suggesting that the last insertions in *E. multilocularis* occurred approximately at the same time as these species diverged.

In summary, we found evidence for retrotransposition of *ta-TRIM* elements after the divergence of the main lineages of Taeniidae, as well as after the splitting of *E. multilocularis* and *E. granulosus*, and after the splitting of *T. solium* and *T. asiatica*. These elements may still be active (or may have been active until very recently) in *T. solium*, whereas in *E. multilocularis* and *T. taeniaeformis*, it seems that they do not mobilize any longer.

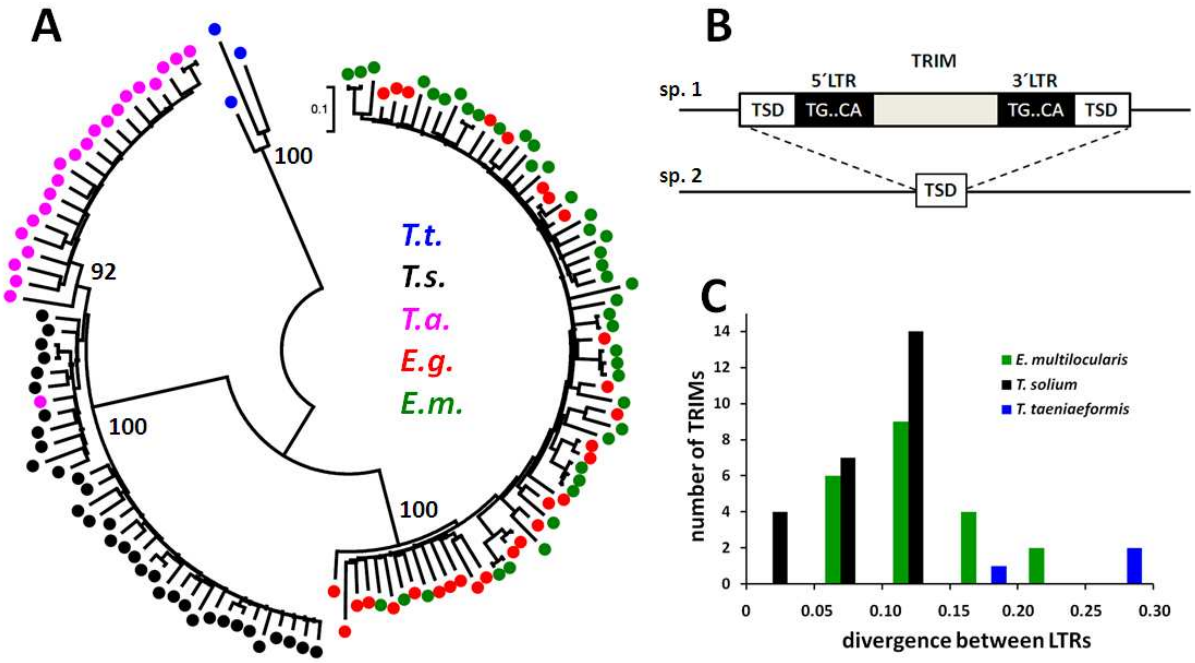

Figure 2. Evolution and insertions of *ta-TRIMs*. A. Phylogenetic tree of ta-TRIMs from taeniid species, inferred by Maximum Likelihood analysis (Kimura 2-parameter model with gamma distributed sites). Bootstrap values (1000 replicates) are indicated next to selected nodes. *Eg*, *E. granulosus*; *Em*, *E. multilocularis*; *Ta*, *T. asiatica*; *Ts*, *T. solium*; *Tt, T. taeniaeformis*. B. Diagram explaining the identification of insertion sites between closely related species (sp.1 and sp.2). C. Histogram showing the divergence of 5´and 3´ LTRs for *ta-TRIMS* of three taeniid species (see the text for details).

A candidate autonomous element for the mobilization of *ta-TRIM*s *in trans*

So far, no specific retrotransposons have been proposed to be responsible for the mobilization of TRIMs in any species (Schulman 2012), probably because the similarity between them may be very limited. Initially, we unsuccessfully looked for candidate retrotransposons in *E. multilocularis* by searching for a short distance (<20 kb) between blastn searches for *ta-TRIM*s and tblastn searches for reverse transcriptases (data not shown). As an alternative, we characterized some of the most complete LTR-retrotransposons in the *E. multilocularis* genome, and compared their sequence to the *E. multilocularis ta-TRIM*s. We found one family of LTR-retrotransposons (which we have dubbed *lennie*) that has characteristics suggesting that it may have fulfilled this role (Supplementary Data 6). In particular, the first 8 bases of the LTR which are crucial for interaction with IN (Zhou et al. 2001) are identical between *ta-TRIM*s and *lennie*. Furthermore, since the cognate tRNAs are specifically packaged into VLPs during the retrotransposition cycle (Boeke and Stoye 1997; Mak and Kleiman 1997), any autonomous elements mobilizing *ta-TRIM*s should have the same PBS. *lennie* has a PBS of 8 bases that is complementary to the same ^{Leu}tRNA as *ta-TRIM*, and is positioned at the same distance from the 5′ LTR. Finally, the length of the TSD generated is characteristic for each IN group (Wu et al. 2005; Ballandras-Colas et al. 2013). Most TSDs of *ta-TRIM*s and solo-LTRs in *E. multilocularis* are 4 bases long (18/19 analyzed cases, with one case of 5 bases), which is coincident with the length of the TSDs for *lennie* elements. We were unable to detect intact copies of *lennie* in the *E. multilocularis* genome (all had at least one frameshift in *pol*). If *lennie* was the element mobilizing *ta-TRIMs in trans*, then the lack of intact *lennie* elements could explain the absence of recent *ta-TRIM* retrotransposition events in *E. multilocularis*.

Due to the draft status of the genome assemblies of *Taenia* spp., we were unable to determine if intact *lennie* elements are present in these species. However, in all the analyzed *Taenia* spp., the TSDs of *ta-TRIM*s were 5 bases long (*T. solium*, 6/6 events; *T. asiatica*, 2/2 events; *T. taeniaeformis*, 2/2 events; the proportions of 4 base long and 5 base long TSDs are significantly different between *T. solium* and *E. multilocularis* by Fisher´s exact test, $p < 0{,}0001$). This suggests that the element mobilizing the *ta-TRIMs* may have been different in *Taenia* spp.

Massive expression of *ta-TRIM*s and generation of novel transcripts from solo-LTRs

Originally, the transcripts of *ta-TRIM*s were noticed in *E. granulosus* due to their massive expression (*ca*. 10% of all ESTs in oligo-capped libraries (Parkinson et al. 2012)). Here, we analyzed a small collection of full length ESTs from *E. multilocularis* metacestodes, and found that also in this species, *ta-TRIMs* are very highly expressed (1.8% showed significant [< e-5] similarity to *ta-TRIM*s by blastn, n = 4195 ESTs). In *T. solium*, a similarly high proportion of ESTs in GenBank showed similarity to *ta-TRIM*s, (1.4 %, n = 74730 ESTs).

By using diverse EST libraries of *E. multilocularis* (see materials and methods) we searched for *ta-TRIM*-like transcripts by blastn and mapped them to the genome of *E. multilocularis* under stringent requirements (single mapping position in the genome with >99% identity to the EST). In this way, we identified 73 different loci with similarity to *ta-TRIM*s and with strong evidence of transcriptional activity, which we then manually curated. For 63 loci, transcription was apparently originated from within an LTR (Figure 2 and Figure 4; Supplementary Data 4), strongly indicating that it was generated from an LTR promoter and not by readthrough from upstream genes.

25 loci corresponded to full-length *ta-TRIM*s, which in most cases showed several deletions and substitutions of presumably important sites, but which nonetheless had two LTRs (Figure 3A). Alternative *cis*-splicing events were sometimes detected within the *ta-TRIM* for these loci, and were confirmed for one locus by 3´ RACE (Figure 3A). No transcriptional readthrough was detected downstream of the U5 region of the 3´ LTR for complete *ta-TRIM*s. The other 38 loci corresponded to transcription initiation from solo-LTRs, and these showed two main distinct behaviors. In some cases, solo-LTRs generated internal transcripts, from the U3/R limit to the R/U5 limit, indicating that in the absence of *ta-TRIM* sequences downstream to the LTR, short "abortive" transcripts are generated (Figure 3B, example 3). These are reminiscent of short transcripts originating from mutant retroviruses in which polyadenylation is no longer repressed in the 5´ LTR (Schrom et al. 2013). For 16 loci, only this kind of transcripts was found. Other solo-LTRs (22 loci) showed transcriptional readthrough

into the downstream neighboring regions, accompanied in some cases by short internal transcripts. In most cases this resulted in the generation of lncRNAs, which were in many cases *cis*-spliced (Figure 3B, panels 1 and 2). In 5 loci, the solo-LTR promoter initiated transcripts that were fused to a downstream coding gene, generating an alternative isoform under the control of the solo-LTR (Figure 4). The predicted amino acid sequences of the downstream genes were always conserved (at least among all cestodes analyzed) strongly indicating that they correspond to protein-coding genes.

We further confirmed by RT-PCR these transcriptional fusions for 3 out 4 investigated loci (the fourth transcriptional fusion may also occur, but the RT-PCR unspecifically amplified a transcript from a different *ta-TRIM* locus). Control RT-PCRs in which the forward primer was located ≤200 bp upstream of the solo-LTRs, as well as in the U3 region within the LTR, gave no amplification, providing strong confirmatory evidence that the transcript is initiated within the solo-LTR (data not shown). For most loci, analysis of RNAseq data suggested that the new LTR promoter is a minor alternative one, but in the case of locus 8 (shown in Figure 4B) it seems to be the main or only promoter (data not shown).

Very interestingly, three of these loci were found to differ between *E. multilocularis* and *E. granulosus*. In one case, a complete *ta-TRIM* element was found in the corresponding *E. granulosus* region, which presumably would not generate fusion transcripts (locus 64, Figure 4G). No *ta-TRIM* or solo-LTR was found for the other two cases in *E. granulosus* (loci 8 and 21), and because the loci are collinear except at the precise position of the solo-LTR, this suggests that a *ta-TRIM* was inserted and reduced into a solo-LTR after the divergence of both species (Figure 4F and data not shown). The *E. granulosus* ortholog of locus 21 is a trans-spliced gene (evidence from two independent ESTs, BI244081.2 and CV681147.1, containing the *E. granulosus* spliced leader (Brehm *et al*., 2000) at the 5´end). In *E. multilocularis* the LTR-initiated transcript is spliced in *cis* to an exactly corresponding splice acceptor site (Figure 4C), suggesting that it competes for this site with the spliced-leader.

In summary, *ta-TRIM*s and derived solo-LTRs are massively transcribed in *E. granulosus*, *E. multilocularis* and *T. solium*. In *E. multilocularis*, we provide strong evidence for the generation from dispersed solo-LTRs of novel lncRNA and alternative

splicing isoforms for coding genes. Some of these *ta-TRIM* elements are absent in the corresponding regions in *E. granulosus*, suggesting that these differences were generated during or after their speciation.

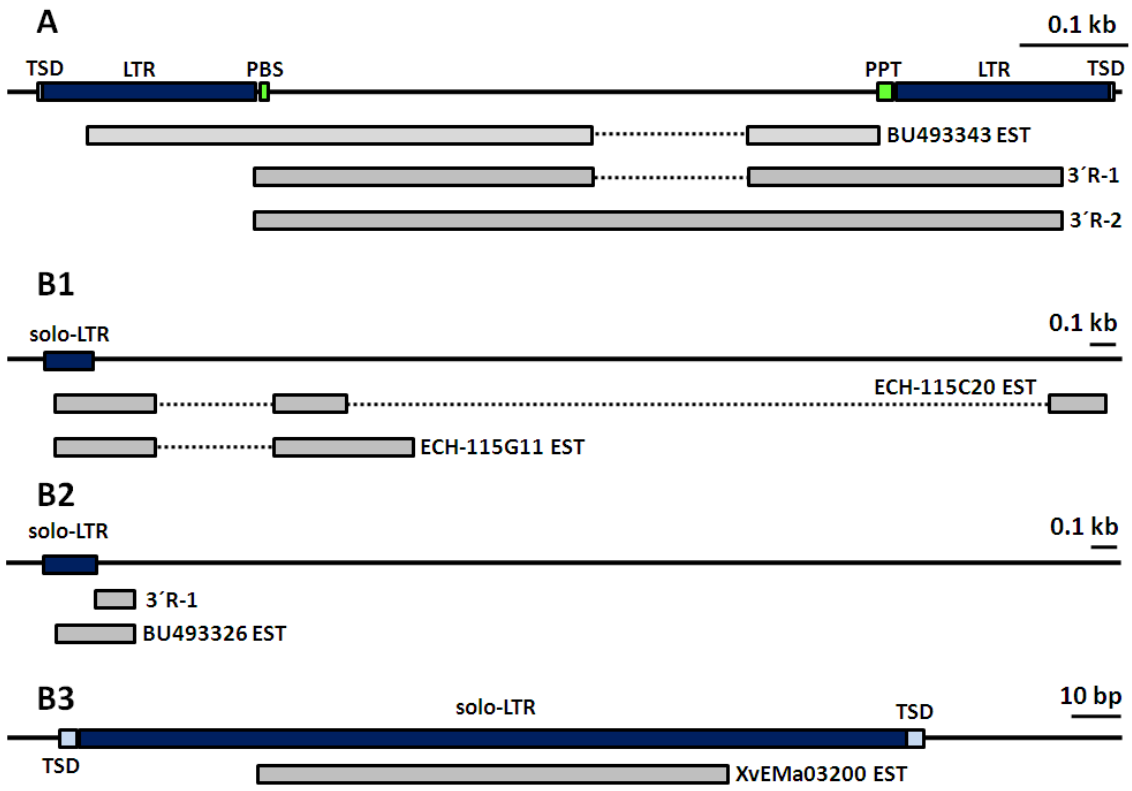

Figure 3. Transcription of *ta-TRIM* and derived elements in *E. multilocularis*. Continuous lines indicate the genomic locus, and EST and 3´RACE (3´R) data are shown below, with mapped regions drawn as grey rectangles, and intervening introns as dotted lines connecting them. A. Example of a full length *ta-TRIM*. B1-B3, examples of solo-LTRs initiating the transcription of diverse non-coding RNAs (see the main text for details).

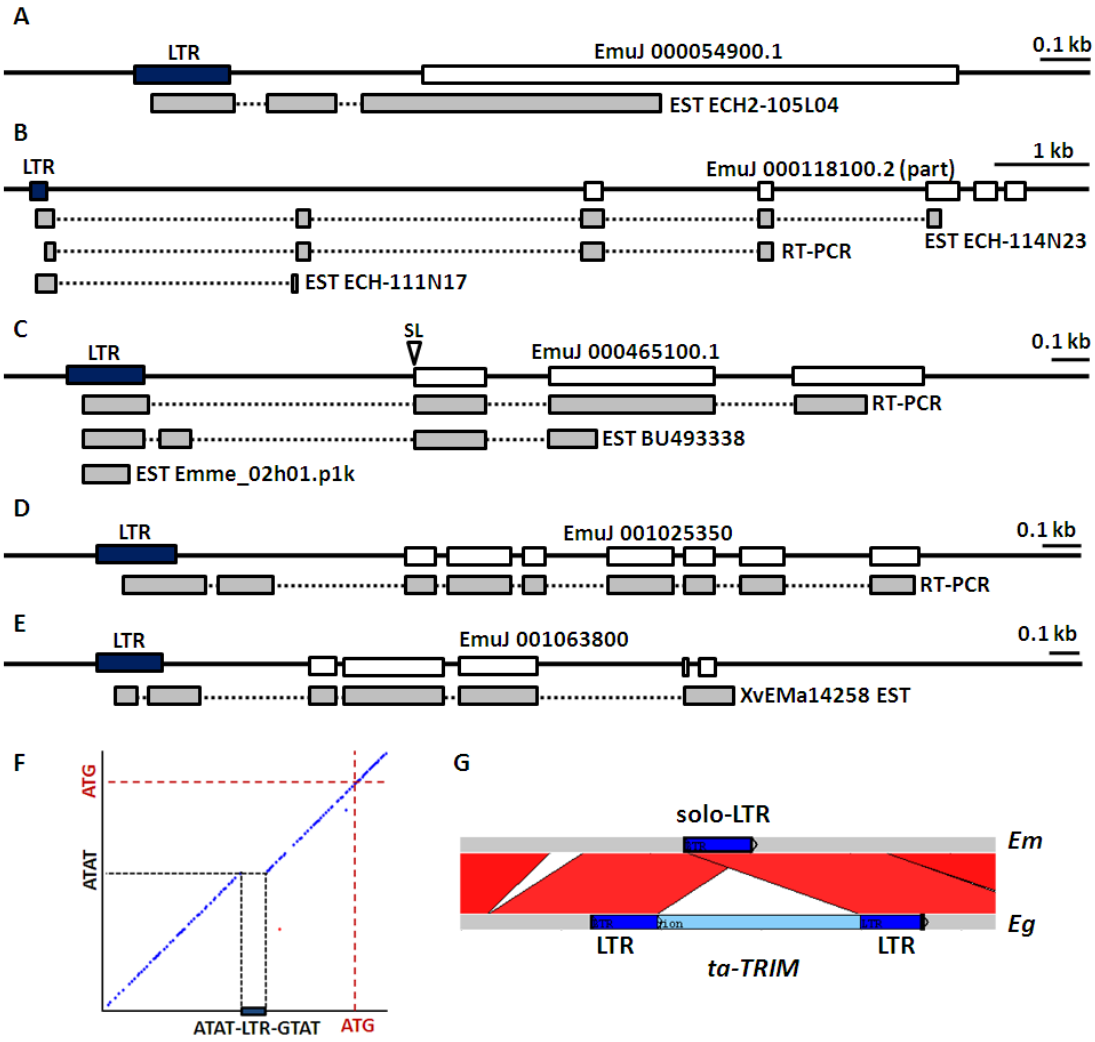

Figure 4. Transcriptional fusions of solo-LTRs and downstream coding genes. Drawings are as in Figure 3. "RT-PCR" indicates sequenced RT-PCR products obtained in this work. The white arrowhead ("SL") in panel C indicates the position of the trans-splicing acceptor site in the ortholog of *E. granulosus*. Not all alternative splicing isoforms that were obtained are shown. A. Locus 2. B. Locus 8. C. Locus 21. D. Locus 60. E. Locus 64. F. Dot plot (identity within 10 bp windows is shown as blue dots) of the 2 kb region upstream of the start codon (ATG) of EmuJ_000465100 (Locus 21) and the ortholog region of *E. granulosus*. The solo LTR (blue rectangle) is precisely lacking in *E. granulosus*, and a similar sequence is seen at this position as in the TSDs of the solo-LTR of *E. multilocularis*. G. Comparison of the upstream region of locus 64 in *E. multilocularis*, where a solo-LTR found, with the ortholog region in *E. granulosus*, containing a full length *ta-TRIM*. Red bars indicate blastn hits. Drawing generated with WebACT (Abbott et al. 2005).

Expression of *ta-TRIM*s in *E. multilocularis* germinative cells

Finally, we performed whole-mount in situ hybridization (WMISH) with a *ta-TRIM* probe to analyze at the cellular level the expression of *ta-TRIM*s during the development of the metacestode larva of *E. multilocularis*. Within the metacestode cysts, the cells are organized as a thin layer (the germinal layer), which has dispersed germinative cells (stem cells). These germinative cells are the only proliferating cell type in the larva, whereas all differentiated cells are post-mitotic (Koziol et al. 2014). The *ta-TRIM* probe showed a strong and specific signal in dispersed cells with the characteristic morphology of the germinative cells (small sized, pear-shaped to fusiform cells with a high nucleo-cytoplasmic ratio, and one or more large nucleoli (Gustafsson 1990; Reuter and Kreshchenko 2004; Koziol et al. 2014)) (Figures 5A and 5H). Furthermore, they were in average 23 % of all cells in the germinal layer (n = 2 independent WMISH experiments with two different isolates, 1130 total cells counted), which corresponds well to the proportion of germinative cells as estimated by morphology (21 % to 25 % of all cells, (Koziol et al. 2014)). Finally, the *ta-TRIM* signal is observed in 94.3 % of all cells undergoing S-phase, as determined by their incorporation of the thymidine analog 5-Ethynyl-2′-deoxyuridine (EdU) (n = 3 independent WMISH experiments with three different isolates, 427 total cells counted). All of these results strongly indicate that *ta-TRIM*s are specifically expressed in the germinative cells, and only very low or null levels can be seen in other cells. Furthermore, *ta-TRIM*s appear to be expressed in almost all of the proliferating germinative cells, given the high co-localization of *ta-TRIM*s with EdU incorporation.

Throughout the development of protoscoleces from the germinal layer, the *ta-TRIM*+ cells show the stereotypical distribution of the germinative cells (Koziol et al. 2014) and continue to incorporate EdU (Figure 5B-G). They massively accumulate during the early budding process that leads to the formation of brood capsules (thickenings of the germinal layer that invaginate into the cyst, where protoscolex development proceeds (Koziol, Krohne, and Brehm 2013), Figure 5 B), as well as during early and intermediate protoscolex formation, except at the apical most region were no proliferation is observed (Figure 5C and 5D). At the last stages of development,

expression is restricted to ever decreasing cell numbers in the posterior body, whereas in the scolex (the head of the protoscolex with the attachment organs) expression is only observed in the proliferative region at the base of the suckers (Galindo et al. 2003; Koziol et al. 2014) (Figures 5 E-G). In summary, during the development of the metacestode larva, the *ta-TRIM* WMISH signal is strongly and specifically observed in the germinative cells.

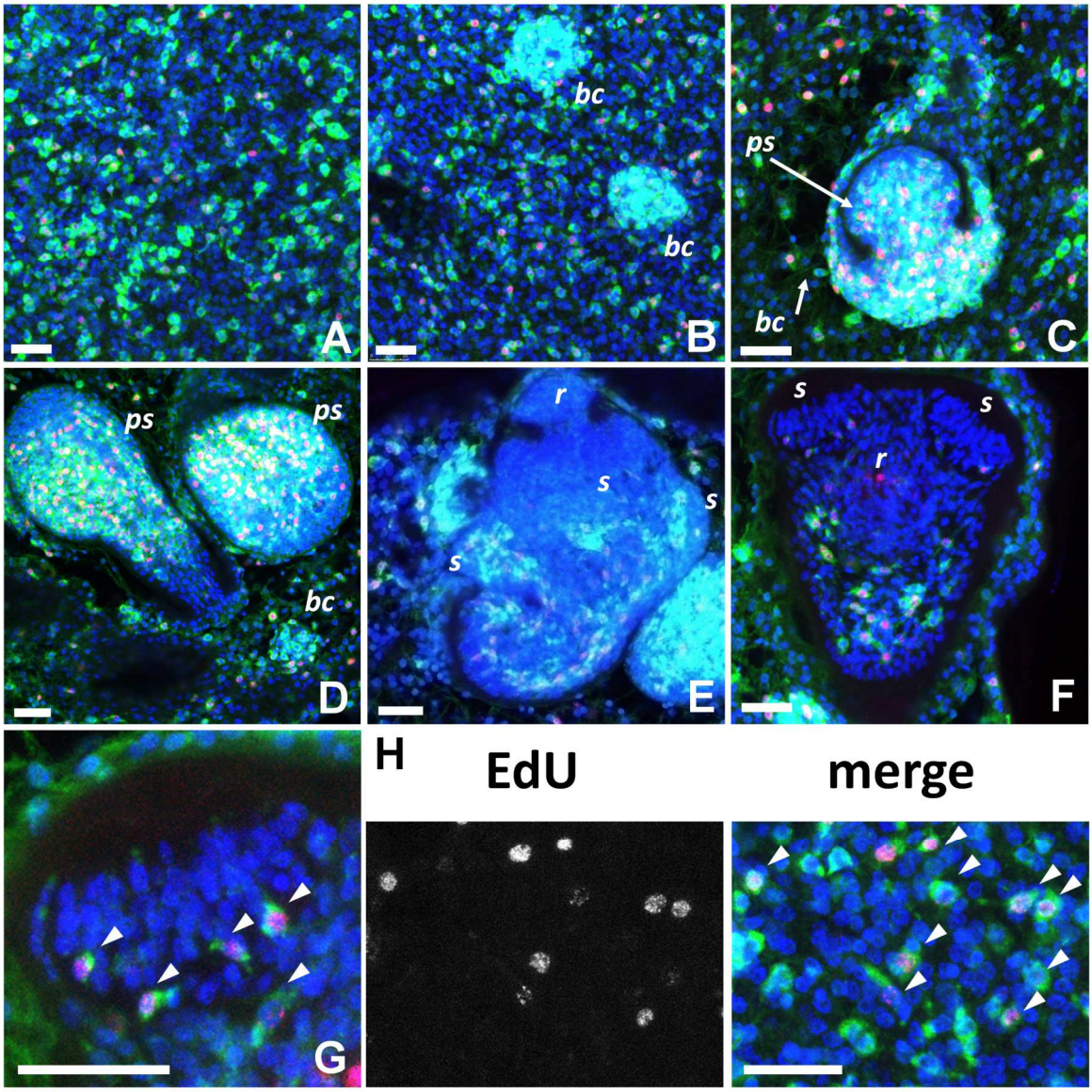

Figure 5. WMISH analysis of *ta-TRIM* expression during *E. multilocularis* larval development. In all panels, the *ta-TRIM* WMISH signal is shown in green, DAPI (all nuclei) in blue, and EdU detection in red (EdU was incorporated during a 5 hour, 50 µM pulse, *in vitro*). Staging follows the system of Leducq and Gabrion (1992). **A.** Germinal layer. **B.** Early formation of brood capsule buds (bc) from the germinal layer. **C.** Early formation of the protoscolex (ps; stage 1). **D.** Early formation of the protoscolex (ps; stage 2). **E.** Intermediate protoscolex development (stage 3-4). *r*, rostellum; *s*, sucker primordia. **F.** Late protoscolex development (already invaginating, stage 6). *r*, rostellum (red signal in rostellum comes from auto-fluorescence of the hooks); *s*, suckers. **G.** Detail of the sucker of the protoscolex shown in (F). Arrowheads point at EdU^+ *ta-TRIM* $^+$ cells at the base of the developing suckers. **H.** Detail of the germinal layer. Arrowheads point at EdU^+ *ta-TRIM* $^+$ cells. Bars, 25 µm.

Discussion

Convergent reductive evolution of LTR-retrotransposons into TRIMs

In this work, we describe a new family of TRIM elements that is found exclusively in taeniid cestodes, and has expanded during the divergence of this family. So far, TRIM-like elements have been described in plants (Witte et al. 2001; Kalendar et al. 2008), fungi (Dos Santos et al. 2012) and in two distant metazoan groups: ants (Zhou and Cahan 2012), and taeniid cestodes (this work). The TRIM elements of each of these taxonomic groups show no similarity to each other, and are therefore a likely case of convergent reductive evolution, in which different retrotransposons are stripped of all non-essential sequences as they parasitize autonomous elements for retrotransposition (Schulman 2012). As such, TRIM-like elements are probably widely present in the genomes of other groups, but their discovery is difficult since they possess no similarity to other TRIM-like elements, have only short LTRs, and lack coding sequences. In our case, the discovery was prompted by the high expression of these elements in cestodes, but silent or lowly expressed TRIMs would easily escape detection.

The distribution of individual TRIM families in animals seems to be more restricted than in plants, since similar TRIM elements are found throughout mono and dicotyledons (Witte et al. 2001; Kalendar et al. 2008). Interestingly, very similar TRIMs have been described in distant ant species and the tree of TRIM elements in ants shows no correspondence with the species tree, suggesting horizontal transfer events between species (Zhou and Cahan 2012). In sharp contrast, we find that phylogenetic clades of *ta-TRIM*s are specific to individual taeniid lineages (Figure 2A). This is strong evidence against horizontal transference of these elements, and suggests that independent expansions of *ta-TRIM*s occurred in each lineage. Further support for this comes from the fact that the distribution of estimated insertion dates are significantly different for *ta-TRIM*s of each species investigated (Figure 2C), and that specific insertions occurred after the divergence of closely related species (Figure 2B). However, we cannot rule out the possibility that the phylogenetic pattern is caused by extensive gene conversion between *ta-TRIM* elements in each genome. In general, ectopic gene conversion would not be expected to maintain sequence similarity for such a large number of elements

widespread throughout the chromosomes (Chen et al. 2007). However, it has been shown that LTR-retrotransposons in *Saccharomyces cerevisiae* can undergo ectopic gene conversion between the genomic DNA copies and the cDNA intermediates (Melamed, Nevo, and Kupiec 1992), and similar mechanisms have been proposed to mediate gene conversion between non-linked loci in other organisms (Kass, Batzer, and Deininger 1995; Benovoy and Drouin 2009). Therefore, high levels of rtnDNA could result in genome-wide gene conversion events. Furthermore, we observed evidence for ongoing gene conversion in *T. solium*. At this point, it is not possible to decide between both explanations for the observed phylogenetic pattern, but large scale studies of synteny of *ta-TRIM*s in all the species may be able to distinguish between them, once less fragmentary genomic assemblies are available.

Except for a few cases in which the retrotransposon and the NA-element showed extensive sequence similarity (*e.g.* the LARD *Dasheng* and the retrotransposon *RIRE-2* in rice, (Jiang, Jordan, and Wessler 2002)), few pairs of NA-elements and their possible mobilizing retrotransposons *in trans* have been proposed. In the case of TRIMs, no candidate has been identified so far. It is possible that in TRIMs, extensive sequence reduction has limited similarity to a few key positions for interaction with RT and the primer tRNA (the PBS and PPT) and with INT (the ends of the LTRs), and that most of the specificity is achieved by the specific packaging of the TRIM RNA into the VLP particle (Friedl et al. 2010). Packaging is dependent on the PSI element, which is only conserved at the secondary structure level (Wicker et al. 2007) and therefore difficult to identify. Based on this, we propose that the element *lennie* may have been the factor mobilizing *ta-TRIM*s in *E. multilocularis*. The absence of identifiable intact *lennie* elements in the genome could explain the lack of recent retrotransposition events in *E. multilocularis*, as well as the absence of gene conversion events (since no cDNA copies would be produced). Furthermore, it would be expected that competition with highly expressed *ta-TRIM* elements could drive the extinction of an autonomous retrotransposon group such as *lennie*, as the rate of their own retrotransposition decreases and the existing copies accumulate deleterious substitutions (Schulman 2012). In *Taenia* spp., the different size of TSDs as compared with *E. multilocularis* gives evidence that a different element may be the mobilizing factor in *trans*, since TSD size is specific for each IN group (Zhou et al. 2001; Ballandras-Colas et al. 2013). This

implicates a unique shift of "host" (mobilizing factor) during the evolution and divergence of *ta-TRIM*s in taeniids.

Expression of *ta-TRIM* elements and the generation of new transcripts

The EST evidence suggests that in all the analyzed taeniid species, TRIMs are transcribed at very high levels (> 1 % of all polyadenylated RNAs). Furthermore, the presence of solo-LTRs has a clear effect in the expression of downstream sequences in *E. multilocularis*, resulting in many new lncRNA, and in alternative promoters for coding genes (Figures 3 and 4). Therefore, although the elements may no longer be active for retrotransposition in *E. multilocularis*, they have extensively modified its transcriptome. The evidence we show here is very conservative: more examples of lncRNA originating from solo-LTRs can be found when using slightly lower stringency values for the mapping of ESTs (data not shown), and it is likely that many more examples will be found with larger datasets, given the number of positions (> 1000) with similarity to *ta-TRIM*s in the genome. Usage of retrotransposons as alternative promoters and as a source of new lncRNA has been described for many individual examples, and also at a large global scale for model organisms such as humans, mice and Drosophila (Peaston et al. 2004; Cohen, Lock, and Mager 2009; Faulkner et al. 2009; Kelley and Rinn 2012; Lenhard, Sandelin, and Carninci 2012; Batut et al. 2013). It has been proposed that this can result in evolutionary innovation in the expression patterns of the involved genes, and may lead to the coordinately regulated expression of various genes, as they acquire the expression pattern of the invading retrotransposons (Peaston et al. 2004; Batut et al. 2013). The finding of splicing between a solo-LTR and an ancestral trans-splicing acceptor site (Figure 4C) provides a novel and simple evolutionary mechanism by which LTR retrotransposons can be "captured" as alternative promoters. In this model, the pre-existing trans-splicing acceptor site (as found in *E. granulosus*) is spliced to an appropriate splice-donor site originating from the new LTR. This donor site may be there by mere chance, since it does not need to be a particularly strong one (*e.g.* a simple 5′-GT-3′ motif). This is because the spliceosome has a "donor-first" syntaxis, in which a cis-splicing site efficiently out-competes the spliced-leader for a downstream splicing acceptor site (Hastings 2005).

The generation of lncRNA from solo-LTRs seems to be a simple consequence of downstream transcriptional readthrough. However, lncRNAs have been recently shown to have many functions for the regulation of gene expression *in trans*, and the transcription of lncRNA itself may also alter gene expression *in cis* (Mercer, Dinger, and Mattick 2009; Kornienko et al. 2013). Therefore, some of these new lncRNAs may have been exapted for new functions in *E. multilocularis*.

The differences in *ta-TRIM* transcriptional fusions between *E. multilocularis* and *E. granulosus* suggest that they could lead to differences in gene regulation between both species. Furthermore, because of the stem cell specific expression of *ta-TRIM*s (Figure 5), this could lead to novel stem-cell specific transcripts. Future comparative analyses of the *ta-TRIM* derived transcriptome of both species may identify many more examples. It is possible that the differences in *ta-TRIM* derived transcripts between *Echinococcus* spp. have contributed to some of the important differences in morphology and development found between these closely related species (Thompson 1986), particularly since the gene complement of both species is almost identical (Olson et al. 2011; Tsai et al. 2013).

ta-TRIMs as a germinative cell marker in *E. multilocularis*

The WMISH experiments (Figure 5) provide very strong evidence of a germinative cell specific expression of *ta-TRIM*s throughout the development of the metacestode larva from the cyst wall to the mature protoscolex. The germinative cells of *E. multilocularis* larvae are a morphologically homogeneous population of undifferentiated cells, which however show heterogeneity at the molecular level in the expression of conserved stem cell regulators such as *nanos* and *argonaute* genes (Koziol et al. 2014). This suggests that there may be in reality several sub-populations with different proliferation and/or self-renewal potencies. In contrast, it seems that *ta-TRIM*s are expressed in almost all of the morphologically defined germinative cells, and are therefore the best molecular marker so far for the total germinative cell population. The small number of EdU^+ *ta-TRIM* $^-$ cells (*ca*. 5 % of all EdU^+ cells) could indicate the existence of a different small sub-population of germinative cells, or could be the result of fluctuating silencing of these elements in the germinative cells. At this point, nothing

is known about the mechanism by which cestodes silence MGEs in the absence of a canonical Piwi pathway (Skinner et al. 2014), but a comparison of the chromatin structure and histone modifications between *ta-TRIM* loci and autonomous, silenced retrotransposons may provide a first experimental strategy towards its elucidation. It is possible that taeniid cestodes control the expansion of *ta-TRIM*s by simply repressing the autonomous element mobilizing *ta-TRIMs in trans*. This would explain the absence of strong deleterious effects in the face of massive *ta-TRIM* expression.

From an evolutionary point of view, expression of *ta-TRIM*s in somatic stem cells which will eventually form all of the tissues of the next life stage (including the germ line) would allow the expansion and transmission of *ta-TRIM*s in the genome of the next generation. At this point, we do not know if *ta-TRIM*s are also expressed in the germ line in the gonads of the adult stage. However, published RNAseq data (Tsai et al. 2013) show expression in the adult stage, suggesting that this is possible (data not shown). It would be interesting to determine if in planarians, which can also generate the germ line from somatic stem cells after embryonic development, specific retrotransposon families also show a stem-cell specific expression.

The expression of retrotransposons in somatic stem cells of *E. multilocularis* is analogous to the highly specific expression of several endogenous retrovirus families during early mammalian development, before the specification of the germ line (Brulet et al. 1985; Evsikov et al. 2004; Peaston et al. 2004), as well as in the germ line itself (Dupressoir and Heidmann 1996): only expression at these stages may result in the expansion of endogenous retroviruses in the genome of the following generation. Indeed, expressed endogenous retroviruses have been shown to be excellent markers for totipotency or pluripotency in the early mammalian embryo and in embryonic stem cells (Santoni, Guerra, and Luban 2011; Macfarlan et al. 2012). It has been shown that many genes specifically expressed in pluripotent embryonic cells are transcribed from similar upstream LTR promoters (Macfarlan et al. 2012; Fort et al. 2014), and this has been proposed to result in the concerted expression of genes important for pluripotency. The widespread presence in *E. multilocularis* of transcription from solo-LTRs and their presumably stem-cell specific expression suggest that similar mechanisms may be at play in the stem cells of taeniid cestodes.

Materials and methods

ESTs and genomic assemblies.

Genomic assemblies from *Echinococcus multilocularis*, *Echinococcus granulosus*, *Taenia solium* and *Hymenolepis microstoma* (Tsai et al. 2013) as well as *Schistosoma mansoni* (Berriman et al. 2009) were downloaded from the GeneDB database at the Wellcome Trust Sanger Institute (genedb.org). Draft assemblies of *Taenia asiatica*, *Taenia taeniaeformis*, *Mesocestoides corti* and *Diphyllobothrium latum* were generated by the Parasite genomics group of the Wellcome Trust Sanger Institute in the context of the 50 helminth genomes initiative, and are available at ftp://ftp.sanger.ac.uk/pub/project/pathogens/HGI. ESTs from *Taenia solium* were downloaded from GenBank, and ESTs from *Echinococcus* spp. were collected from GenBank, GeneDB and the *Echinococcus* Full-Length cDNA project (http://fullmal.hgc.jp/index_em_ajax.html).

Search *for ta-TRIM* ESTs and genomic loci

Initially, we performed blastn searches of *Echinococcus* spp. ESTs and genomic loci with similarity to the previously described Cluster A of lncRNAs of *E. granulosus* (Parkinson et al. 2012), as well as against the EgRep repetitive element (Marin et al. 1993). Once the loci were recognized due to their characteristics as possible TRIMs, complete *ta-TRIM* elements from *E. multilocularis* were used for blastn searches in other cestodes and flatworms. Because of the divergence between *ta-TRIM* sequences in different taeniid species, the manually identified *ta-TRIM* sequences from each species were used for new blastn searches, in the same as well as in other species. A list of complete and almost complete elements was extracted for each species from these blastn results, which was used for analysis of TSD sites, LTR divergence and comparison of synteny between species. A longer list containing all fragments longer than 800 bp from each species was compiled for phylogenetic analyses.

5. Results

ESTs of *E. multilocularis* with similarity to *ta-TRIMs* were mapped by blastn, eliminating all hits with < 99 % identity to the genome or smaller than 50 bp, as well as those which mapped to more than one region in the genome with > 99 % identity. The resulting loci, plus a duplicated genomic locus which was supported from 3´RACE experiments, were collected and manually analyzed to determine if they were complete *ta-TRIMS* or solo-LTRs, whether transcription was likely initiated from within an LTR, and whether there was downstream transcriptional readthrough into neighboring intergenic regions or coding genes.

Identification of the *ta-TRIM* primer binding site (PBS).

A list of *E. multilocularis* tRNA genes was generated from the genomic assembly with tRNAscan-SE (Lowe and Eddy, 1997). The 3´ region of these tRNAs was compared to the region immediately downstream of the 5´ LTR. Only a family of ^{Leu}tRNA genes was identified as having complementarity for 8 or more bases in this region.

Phylogenetic analysis

An alignment of complete *ta-TRIM* elements and fragments longer than 800 bases from all species was performed with ClustalW (Thompson, Higgins, and Gibson 1994), and the region corresponding to the 5´ LTR was removed (since it is not independent from the 3´ LTR sequence). Maximum Likelihood phylogenetic analysis was performed using MEGA 5.0 (Tamura et al. 2011), under a Kimura 2-parameter model with gamma distributed sites (K2P+G, gamma parameter = 1), which was the model that gave the best fit to the data using the "find best DNA/protein models (ML)" feature.

Comparison of *ta-TRIM* loci between taeniid species

When comparing *ta-TRIM* loci for evidence of integration, each locus with a complete or almost complete *ta-TRIM* of *E. multilocularis* was blasted together with 2

kb of upstream and downstream flanking sequence to the *E. granulosus* genome. Blast hits with <80% identity upstream or downstream of the *ta-TRIM* were discarded, and the retrieved sequences were aligned with ClustalW and manually inspected. The same procedure was performed when comparing *T. solium* and *T. asiatica*.

Search for gene conversion

Alignments of *ta-TRIM*s for each taeniid species were analyzed using the program GENECONV (Sawyer 1999), which looks for statistically significant tracts of identity between two sequences, given their overall divergence. Global *p*-values below 0.05 were considered significant.

Estimates of substitution rates from introns and divergence between LTRs

Introns from the *elp* and *pold* genes from *E. vogeli* and *E. oligarthrus* (Knapp et al. 2011) were retrieved from GenBank and aligned using ClustalW. The first 10 and the last 30 bases of each alignment were discarded (to remove functional splice sites, Hoffman and Birney 2007) and the substitutions per site (transitions and transversions only) under a K2P+G model were estimated using MEGA 5.0 (Tamura et al. 2011). The intron neutral substitution rate was estimated from the average of K2P+G estimates of both genes using the formula r = s / 2t, where r is the substitution rate, s the estimated substitutions per site, and t the time of divergence (set as 3 million years for *E. vogeli* and *E. oligarthrus*). For *E. multilocularis*, *E. granulosus* and *T. solium*, divergence values were also estimated for other well characterized genes (*emmpk2*, *emsmadC*, *emmpk1*, *emraf*, *emegfr*, and *emir1* from *E. multilocularis* (Spiliotis, Kroner, and Brehm 2003; Spiliotis et al. 2005; Spiliotis et al. 2006; Gelmedin, Caballero-Gamiz, and Brehm 2008; Zavala-Gongora et al. 2008; Hemer et al. 2014), *egpum1* from *E. granulosus* (Koziol, Marin, and Castillo 2008), and their orthologs retrieved from the other species). When comparing *T. solium* and *E. multilocularis*, only the shortest introns showing trustworthy alignments were included, and therefore the divergence values between both species are conservative.

The 5′ LTR and 3′ LTR was aligned for each complete and almost complete *ta-TRIM* element from each species. The actual per site divergence, as well as the total estimated substitutions per site (transitions and transversions only) under a K2P+G model, were calculated using MEGA 5.0 (Tamura et al. 2011).

3′ Rapid amplification of cDNA ends (RACE) and RT-PCR.

Reverse transcription was performed with 700 ng of total RNA from *in vitro* cultured *E. multilocularis* larvae (Spiliotis and Brehm 2009) using Prime-Script reverse transcriptase (Takara) as instructed by the manufacturer, with the primer AAGCAGTGGTATCAACGCAGAGTAC-T_{30}-VN. RT-PCRs were performed with 2 µl of cDNA per reaction using KOD polymerase (Millipore). For 3′ RACE, a semi nested RT-PCR approach was performed, using degenerate forward nested primers for the U5 region of several *ta-TRIM*s (TGTGTCTTCTTTCGTNTTCAGGGAG and TCAGGGAGTCYYGGGAYGCTACA for the first and second PCR reactions, respectively) and the reverse primer AAGCAGTGGTATCAACGCAGAGTAC. For confirming the transcriptional fusions between solo-LTRs and downstream coding genes, the following primer combinations were used: locus 8, TTCGTCTTCTTTCGTCTTCAGAGAG and GCATCCTTGATCGAAGTTTGGG (fusion to EmuJ_000118100); locus 21, CTTTTGTACTTTGAGTTAGCCCCTTGTAC and CCATGGCGAAATCGACCAC (fusion to EmuJ_000465100); locus 60, CCTTGTACCTAGCTAAGAGGGCTGAC and CGACGTAGGCACTCAAGCAAG (fusion to EmuJ_001025350); locus 2 (the only one for which RT-PCR was unsuccessful, due to unspecific amplification from another *ta-TRIM* element), CCGAGTATTGTGTCTTCTTTCGTCTTC and CGGAATGACATTTGGCAAAGTC (fusion to EmuJ_000054900). All products of the expected size were gel-purified, cloned into pJET1.2 (Thermo-Scientific), and several clones were sequenced for each product.

Whole-mount in situ hybridization (WMISH)

Fluorescent WMISH of *in vitro* cultured *E. multilocularis* larvae was performed with a digoxigenin-labeled antisense probe, corresponding to the region interior to the LTRs of the *ta-TRIM* locus 39 of *E. multilocularis* (Supplementary Data 3), as described (Koziol et al. 2014). Primers TTGGTGGCAGCGGAAAGC and CCTCTTTTGAGTGTTATCCCCAGC were used to amplify the probe region from genomic DNA of *E. multilocularis*, and the product was cloned into pJET1.2 (Thermo-Scientific). Three independent experiments with different laboratory isolates were performed. These isolates were GH09 and Ingrid/10, obtained from accidental infections of Old World Monkeys in a breeding exclosure (Tappe et al. 2007), and MS10/10, obtained from an infected dog. All isolates had been kept in the laboratory by serial peritoneal injection into *Meriones unguiculatus* for 4 years or less. Control WMISH experiments using the corresponding sense probe were always negative (data not shown). *In vitro* EdU labeling (50 μM for 5 hours) and detection were performed as previously described (Koziol et al. 2014).

Supplementary data

Supplementary Data 1. Alignment of examples of *ta-TRIM* elements from taeniids.

Supplementary Data 2. Target Duplication Sites (TSDs) found in *ta-TRIM* elements from taeniids. Abbreviations are as for Figure 2A.

Supplementary Data 3. List of *E. multilocularis* loci with similarity to *ta-TRIM*s and with evidence of transcription from ESTs and 3' RACE analyses. Locus number and the position of ESTs and 3' RACE sequences (mapped by blastn analyses) are indicated, as well as the manual annotation of the loci. Note that one EST may have several discontinuous blast hits due to the presence of introns.

Supplementary Data 4. Distribution of *ta-TRIM*-like sequences in *E. multilocularis* chromosomes and unplaced contigs.

Supplementary Data 5. Examples of integrations of *ta-TRIM*s after the divergence of *Echinococcus* spp., and of *Taenia* spp. Alignment of a *ta-TRIM* element and its surrounding region from *E. multilocularis* with the ortholog region of *E. granulosus*, and of a *ta-TRIM* element and its surrounding region from *T. solium* with the ortholog region of *T. asiatica.*

Supplementary Data 6. Example of *lennie* element from *E. multilocularis*.

5.3. CHAPTER 3: Further experimental results regarding the *E. multilocularis* stem cell system.

In this chapter, I will describe further experiments that I performed for the characterization of the *Echinococcus multilocularis* stem cell system, which were not included in the previous articles. Some of these results were included within other articles of which I am a co-author, as indicated.

5.3.1. The cell-cycle kinase *em-plk1* is expressed in *E. multilocularis* germinative cells

Polo-like kinases (PLKs) are a family of Serine/Threonin kinases with important roles in the regulation of cell-cycle progression in eukaryotes (Archambault and Glover 2009). Within this family, PLK-1 is specifically expressed during the late G2 and M phases of the cell-cycle, and has a key conserved role in regulating the transition through mitosis (Winkles and Alberts 2005). PLK-1 homologs were also shown to be expressed in the neoblasts of planarians and neoblast-like cells of the trematode *Schistosoma mansoni* (Labbe et al. 2012; Collins et al. 2013).

During his doctoral thesis, Andreas Schubert characterized *em-plk1*, the *E. multilocularis* ortholog of *plk-1*. Because in *E. multilocularis* only the germinative cells proliferate, it was likely that *em-plk1* was specifically expressed in these cells. As part of the characterization of *em-plk1*, I determined its gene expression pattern during *E. multilocularis* larval development by means of WMISH (Figure R3.1). Cells expressing *em-plk1* (*em-plk1*$^+$) were observed dispersed throughout the germinal layer, and accumulate in early brood capsules and in the proliferative region of developing protoscoleces. During late protoscolex development, *em-plk1*$^+$ cells are observed to accumulate at the base of the suckers, similarly to what is observed for EdU$^+$ and *em-h2b*$^+$ cells (see Chapter 1; (Koziol et al. 2014)). Overall, these data strongly support the hypothesis that *em-plk1* is specifically expressed in *E. multilocularis* proliferating germinative cells. It is likely that these consist of cells in the late G2 and M phases of the cell cycle, and as such *em-plk1* would be a complementary marker for EdU incorporation and *em-h2b* expression (Koziol et al. 2014).

These results have already been published as Schubert *et al*., 2014, PloS Neglected Tropical Diseases 8(6): e2870.

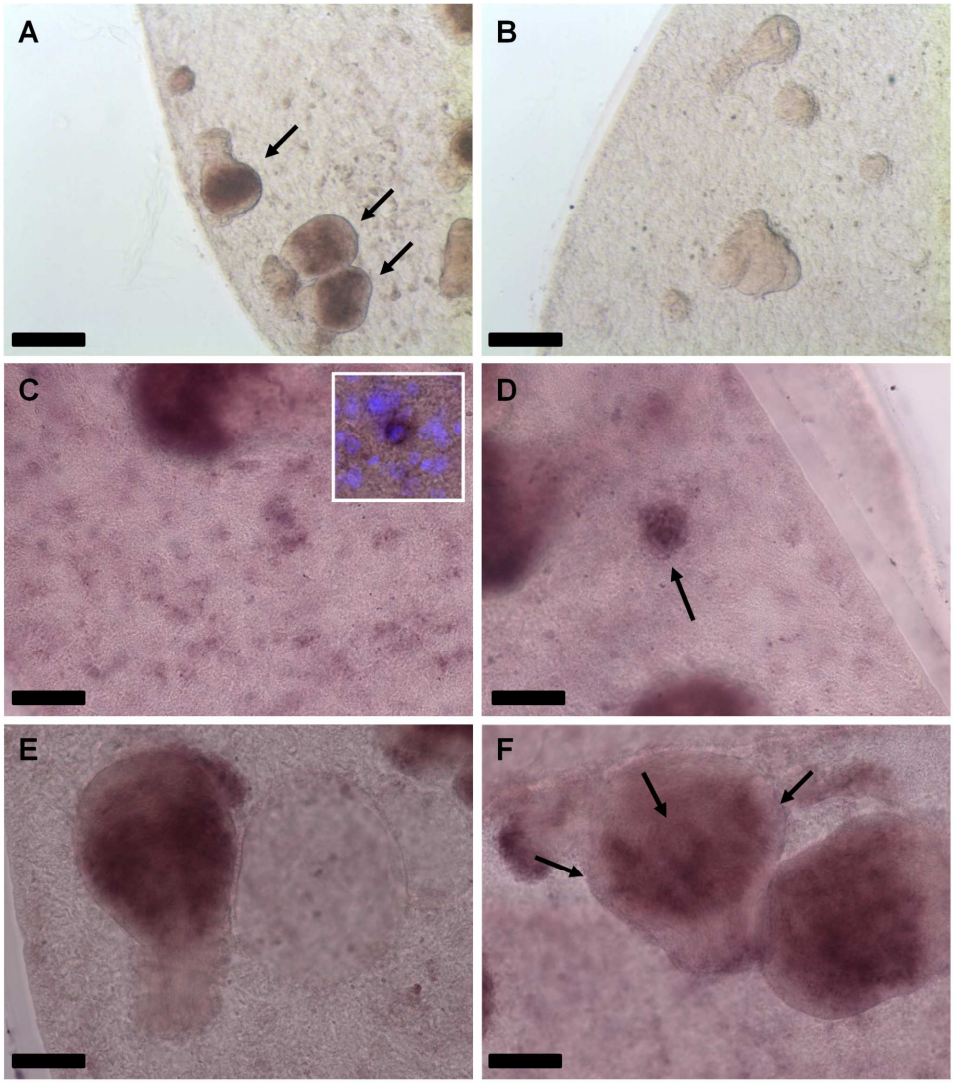

Figure R3.1. **WMISH detection of *em-plk1* transcripts. A.** General view of a metacestode hybridized with the *emplk1* antisense probe. Note the accumulation of *em-plk1* positive cells in the developing protoscoleces (arrows). **B.** General view of a metacestode hybridized with the *em-plk1* sense control probe. No signal is detected. **C-F**. Details of *em-plk1* WMISH detection in different developmental stages. **C.** Detail of the metacestode germinative layer, in which disperse *emplk1* positive cells can be distinguished (inset: higher magnification of a positive cell, combined with 4',6-diamidino-2-phenylindole (*DAPI*) nuclear staining). **D.** Accumulation of *em-plk1* positive cells in the early brood capsule bud (arrow). **E.** Early protoscolex development, with abundant *emplk1* positive cells in the interior. **F.** Late protoscolex development. *em-plk1* positive cells accumulate at the base of the developing suckers (arrows). Bars represent 200 µm (A, B) and 50 µm (C-F). Figure and legend have been previously published as a part of Schubert et al., 2014.

5.3.2. The insulin receptor *emir2* is expressed in the proliferating region of the developing protoscolex

Previously, it was shown in our laboratory that physiologically relevant concentrations of human insulin can promote cell proliferation, glucose uptake and metacestode growth and regeneration of *E. multilocularis in vitro*. Two insulin receptor homologs (*emir1* and *emir2*) were found in the *E. multilocularis* genome, and both were shown to bind to human insulin in yeast-two hybrid experiments. Furthermore, addition of insulin induced tyrosine phosphorylation of EmIR1 and phosphorylation of conserved canonical downstream targets. In sum, the experiments showed that insulin can promote the development of the parasite, and that this is probably mediated through the activation of conserved canonical insulin receptors and signaling pathways (Hemer et al. 2014).

The EmIR1 protein was shown to be expressed at low levels in the germinative cells, and at particularly high levels in the glycogen storage cells. It was therefore proposed that EmIR1 mediated the increase of glucose uptake after insulin stimulation (Hemer et al. 2014). Expression of EmIR2 was highest in primary cell preparations as compared to metacestodes and protoscoleces, and it was proposed that it could be expressed in the germinative cells, although immunohistofluorescence experiments were not conclusive in this regard. As a complementary approach, I studied the expression of *emir2* mRNA by WMISH during metacestode and protoscolex development. No expression could be detected in the germinal layer, but strong expression could be seen in the proliferative region (rich in EdU^+ cells) during early protoscolex development (Figure R3.2). Although the signal was not defined enough to confirm that individual EdU^+ cells were also *emir2*$^+$, these results indicate that *emir2* may be specifically expressed in parasite stem cells or, at least, in parasite tissues that are actively proliferating during development. These results were previously published as Hemer *et al*. (2014), BMC Biology 12:5.

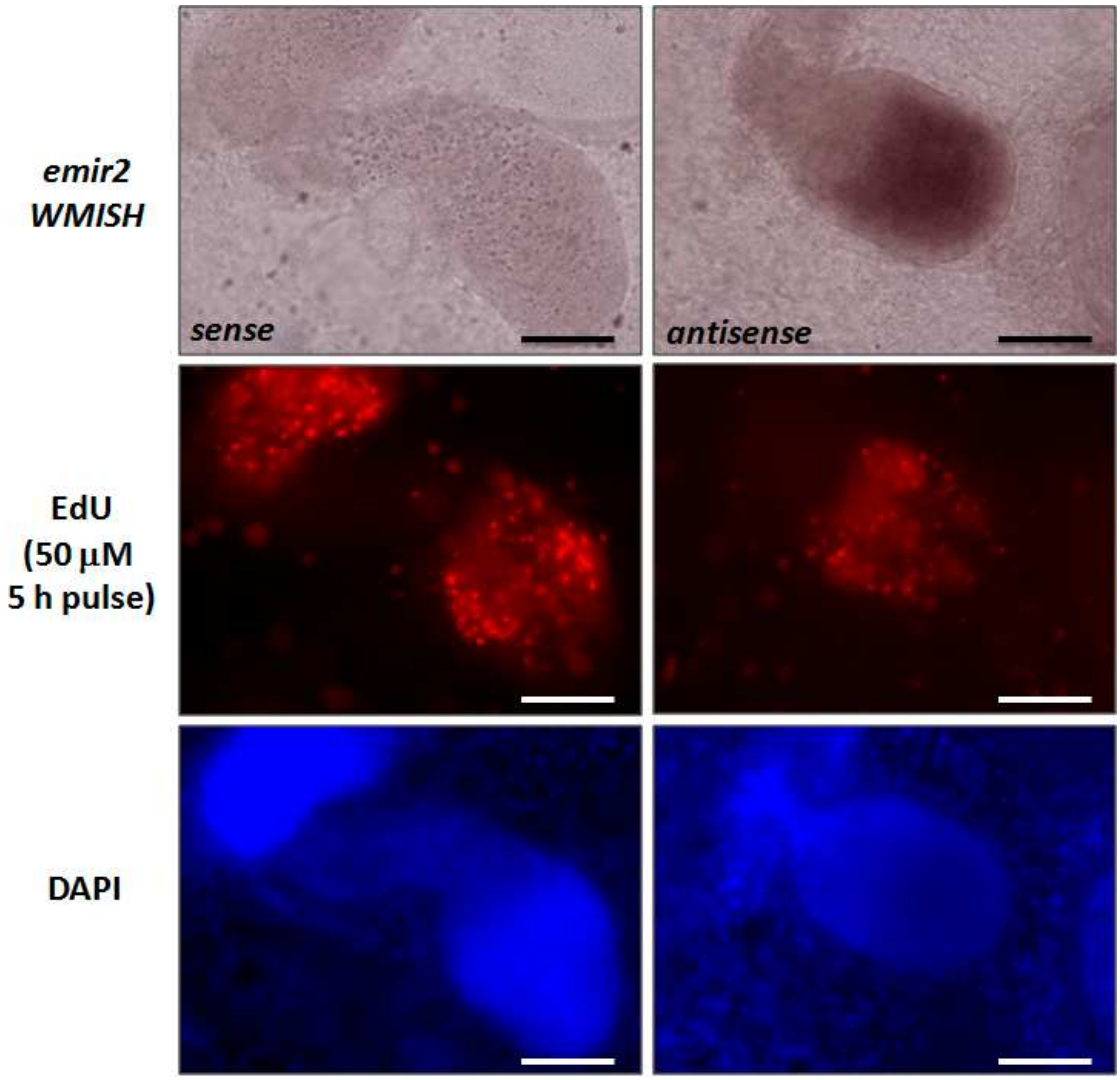

Figure R3.2. WMISH detection of *emir2*. Germinal layer with developing protoscoleces stained for *emir2* WMISH (upper panel), EdU incorporation (mid panel) and DAPI (lower panel). Sense (left) and antisense (right) probes have been used as indicated. Bar represents approximately 50 µm. Figure and legend have been previously published as a part of Hemer et al., 2014.

5.3.3. Expression of FGF receptor homologs of *E. multilocularis*

Previous results from Dr. Sabine Förster demonstrated that human FGF-1 and FGF-2 are capable of stimulating cell proliferation, growth and regeneration in *E. multilocularis* metacestodes and primary cells (Förster 2012). Furthermore, two genes coding for FGF receptors (FGFRs) were previously found in the *E. multilocularis* genome: *emfr1* (previously denominated *emfr*) and *emfr2* (Förster 2012). However, no canonical FGF ligand could be found (Förster 2012). Both EmFR1 and EmFR2 were shown to be activated by human FGF-1 and FGF-2 after heterologous expression in the *Xenopus* oocyte system. Therefore, it was concluded that human FGF ligands can activate the cognate FGFRs of *E. multilocularis*, and that this promotes metacestode growth and development (Förster 2012).

Given that genes coding for FGFRs are expressed in stem cells in other flatworms (Ogawa et al. 2002; Collins et al. 2013), and that human FGF ligands induce metacestode growth and development, I investigated in this work the expression patterns of FGFR genes during *E. multilocularis* larval development, and performed phylogenetic analyses in order to establish orthology relationships among flatworm FGFRs. While searching for other tyrosine kinase receptors for constructing the phylogenetic tree, I discovered a third FGFR in *E. multilocularis*, *emfr3*, which was previously unnoticed (since it had not been included in the original automatic gene predictions). Sequence analysis after cloning of the complete coding domain sequence (CDS, corrected in the 3′ region from the original gene model) showed that the predicted EmFR3 protein has all of the typical FGFR domains and motifs, including (from N-terminal to C-terminal): a signal peptide, at least two immunoglobulin-like domains, a single-pass transmembrane region, and a tyrosine kinase (TK) domain (Figure R3.3). The CDS of *emfr3* was sub-cloned (minus the signal-peptide coding region) into pSecTag2/HygroA. This construct was used by C. Dissous and colleagues (Center for Infection and Immunology, Institut Pasteur de Lille, France) for expression in the *Xenopus* oocyte system, by which they demonstrated that EmFR3 is also able to interact with human FGF-1 and FGF-2 (C. Dissous, personal communication to K. Brehm).

Phylogenetic analyses of flatworm FGFR genes had to be restricted to alignments of the TK domain, since other regions did not show sufficient sequence conservation for reliable alignments to be made. This limited the information for phylogenetic inference, resulting in low support values throughout most of the tree. However, one clearly supported node linked *emfr3* with the *Schistosoma mansoni* stem cell-specific *fgfrA* (Collins et al. 2013), indicating that both genes are orthologs (Figure R3.4).

Figure R3.3. Diagram of the domain organization of EmFR3. From N-terminal to C-terminal: SP, signal peptide; Ig, immunoglobulin-like domain; TM, trans-membrane region; TK, tyrosine kinase domain. Total length is 883 amino acid residues.

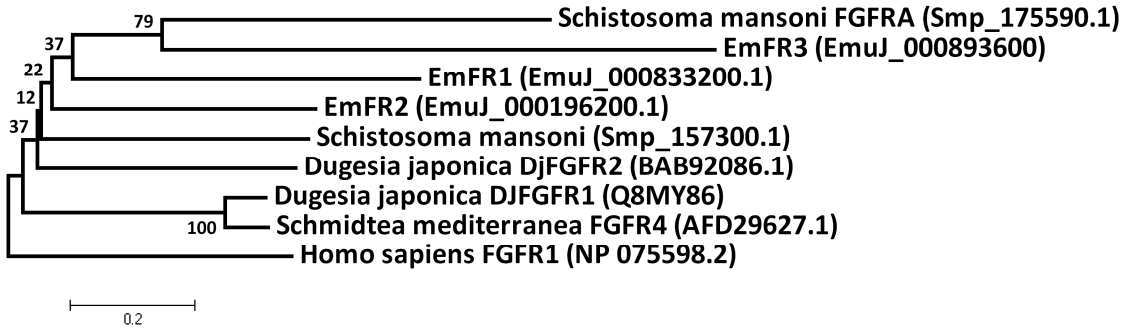

Figure R3.4. Phylogeny of FGFRs from flatworms. The TK domain of FGFRs from *E. multilocularis* (EMFR1-3), *Schistosoma mansoni*, planarians (*Dugesia japonica* and *Schmidtea mediterranea*), and FGFR1 of *Homo sapiens* were aligned, and a neighbor joining phylogenetic analysis was performed with MEGA5.0 using the JTT matrix-based substitution model. Numbers next to the nodes are bootstrap support values (1000 replicates). GeneDB codes (for *E. multilocularis* and *S. mansoni*) or NCBI accession codes (for planarians and *H. sapiens*) are given in parenthesis.

The three receptors showed very different expression patterns in *E. multilocularis* larval stages. *emfr1* was expressed at low levels throughout the germinal layer and especially during the development of protoscoleces (Figure R3.5). The intensity of the signal was heterogeneous, but no clear pattern could be discerned and it was too low to determine with certainty the percentage of positive cells.

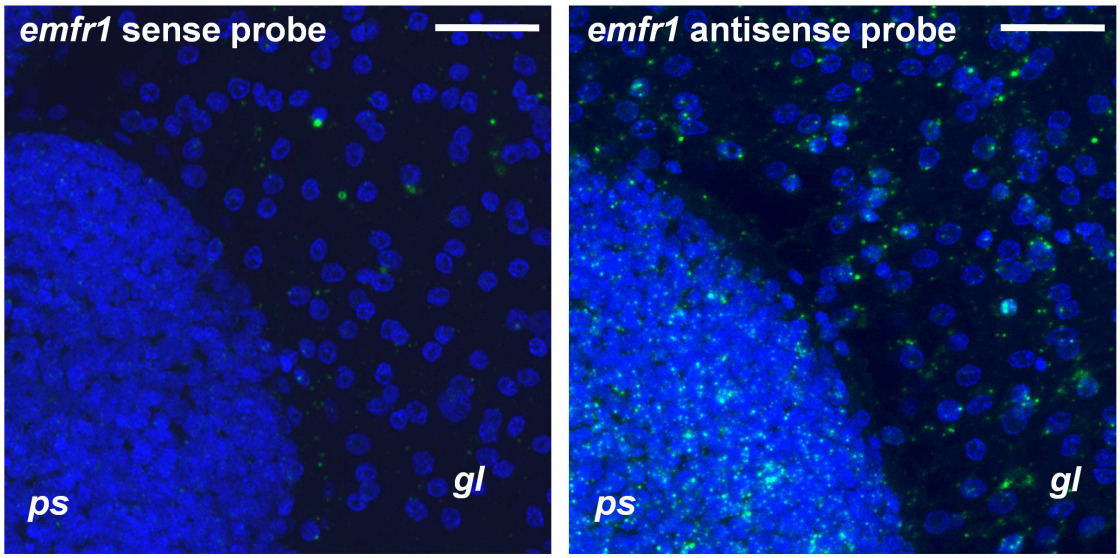

Figure R3.5. WMISH analysis of *emfr1* expression. Left panel, sense probe (negative control). Right panel, antisense probe. *gl*, germinal layer; *ps*, developing protoscolex. Bar: 20 µm.

In contrast, *emfr2* was specifically expressed in a small population of cells, typically of small size, which comprised 1.7% to 6.3% of all cells in the germinal layer (two independent WMISH experiments with isolates H95 and GH09, respectively; Figure R3.6, B-C). Furthermore, none of the *emfr2*$^{+}$ cells were EdU^{+}, indicating that these cells were out of the cell-cycle, and therefore not proliferating germinative cells (n>200 cells from two independent WMISH experiments; Figure R3.7, A). During initial protoscolex development, *emfr2*$^{+}$ cells accumulate in the peripheral-most layer of cells, as well as in the anterior-most region (which will give the rostellum), and in three longitudinal bands of cells in the interior of the protoscolex buds (Figure, R3.6, B and D). Practically none of these cells are EdU+ (<< 1% of *emfr2*+ cells are EdU+, Figure R3.7, B). Later, some *emfr2*+ cells are found in the protoscolex body, but most

accumulate in the developing rostellum and suckers (Figures R3.6, B and R3.7, C-D). Importantly, *emfr2* expression is restricted to the sucker cup, where cells are differentiating into *em-tpm-1.hmw*$^{+}$ muscle cells (Koziol et al. 2014), and not to the sucker base, were EdU^{+} germinative cells accumulate ((Koziol et al. 2014); Figure R3.7, C-D). In summary, *emfr2* is expressed in cells that are not actively cycling, and many of them are likely to be differentiating and/or differentiated muscle cells.

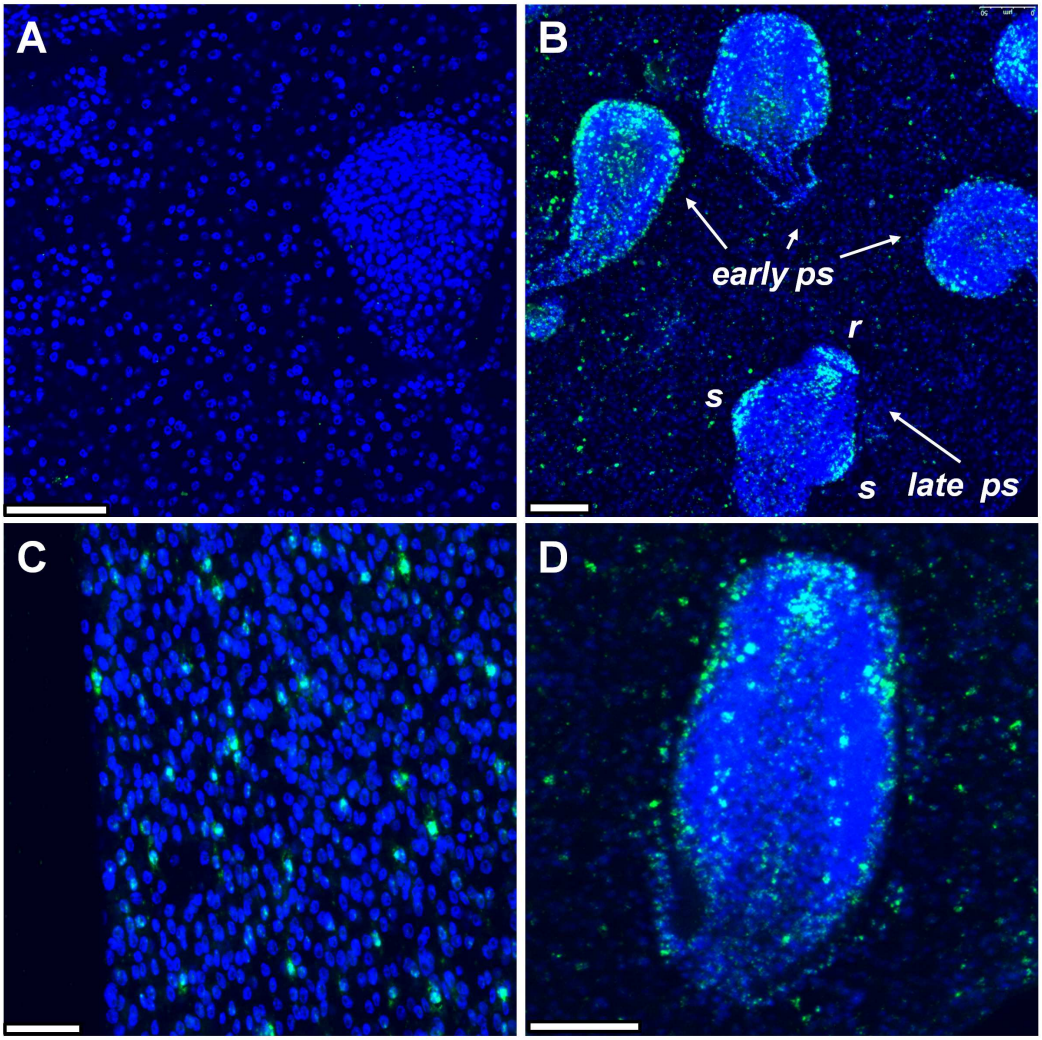

Figure R3.6. WMISH analysis of *emfr2* expression during metacestode development. In all panels the WMISH signal is shown in green, and DAPI nuclear staining is shown in blue. **A.** Sense probe (negative control). **B.** General view of a region of a metacestode with protoscoleces in different stages of development. **C.** Detail of the germinal layer. **D.** Detail of a protoscolex during early development (*ca*. stage 2 of Leducq and Gabrion, 1992). *ps*, protoscolex; *r*, rostellum; *s*, sucker. Bars: 50 µm for A, B and D, 20 µm for C.

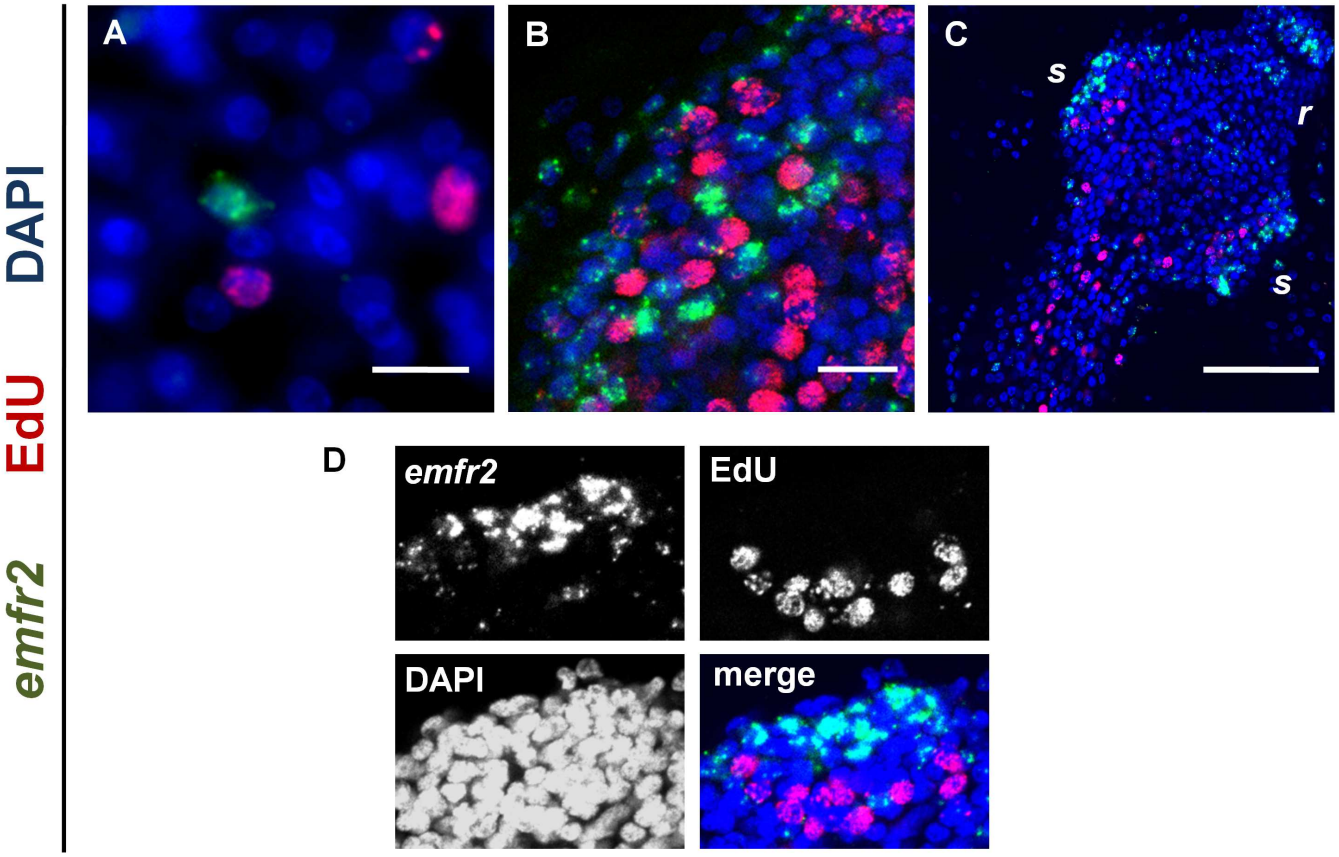

Figure R3.7. Co-detection of *emfr2* WMISH and EdU incorporation during metacestode development. Metacestodes were cultured *in vitro* with 50 µM EdU for 5 hours and were then processed for WMISH and EdU detection. In panels displaying multiple channels, the WMISH signal is shown in green, EdU detection in red, and DAPI nuclear staining in blue. **A.** Germinal layer. **B.** Early protoscolex development. **C.** Late protoscolex development. **D.** Detail of a sucker from the same specimen as in A, maximum intensity projection of a confocal Z-stack. *r*, rostellum; *s*, sucker. Bars: 10 µm for A and B, 50 µm for C.

Finally, *emfr3* is expressed in very few cells in the germinal layer (<<1% of all cells, although the number is difficult to estimate since they are absent in most random microscopy fields). *emfr3*$^{+}$ cells accumulate in small numbers during brood capsule and protoscolex development (Figure R3.8, B-E). Particularly, *emfr3*$^{+}$ cells can be found in characteristic positions at the base of the stalk connecting the developing protoscolex to the brood capsule and in the periphery of the brood capsule itself, as well as in the body of the developing protoscolex. The *emfr3*$^{+}$ cells have a large nucleus and nucleolus (as

compared for example with the *emfr2*$^{+}$ cells) and appear to have the morphology of germinative cells (Figure R3.8, E). Finally, a few *emfr3*$^{+}$ cells are present in the body region at the final stages of protoscolex development, and some signal can be seen in the rostellar region as well (Figure R3.8, F). In the developing protoscolex and in the germinal layer, *emfr3*$^{+}$ EdU^{+} double positive cells can be found (Figure R3.9). Therefore, *emfr3* is expressed in a very small number of proliferating cells with the morphology of germinative cells, indicating that it labels a minor germinative cell sub-population.

In summary, FGFR genes of *E. multilocularis* showed important differences to each other in their complex expression patterns, and also to the expression in most or all neoblasts of planarians and neoblast-like stem cells of *Schistosoma mansoni*.

Figure R3.8 (*next page*). WMISH analysis of *emfr3* expression during metacestode development. In all panels the WMISH signal is shown in green, and DAPI nuclear staining is shown in blue. **A.** Sense probe (negative control). **B.** Early brood capsule formation. **C.** Early protoscolex formation. **D.** Detail of early protoscolex formation, showing an *emfr3*$^{+}$ cell in the region of the stalk connecting the developing protoscolex to the brood capsule. **E.** Detail of early protoscolex formation, showing the morphology of an *emfr3*$^{+}$ cell (inset: only DAPI channel is shown). **F.** Late protoscolex formation. *bc*, brood capsule; *gl*, germinative layer: *ps*, protoscolex; *r*, rostellum; *s*, sucker; *st*, stalk. Bars: 25 μm for B, C, D and F; 10 μm for E.

5. Results

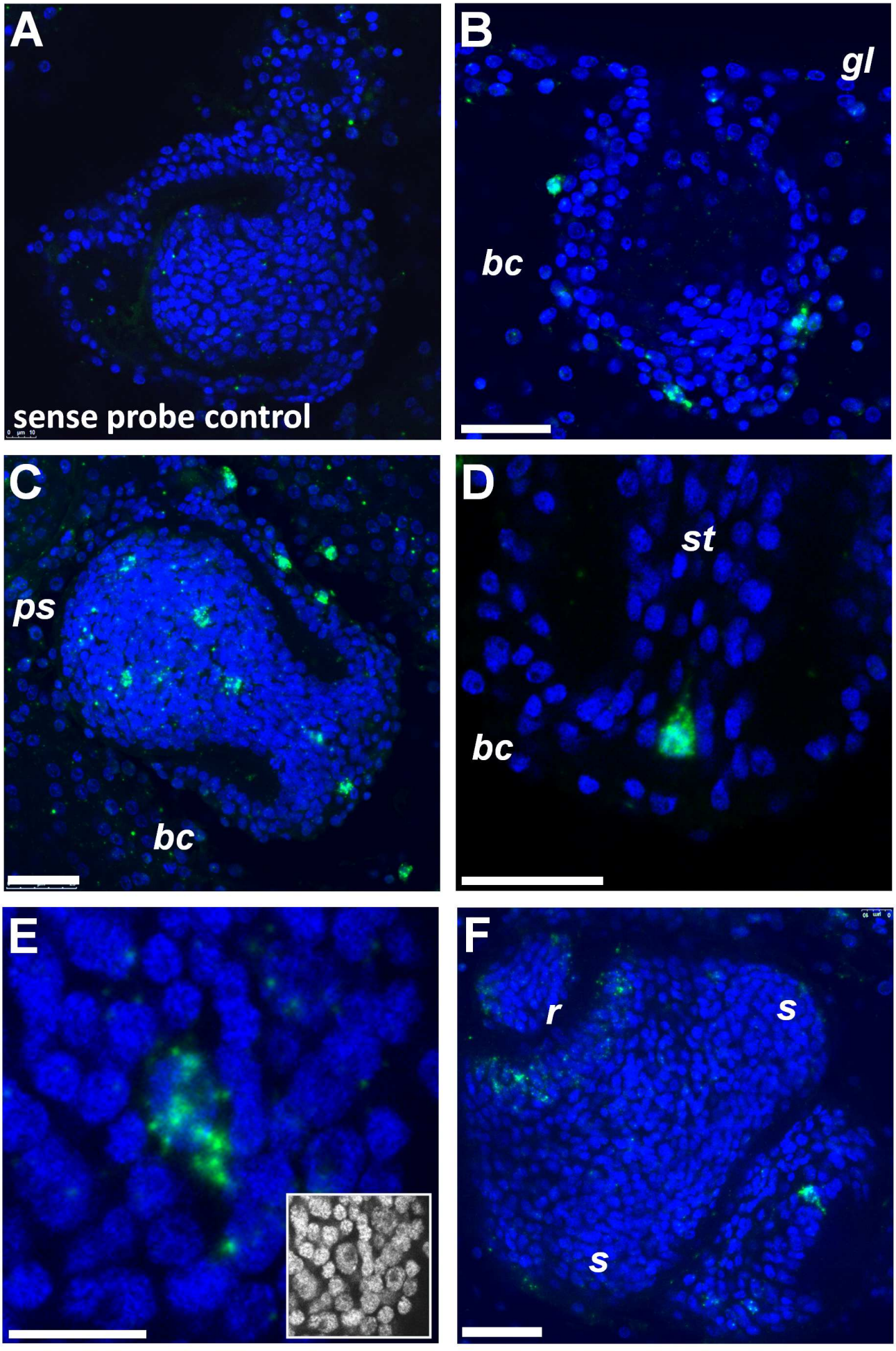

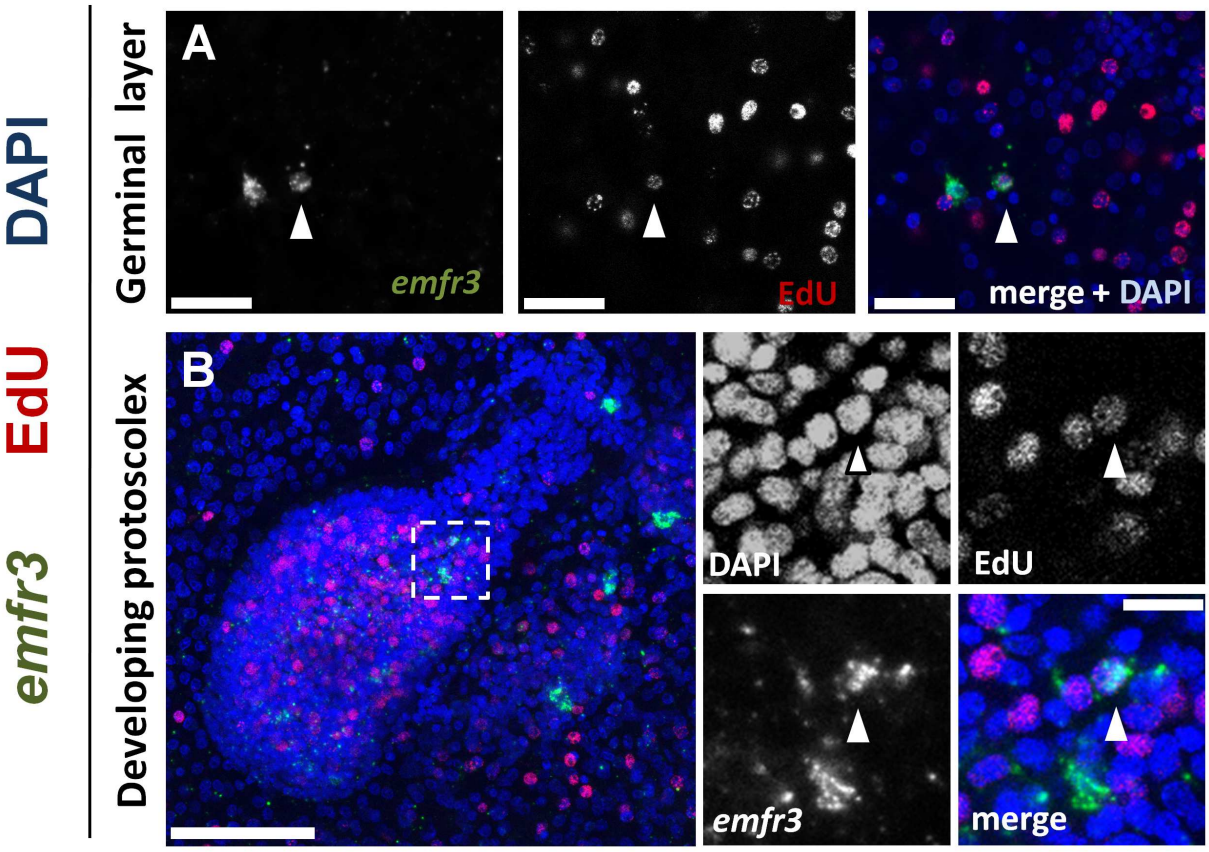

Figure R3.9. Co-detection of *emfr3* WMISH and EdU incorporation during metacestode development. Metacestodes were cultured *in vitro* with 50 µM EdU for 5 hours and were then processed for WMISH and EdU detection. In panels displaying multiple channels, the WMISH signal is shown in green, EdU detection in red, and DAPI nuclear staining in blue. **A.** Germinal layer. **B.** Developing protoscolex. Arrowheads indicate EdU^+ *emfr3*$^+$ double-positive cells

5.3.4. Transcriptomic analysis of HU treated metacestodes – A first glimpse of the germinative cell transcriptome

The previously described gene expression studies of *E. multilocularis* germinative cells were performed based on a candidate-gene approach, by selecting conserved stem cell regulators. However, in order to have a more general, bias-free view of gene expression in *E. multilocularis* germinative cells, we performed transcriptomic analyses by high-throughput RNA sequencing (RNAseq) of vesicles treated *in vitro* for 7 days with 40 mM hydroxyurea, *versus* untreated control vesicles (HU *versus* control groups, both under axenic culture conditions). The rationale behind this approach is that HU specifically depletes the germinative cells after 7 days, but has no appreciable effect on the number of differentiated cells (Koziol et al. 2014). Therefore, many genes specifically depleted in the HU group could be germinative cell-specific.

We performed three biological replicates of comparisons between HU and control groups, which were processed for RNAseq by our collaborators in the Wellcome Trust Sanger Institute (Matt Berrimann and Magdalena Zarowiecki, Cambridge, United Kingdom). M. Zarowiecki performed a preliminary analysis, searching for significantly depleted genes in the HU group, and analyzed this gene set for significant enrichment of Gene Ontology (GO) groups (Table R3.1). In total, 154 genes were less abundantly expressed in the HU group as compared with the controls (although this number is still preliminary). Interestingly, most of the GO terms showing the highest significance were related to cell proliferation, cell cycle regulation, DNA repair and cell fate commitment, which strongly suggested that within the list of HU-depleted genes there is a strong signature of germinative cell-specific genes.

We analyzed the preliminary list of down-regulated genes for further confirmation that germinative cell transcripts could be specifically depleted in the HU group. Markers of tegumental cells (*em-muc-1*, *em-alp-1* and *em-alp-2*) showed no significant difference, nor did *em-phb1*, *em-hdac1*, *em-ago2-A/B/C* and *emfr1*, which were shown in the previous experiments to be widely expressed ((Koziol et al. 2014); see above). In contrast, *em-nos-1*, *em-nos-2*, *emfr3* and *em-plk1*, all of which are

expressed in sub-populations of germinative cells ((Koziol et al. 2014; Schubert et al. 2014); see above), showed a statistically significant depletion in the HU group. *emfr2* was also significantly depleted, suggesting that the post-mitotic cells expressing this gene are mostly differentiating cells.

Few genes related to the germline multipotency program or to post-transcriptional regulation in general were found to be down-regulated after HU treatment (with the exception of a *bruno* homolog, EmuJ_000943000). In particular, none of the orthologs of the Schistosome "*vasa*-like genes" *sensu* Skinner et al. (2012) (EmuJ_000777250, EmuJ_000098400, EmuJ_001183300) showed a significant change after HU treatment. These "*vasa*-like genes" are DEAD box RNA helicases that are paralogs of *vasa*, such as *PL-10* and *p68*.

In contrast, the regulators showing the greatest fold-change and smallest *p*-values were almost invariably transcription factors (a selected list of interesting candidate genes is presented as Table R3.2, including some references to their stem cell and cell differentiation-related functions in other metazoans). Among these, four out of seven *E. multilocularis* Sox-family transcription factors (Kamachi and Kondoh 2013) can be found. Phylogenetic analyses demonstrated that the down-regulated Sox genes belong to two sub-families (Figure R3.10). One gene belongs to the SoxB sub-family, which in other metazoans includes both positive and negative transcriptional regulators, among which is the mammalian ESC pluripotency factor Sox2 (Uchikawa, Kamachi, and Kondoh 1999; Bowles, Schepers, and Koopman 2000). The other three genes group with divergent planarian Sox genes which have been shown to be specifically enriched in neoblasts (Onal et al. 2012; Wagner, Ho, and Reddien 2012).

Besides possible transcriptional and post-transcriptional regulators, I also mined the list of HU-depleted transcripts for signaling receptors and kinases, which could in principle be targeted by pharmacological methods for functional analyses, or eventually as potential therapeutic targets. Few signaling receptors were found in the list of HU-depleted genes. These include *emfr2* and *emfr3*, but also a member of the Frizzled family of receptors for Wnt ligands (Clevers 2006) with conserved roles in the maintenance and expansion of stem cells (EmuJ_000636500). As expected, a large number of homologs of kinases related to cell-cycle regulation and proliferation are

among the transcripts with the most pronounced depletion, including *em-plk1* (see above), the polo-like kinase family member PLK-4 (EmuJ_000104700), cyclin-dependent kinases (CDKs, such as EmuJ_000046100 and EmuJ_000659500), greatwall kinase (EmuJ_000711100), maternal embryonic leucin zipper kinase (EmuJ_000500200), aurora kinase A (EmuJ_001059700) and wee1 kinases (EmuJ_001003100 and EmuJ_000659400). LATS2 (EmuJ_000700100), a kinase of the hippo signaling pathway that limits and coordinates the growth of tissues and organs (Zhao, Li, and Guan 2010) was also depleted. Finally, *emSSY* (EmuJ_000139200) also showed strong depletion after HU treatment. *emSSY* is a paralog of the previously described *emmpk2* p38 MAPK (Gelmedin 2008; Gelmedin, Caballero-Gamiz, and Brehm 2008), but has an unique Ser-Ser-Tyr motif in the kinase activation loop instead of the Thr-Gly-Tyr motif that is universally conserved for p38 MAPK (Kultz 1998). *emSSY* and *emmpk2* are clustered together in the genome of *E. multilocularis* (separated by only one gene), which suggests that *emSSY* originated from a recent duplication of *emmpk2* (Gelmedin 2008). By searching in the genomes of other flatworms and performing phylogenetic analyses, it became clear that this duplication and their clustered arrangement are specific to cestodes (Figure R3.11). The possibility that this could be a cestode-specific and germinative cell-specific p38 kinase with atypical biochemical properties makes it a very interesting target for future studies.

Table R3.1. Gene Ontology (GO) Analysis of transcripts specifically depleted after HU treatment (performed by M. Zarowiecki)

GO Term		Annotated genes	Significant genes	Expected significant genes	P-value
GO:0006270	DNA replication initiation	7	6	0.44	4.00E-07
GO:0007156	homophilic cell adhesion	41	12	2.59	4.90E-06
GO:0006298	mismatch repair	7	5	0.44	1.80E-05
GO:0007050	cell cycle arrest	64	16	4.04	2.10E-05
GO:0051320	S phase	43	11	2.71	6.50E-05
GO:0006865	amino acid transport	24	7	1.51	0.00051
GO:0022403	cell cycle phase	174	40	10.98	0.00057
GO:0006275	regulation of DNA replication	4	3	0.25	0.00095
GO:0006261	DNA-dependent DNA replication	22	11	1.39	0.0016
GO:0000087	M phase of mitotic cell cycle	86	16	5.43	0.00193
GO:0000278	mitotic cell cycle	145	26	9.15	0.00199
GO:0006281	DNA repair	106	22	6.69	0.00219
GO:0000082	G1/S transition of mitotic cell cycle	6	3	0.38	0.00431
GO:0000725	recombinational repair	17	6	1.07	0.00692
GO:0000077	DNA damage checkpoint	7	3	0.44	0.0072
GO:0009219	pyrimidine deoxyribonucleotide metabolic (...)	3	2	0.19	0.01141
GO:0032515	negative regulation of phosphoprotein phosphatase activity	3	2	0.19	0.01141
GO:0032774	RNA biosynthetic process	748	35	47.18	0.0125
GO:0007067	mitosis	48	8	3.03	0.01496
GO:0045165	cell fate commitment	19	5	1.2	0.01532
GO:0010564	regulation of cell cycle process	35	8	2.21	0.02136
GO:0000245	spliceosomal complex assembly	10	3	0.63	0.02141
GO:0007569	cell aging	4	2	0.25	0.02186

GO:0060078	regulation of postsynaptic membrane potential	4	2	0.25	0.02186
GO:0034502	protein localization to chromosome	11	3	0.69	0.02809
GO:0021536	diencephalon development	5	2	0.32	0.03493
GO:0007269	neurotransmitter secretion	5	2	0.32	0.03493
GO:0010863	positive regulation of phospholipase C activity	5	2	0.32	0.03493
GO:0031398	positive regulation of protein ubiquitination	5	2	0.32	0.03493
GO:0014902	myotube differentiation	5	2	0.32	0.03493
GO:0007052	mitotic spindle organization	5	2	0.32	0.03493
GO:0002064	epithelial cell development	5	2	0.32	0.03493
GO:0006468	protein phosphorylation	316	27	19.93	0.03757
GO:0048523	negative regulation of cellular process	218	27	13.75	0.04062
GO:0044093	positive regulation of molecular function	78	9	4.92	0.0455
GO:0006260	DNA replication	103	23	6.5	0.04556
GO:0006259	DNA metabolic process	427	59	26.94	0.04962

Table R3.2. Selection of genes coding for conserved transcription factors that are specifically depleted after HU treatment

GeneDB code	GeneDB description	Roles of homologs
EmuJ_000098000	bhlh factor math6	bHLH proteins have widespread roles in cell-fate determination (Jones 2004), including math6 (Inoue et al. 2001)
EmuJ_000627500	achaete scute transcription factor	Regulates ISC fate (van der Flier et al. 2009)
EmuJ_000344700	neurogenic differentiation factor 1	bHLH proteins have widespread roles in cell-fate determination (Jones 2004)
EmuJ_000215900	GATA binding factor 2	GATA factors 1-3 are essential for hematopoiesis, including HSC/progenitor function and differentiation (Bresnick et al. 2012)
EmuJ_000457300	DNA binding protein inhibitor ID 4	ID proteins inhibit differentiation and promote proliferation of stem cells (Yokota 2001)
EmuJ_000909600	MYB	MYB proteins regulate cell proliferation and differentiation (Oh and Reddy 1999; Prouse and Campbell 2012)
EmuJ_000704700	transcription factor Sox1a	Sox proteins regulate cell fate and differentiation (Kamachi and Kondoh 2013)
EmuJ_000451500	Basic helix loop helix dimerisation region bHLH	bHLH proteins have widespread roles in cell-fate determination (Jones 2004)
EmuJ_000449700	POU specific (from blast, Class III POU)	POU factors have roles in stem cell maintenance (*e.g.* Oct4) and in lineage commitment (*e.g.* Class III POUs) (Tantin 2013)
EmuJ_000191100	transcription factor SOX 14	Sox proteins regulate cell fate and differentiation (Kamachi and Kondoh 2013)
EmuJ_000232900	transcription factor SOX 6	Sox proteins regulate cell fate and differentiation (Kamachi and Kondoh 2013)
EmuJ_000437800	transcription factor SOX 14	Sox proteins regulate cell fate and differentiation (Kamachi and Kondoh 2013)

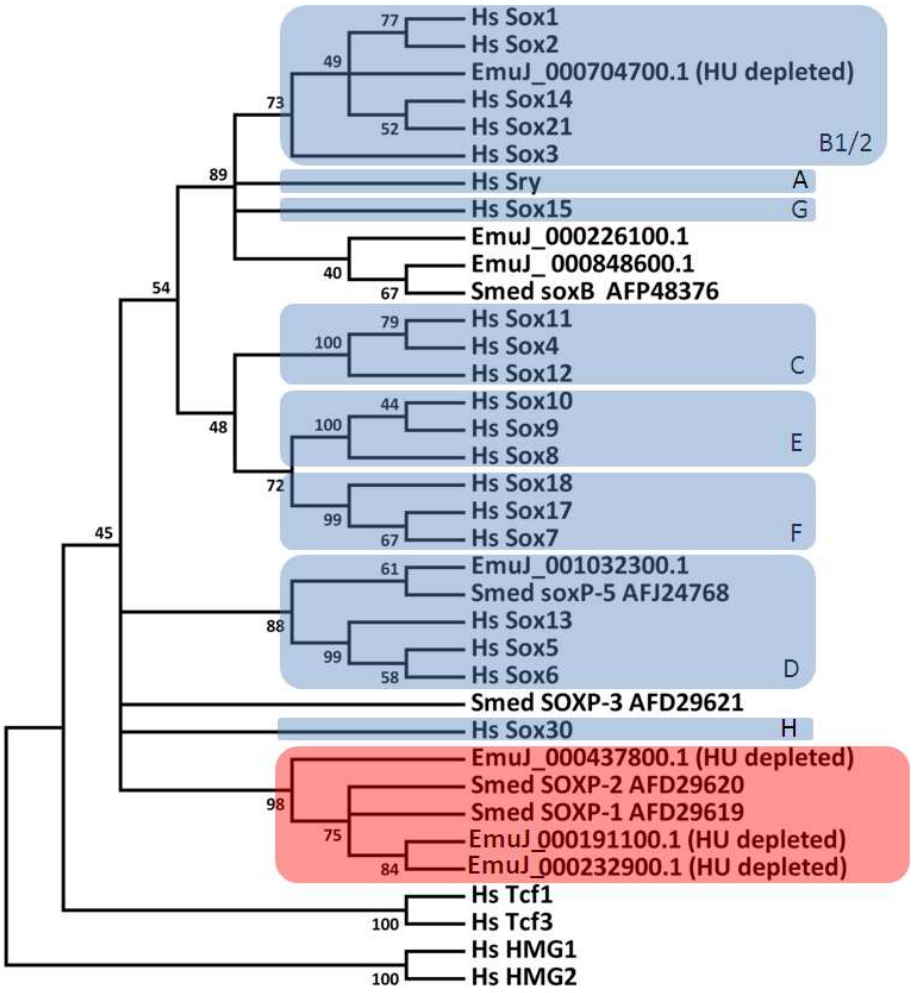

Figure R3.10. Phylogeny of Sox proteins from *E. multilocularis*. The HMG domain of Sox proteins from *E. multilocularis* (Emu), *Homo sapiens* (Hs, from Bowles, Schepers, and Koopman 2000), and published planarian genes (*S. mediterranea*, Smed) were aligned, and a neighbor joining phylogenetic analysis was performed with MEGA5.0 using the JTT substitution model. Numbers next to the nodes are bootstrap support values (1000 replicates). HU-depleted genes of *E. multilocularis* are indicated in parentheses. Blue labeling indicates groups A to H of Sox proteins as defined by Bowles, Schepers, and Koopman, 2000. Red labeling indicates a divergent group of flatworm sequences that cannot be easily classified according to the scheme of Bowles, Schepers and Koopman for vertebrate Sox proteins. Human Tcf1, Tcf3, HMG1 and HMG2 proteins were used to root the tree. GeneDB codes (for *E. multilocularis*) or NCBI accession codes (for *S. mediterranea*) are given.

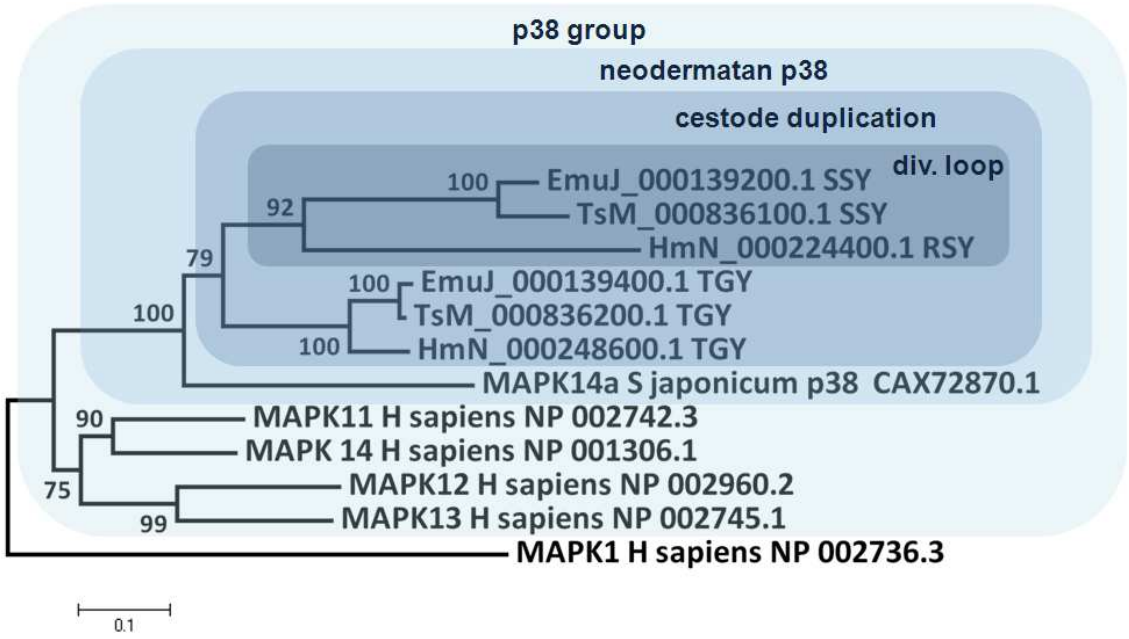

Figure R3.11. Phylogeny of p38 MAPK proteins from neodermatans. Proteins sequences of the p38 MAPK family from *E. multilocularis*, (Emu), *Taenia solium* (Ts), *Hymenolepis microstoma* (Hm) and *Schistosoma japonicum* were aligned with p38 MAPK sequences of *Homo sapiens*, together with an ERK MAPK of *Homo sapiens* (MAPK1) as an outgroup. Neighbor joining phylogenetic analysis was performed with MEGA5.0 using the JTT substitution model. Numbers next to the nodes are bootstrap support values (1000 replicates). The motif found in the kinase activation loop of cestode proteins is indicated to the right. GeneDB codes (for *E. multilocularis*, *T. solium* and *H. microstoma*) or NCBI accession codes (for *S. japonicum* and *Homo sapiens*) are given. "div. loop" indicates the cestode-specific group of divergent p38 MAPKs.

5.3.5. First steps towards the development of clonal analyses of *E. multilocularis* germinative cells

The study of the potency of individual *E. multilocularis* germinative cells will require clonal analyses, but the techniques required for this are not as yet available (see also the Discussion section). We therefore set out to develop transplant experiments for tracing clones originating from individual *E. multilocularis* cells, after introduction into a host metacestode. Ideally, genetically manipulated *E. multilocularis* cells expressing a marker gene, or different *E. multilocularis* isolates with specific antigens could be used. However, transgene integration has not been achieved in *E. multilocularis* yet, and there are no known differential antigens between isolates. Instead, inspired by the classic quail-chick chimera experiments used for cell tracing during chicken embryonic development (Le Douarin and Teillet 1974), we decided to investigate whether *E. multilocularis* primary cells (EmPCs) could be integrated into the metacestode of the related taeniid species *Taenia crassiceps* (TcMC).

Previously, Andreas Schubert had shown that *T. crassiceps* proliferating cells could integrate into *E. multilocularis* metacestodes that had been depleted of proliferating cells by long-term treatment with a PLK-1 inhibitor (A. Schubert, personal communication). This suggested that no histoincompatibility system was present. As a proof of principle, an experiment was performed in which a large number of EmPCs were introduced into TcMC using a simple 26G3/8 syringe. Because TRIM copies are very divergent between taeniid species (*e.g.* only *ca*. 50% identity between *E. multilocularis* and *T. solium* TRIMs), and are highly expressed in the *E. multilocularis* germinative cells, we performed WMISH with a specific *E. multilocularis ta-TRIM* probe ("*emTRIM*") to search for viable *E. multilocularis* germinative cells that had integrated into the TcMC tissues. In transplanted TcMC, many *emTRIM* $^{+}$ cells with germinative cell morphology could be found after 5 days of culture, sometimes in patches that suggested growth from only one or a few founding EmPCs (Figure R3.12; 2/4 specimens). No *emTRIM* $^{+}$ cells were found in control, non-transplanted TcMC (0/3 specimens). In conclusion, EmPCs can integrate into TcMC, and *E. multilocularis* germinative cells can be specifically detected within those tissues. Possible applications

of these results for clonal analysis of *E. multilocularis* germinative cells are proposed in the Discussion section.

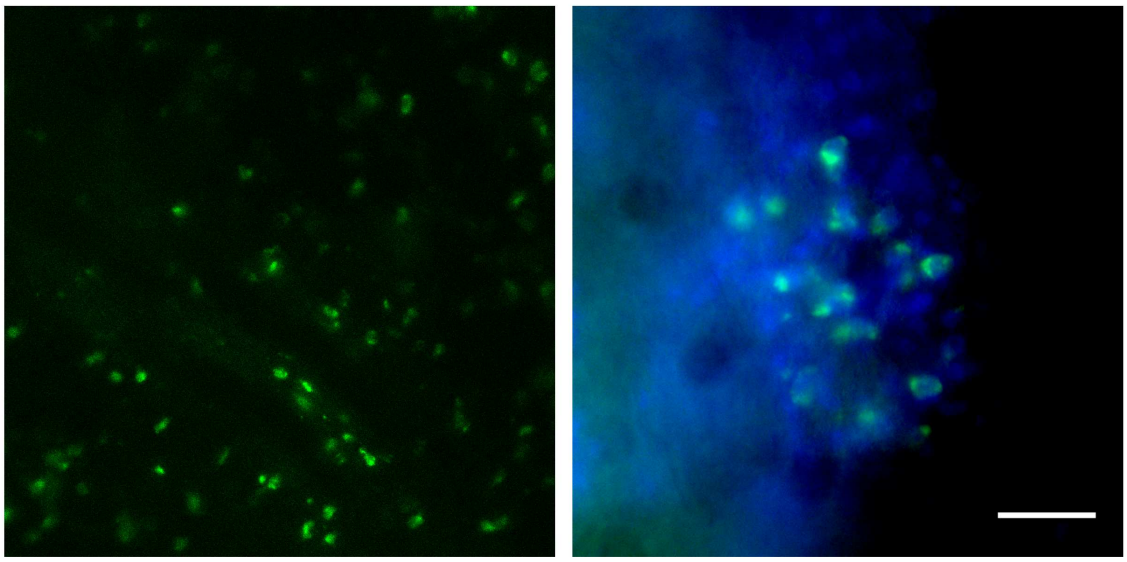

Figure R3.12. Detection of *emTRIM*$^{+}$ cells by WMISH after transplantation of *E. multilocularis* cells into *T. crassiceps*. Left, general view of a region of one transplanted *T. crassiceps* metacestode. Right, detail of an isolated patch of *emTRIM*$^{+}$ cells. Bar: 20 µm.

5.4. CHAPTER 4: "Anatomy and development of the larval nervous system in *Echinococcus multilocularis*"

Originally published as Koziol *et al*. (2013), Frontiers in Zoology 10:24

Author contributions

General study design:

Uriel Koziol and Klaus Brehm

Experimental design and work:

Uriel Koziol designed, performed or participated in all the experiments. Georg Krohne designed, supervised and interpreted the results of electron microscopy experiments.

Analysis of the results:

Uriel Koziol, Klaus Brehm, Georg Krohne

Writing of the manuscript:

Uriel Koziol wrote the first manuscript draft, which was corrected by Klaus Brehm and accepted by all the authors

Anatomy and development of the larval nervous system in *Echinococcus multilocularis*

Uriel Koziol[1,3], Georg Krohne [2], Klaus Brehm[1,*]

[1] University of Würzburg, Institute of Hygiene and Microbiology, Josef-Schneider-Strasse 2, D-97080 Würzburg, Germany

[2] University of Würzburg, Department of Electron Microscopy, Biocenter, D-97078 Würzburg, Germany

[3] Universidad de la República, Facultad de Ciencias, Sección Bioquímica y Biología Molecular, Iguá 4225, CP 11400, Montevideo, Uruguay.

* Corresponding Author

5. Results

Background

The metacestode larva of *Echinococcus multilocularis* (Cestoda: Taeniidae) develops in the liver of intermediate hosts (typically rodents, or accidentally in humans) as a labyrinth of interconnected cysts that infiltrate the host tissue, causing the disease alveolar echinococcosis. Within the cysts, protoscoleces (the infective stage for the definitive canid host) arise by asexual multiplication. These consist of a scolex similar to that of the adult, invaginated within a small posterior body. Despite the importance of alveolar echinococcosis for human health, relatively little is known about the basic biology, anatomy and development of *E. multilocularis* larvae, particularly with regard to their nervous system.

Results

We describe the existence of a subtegumental nerve net in the metacestode cysts, which is immunoreactive for acetylated tubulin-α and contains small populations of nerve cells that are labeled by antibodies raised against several invertebrate neuropeptides. However, no evidence was found for the existence of cholinergic or serotoninergic elements in the cyst wall. Muscle fibers occur without any specific arrangement in the subtegumental layer, and accumulate during the invaginations of the cyst wall that form brood capsules, where protoscoleces develop. The nervous system of the protoscolex develops independently of that of the metacestode cyst, with an antero-posterior developmental gradient. The combination of antibodies against several nervous system markers resulted in a detailed description of the protoscolex nervous system, which is remarkably complex and already similar to that of the adult worm.

Conclusions

We provide evidence for the first time of the existence of a nervous system in the metacestode cyst wall, which is remarkable given the lack of motility of this larval stage, and the lack of serotoninergic and cholinergic elements. We propose that it could function as a neuroendocrine system, derived from the nervous system present in the bladder tissue of other taeniids. The detailed description of the development and anatomy of the protoscolex neuromuscular system is a necessary first step toward the understanding of the developmental mechanisms operating in these peculiar larval stages.

Keywords:

***Echinococcus*; metacestode; protoscolex; nervous system; neuropeptide; serotonin; acetylated tubulin**

Introduction

The metacestodes of *Echinococcus multilocularis* and *Echinococcus granulosus* are the causative agents of alveolar and cystic echinococcosis (AE, CE), respectively. These larvae develop from onchospheres after oral ingestion of infectious eggs by their natural intermediate hosts (rodents for *E. multilocularis* and different ungulate species for each lineage of the *E. granulosus* species complex), but humans can also serve as accidental intermediate hosts. Most commonly, metacestode growth occurs in the liver (especially in the case of *E. multilocularis*), but other parenteral sites can also be infected. AE is one of the most dangerous zoonotic diseases in the Northern Hemisphere, while the more widely distributed CE is a neglected tropical disease of both medical and veterinary importance (Eckert and Deplazes 2004).

Echinococcus metacestode larvae consist of fluid-filled cysts that are covered by an acellular laminated layer. Within the cysts, the cells are organized as a thin layer, the germinal layer or "germinal membrane", which is juxtaposed to the laminated layer. This layer consists of several cell types such as tegumental cells, which compose the tegumental syncitium that covers the cyst's interior and secretes the laminated layer. Other cell types have been described within the germinal layer, including glycogen storing cells, calcareous corpuscle cells, cells forming the excretory ducts (and in the case of *E. granulosus* also flame cells), muscle cells and undifferentiated stem cells (Morseth 1967b; Sakamoto and Sugimura 1969; Sakamoto and Sugimura 1970; Lascano, Coltorti, and Varela-Diaz 1975). In the case of *E. granulosus*, each larva grows typically as a single cyst, whereas the *E. multilocularis* metacestode proliferates as a labyrinth of small interconnected vesicles that infiltrates the tissues of the host.

Within the cysts, brood capsules are formed from the germinal layer. These are vesicular structures, with a cavity lined by a tegumental syncytium (that is, with the opposite polarity to that of the cyst wall, in which the tegumental syncytium covers the external side). Two theories have been proposed for the mechanism of formation of the brood capsules, based on histological and electron-microscopical investigations: that they are formed by cavitation of a solid mass of cells that accumulates as a bud in the germinal layer (Sakamoto and Sugimura 1970; Thompson 1976), or by invagination and

posterior constriction of a thickened region of the germinal layer (Goldschmidt 1900; Leducq and Gabrion 1992).

Within the brood capsules, protoscoleces are formed, which are the infective stage for the definitive hosts (canids). The protoscolex contains a scolex with four suckers and an armed rostellum, already very similar in morphology to the scolex of the adult worm. The scolex is invaginated, but after ingestion by the definitive host the scolex evaginates and the protoscolex establishes in the intestine, were it develops into the adult worm. The formation of protoscoleces within the brood capsule has been described by several authors (Goldschmidt 1900; Rausch 1954; Mankau 1956; Thompson 1976; Leducq and Gabrion 1992): initially, a small bud develops on the inner side of the brood capsule wall, covered by the brood capsule tegument, and grows into the brood capsule cavity. Early during development, the rostellar primordium can be distinguished at the tip of the protoscolex bud, and later the primordia of the suckers become apparent. Once the development of the rostellum and the suckers is complete, the scolex invaginates into the posterior body, which is now only connected to the brood capsule by a thin stalk (however, the invagination of the scolex before development is completed has also been described (Goldschmidt 1900; Slais 1973)). The formation of multiple protoscoleces within each cyst results in asexual multiplication in the intermediate host, a process that is rare in cestodes but relatively common within the family Taeniidae (genera *Taenia* and *Echinococcus* (Slais 1973; Moore and Brooks 1987; Hoberg et al. 2000; Loos-Frank 2000; Swiderski et al. 2007)).

Few ultrastructural, histochemical or immunohistochemical studies have been conducted on the nervous system of *Echinococcus*, resulting in a rather incomplete picture of its morphology and development. The elements of the nervous system have been best described for the adult form of *E. granulosus*, by acetylcholinersterase histochemistry (AChE HC) (Shield 1969) and by immunohistofluorescence (IHF) against 5-hydroxytryptamine (serotonin; 5-HT) (Brownlee et al. 1994), with similar but also complementary results (not all elements could be described with each technique). Briefly, in the scolex, it consists of two main lateral ganglia connected to each other by transverse and ring commisures, two postero-lateral ganglia, and a rostellar nerve ring and paired rostellar ganglia. Ten longitudinal nerve cords run in the strobila, that are

interconnected by numerous transverse commisures. Neurites emanate from the nerve cords forming a subtegumental plexus innervating the subtegumental musculature. In the protoscolex of *E. granulosus*, the nervous system was partially described by a pioneering IHF study using antibodies against 5-HT and against mammalian neuropeptides (Fairweather et al. 1994). It was suggested that the nervous system was similar but simpler than that of the adult worm, with fewer 5-HT positive cells, and lacking for example the postero-lateral ganglia. No detailed IHF study has been performed with other neural markers for protoscoleces of *Echinococcus* spp., no study has been conducted in *E. multilocularis* and to the best of our knowledge, there has been no study on the cyst wall of the metacestode.

In this work, we use phalloidin staining and IHF with antibodies against several nervous system markers to describe the muscle and nervous systems in the germinal layer and protoscolex of *E. multilocularis*. We provide evidence for the first time of nerve cells in the germinal layer of the cyst wall, and describe the development of the muscle and nervous systems of the protoscolex during asexual multiplication. Finally, we provide the most detailed account of the neuroanatomy of the mature protoscolex available to date.

Results

The muscle system in the cyst wall

Phalloidin staining revealed long muscle fibers in the metacestode cyst wall, situated below the tegument, external to all the nuclei of the cells of the germinal layer (subtegumental muscle layer) (Figures 1, 2 and 3). The fibers show no particular arrangement at a global level, but locally bundles of parallel fibers can be seen. Muscle fibers had been previously described by TEM in the cyst wall of both *E. granulosus* and *E. multilocularis* (Sakamoto and Sugimura 1969; Sakamoto and Sugimura 1970; Lascano, Coltorti, and Varela-Diaz 1975). Larger vesicles show a denser array of fibers and fiber bundles, especially in the case of *in vitro* cultured vesicles, whereas smaller vesicles show scarcer, isolated fibers. Fully mature vesicles obtained *in vivo* become packed with protoscoleces and calcareous corpuscles, with a very thin germinal layer that has few or no muscle fibers (data not shown).

The nervous system in the cyst wall

Acetylated tubulin-α immunoreactivity (AcTub-IR) in the cyst wall revealed a discontinuous nerve net of multipolar cells, with perykarya sunken in the deeper levels of the germinal layer, and long branching neurites projecting towards the subtegumental muscle layer, in many cases contacting the neurites from other nerve cells (Figures 2 and 3 A, 3 B). Also, a smaller number of other AcTub-IR nerve cells were found, with longer and much less branched projections (Figure 2 E). The neurites of these cells run deeper in the germinal layer, below most of the subtegumental muscle fibers.

The AcTub-IR nerve net was found in vesicles from both *in vivo* and *in vitro* cultures, being most developed in larger vesicles with a well developed muscle layer and a thicker germinal layer, while in smaller vesicles fewer nerve cells were apparent. Upon *in vitro* cultivation, the nerve net was clearly observable in all vesicles, distributed throughout the cyst wall. In *in vivo* generated material, the nervous system was observable in some but not all the vesicles. Particularly, degenerating and fully mature vesicles, with a thin germinal layer, showed few or no nervous elements. Also, in very

young and small vesicles, with a thin germinal layer (Rausch 1954; Thompson 1976), muscle fibers were sometimes not apparent, and the nerve cells were few, distributed in small patches in the cyst wall. From whole-mount preparations of in vitro cultured material, we estimated that AcTub-IR nerve cells represented 0.2% to 1.9% of all cells in the germinal layer.

The only cells labeled in the cyst wall with the antibody against AcTub were the nerve cells and some very rare flame cells, which were only observed in material from *in vivo* cultivation. These are easily distinguishable from the nerve cells given their morphology (including an AcTub-IR bundle of cilia or "flame", and a roundish cell body that is also strongly AcTub-IR), and by their co-staining with phalloidin in a basal ring surrounding the bundle of cilia (Wahlberg 1998; Valverde-Islas et al. 2011). Their morphology is however somewhat abnormal as compared to the morphology of flame cells in the protoscolex, since the phalloidin ring and the bundle of cilia are small and irregularly shaped [Additional File 1]. AcTub-IR has also been described in gland cells and glandular ducts in other flatworms (see for example (Hartenstein and Jones 2003)), but because of the morphology of the AcTub-IR cells in the cyst wall, we conclude that most, if not all, the AcTub-IR positive cells that are not flame cells correspond to nerve cells.

A small subpopulation of the cells in this nerve net was revealed by FMRFa immunoreactivity (FMRFa-IR), that was localized to a few nerve cells extending long, varicose projections with little branching (Figure 3 C). Staining was seen in the nerve cell bodies and in the varicose neurites. Similarly, RYamide immunoreactivity (RYa-IR) and FVamide immunoreactivity (FVa-IR) was revealed in even smaller numbers of nerve cells with similar morphology, and in many cases only the nerve projections were apparent, the perykarya being indistinct (Figure 3 D and data not shown).

Interestingly, no clear evidence was obtained for the existence of serotoninergic or cholinergic nerve cells, although 5-HT and acetylcholine are two of the best characterized classical neurotransmitters in cestodes (Maule, Marks, and Day 2006), and both kinds of elements are detectable in the protoscolex ((Fairweather et al. 1994); see below). Only some (presumably non-specific) 5-HT-immunoreactivity (5-HT-IR)

was observed surrounding the calcareous corpuscles (data not shown). Furthermore, no acetylcholinersterase activity was observed in the nerve cells by HC. Only some very rare cells, apparently lacking projections, were positive for acetylcholinesterase HC, and these were all negative for AcTub-IR [Additional File 2].

The finding of a nervous system in the cyst wall was unexpected, since it is a non-motile stage, and a nervous system has never been described in previous ultrastructural studies on *Echinococcus* (Morseth 1967b; Sakamoto and Sugimura 1969; Lascano, Coltorti, and Varela-Diaz 1975). Therefore, we performed our own TEM studies with *in vitro* cultured vesicles [Additional File 3 A, B]. In sections tangential to the cyst wall, we found long, thin cellular projections, packed with microtubuli, and in some cases containing mitochondria and some few small electron-dense vesicles. We interpret these as the projections of nerve cells. They are few, small, and rather inconspicuous, possibly explaining why they have not been previously described. We have found in rare occasions cell bodies connected to such projections, which we identify as the putative nerve cells, containing cytoplasm with numerous free ribosomes and mitochondria, and with regions packed with microtubuli in parallel arrays and occasional vesicles [Additional File 3 C].

Formation of brood capsules

Brood capsule formation begins as a compact, bud shaped accumulation of cells in the germinal layer. By confocal microscopy of whole-mounts and sections, we were able to clearly confirm that the brood capsule forms from an invagination of the germinal layer that is not accompanied by the laminated layer (Leducq and Gabrion 1992) (Figure 1) [Additional Files 4, 5 and 6]. Furthermore, there is a reorganization of the subtegumental muscle layer, as muscle fibers with a circular disposition accumulate surrounding the invagination. Later, the base narrows, forming a stalk that connects the brood capsule proper to the germinal layer, but even in this and later stages this stalk is hollow and internally covered by muscle fibers, that are predominantly circular. The other end becomes dilated, with the walls becoming thinner. Thus, the subtegumental layer of muscle fibers in the cyst wall is continuous with the muscle layer in the brood capsule stalk and wall. The muscle fibers in the dilated brood capsule do not initially

show any particular arrangement, but when the protoscolex bud emerges as a thickening in the brood capsule wall, the muscles become rearranged, showing a clear grid of longitudinal and circular muscles that extend from the brood capsule into the developing protoscolex (see also below). The rest of the brood capsule becomes a thin layer of germinal tissue as protoscolex development proceeds, with sparser and less organized muscle fibers.

We found no evidence of nerve cell bodies within the brood capsule itself. However, AcTub-IR perykarya were seen at the base of some brood capsules, and projections from the nerve cells in the cyst wall sometimes entered the base of the early brood capsules. No connection was observed between the nervous system of the cyst wall and the developing protoscolex.

Figure 1 (next page). Muscle fibers in the germinal layer and during brood capsule formation. All specimens stained with Phalloidin. A. Early brood capsule development (*bc*, brood capsule; *gl*, germinal layer; *h*, host tissue; *ll*, laminated layer). B. Brood capsules containing protoscolex buds (*ps*). C. Brood capsules during late protoscolex development. D. Whole-mount preparation showing an early brood capsule seen from above (inset shows merge with DAPI staining). Note the organization of the muscle fibers in the brood capsule region. E. General arrangement of the muscle fibers in the metacestode and brood capsules. A, B and C are sections from *in vivo* cultured material; D and E are whole-mount preparations of *in vitro* cultured material. Bars represent 50 μm.

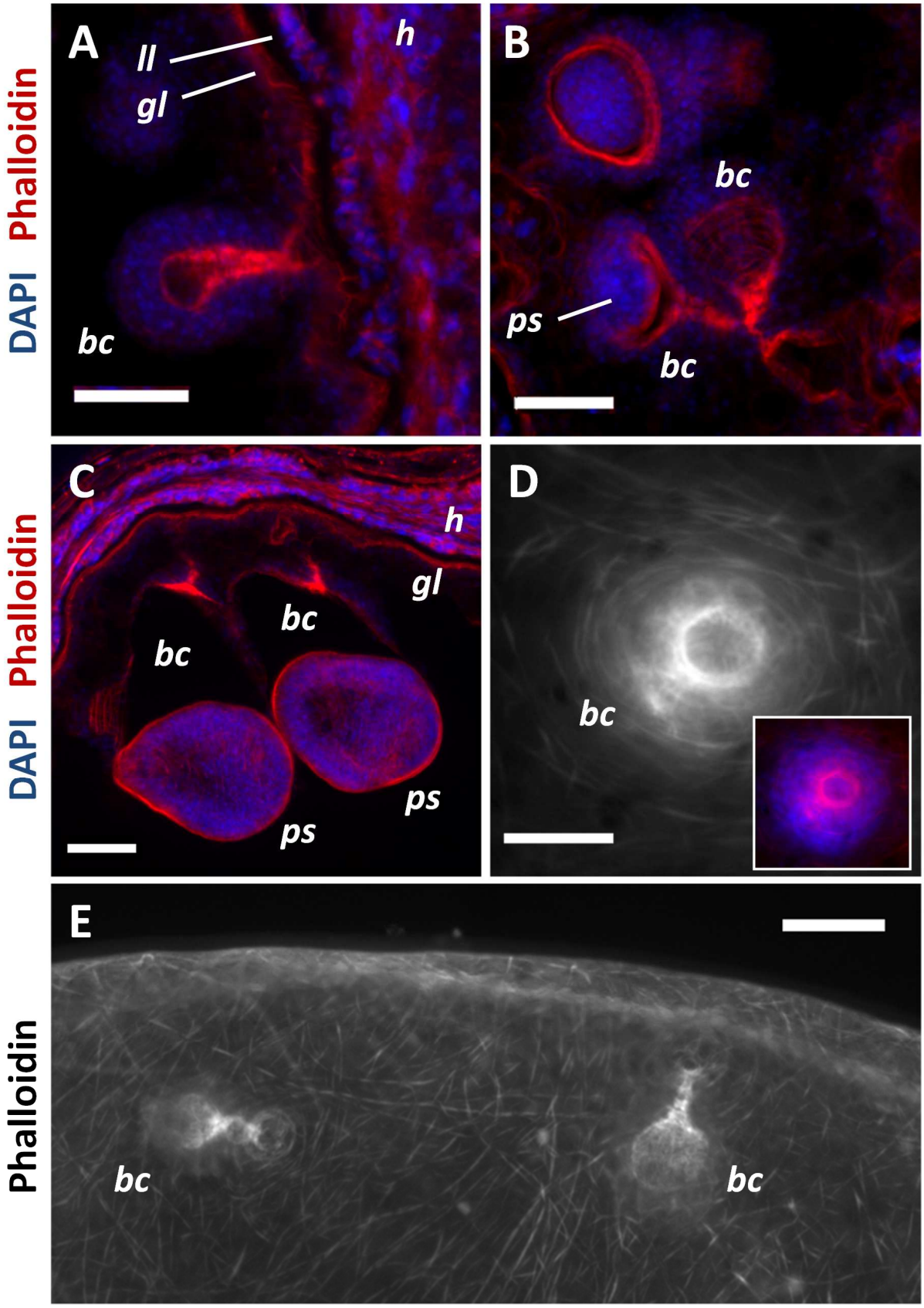
A
ll
gl
h
bc
B
bc
ps
bc
DAPI Phalloidin
C
h
gl
bc
bc
ps
ps
D
bc
DAPI Phalloidin
E
bc
bc
Phalloidin

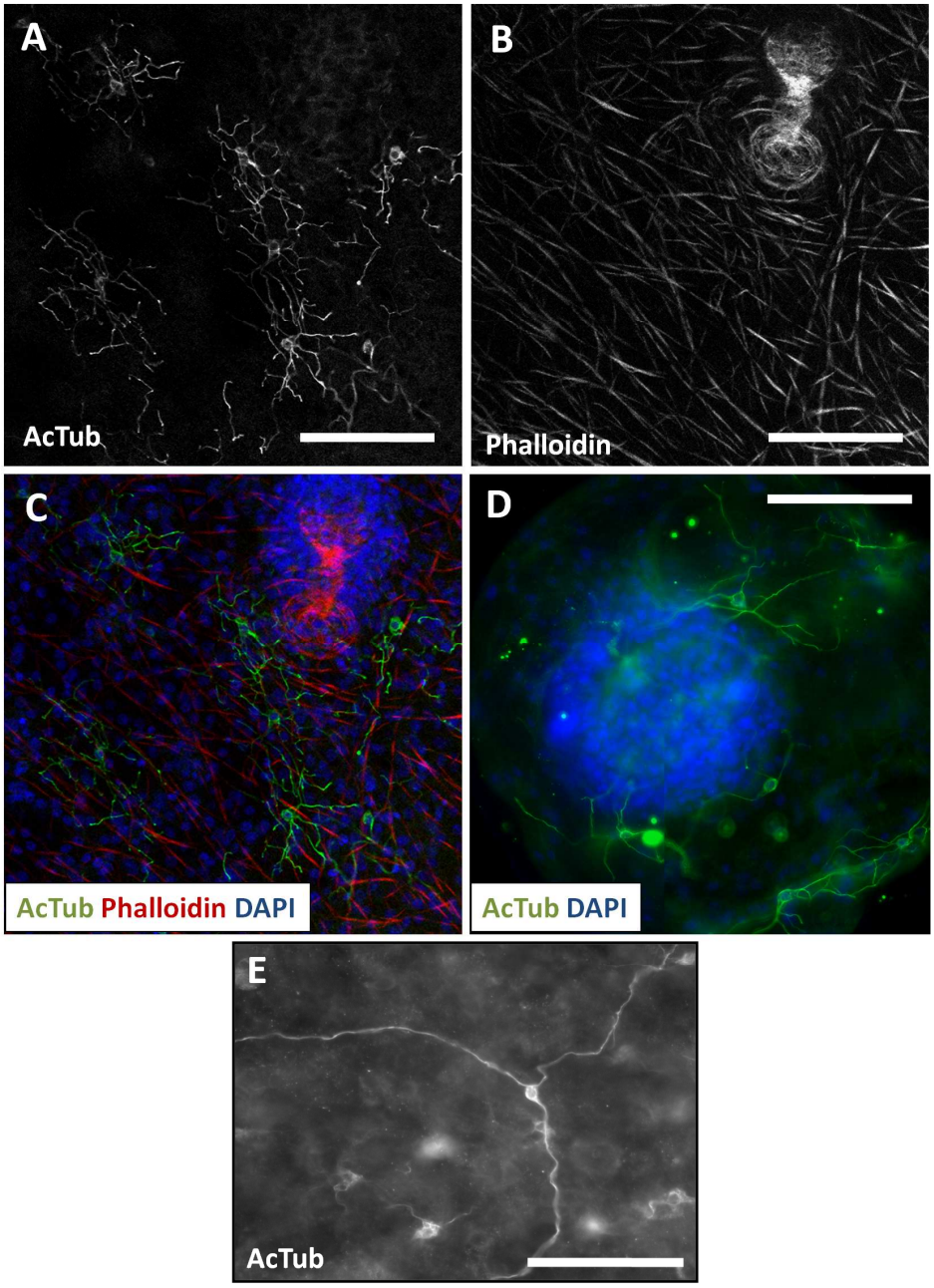

Figure 2. AcTub-IR in whole-mount preparations of the germinal layer. A. AcTub-IR nerve cells in the germinal layer (*in vitro* cultured cyst, analyzed by confocal microscopy). B. Corresponding image of Phalloidin staining. C. Merge of AcTub-IR and Phalloidin staining combined to DAPI staining. Notice the lack of AcTub-IR cell bodies in the brood capsule. D. AcTub-IR nerve cells in a very small vesicle obtained from *in vivo* culture, containing only one brood capsule with a protoscolex bud (this image is a mosaic of three pictures and an overlay of several focal plains of epifluorescence microscopy). E. Unusual AcTub-IR nerve cell with long, unbranched neurites (*in vitro* cultured material). Neurites from other nerve cells are outside of the focal plane. Bars represent 50 μm.

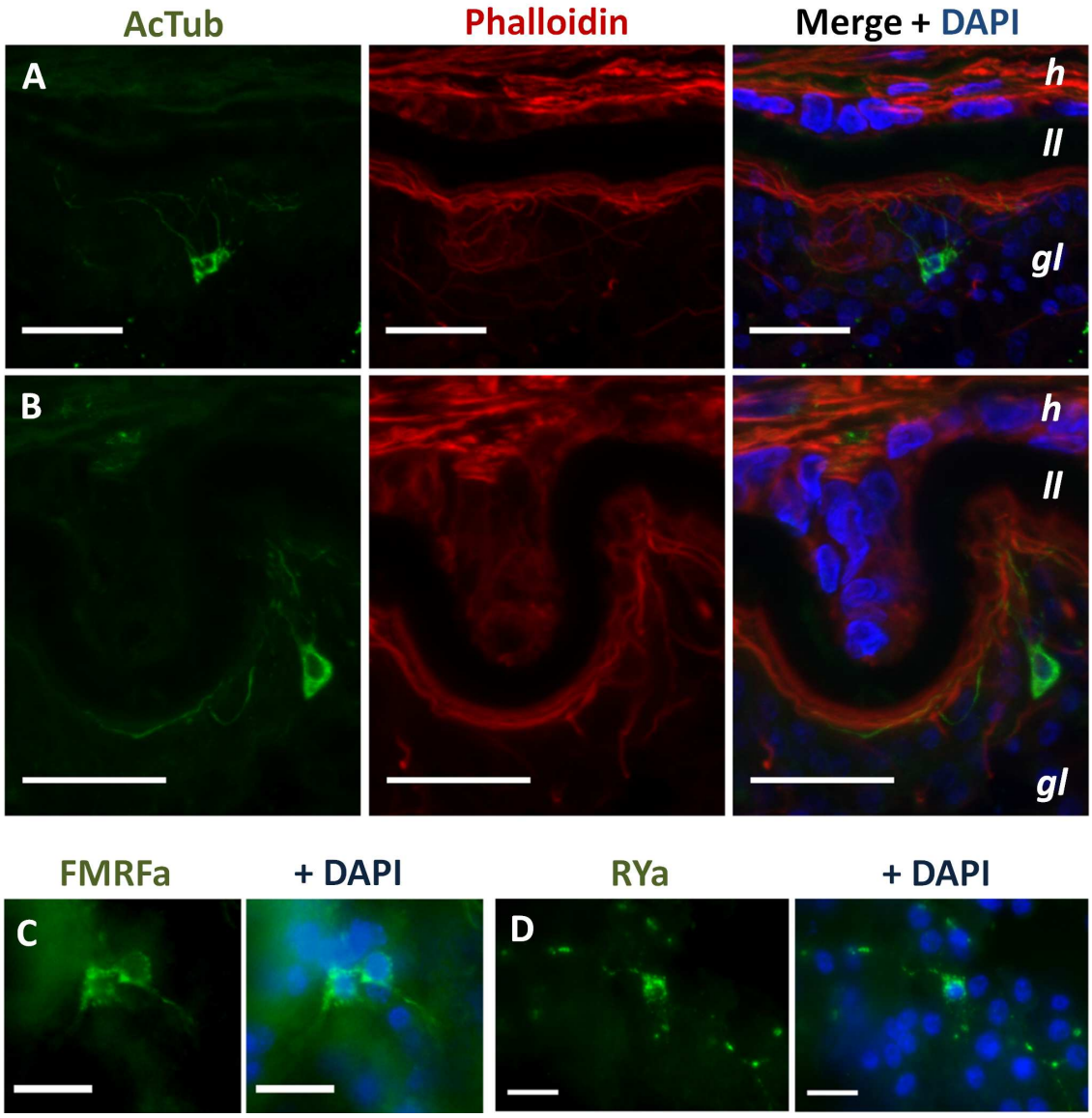

Figure 3. AcTub-IR, FMRFa-IR and RYa-IR in sections of the germinal layer. A. multipolar AcTub-IR cell. Note the neurites projecting towards the subtegumental muscle layer. B. Pseudounipolar AcTub-IR cell. C. FMRFa-IR in two cell bodies and their projections. D. RYa-IR in a nerve cell body and projections in a tangential section of the germinal layer. A and B are confocal microscopy images from *in vivo* cultured material; C and D are epifluorescence images from *in vitro* cultured material. Abbreviations are as in Figure 1. Bars represent 20 µm in A, B and 10 µm in C, D.

5. Results

The muscle system of the mature protoscolex.

For the sake of clarity, we will first describe the muscular and neural anatomy of the mature protoscolex, as observed after evagination (Figures 4 and 5). The muscle system was described by classical histological methods for *E. granulosus* by Coutelen *et al*. (Coutelen et al. 1952), and our results are, with few exceptions, comparable to theirs, so the musculature will be discussed only briefly.

The subtegumental muscle layer consists of a grid of outer circular and inner longitudinal muscle fibers. The longitudinal muscle fibers traverse all along the anteroposterior axis, from the rostellum to the stalk and excretory pore, except for those fibers that are interrupted by the suckers. The circular fibers are found throughout the body except at the level of the suckers. Closely beneath the subtegumental muscles of the scolex, there are groups of muscle fibers projecting more or less radially from the margin of the suckers, connecting each sucker to the others and to the rostellum. Some of the muscles project from the antero-medial border of one sucker, crossing the midline towards the postero-medial border of the adjacent sucker on the same side of the scolex. Other muscle fibers emanating from the margin of the suckers, that are fixed more anteriorly, also cross the midline and connect each sucker to the diagonally opposite sucker, on the other side of the scolex, while still other fibers connect each sucker to the rostellum. Dorso-ventrally opposed suckers are connected by fibers emanating from the lateral margin of each sucker, but also by deep muscle fibers that are fixed to their bases.

Deep in the parenchyma, there is a group of few but prominent longitudinal fibers, connecting the rostellar pad to the posterior of the protoscolex. These muscles are probably associated with the invagination of the scolex.

The suckers themselves are complex muscular organs, with circular fibers both at the opening of the sucker, and also surrounding the wall of the sucker, forming a grid with longitudinally oriented fibers. On the outer face of the sucker, beneath the tegument, there is also a grid of longitudinal and traverse muscles. The most important

group of muscle fibers in the sucker are the perpendicular fibers, connecting the base and the outer face of the sucker.

The rostellar pad, beneath the hooks, is similar in its constitution to the suckers, being surrounded at its outer wall by circular and longitudinal muscles, and with powerful perpendicular fibers connecting the base to the tip of the pad.

Finally, there are numerous muscle fibers in the scolex that are not so intricately organized, including dorso-ventral fibers and transverse fibers. In particular, there is a great accumulation of radial fibers beneath the rostellar pad proper. These could be of importance for the evagination of this organ. Few other fibers can be seen in the body of the protoscolex.

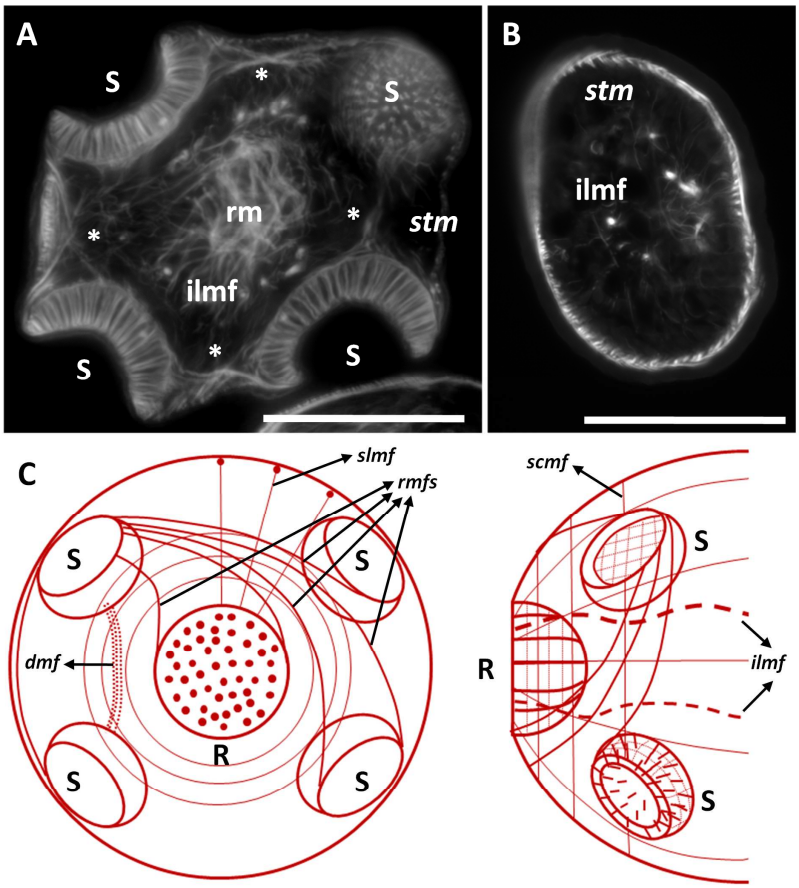

Figure 4. The muscle system of the protoscolex. A. Phalloidin staining of a transverse section of the scolex. B. Phalloidin staining of a transverse section of the posterior body. C. Diagram showing the main groups of muscle fibers in the scolex (left, frontal view; right, dorsal view). See the main text for details. Abbreviations: *dmf*, deep muscle fibers connecting dorso-ventrally adjacent suckers; *ilmf*, inner longitudinal muscle fibers; S, sucker; *slmf*, subtegumental longitudinal muscle fibers, *scmf*, subtegumental circular muscle fibers; *stm*, subtegumental muscles (referring to both longitudinal and circular muscle fibers); R, rostellum, *rm*, radial muscles below the rostellar pad; *rmfs*, radial muscle fibers connecting each sucker to the others and to the rostellum. Asterisks mark several groups of muscle fibers connecting the suckers to each other. Bars represent 50 µm.

5. Results

The nervous system of the mature protoscolex.

Patterns obtained with antibodies

The nervous system of the protoscolex was reconstructed from confocal sections of whole mount material and minor details were obtained from cryosections. AcTub-IR revealed the perinuclear cytoplasm and the neurites of nerve cells, as well as the body and cilia of the flame cells (Figure 5), [Additional File 7]. Because of their morphology and distribution in the nervous system, we conclude that most of the cells labeled by AcTub-IR in the protoscolex, excluding the flame cells, are nerve cells. The flame cells possessed thin AcTub-IR protrusions projecting from the cell bodies, that sometimes appeared to contact the nerve cords. They were nonetheless easily distinguished from nerve cells thanks to their characteristic morphology and by the co-labeling with phalloidin at the base of the flame. A large number of nerve cells were detected by this method, resulting in exquisite detail, but at the same time obscuring in some instances the general layout of the nervous system. The FMRFa-IR, on the other hand, strongly stained all the main and minor nerve tracts in the scolex, the nerve cords and connecting commisures, as well as several minor projections from the nerve cords, giving the best results for the reconstruction of the general layout of the nervous system, although it was very difficult to recognize the perikarya of individual nerve cells (Figure 6), [Additional File 8]. The pattern of RYa-IR was essentially indistinguishable to that obtained by FMRFa-IR, and the pattern or FVa-IR was similar, except that IR was typically low in the nerve cords as compared to the scolex [Additional File 9]. Finally, 5-HT-IR identified a small subset of nerve cell bodies and their neurites, that follow the main nerve tracts, the nerve cords, and some minor tracts and projections (Figure 7). In combination, these markers allowed for a detailed description of the nervous system of the protoscolex.

Neuroanatomy

The nervous system in the scolex of the protoscolex of *E. multilocularis* is very similar to that of the adult stage of *E. granulosus*. All the main elements observed by 5-HT IHF and/or acetylcholinesterase HC (Shield 1969; Brownlee et al. 1994) were

revealed by AcTub and FMRFa IHF, as well as some minor elements and details not previously described.

Two lateral ganglia are situated in the scolex at the level of the anterior border of the suckers. These contain numerous AcTub-IR nerve cell bodies, but it was not possible to distinguish a distinct neuropile within the ganglia, probably due to their small size. These ganglia are connected by a main transverse commissure and by an anterior ring commissure; the main transverse commissure displayed relatively low AcTub-IR, and in some FMRFa and AcTub IHF preparations it appeared to be formed by two individual commissures. From each lateral ganglion, two connectives are emitted towards a rostellar nerve ring at the base of the rostellar pad. These connectives are very closely juxtaposed, and only distinguishable by reconstruction from confocal sections. One pair of dorsal and one pair of ventral medial connectives also connect the anterior ring commissure to the rostellar ring and are the continuations of the minor medial nerve cords (see below). Each of these dorsal and ventral nerve pairs are further connected midway to the rostellum by a short commissure. Finally, a pair of dorso-ventral connectives, termed the 'X-commissure' by Shield [21], directly connect the dorsal and ventral medial nerve cords to the main transverse commissure, resulting in a characteristic cross as seen in cross-sections (Figures 6B, 6D).

The rostellar nerve ring itself appears as a smooth FMRFa-IR ring and has numerous AcTub-IR bipolar nerve cell bodies, that give rise to two coronae of long neurites innervating the rostellum. The neurites of the external corona surround the rostellar pad and reach the apex of the rostellum where the hooks are inserted (this region was denominated the ´rostellar cone´ by Galindo *et al.* (Galindo, Schadebrodt, and Galanti 2008) , and is probably the precursor of the so-called "rostellar gland" of the adult, composed by modified tegumental cells with secretory properties (Thompson, Dunsmore, and Hayton 1979)). The internal corona is composed of neurites that reach and presumably traverse into the rostellar pad. Within the rostellar pad itself few AcTub+ neurites or cell bodies are visible. There seemed to be no indication of distinct lateral rostellar ganglia *sensu* Fairweather *et al*. (Brownlee et al. 1994), but rather the whole rostellar nerve ring seemed to be ganglionic in nature.

To the posterior, the lateral ganglia emit two thick connectives towards the postero-lateral ganglia, located at the same level as the posterior border of the suckers. By FMRFa-IR, the lateral ganglia, the thick connectives and the postero-lateral ganglia appear as a continuous mass of nervous tissue. The postero-lateral ganglia are connected to each other by a posterior ring commissure. The two main lateral nerve cords are born from the postero-lateral ganglia, and each of them is accompanied by a dorso-lateral and a ventro-lateral minor nerve cord, that are born at the point where the posterior ring commissure fuses with the sucker nerve ring (see below; Figures 6A, 6B; Additional File 8).

Each sucker is surrounded at its base by an external nerve ring, that fuses at its medial margin with the medial nerve cords and at its anterior and posterior margins with the anterior and posterior ring commisures. The sucker nerve ring has numerous AcTub+ IR cells projecting neurites that either surround the body of the sucker and result in nerve terminals at its opening, or go deep into the body of the sucker and connect to an internal sucker nerve ring. AcTub-IR nerve cell bodies are also present in this ring (Figure 5 C), but only neurites are labeled by 5-HT-IR and FMRFa-IR. They appear to be bipolar, and extend long neurites towards the surface of the sucker.

In the posterior body, the five pairs of longitudinal nerve cords are connected by transverse ring commissures, forming a typical orthogonal plan (Halton and Gustafsson 1996; Reuter, Mäntylä, and Gustafsson 1998), although the neurites connecting each pair of adjacent nerves are not completely aligned to each other. Along the main nerve cords, the bodies of nerve cells can be distinguished by AcTub-IR, FMRFa-IR, RYa-IR and 5-HT-IR (Figures 6A, 7A, Additional File 9C and data not shown). From these cell bodies neurites extend towards the subtegumental region, where they form a peripheral plexus. Among the AcTub-IR neurites, some of their terminals are located in the subtegumental region, presumably innervating the subtegumental muscles, while others traverse the tegument and are therefore probably sensory terminals (such as those previously described by TEM in *E. granulosus* adults by Morseth (Morseth 1967a); Figure 5E). There are many medial AcTub-IR neurites, that make the medial nerve cords untraceable with AcTub-IR (but they are readily distinguished by IR to the other

antibodies). In the scolex, the nerve terminals of the peripheral plexus are very densely distributed (Figure 5A).

Throughout this description, 5-HT-IR was scarcely mentioned because of the similarity to previous results in *E. granulosus* adults (Brownlee et al. 1994). An important distinction, however, lies in the number of 5-HT-IR nerve cells observed. We observed that although the positions of the 5-HT-IR cells were relatively fixed, the number of cells in each position and the total number in each protoscolex showed some variation. This variation occurred in completely mature protoscoleces, as judged by the morphology of the suckers and the rostellum, and also by the low levels of cell proliferation as determined by 5-ethynyl-2′-deoxyuridine (EdU) incorporation assays (U. Koziol and K. Brehm, unpublished results; see (Galindo et al. 2003)). 5-HT-IR nerve cell bodies were located in the rostellar nerve ring (mode = 3, range = 2-4), in each lateral ganglion (mode = 1, range = 1-2), on the region of the anterior commissure (mode = 1, range = 0-3), in each postero-lateral ganglion (mode = 2, range = 1-3), on the main lateral nerve cords (mode = 2, range = 1-3) and rarely on the medial nerve cords (mode = 0, range = 0-2) (Figure 7). More rarely, we observed ectopically positioned 5-HT-IR nerve cell bodies (e.g. between nerve cords). The total number of 5-HT-IR cells was therefore variable, with an average of 15.2 cells per protoscolex (n = 74), and the majority had between 14 and 17 5-HT-IR cells (Figure 7 C). This was the case for both GH09, an isolate kept by intraperitoneal serial passage in *M. unguiculatus* for 3 years (average = 15.3 5-HT-IR cells / protoscolex), as for J2012, that had only been passaged for 6 months (average = 15.2 5-HT-IR cells / protoscolex; n = 37 for each isolate). This indicates that this variation is a typical feature of the *E. multilocularis* protoscolex and not an abnormal characteristic of a specific laboratory isolate.

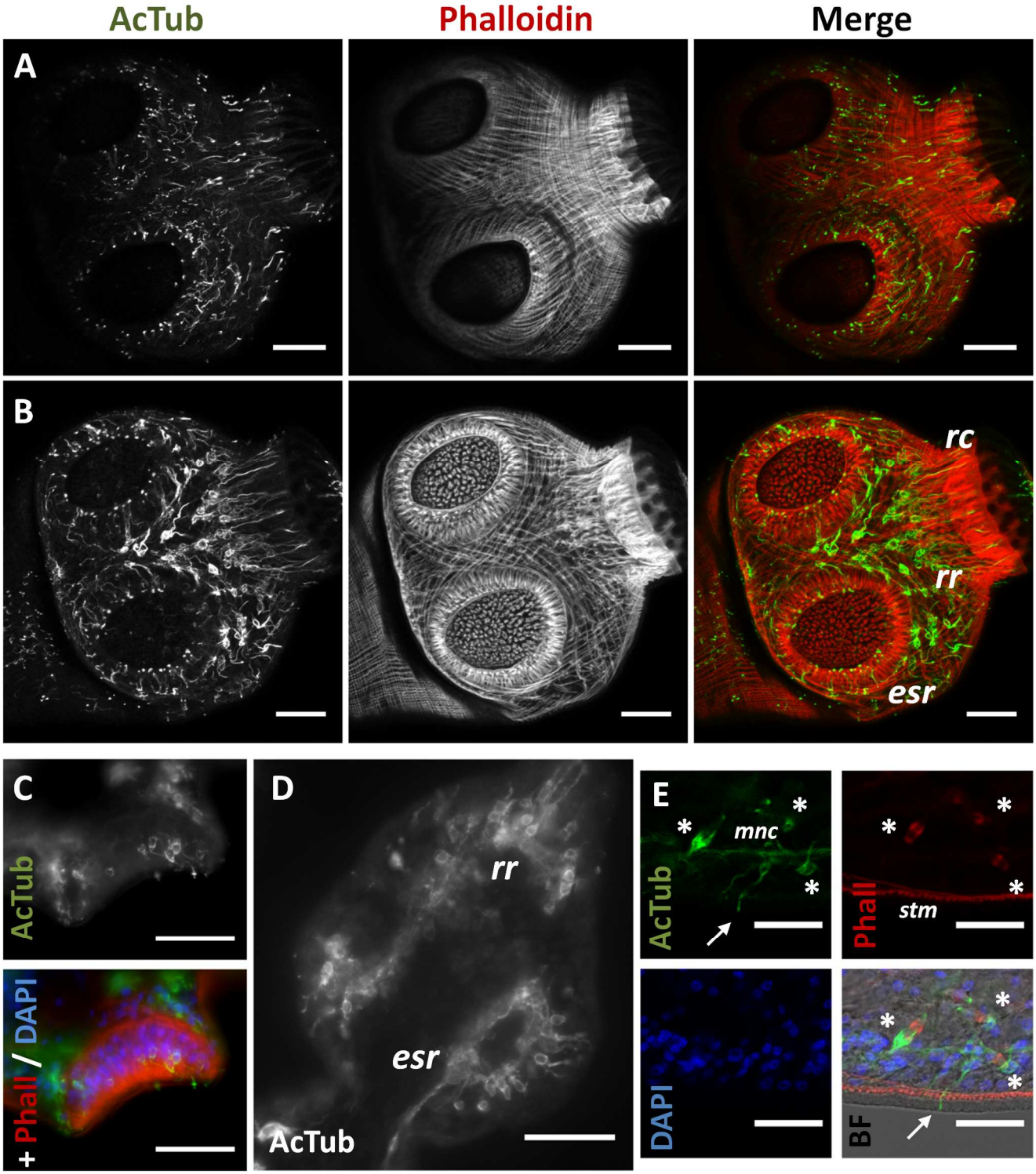
AcTub
Phalloidin
Merge
A
B
rc
rr
esr
C
AcTub
+ Phall / DAPI
D
rr
esr
AcTub
E
mnc
AcTub
DAPI
Phall
stm
BF

Figure 5. AcTub-IR in the protoscolex (previous page). A. AcTub-IR in the nerve terminals in the surface of the protoscolex (confocal microscopy, merge of 3 optical sections). B. AcTub-IR in the nerve cell bodies and neurites below the sections shown in A (confocal microscopy, merge of 3 optical sections). C. AcTub-IR cells and their projections in the internal sucker nerve ring (section). D. AcTub-IR cell bodies and their projections deep within the scolex (section). E. Detail showing a nerve terminal penetrating and traversing the tegument (arrow). Asterisks mark flame cells. (In panel BF, bright field microscopy is added to the merge of the fluorescence channels). Abbreviations: *esr*, external sucker ring; *mnc*, main nerve cords; *rc*, coronae of neurites projecting from the rostellar ring; *rr*, rostellar ring; *stm*, subtegumental muscle layer. Bars represent 25 μm in A, B, and D, 50 μm in C and 20 μm in E.

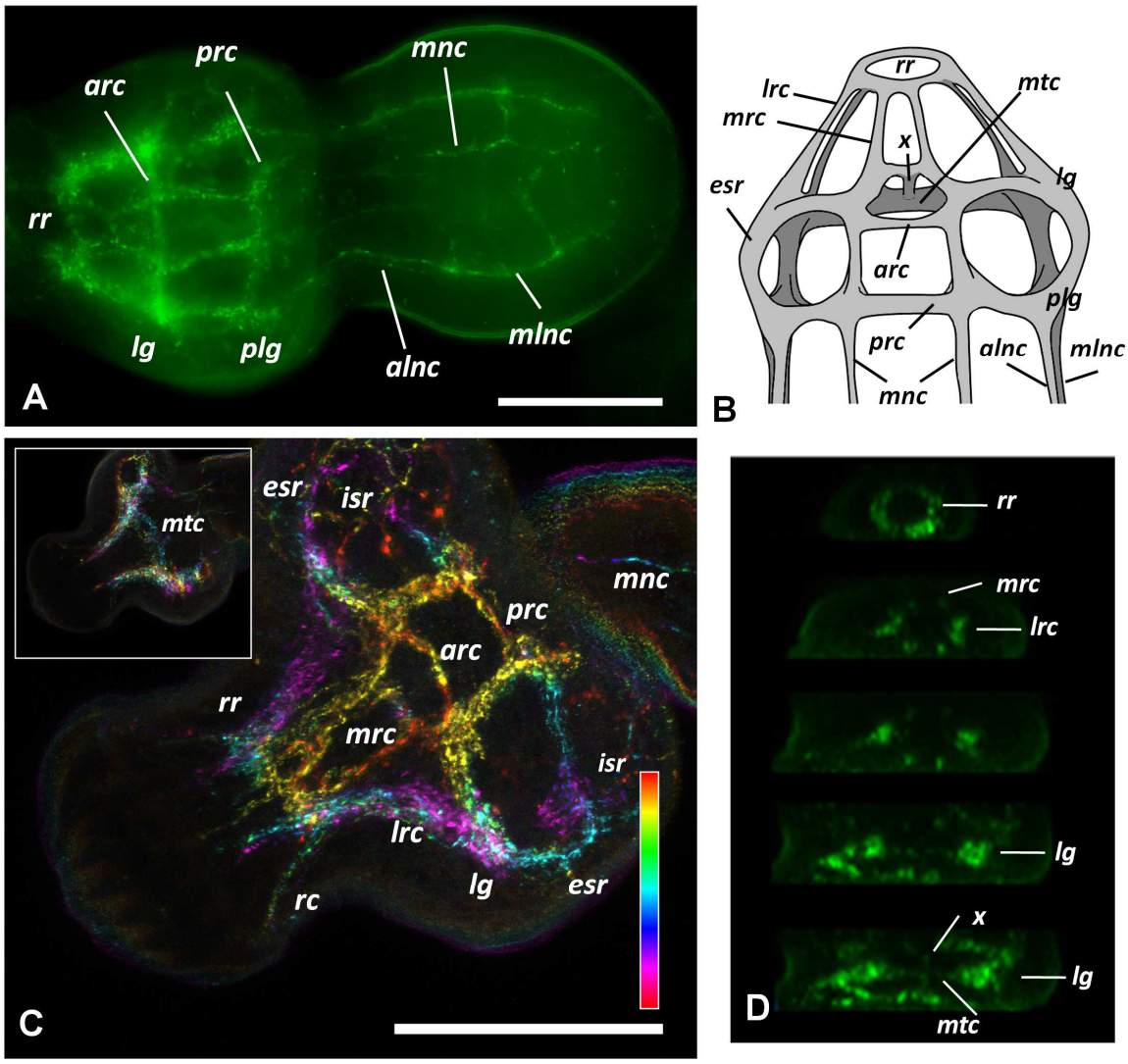

Figure 6. FMRFa-IR in the protoscolex. A. General view of the protoscolex; merge of several focal planes of epifluorescence microscopy, anterior is to the left. B. Diagram showing the main elements of the central nervous system in the scolex as identified by FMRFa-IR. C. Detail of FMRFa-IR in the scolex, confocal projection of 10 um of optical sections with color-coded depth; the inset shows another projection of 10 um thickness, deeper within the scolex, where the main transverse commissure can be seen. Anterior is to the left. D. Serial transverse sections (from anterior to posterior), reconstructed from the confocal sections of C. Abbreviations: *alnc*, accessory lateral nerve cord; *arc*, anterior ring commissure; *esr*, external sucker ring; *isr*, internal sucker ring; *lg*, lateral ganglia; *lrc*, lateral rostellar connectives; *mlnc*, main lateral nerve cords; *mnc*, medial nerve cords; *mrc*, medial rostellar connectives; *mtc*, main transverse commissure; *plg*, postero-lateral ganglia; *prc*, posterior ring commissure; *rr*, rostellar ring; *rc*, coronae of rostellar ring projections; *x*, x-commissure. Bars represent 50 μm.

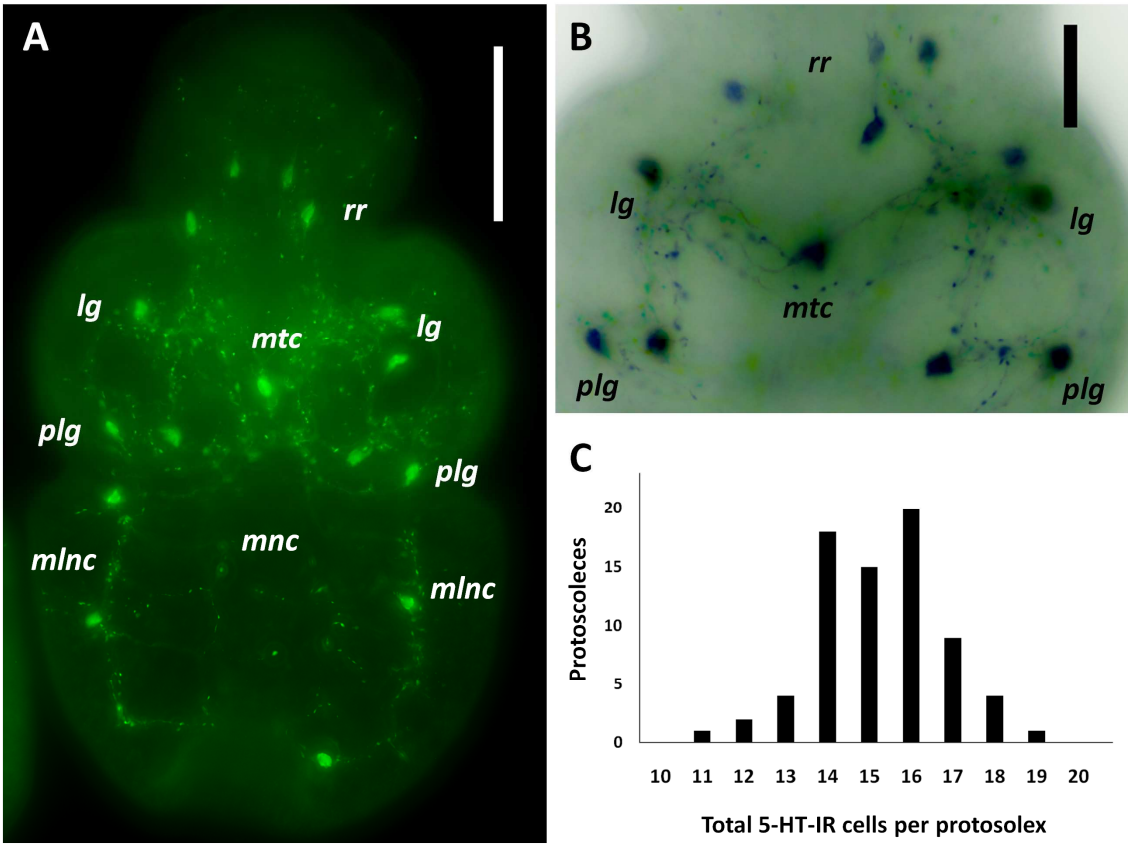

Figure 7. 5-HT-IR in the protoscolex. A. General view of the protoscolex. B. Detail of the scolex (different specimen). A and B are merges of several focal planes of epifluorescence microscopy, anterior is to the top. C. Histogram showing the frequency of the abundance of 5-HT-IR nerve cells per protoscolex. Abbreviations are as in figure 6. Bars represent 50 µm in A, 20 µm in B.

5. Results

The development of muscle fibers and the nervous system in the protoscolex

IR patterns obtained with each antibody during development

Phalloidin staining revealed the development of the muscle fibers throughout protoscolex development. In the case of the nervous system, 5-HT-IR was detectable from early stages of development, clearly labeling the cell bodies of nerve cells, and later the projections from these cells. FMRFa-IR was detectable either at the same stages of development as 5-HT, or usually slightly later, showing similar patterns. Finally, AcTub-IR appeared relatively late during development, only in those regions of the nervous system that could be previously detected by the other antibodies. However, a greater number of nerve cells could be detected at this point with this antibody.

Developmental stages

We have adopted the staging system of Leducq and Gabrion (Leducq and Gabrion 1992) for describing the development of the protoscolex. In stage 1, the initial protoscolex bud appears in the wall of the brood capsule, without any external distinctive features. Already at this stage, there is a well defined grid of longitudinal and circular subtegumental muscles [Additional File 10], that continue into the wall of the brood capsule, and several transverse muscle fibers. It is at this stage that 5-HT-IR appears, as a pair of 5-HT positive cells close to the tip of the bud, without any projections except that they are connected to each other by a short commissure (Figure 8 A). Rarely, faint FMRFa-IR also appears in a pair of cells in a similar position (Figure 8 A). These cells mark the beginning of the development of the rostellar nerve ring. The development of the nervous system then proceeds towards the posterior, resulting in a developmental gradient along the antero-posterior axis.

In stage 2, the rostellar primordium becomes apparent at the tip, composed of an apical rostellar bulb, that will differentiate into the muscular rostellar pad, and a fold (the prebulbar region) at its base. Some of the deep longitudinal muscle fibers can already be seen at this stage. [Additional File 11]. The nerve cells in the developing

rostellar ring form anterior projections towards and into the rostellar bulb, and in some cases 5-HT-IR and FMRFa-IR cells can be seen at this and later stages within the rostellar bulb (however, these probably become relocated later during development since no such cells were observed in the mature rostellar pad). At the same time posterior projections are formed towards the developing lateral ganglia, in which some 5-HT-IR cells with varying labeling intensity can already be seen, already connected by the main nerve commissure (Figure 8 A), [Additional File 11]. The longitudinal nerve cords cover part of the antero-posterior axis. Sometimes supernumerary 5-HT-IR cells or positive cells with atypical positions can be seen (Figure 8 A). The fate of these cells is not clear; presumably these are eliminated or relocated later in development. The FMRFa-IR pattern closely matches the 5-HT-IR, except that it extends more posteriorly in the developing longitudinal nerve cords (Figure 8 A). No AcTub-IR is usually seen at this stage.

In stages 3 to 4, the region that will become the scolex becomes distinct from the posterior body, and cells begin to accumulate at the site where the suckers will be developed. At the same time, the histogenesis of the hook begins at the side of the prebulbar fold. At these stages, the rostellar ring and its coronae, the lateral ganglia, the main transverse commissure and the anterior ring commissure are clearly evident by 5-HT and FMRFa IHF, and weakly 5-HT-IR cells can be seen at the position of the postero-lateral ganglia (Figure 8 A). The main lateral nerve cords are seen extending posteriorly and the anterior portion of the medial nerve cords is also distinct. At this point, AcTub-IR brightly labels the cells of the rostellar nerve ring and the coronae of rostellar projections, directed towards the bulb (internal corona) and the prebulb (external corona) (Figure 8 B).

In stages 5 to 6, the development of the suckers and their associated muscles and nerve rings proceeds. At the same time, the folds of the rostellar prebulb, carrying the developing hooks, grow and engulf the rostellar bulb, coalescing over it. Therefore, the rostellar bulb becomes sub-apical, with the hooks and the prebulb covering it as is found in the mature rostellum. At this point minor connectives and commissures in the scolex are developing, and the postero-lateral ganglia and the posterior ring commissure are well formed. FMRFa-IR labels the main nerve cords all the way towards the posterior of

the protoscolex soma; 5-HT-IR usually labels the cords only to a more anterior position, but positive cells can already be found on the main nerve cords. Finally, at stage 7 the development is complete and the scolex lies invaginated within the posterior body.

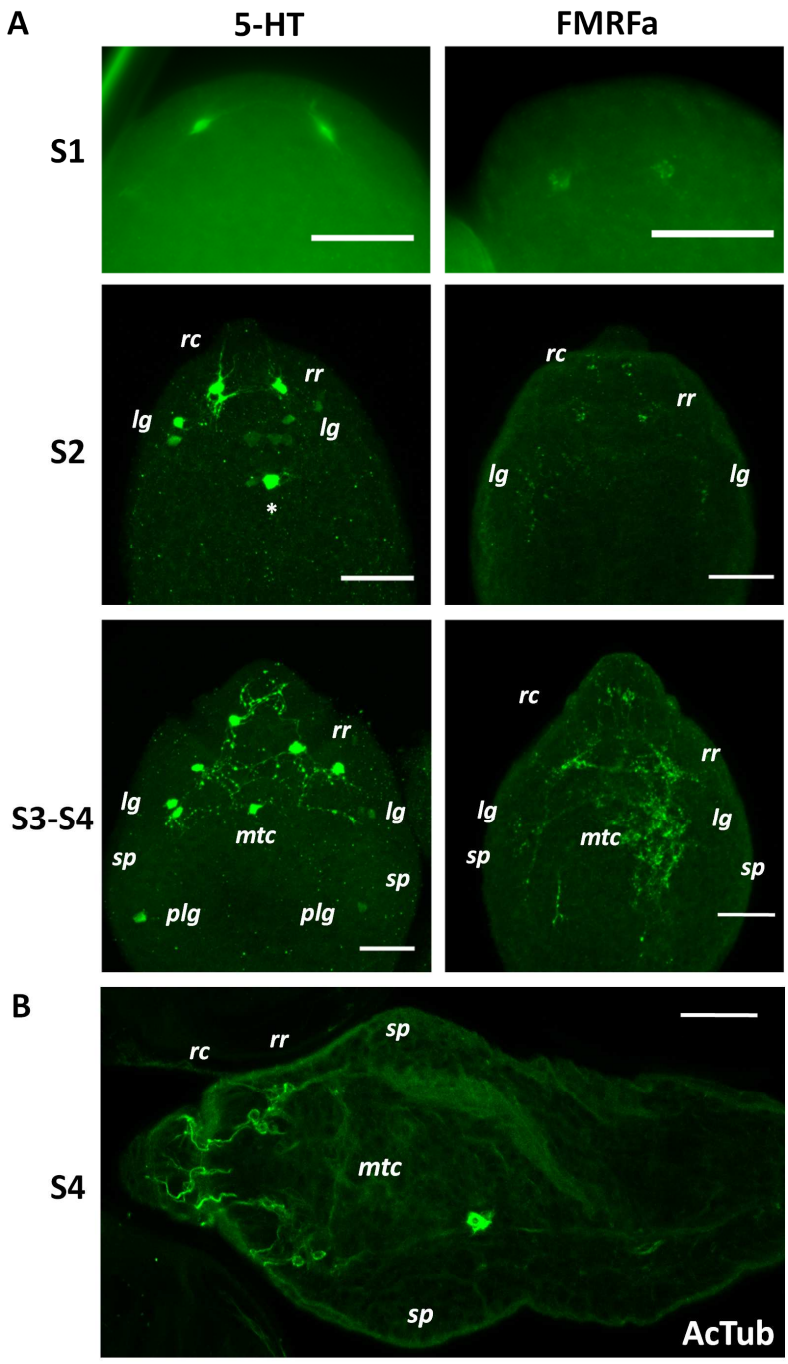

Figure 8. Development of the protoscolex nervous system. A. 5-HT-IR and FMRFa-IR in the early stages of protoscolex development. Abbreviations are as in figure 6 and *sp*, sucker primordium. The asterisk marks a 5-HT-IR cell in an unusual position, perhaps in the developing *mtc*. Note also some supernumerary 5-HT-IR cells with low signal levels next to the lateral ganglia. B. AcTub-IR in late protoscolex development. S1, S2, S3, S4 are stages 1 to 4, respectively. Bars represent 20 µm.

Discussion

This work represents the first detailed description of the nervous and muscle systems in the development of the post-onchosperal larvae of *Echinococcus*, including the first description, to the best of our knowledge, of nervous elements in the germinal layer of the metacestode. The presence of muscle fibers and nerve cells in the germinal layer of the metacestode is intriguing, since this larval stage is a non-motile cyst. However, possible functions for these systems can be hypothesized. In the case of the muscle system, the accumulation of circular fibers around the invaginating brood capsule suggests that they could be involved in the mechanism of invagination and in the constriction of the stalk. Furthermore, the muscle layer in the cyst wall is continuous to that of the brood capsule and the protoscolex. In the case of the nervous system, although the projecting neurites of the nerve cells are in close apposition to the muscle fibers, a myoregulatory role seems improbable, given the lack of motility and the absence of serotoninergic and cholinergic elements (which are the best characterized myomodulatory neurotransmitters in flatworms (Ribeiro, El-Shehabi, and Patocka 2005; Maule, Marks, and Day 2006)). Furthermore, this nervous system is independent from that of the developing protoscolex, suggesting that it would not serve as a scaffold for the development of the protoscolex nervous system. An attractive hypothesis is that it could represent a neuroendocrine system, secreting factors that regulate the development of the metacestode. Relatedly, possible neuroendocrine secretory terminals have been described at the ultrastructural level in the nervous system of cestodes (Halton and Maule 2003), and in free living flatworms there are several lines of evidence suggesting a role of the nervous system in regulating cell proliferation and pattern formation during asexual reproduction and regeneration (Reuter and Gustafsson 1996; Rossi, Iacopetti, and Salvetti 2012). In other systems, muscle fibers or myofibroblasts can also be a source of growth factors stimulating stem cell proliferation and maintenance in superjacent epithelia (Powell et al. 1999; Takashima, Gold, and Hartenstein 2013). If such a role was demonstrated for the neuromuscular system in *Echinococcus* cysts, it would open new areas for drug research targeting these signaling systems, offering a potential link to many present efforts targeting the neuromuscular system in trematodes (Mousley et al. 2005) .

The nervous and muscle systems in *E. multilocularis* are probably homologous to those present in the motile bladder tissue from *Taenia* spp., although modified because of the lack of motility in *Echinococcus* cysts. Indeed, the limited reports regarding the nervous system in the bladder of *Taenia* spp. indicate that RFamide-IR and acetylcholinesterase positive (AChE+) fibers are present (Fairweather et al. 1991; Vasantha et al. 1992). Furthermore, we have confirmed the presence of FMRFa-IR, AcTub-IR and AChE+ elements in the bladder tissue of *in vitro* cultured *Taenia crassiceps*, together with a well organized grid of subtegumental longitudinal and circular muscles [Additional File 12].

In another publication (Tsai et al. 2013) we performed a bioinformatic search for neuropeptide-encoding genes in the genomes of *E. multilocularis* and other cestodes, finding several genes that showed significant expression in the germinal layer (as determined by high throughput RNA sequencing and RT-PCR). It is thus possible that some of these neuropeptides are expressed in the nerve net of the germinal layer.

Surprisingly, there is no AcTub-IR during the early development of the protoscolex nervous system, which is at odds with the occurrence of AcTub-IR in pioneer neurons during the development of many metazoans (Jellies et al. 1996; Younossi-Hartenstein, Ehlers, and Hartenstein 2000; Younossi-Hartenstein and Hartenstein 2000; Younossi-Hartenstein, Jones, and Hartenstein 2001). It seems that in the case of *E. multilocularis*, tubulin-α acetylation occurs only at late stages of neurogenesis. Interestingly, 5-HT and FMRFa-IR were detected from very early time points, even in young nerve cells with few short projections. Similar results have been described in the development of other invertebrates (Voronezhskaya and Elekes 1996; Dickinson, Croll, and Voronezhskaya 2000; Franchini 2005) , and the early expression of neurotransmitter molecules could have regulatory roles during the development of the nervous system (Cameron, Hazel, and McKay 1998; Nguyen et al. 2001; Daubert and Condron 2010) .

This description of the nervous system in the scolex is the most detailed to date, benefiting from the use of several different markers in combination with confocal

microscopy. In particular, the use of AcTub-IR resulted in great detail, and allowed us to identify large numbers of nerve cell bodies not previously detectable with 5-HT-IR, AChE HC or IR against mammalian neuropeptides (Shield 1969; Brownlee et al. 1994; Fairweather et al. 1994). Prominent examples of this include the rostellar ring, which appears as fully ganglionic by AcTub-IR (whereas it appeared to be composed of two individual ganglia by 5-HT-IR) and the inner sucker nerve ring, that has numerous AcTub-IR cell bodies but that was only described as a network of nerve processes in previous studies (Brownlee et al. 1994; Fairweather et al. 1994). On the other hand, FMRFa-IR gave the best results for the reconstruction of the general layout of the nervous system, and for tracing the main commisures and connectives. Indeed, it allowed the detection of all nervous elements previously described from 5-HT-IR and/or AChE HC, together with fine details not previously described [Additional File 13].

Once the development of the nervous system is complete in the protoscolex, its morphology is already similar to that of the scolex of the developed adult, with no major rearrangements produced during adult development. This is probably related to the fact that the scolex, once evaginated, must be fully functional to avoid being dispelled from the host. However, the number of 5-HT-IR cells in the scolex of adult *E. granulosus* is higher, and has been described as fixed for each region (e.g., exactly five 5-HT-IR cells have been described in the postero-lateral ganglia, 3 in the rostellar ring, etc. (Brownlee et al. 1994)). Therefore, assuming that the nervous system of the adult of *E. multilocularis* is identical to that of *E. granulosus*, new nerve cells must be incorporated into the nervous system of the scolex during adult development (as has been described for example for peptidergic neurons of *Hymenolepis diminuta* (Fairweather et al. 1988)). The final numbers of 5-HT-IR cells might become fixed in adults as compared to the protoscolex, but there is little information about the constancy in the number and position of individually identifiable neurons in flatworms in general (Halton and Gustafsson 1996; Younossi-Hartenstein, Ehlers, and Hartenstein 2000). The general structure of the nervous system in the scolex of *Echinococcus* is also remarkably similar to classical descriptions of the related *Taenia* spp. (Cohn 1899; Vasantha et al. 1992), although the scolex in these species is at least one order of magnitude larger. It is also worth mentioning the similarities observed in the

development of the scolex of *Echinococcus* spp. ((Goldschmidt 1900); this work) and that of *Taenia* spp. (Crusz 1947; Mount 1970; Shield, Heath, and Smyth 1973). In both cases the rostellar bulb and prebulb are the first signs of differentiation appearing on a thickened scolex primordium in the brood capsule (*Echinococcus*) or bladder wall (*Taenia*). Later, as the prebulb carrying the hooks grows and engulfs the bulb, the primordia of the suckers are formed.

The highly detailed description of the nervous system in these larval stages is a necessary first step towards future studies regarding the function of the nervous system, and of particular neurotransmitters, neuropeptides and their signal transduction systems in the biology and development of *E. multilocularis*. Furthermore, the use of axenic *in vitro* cultivation systems for *E. multilocularis* metacestodes (Spiliotis and Brehm 2009) provides the opportunity, for the first time, to study the mechanisms behind the peculiar developmental processes of these organisms, including their developmental plasticity, unusual asexual multiplication by protoscolex formation, and the continuous growth and exogenous budding of metacestodes, all of which are based on the presence of a totipotent population of stem cells (the so-called germinative cells or neoblasts) (Sakamoto and Sugimura 1970; Reuter and Kreshchenko 2004; Brehm 2010b; Koziol et al. 2010). Also in this case, a careful description of developmental sequences such as the development of the neuromuscular system described herein is an essential first step.

Conclusions

E. multilocularis is an important human parasite and a recently emerging model system to study host-dependent parasite development *in vitro* [63]. We herein provide the most detailed description to date of the morphology of the nervous system of protoscoleces throughout development. We found a remarkable complexity of the protoscolex nervous system, comparable to that observed in many adult cestodes. The data we provide will be important for future studies on parasite developmental plasticity and functional and evolutionary analyses on cestodes in general, and taeniids in particular. Furthermore, we demonstrate for the first time that the cystic metacestode stage, which grows tumor-like within the intermediate host, contains a nerve net with peptidergic elements. Although the function of this nerve net cannot yet be clearly

determined, we suggest that it could act as a neuroendocrine system that regulates parasite development within the host. As such, it could be a potential target for the development of novel anti-parasitics. Using the information provided by our study, and the recently determined *E. multilocularis* genome sequence [42], we are currently characterizing parasite neuropeptides that are expressed in the metacestode in order to determine their function in parasite physiology.

Materials and Methods

Parasite culture and fixation

Parasite isolates were maintained by serial intraperitoneal passage in *Meriones unguiculatus* as previously described (Spiliotis and Brehm 2009). Isolates were originally obtained from accidental infections of Old World Monkeys in a breeding exclosure (Tappe et al. 2007), and had been passaged at the time of this study for between six months and four years. All experiments were carried out in accordance with European and German regulations on the protection of animals (Tierschutzgesetz). *In vitro* co-culture of parasite vesicles with rat Reuber hepatoma cells was performed as previously described (Spiliotis and Brehm 2009). Protoscoleces were isolated from *in vivo* parasite material and either activated by successive treatments with pepsin at low pH and taurocholate (Gelmedin, Spiliotis, and Brehm 2010) , or alternatively set into culture in DMEM (Gibco) plus 10% fetal calf serum (Biochrom) for 12 hours, that also resulted in significant scolex evagination. Parasite vesicles obtained *in vitro* (Spiliotis and Brehm 2009) were gently opened using a syringe tip in order to allow the entry of the fixative and other reagents during immunohistofluorescence. The material analyzed from *in vivo* cultures consisted of small pieces of metacetode tissue surrounded by host liver tissue. All samples for IHF were fixed in 4% paraformaldehyde (PFA) buffered in phosphate buffer saline (PBS), for 1 to 4 hours at room temperature.

Antibodies

We used a suite of antibodies typically employed for the description of the nervous system in diverse invertebrates:

1) Anti-acetylated tubulin-α (AcTub), mouse monoclonal antibody (Santa Cruz, clone 6-11B-1; diluted 1:100; (Piperno and Fuller 1985)). Tubulin-α acetylation is a post-translational modification that occurs in highly stable microtubuli, mainly occurring in the neuronal cytoskeleton (neurotubuli) and in cilia and flagella. Because it is able in

principle to label all nerve cells independently of their neurotransmitter, AcTub immunoreactivity (IR) has been used to describe in detail the complete nervous system of numerous invertebrates, including free living flatworms and onchospheres (Siddiqui et al. 1989; Muller and Westheide 2000; Younossi-Hartenstein, Ehlers, and Hartenstein 2000; Younossi-Hartenstein and Hartenstein 2000; Younossi-Hartenstein, Jones, and Hartenstein 2001; Orrhage and Müller 2005; Persson et al. 2012). Furthermore, it has been used to study the development of the nervous system in both vertebrates and invertebrates, since many pioneer axons show AcTub-IR (Chitnis and Kuwada 1990; Jellies et al. 1996; Younossi-Hartenstein, Ehlers, and Hartenstein 2000; Younossi-Hartenstein and Hartenstein 2000; Younossi-Hartenstein, Jones, and Hartenstein 2001).

2) Anti-FMRFamide (FMRFa), rabbit polyclonal antibody (Immunostar, diluted 1:300). Antibodies against the neuropeptide FMRFa have also been used extensively for the characterization of invertebrate nervous systems. It is acknowledged that anti-FMRFa antibodies, and in particular the one used in this and other studies, can recognize most neuropeptides containing a C-terminal RFamide motif (Brennan et al. 1993; Hartenstein and Jones 2003; Orrhage and Müller 2005; Harzsch and Muller 2007).

3) Anti-RYamide (RYa; 1:250 dilution) and Anti-FVamide (FVa; 1:125 dilution), rabbit polyclonal antibodies, kindly provided by Markus Conzelmann (Max Planck Institute for Developmental Biology, Tübingen, Germany). These antibodies recognize small amidated dipeptide motifs frequently found in neuropeptides of invertebrates, and are highly specific (Conzelmann and Jekely 2012). For instance, the anti-RYa antibody does not cross- react with neuropeptides with an RFamide motif. Anti-FLamide was also used but no IR was found in *E. multilocularis* (data not shown).

4) Anti-5-HT, rabbit polyclonal antibody (Immunostar, diluted 1:300). Antibodies against 5-HT have been extensively used to characterize the serotoninergic components of the nervous system in invertebrates in general and flatworms in particular (see for example (Brownlee et al. 1994; Fairweather et al. 1994; Orrhage and Müller 2005; Maule, Marks, and Day 2006))

Immunohistofluorescence in whole-mounts (WMIHF) and in cryosections

We followed the WMIHF protocols described by Collins *et al*. (Collins et al. 2011) for *Schistosoma mansoni*, with some modifications. After fixation, samples were washed three times for 10 min with PBS with 0.3% Triton X-100 (PBS-T). After this, permeabilization was achieved by either A) 20 min incubation in PBS with 1% sodium dodecyl sulfate (SDS) for metacestode vesicles or B) a 5 min treatment with proteinase K (Fermentas, 2 µg/ml in PBS-T plus 0.5% SDS), followed by re-fixation with 4% PFA buffered in PBS for 10 min at room temperature (proteinase K treatment was essential for protoscolex WMIHF). After permeabilization, samples were washed three more times with PBS-T and blocked for 2 h in PBS-T with 3% bovine seralbumin (BSA, Sigma-Aldrich) and 5% normal sheep serum (Sigma-Aldrich). Incubation with the primary antibody, diluted in PBS-T with 3% BSA, was carried overnight at 4 º C. Then, samples were washed five times for 30 min with PBS-T, and incubated overnight with the FITC conjugated secondary antibody (donkey anti-mouse or donkey anti-rabbit as required, Jackson Immunoresearch) at 4 º C. Finally the samples were washed five times for 30 min with PBS-T, and co-stained with 4',6-diamidino-2-phenylindole (DAPI) and TRITC-conjugated Phalloidin (Sigma-Aldrich) as previously described (Koziol et al. 2011). Negative controls lacking the primary antibody were performed, which showed no signal. Cryosections were prepared as previously described (Koziol et al. 2010), and processed for IHF with a similar protocol, except that no detergent was added to PBS for the washes, permeabilization was achieved using 0.1% Triton X-100 in PBS, and all incubation times were reduced. Samples were analyzed by confocal microscopy (Leica TCS SP5) and by epifluorescence microscopy (Zeiss Axio Imager.Z1).

Acetylcholinesterase Histochemistry. (AChE HC).

AChE HC was carried out as described by the direct method of Karnovsky and Roots (Karnovsky and Roots 1964).

Transmission electron microscopy

5. Results

Metacestode vesicles obtained after 3 months of *in vitro* culture of the GH09 isolate (containing brood capsules) were fixed, processed and analyzed by TEM, essentially as previously described (Spiliotis et al. 2008).

Acknowledgments

This work was supported by grants from the Deutsche Forschungsgemeinschaft (DFG; BR 2045/4-1) and the Wellhöfer Foundation (all to KB). UK was supported by a grant of the German *Excellence Initiative* to the Graduate School of Life Sciences, University of Würzburg. The authors wish to thank Monika Bergmann and Dirk Radloff for excellent technical assistance, and Hilde Merkert, of the Institute for Molecular Infection Biology, Würzburg, for her assistance with confocal microscopy. This publication was funded by the German Research Foundation (DFG) and the University of Würzburg in the funding programme Open Access Publishing.

Authors' contributions

UK carried out or participated in all experiments. UK and KB designed the study and drafted the manuscript. GK designed and interpreted the results of TEM studies. All authors read and approved the final manuscript.

Competing interests

The authors declare that they have no competing interests.

Additional files

Additional File 1 - Supplementary figure (.tif format). Unusual flame cell in the germinal layer of *Echinococcus multilocularis*. Confocal microscopy, section of *in vivo* cultured material**.** The bar represents 10 μm.

Additional File 2 – Supplementary figure (.tif format). AChE histochemistry in *Echinococcus multilocularis*. A. Double labeling of AChE HC and AcTub-IR; note the single AChE HC positive cell without any projections (asterisk), and negative to AcTub-IR. AcTub-IR cell bodies are indicated by arrows. The bar represents 50 μm. B. AChE HC reaction in the nervous system of the protoscolex.

Additional File 3 – Supplementary figure (.tif format). Transmission electron microscopy of the germinal layer of *Echinococcus multilocularis*. Nerve projections (A, B, C, arrows) and a putative nerve cell body (C, asterisk) are highlighted in red. Abbreviations: *mc*, mitochondria; *nu*, nucleus; *tu*, microtubules; *ve*, vesicles. Bars represent 1 μm.

Additional File 4 – Supplementary movie (.avi format). Early brood capsule. Serial confocal sections of an early developing brood capsule from *in vivo* cultured material of *Echinococcus multilocularis* stained for AcTub-IR (green), Phalloidin (red) and DAPI (blue).

Additional File 5 – Supplementary movie (.avi format). Stalked brood capsule. Serial confocal sections of a brood capsule with a stalk from *in vivo* cultured material of *Echinococcus multilocularis* stained for Phalloidin (red) and DAPI (blue).

Additional File 6 – Supplementary movie (.avi format). Brood capsule with developing protoscolex. Serial confocal sections of a brood capsule with a protoscolex bud in a whole-mount *in vitro* cultured cyst of *Echinococcus multilocularis*, stained for AcTub-IR (green), Phalloidin (red) and DAPI (blue).

Additional File 7 – Supplementary movie (.avi format). AcTub-IR in the protoscolex of *Echinococcus multilocularis*. Serial confocal sections of a whole-mount specimen.

Additional File 8 - Supplementary movie (.avi format). FMRFa-IR in the protoscolex of *Echinococcus multilocularis*. Serial confocal sections of a whole-mount specimen stained for FMRFa-IR (green), Phalloidin (red) and DAPI (blue).

Additional File 9 – Supplementary figure (.tif format). FVa-IR and RYa-IR in the protoscolex of *Echinococcus multilocularis*. A. Developing protoscolex, FVa-IR (whole-mount). B. Transverse section of the scolex, FVa-IR. C. Mature protoscolex, RYa-IR (whole-mount). D. Section of developing protoscolex, RYa-IR. Abbreviations are as in figures 4 and 6, and *cns*, central nervous system; *px*, subtegumental plexus. Bars represent 50 μm in A, C and D, and 25 μm in B.

Additional File 10 – Supplementary movie (.avi format). Subtegumental muscle fibers in a stage 1 protoscolex bud of *Echinococcus multilocularis*. Serial confocal sections of a whole-mount protoscolex bud partially surrounded by the remains of the brood capsule, stained with Phalloidin.

Additional File 11 – Supplementary movie (.avi format). 5-HT-IR in a stage 2 developing protoscolex of *Echinococcus multilocularis*. Serial confocal sections of a whole-mount specimen stained for 5-HT-IR (green) and Phalloidin (red).

Additional File 12 – Supplementary figure (.tif format). Muscle and nervous systems in *Taenia crassiceps* bladder tissue cultured *in vitro*. This is a laboratory strain passaged in *M. unguiculatus*. It multiplies by budding but is unable to produce scoleces, generating only bladder tissue. Samples were processed identically to the *E. multilocularis* cysts. A. Phalloidin staining; note the longitudinal and circular muscle fibers (whole-mount). B. AcTub-IR in the subtegumental layer; inset shows the flame cells in detail (whole-mount). C. FMRFa-IR in the subtegumental layer (whole-mount). D. AChE HC (section). Bars represent 200 μm in A, 50 μm in B and C, 20 μm in the inset in B.

Additional File 13 – Supplementary table (.doc format). Comparison of the description of the protoscolex nervous system in this and in previous investigations.

5.5. CHAPTER 5: Further experimental results regarding the *E. multilocularis* neuromuscular system.

In this chapter, I will describe further experiments that I performed for the characterization of the *Echinococcus multilocularis* neuromuscular system, which were not included in the previous article. Some of these results were included in another article of which I am a co-author, as indicated.

5.5.1. Persistence of the nervous system during the development from protoscoleces to metacestode vesicles

Another peculiarity of the development of *Echinococcus* larval stages is the ability of protoscoleces to develop into metacestode vesicles if they are released in the intermediate host, as well as *in vitro* (Yamashita, Ohbayashi, and Sakamoto 1960; Yamashita et al. 1962; Smyth, Howkins, and Barton 1966; Rogan and Richards 1986; Rogan and Richards 1989; al Nahhas et al. 1991; Cucher et al. 2013). This ability is more marked and has been studied in greater detail for *E. granulosus,* and spillage of protoscoleces from ruptured cysts is the main source of secondary cysts in CE (Brunetti, Kern, and Vuitton 2010).

Under the typical *in vitro* co-culture conditions used in our laboratory, a small proportion (<1%) of protoscoleces were able to complete this developmental transition, following similar developmental stages as the ones described for *E. granulosus* (Rogan and Richards 1986) (Figure R5.1). A large fraction of protoscoleces never begins the transformation into metacestode vesicles, while many others die during the process. Initially, the protoscoleces swell and adopt a vesiculated shape, and many cells disappear. Rudimentary suckers and rostellum remain, as well as internal "filaments" connecting the scolex to the posterior of the body. Eventually, the laminated layer appears, and only shapeless tissue remnants are found in the original position of the scolex, which are usually still are connected to the posterior region of the body through the "filaments". The process took at least 50 days, under our culture conditions, from the start of the culture until the laminated layer becomes apparent by standard microscopy. After 105 days of culture, these protoscolex-derived vesicles showed a strong positive reaction for alkaline phosphatase in the tegument, as is characteristic for the metacestode germinal layer, but not for protoscoleces (Koziol et al. 2014) (Figure R5.2). Furthermore, small accumulations of proliferating cells, reminiscent of early brood capsule formation, could be seen in some of the metacestode vesicles obtained after 105 days of culture (see below). These results suggest that the transformation of protoscoleces into metacestode vesicles was complete.

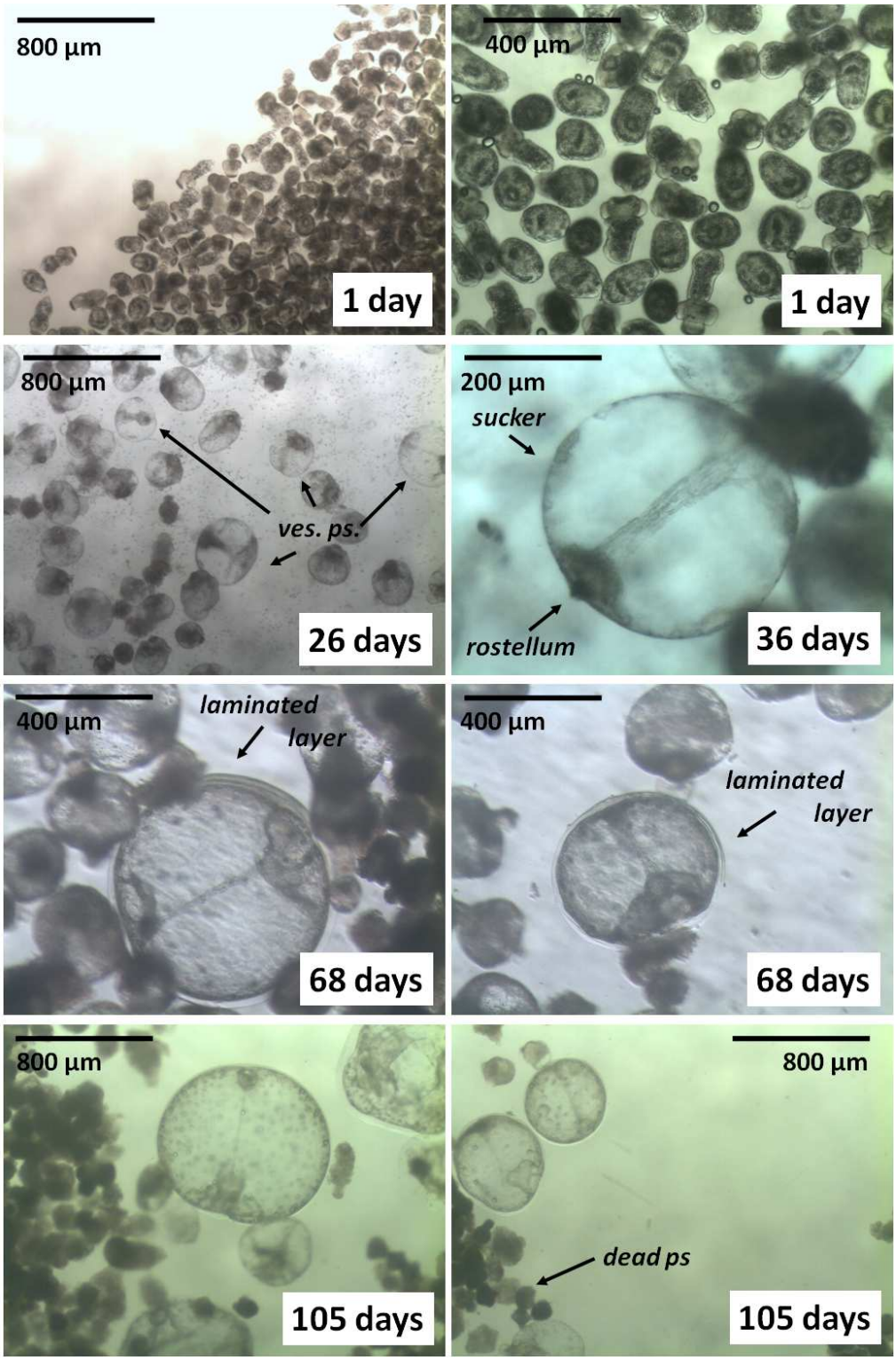

Figure R5.1. Developmental stages of the transformation of protoscoleces into metacestode vesicles *in vitro*. Time elapsed since the beginning of *in vitro* culture is indicated on the bottom right corner. *dead ps*., dead protoscoleces; *ves. ps*., vesiculating protoscoleces.

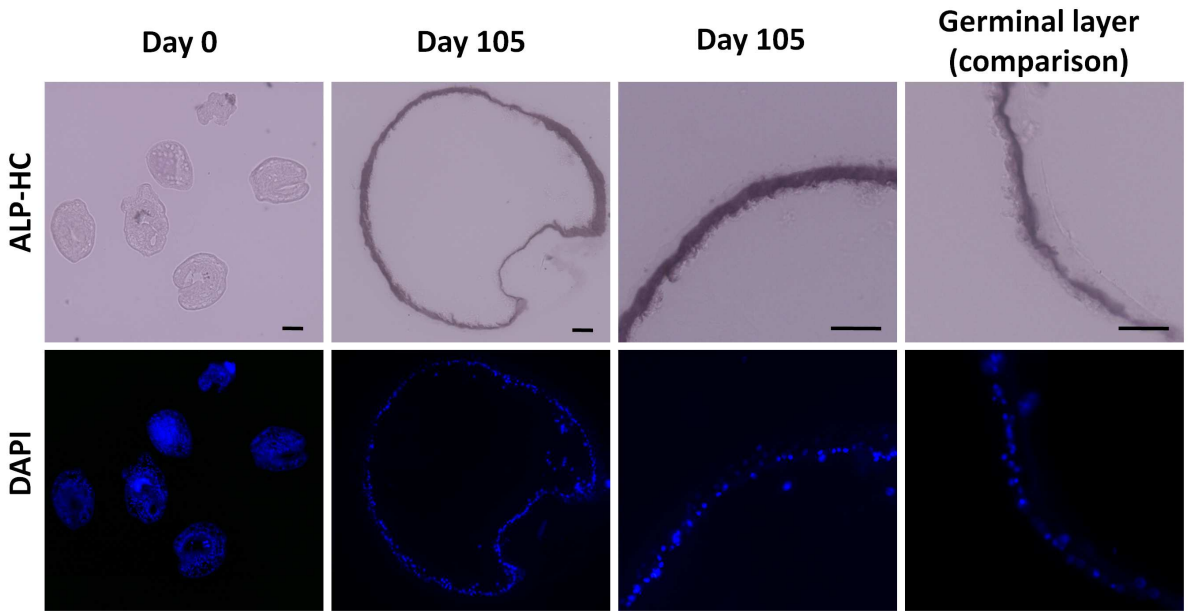

Figure R5.2. Alkaline phosphatase histochemistry (ALP-HC) of protoscoleces during transformation into metacestode vesicles *in vitro*. Protoscoleces before culture (day 0) and after transformation into metacestode vesicles *in vitro* (day 105 of culture) were analyzed for alkaline phosphatase activity in the tegument by ALP-HC in cryosections. For comparison, the same experiment was performed in parallel for metacestode vesicles obtained by standard *in vitro* co-culture of parasite material with feeder cells. Bars: 40 µm.

Previous histological and ultrastructural studies of the transition from the protoscolex to the vesicle stage have focused on the tegumental syncitium and the *de novo* formation of the laminated layer (Rogan and Richards 1989; al Nahhas et al. 1991), but little is known about the fate of the neuromuscular system and the germinative cells. Recently, it was shown that the serotoninergic nervous system of *E. granulosus* disappears very quickly during this transition (Camicia et al. 2013). We investigated the fate of the muscular and nervous systems by phalloidin staining and acetylated α-tubulin (AcTub) immunohistofluorescence. The muscular system became quickly disorganized after just one week, and it largely disappeared from the body of the protoscolex after one month, although it could be seen in the posterior-most region of the body, and more prominently in the suckers and rostellum. As many tegumental cells disappeared, most remaining cells were found in the remains of the scolex and next

to the “filaments”. Interestingly, the “filaments” are $AcTub^+$ and are actually the persisting nervous system, which although somewhat disorganized, remains in the scolex and in the body (Figure R5.3). At the same time, the remaining proliferating (EdU^+) cells cluster around the $AcTub^+$ nerve cords and the remains of the scolex (Figure R5.4, A). At the final stages of development, the EdU^+ cells are still found close to the remains of the scolex, but appear to be dispersing into the rest of the developing vesicle, and new cells can be found in the subtegumental region (Figure R5.4, B). Unfortunately, we were unable to determine if the “filaments” were still $AcTub^+$ at this stage due to insufficient availability of specimens. Finally, when the laminated layer is apparent, the germinal layer has a typical morphology, with dispersed EdU^+ cells which sometimes accumulate to form structures reminiscent of early brood capsules (Figure R5.4, C-D). In summary, although the muscular system is largely lost, the nervous system persists until later stages, and the remaining proliferating cells accumulate in its proximity during the transition to the vesicle stage. In general, the persistence of the nervous system and its proximity to the remaining proliferating cells suggests that it may play a role during this developmental transition, and is reminiscent of the close apposition of neoblast populations and the nerve cords of free-living flatworms (Bode et al. 2006; Rossi, Iacopetti, and Salvetti 2012).

.

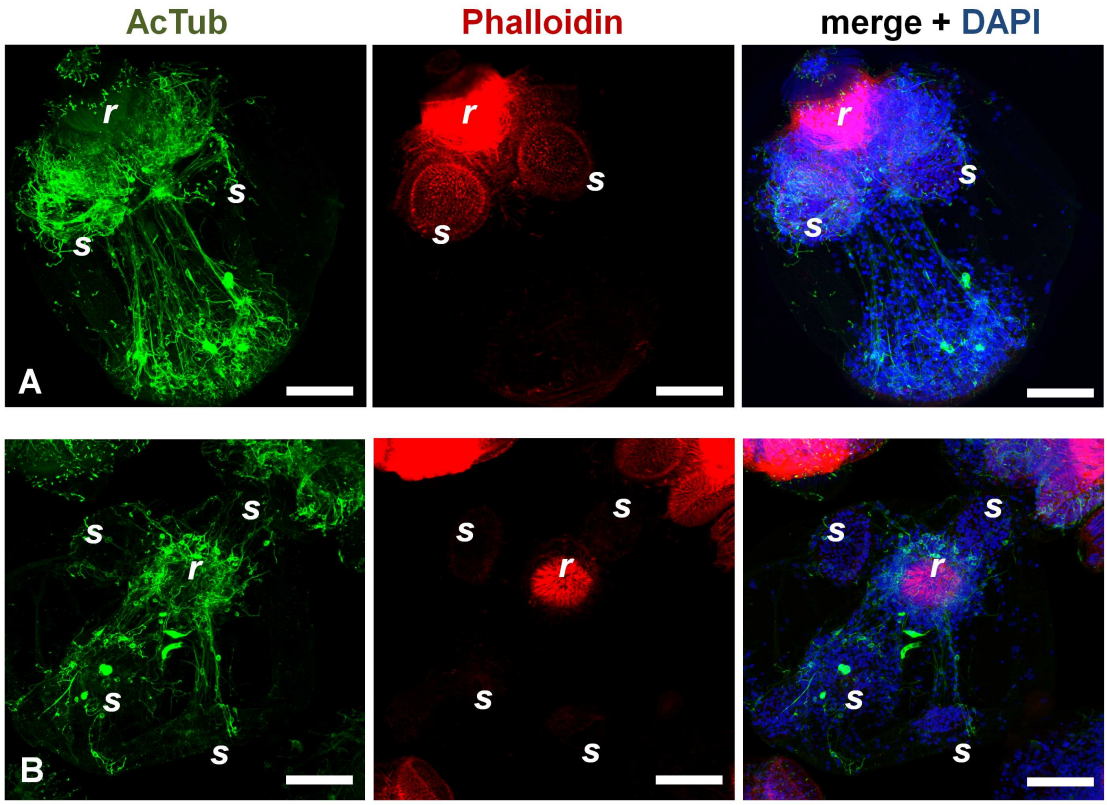

Figure R5.3. AcTub immunohistofluorescence and phalloidin staining of protoscoleces during transformation into metacestode vesicles *in vitro*. Two different specimens are shown (**A, B**). The phalloidin signal is essentially lost in the body, and very reduced in the suckers; only the signal in the rostellum remains (compare for example with the non-vesiculating protoscoleces in the top left corner in B). t. *r*, rostellum; *s*, sucker. Bars: 50 µm.

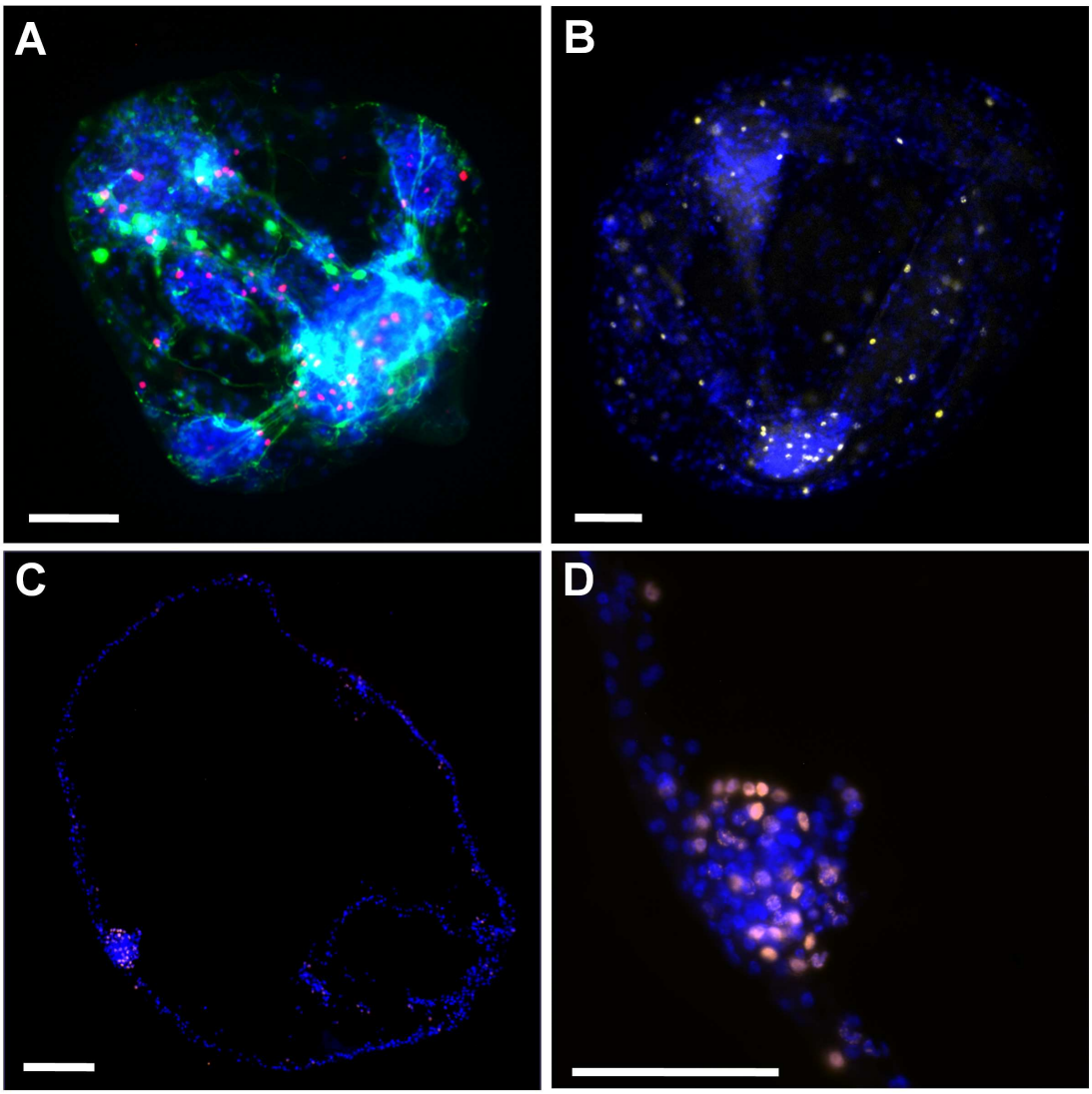

Figure R5.4. EdU incorporation in protoscoleces during transformation into metacestode vesicles *in vitro*. Specimens were cultured *in vitro* with 50 µM EdU for 5 hours and were then processed for AcTub immunohistofluorescence (IHF) and/or EdU detection. **A.** Early vesiculating protoscolex, stained in whole-mount for EdU detection (red), AcTub IHF (green), and DAPI (blue). Note the proximity of the EdU^+ cells to the $AcTub^+$ nervous system in the scolex and in the "filaments". **B.** Late vesiculating protoscolex, stained in whole-mount for EdU (yellow) and DAPI (blue). **C.** Specimen after complete transformation into a metacestode vesicle (with a laminated layer, at day 105 after the beginning of culture), stained in cryosections for EdU (yellow) and DAPI (blue). **D.** Detail of C, showing a structure similar to an early brood capsule bud containing numerous EdU^+ cells. Bars: 50 µm.

5.5.2. Discovery of neuropeptide-encoding genes in *E. multilocularis*

Neuropeptides (*i.e.* bioactive peptides or peptide hormones, abbreviated as NPs) are structurally and functionally diverse in metazoans, having prominent roles as modulators in the nervous system, reproductive system, and in many other tissues. Typically, NPs serve as ligands for signaling through G-protein coupled receptors (GPCRs) of the Rhodopsin and Secretin families (Frooninckx et al. 2012; Hoyer and Bartfai 2012). Drugs targeting these receptors and signaling systems have been proposed as promising targets for anthelminthics (Mousley et al. 2005; Marks and Maule 2010).

NPs are processed from larger pre-prohormone precursors, and this processing is essential for their biological activity (Li and Kim 2008). It is common for individual precursors to code for several different peptides which are processed into individual NPs, in many cases with similar sequence and activity to each other. Initially, the pre-prohormone enters the secretory pathway, and its signal peptide is cleaved as it enters the rough endoplasmic reticulum. Then, the active peptide is proteolitically cleaved from the prohormone at dibasic sites (or more rarely monobasic sites) by proprotein convertases, in particular by members of the PC1 and PC2 subfamilies (Steiner 1998; Seidah et al. 2008). The basic C-terminal residues are removed by carboxypeptidase E, and finally, peptides containing a C-terminal glycine residue are amidated (the glycine residue is lost, and the resulting C-terminal α-amide group comes from the glycine residue itself) (Bradbury and Smyth 1991; Attenborough et al. 2012). Amidation is in many cases essential for the interaction of the NPs with their receptors (Li and Kim 2008).

As shown in the previous chapter, nerve cells showing immunoreactivity to different invertebrate neuropeptides can be detected in the germinal layer of *E. multilocularis* metacestodes. Because of the possible role of NPs in regulating development in flatworms, we were interested in determining which NP-encoding genes are expressed during larval development. Although much progress has been achieved in the discovery of NPs in other flatworms (McVeigh et al. 2009; Collins et al. 2010), almost nothing was known before this work about the diversity of NP genes in cestodes.

5. Results

Only two neuropeptide sequences had been published (NPF and GNFFRFamide from *Moniezia expansa* (Marks and Maule 2010)), and two ESTs from taeniids had been proposed to code for NPs (McVeigh et al. 2009) (*E. granulosus npp-6* and *Taenia solium npp-20*; re-named *npp-20.3* in this work). Recently, two insulin-like peptides (*emilp1* and *emilp2*) were also described for *E. multilocularis* in this laboratory (Hemer et al. 2014). Therefore, the first step was to obtain a list of NP-encoding genes for *E. multilocularis*. The following results were previously included as part of Tsai *et al*. (2013), Nature 496:57-63.

Because the biologically relevant peptides are short stretches of moderately conserved amino acid residues (usually 3–40 residues), identifying genes coding for NPs by purely bioinformatic methods is challenging. In this work, two strategies were performed in order to identify NP genes in the genome of *E. multilocularis* and other cestodes (*E. granulosus*, *Taenia solium* and *Hymenolepis microstoma*). First, a blastp search was conducted for known invertebrate NP genes against the predicted proteome of *E. multilocularis*, and hits were manually examined for important conserved sequences in the active peptides. Pre-propeptides were also examined for the presence of a signal peptide sequence (Petersen et al. 2011) and then scanned for mono and di-basic cleavage sites for prohormone convertases. In this way, a few conserved NP genes could be found, but this strategy would not recover divergent or novel cestode NP genes.

The initial results indicated that cestodes are peculiar among invertebrates, since cestode NP genes typically encode only one or at most two copies of similar mature neuropeptide sequences per propeptide, and the mature NP sequence is often in the C-terminus of the propeptide, not requiring a downstream proprotein convertase site. Therefore, systematic searches for multiple proprotein convertase sites (e.g. $\{[K/R][K/R]X_{4\text{-}20}[K/R][K/R]\}_{>2}$) as described for other invertebrates (Nathoo et al. 2001; McVeigh et al. 2009) are not adequate. Instead, we took advantage of the observation that mature NP sequences are highly conserved between *E. multilocularis* and *Hymenolepis microstoma*, whereas the surrounding regions are poorly conserved but usually still detectable by blast (an example is shown in Figure R5.5). Therefore, a novel homology-based strategy was developed for discovering conserved cestode NPs (see the Materials and Methods section). Briefly, a wide list of possible NP genes from

E. multilocularis, with a very high proportion of false positives, was filtered by checking for high conservation of the predicted active peptide and cleavage sites but lower conservation in the rest of the CDS in *H. microstoma* orthologs. The resulting candidates were further checked for the presence of a signal peptide, and homologs of the candidates were also searched for in *E. granulosus*, *T. solium*, *S. mansoni* and free living flatworms. For one gene (EmuJ_000530500), the correct 5' end containing a putative signal peptide was obtained by 5´ Rapid Amplification of cDNA Ends (5´ RACE).

```
Query: 1      MRGTFISILTLF---YFASSLRLHDYDGEAEPTVSAATPVGEAEDDIDFFPPRYGVAKRY 57
              M    IS+L L    YF +S R+   + +  P +         ++DIDF P  Y + KR
Sbjct: 449033 MHSLHISLLPLLFFVYFVNSFRVSSLEPK-RPFIG--------DEDIDFIPYPYRLYKRI 185

Query: 58     PLLSDLDEGMMIENPYWAK-EISRRSPQFAWRPHSRFGRR 96
               L  +L EG++ E+P    + E+ RRSPQFAWRPHSR+GRR
Sbjct: 449186 SLQPELAEGVIQEDPLMTESEVYRRSPQFAWRPHSRYGRR 305
```

Figure R5.5. Example of tblastn analysis for the discovery of cestode NP genes. One candidate NP gene from *E. multilocularis* (Query) was blasted (tblastn) against the genome of *H. microstoma* (Sbjct). Notice the great similarity in the predicted mature peptide (green), including a C-terminal glycine which could result in C-terminal amidation (blue), and in the putative proprotein convertase sites (red), as compared to the rest of the protein. Furthermore, both proteins contain a predicted signal peptide (not shown). This blast analysis resulted in the discovery of the sequelog group *npp-34*, not previously known for flatworms but with similarity to Luqins from other lophotrochozoans (see the main text).

5. Results

In total, we found 22 groups of NP genes conserved between *E. multilocularis, E. granulosus*, *T. solium*, and *H. microstoma* (Table R5.1). Of these groups, 16 could be assigned to 11 previously described flatworm "sequelogs" (groups of genes coding for similar peptides but of uncertain homology due to the short length of the conserved peptides) or to specific flatworm sequences (groups *npp-4*, *npp-5*, *npp-2*, *npp20.1*, *npp20.2*, *npp20.3*, *npp20.4*, *npp20.5*, *npp-6*, *npp-24*, *npp-27*, *npp-14*, *npp-15.1*, *npp15.2*, *spp-3*, *spp-18* (McVeigh et al. 2009; Collins et al. 2010); note that we have divided the *npp20* sequelog into 5 sub-families). For three other groups we found similar peptides in *Schistosoma*, founding three new flatworm sequelog groups (*npp-29*, *npp-31*, and *npp-32*). For one group, general similarity was found with other RL-amides, but not to any group in particular, and a new sequelog group was founded (*npp-30*). Finally, for two genes, no evidence of conservation was found in other flatworms, resulting in two candidate cestode-specific sequelog groups (*npp-33* and *npp-34*). However, *npp-34* shows similarities with Luqins, a family of NPs found in mollusks and annelids (Veenstra 2010; Veenstra 2011), suggesting a common origin, and that *npp-34* sequences may eventually be discovered in other flatworms as well.

The total number of conserved NP genes was 21 to 22 in taeniids and 25 in *H. microstoma* (which has three specific gene duplications of groups *npp-20.3, npp-27* and *npp-29*, with duplicated genes clustered (<21 kb distance) to each other in the genome). With the exception of these duplicated genes from *H. microstoma*, and of the conserved and clustered duplicated genes *npp-15.1* and *npp-15.2*, no other significant clustering of NP genes was observed in any genome. The total number of conserved predicted mature peptides was found to be between 27 and 29. These numbers are in broad concordance with the number of predicted peptide GPCRs in the genomes of cestodes (e.g. 29 predicted peptide GPCR receptors in *E. multilocularis*, (Tsai et al. 2013)), suggesting that a large proportion of the cestode NP genes has been found.

The discovered cestode NPs are dominated by R(F/Y)amides, (I/L/M)amides (McVeigh et al. 2009; McVeigh et al. 2011), and by an expansion of neuropeptide F family genes (groups *npp-20.1* to *npp-20.5*, similar to the expansion in the planarian *Schmidtea mediterranea* (Collins et al. 2010)). As previously discussed (McVeigh et al. 2009; McVeigh et al. 2011), most of these sequelogs show little to no similarity to vertebrate NPs. Even neuropeptide F genes show divergent features, such as a C-

terminal GRARF-amide motif in *npp-20.2* genes, instead of the highly conserved GRPR(F/Y)-amide motif, and a tryptophan residue in position -10 of *npp-20.3* genes instead of the highly conserved tyrosine. Finally, cestodes appear to have lost several neuropeptide and peptide hormones (*e.g.* FMRFamide, vasopressin/oxytocin-like peptides, Gonadotropin Release Hormone-like peptides and GPA2/GPB5 heterodimeric glycoproteins) that are widely conserved in metazoans, including annelids and mollusks (*i.e.* groups that are phylogenetically close to the Platyhelminthes) (Veenstra 2010; Veenstra 2011).

Table R5.1. Predicted neuropeptide / peptide hormone genes in cestodes

Species	Sequelog	Gene code [2]	Predicted peptide(s) (only conserved peptides shown)	Peptide structural family[3]	Signal Peptide
E. multilocularis	spp-18	EmuJ_000092400.1	GLHFFRL	Non amidated peptide	YES
E. granulosus	spp-18	EgrG_000092400.1	GLHFFRL	Non amidated peptide	YES
T. solium	spp-18	TsM_001104400.1*	GLHFFRL	Non amidated peptide	YES
H. microstoma	spp-18	HmN_000234350	GLHFFRL	Non amidated peptide	?
E. multilocularis	npp-14	EmuJ_000740500	GIMKMRI-amide; ASIRRMRM-amide	(L/M/I)amide	YES
E. granulosus	npp-14	EgrG_000740500	GIMKMRI-amide; ASIRRMRM-amide	(L/M/I)amide	YES
T. solium	npp-14	TsM_001092400.1	GIMKMRI-amide; AGIRRMRM-amide	(L/M/I)amide	YES
H. microstoma	npp-14	HmN_000787500.1	GIRKMRI-amide; GIMKMRI-amide; AGIRRMRM-amide	(L/M/I)amide	YES
E. multilocularis	npp-15.1	EmuJ_000945400.1	AQFLRL-amide	(L/M/I)amide	YES
E. granulosus	npp-15.1	EgrG_000945400.1	AQFLRL-amide	(L/M/I)amide	YES
T. solium	npp-15.1	TsM_000537100.1	AQFLRL-amide	(L/M/I)amide	YES
H. microstoma	npp-15.1	HmN_000592500.1	AQFLRL-amide	(L/M/I)amide	YES
E. multilocularis	npp-15.2	EmuJ_000945300.1	AQFLRI-amide	(L/M/I)amide	YES
T. solium	npp-15.2	TsM_000537000.1	AQFLRI-amide	(L/M/I)amide	NO
H. microstoma	npp-15.2	HmN_000592400	AQFLRI-amide	(L/M/I)amide	YES
E. multilocularis	npp-2	EmuJ_000530500	RGFI-amide (2x)	(L/M/I)amide	YES
E. granulosus	npp-2	EgrG_000530500	RGFI-amide (2x)	(L/M/I)amide	YES
T. solium	npp-2	TsM_001095700.1*	RGFI-amide (2x)	(L/M/I)amide	YES
H. microstoma	npp-2	HmN_000050100.1	RGFI-amide (2x); RSFL-amide	(L/M/I)amide	YES
E. multilocularis	npp-20.1	EmuJ_001070600	ADPLSIINPPESVLSN PAALRDYLRQVNEYF AIIGRPRF-amide	Neuropeptide F	YES
E. granulosus	npp-20.1	EgrG_001070600	ADPLSIINPPESVLSN PAALRDYLRQVNEYF AIIGRPRF-amide	Neuropeptide F	YES
T. solium	npp-20.1	TsM_000819400.1*	ADPLSIVNPPESVLN NPAALRDYLRQVNE	Neuropeptide F	YES

[2] Wellcome Trust Sanger Institute GeneDB codes

[3] Modified from McVeigh et al 2009

			YFAIIGRPRF-amide		
H. microstoma	npp-20.1	HmN_000462100	AEADLTDRILNDPAALRDYLRQINEYFAIIGRPRF-amide	Neuropeptide F	YES
E. multilocularis	npp-20.2	EmuJ_000043400.1	?-KDLFKYMAQLNDYYVLFGRARF-amide	Neuropeptide F	YES
E. granulosus	npp-20.2	EgrG_000043400.1	?-KDLFKYMAQLNDYYVLFGRARF-amide	Neuropeptide F	YES
T. solium	npp-20.2	TsM_000527100.1	?-KDLFKYMAQLNDYYMLFGRARF-amide	Neuropeptide F	YES
H. microstoma	npp-20.2	HmN_000295600	SRSLEEILSDPEFMEWLNSKFPNIAFFLSGRNQEPSTETVREIFRFMAELNNYYAIYGRARF-amide	Neuropeptide F	YES
E. multilocularis	npp-20.3	EmuJ_001194600	QIFRNVREFRRYLQRLDEWLAITGRPRF-amide	Neuropeptide F	NO; but SP after DS ATG
E. granulosus	npp-20.3	EgrG_001194600	QIFRNVREFRRYLQRLDEWLAITGRPRF-amide	Neuropeptide F	NO
T. solium	npp-20.3	NOT PREDICTED	QIFRNVKEFRRYLQRLDEWLAITGRPRF-amide	Neuropeptide F	NO
H. microstoma	npp-20.3.1	HmN_000069000.1	PLFRTARELRRYLEQLDEWLAITGRPRF-amide	Neuropeptide F	YES
H. microstoma	npp-20.3.2	HmN_000069100	PVFRNVQELRRYLEQLDEWLAITGRPRF-amide	Neuropeptide F	NO
E. multilocularis	npp-20.4	EmuJ_000926000.1	SHPTVPLLPQYLERLKKFQSLKDKEKYVAALNSYYMIFGRPRF-amide	Neuropeptide F	YES
E. granulosus	npp-20.4	EgrG_000926000.1	SHPTVPSLPQYLERLKKFQSLKDKEKYVAALNSYYMIFGRPRF-amide	Neuropeptide F	YES
T. solium	npp-20.4	TsM_000401700.1	SRPTVPSLPQYLERLKKFHSLRDKEKYVAALNSYYMIFGRPRF-amide	Neuropeptide F	YES
H. microstoma	npp-20.4	HmN_000206600	NDITYLPKRFKTAKDMERYMAALNAYYMIFGRPRF-amide	Neuropeptide F	YES
E. multilocularis	npp-20.5	EmuJ_000706000.1	EPQTSGWDLADDLGTLESGEDFNDINDAV	Neuropeptide F	NO; but SP DS ATG

			LSSEKTSLTREEIQRYL AQMKAYYLKNGMP RY-amide		
E. granulosus	npp-20.5	EgrG_000706000.1	EPQTSGWDLADDLG TLESGEDFNDINDAV LSSEKTSLTREEIQRYL AQMKAYYLKNGMP RY-amide	Neuropeptide F	NO; but SP after DS ATG
T. solium	npp-20.5	TsM_000781400.1*	EPQAGGWDLADDL GTLGTGEDFGDINDA VLSSEKTSLTREEIQR YLAQMKAYYLKNGM PRF-amide	Neuropeptide F	NO; but SP after DS ATG
H. microstoma	npp-20.5	HmN_000096800.1	DFSISDSWDLDDDLI EDDDLKEANDAVMA SAKTALTEEEAQKYL AQMKAYYLKNGMP RF-amide	Neuropeptide F	NO
E. multilocularis	npp-24	EmuJ_001046700.1	FKPKMPIFLGLI-amide	(L/M/I)amide	YES
E. granulosus	npp-24	EgrG_001046700.1	FKPKMPIFLGLI-amide	(L/M/I)amide	YES
T. solium	npp-24	TsM_000993300.1*	FKPKMPIFLGLI-amide	(L/M/I)amide	YES
H. microstoma	npp-24	HmN_000377100.1	SRSPIFHGLL-amide	(L/M/I)amide	YES
E. multilocularis	npp-27	EmuJ_000347700	RLPYLIGGIRY; ALDYLYGGVRY	Non amidated peptide	YES
E. granulosus	npp-27	EgrG_000347700	RLPYLIGGIRY ; ALDYLYGGVRY	Non amidated peptide	YES
T. solium	npp-27	TsM_000472700.1	RLPYLIGGIRY; ALDYLYGGVRY	Non amidated peptide	NO
H. microstoma	npp-27.1	HmN_000326200.1	ALDYLYGGVRY	Non amidated peptide	YES
H. microstoma	npp-27.2	HmN_000326100.1	SLDYLYGGVRY	Non amidated peptide	YES
E. multilocularis	npp-29	EmuJ_000229800	MLYW; MVYW	Non amidated peptide	YES
E. granulosus	npp-29	EgrG_000229800	MLYW ; MVYW	Non amidated peptide	YES
T. solium	npp-29	NOT PREDICTED	MLYW; MVYW	Non amidated peptide	YES
H. microstoma	npp-29.1	HmN_000212550	MIYW (2x)	Non amidated peptide	YES
H. microstoma	npp-29.2	HmN_000212650	MIYW (2x)	Non amidated peptide	YES
E. multilocularis	npp-30	EmuJ_000489700.1	GFLHSGRL-amide; GFLTASRL-amide	(L/M/I)amide	YES
E. granulosus	npp-30	EgrG_000489700.1	GFLHSGRL-amide; GFLTASRL-amide	(L/M/I)amide	YES
T. solium	npp-30	TsM_000991300.1	GFLHSGRL-amide ;	(L/M/I)amide	YES

			GFLTASRL-amide		
H. microstoma	npp-30	HmN_000183900	GFLTSSRL-amide; GFLTAGRL-amide	(L/M/I)amide	YES
E. multilocularis	npp-31	EmuJ_000076000.1	APEMLWDIE	Non amidated peptide	YES
E. granulosus	npp-31	EgrG_000076000.1	APEMLWDIE	Non amidated peptide	YES
T. solium	npp-31	TsM_000528000.1	APEMLWDIE	Non amidated peptide	YES
H. microstoma	npp-31	HmN_000223650	APELIWDIE	Non amidated peptide	YES
E. multilocularis	npp-32	EmuJ_000179900.1	GPEIFIPLMEA	Non amidated peptide	YES
E. granulosus	npp-32	EgrG_000179900.1	GPEIFIPLMEV	Non amidated peptide	YES
T. solium	npp-32	TsM_000448600.1*	GPEIFIPLMEA	Non amidated peptide	YES
H. microstoma	npp-32	HmN_000205400.1	GPELFIPYMEA	Non amidated peptide	YES
E. multilocularis	npp-33	EmuJ_000829900.1	TMPYSGGIF-amide	IFamide	YES
E. granulosus	npp-33	EgrG_000829900.1	TMPYSGGIF-amide	IFamide	YES
T. solium	npp-33	TsM_000416300.1*	TMPYSGGIF-amide	IFamide	YES
H. microstoma	npp-33	HmN_000514300	TPYSGGIF-amide	IFamide	YES
E. multilocularis	npp-34	EmuJ_000316500	SPQFAWRPHSRF-amide	R(F/Y)amide	YES
E. granulosus	npp-34	EgrG_000316500	SPQFAWRPHSRF-amide	R(F/Y)amide	YES
T. solium	npp-34	TsM_001139300.1*	SPQFAWRPHSRF-amide	R(F/Y)amide	YES
H. microstoma	npp-34	HmN_000315550	SPQFAWRPHSRY-amide	R(F/Y)amide	YES
E. multilocularis	npp-4	EmuJ_000240300.1	GNFFRF-amide	R(F/Y)amide	YES
E. granulosus	npp-4	EgrG_000240300.1	GNFFRF-amide	R(F/Y)amide	YES
T. solium	npp-4	TsM_000895400.1	GNFFRF-amide	R(F/Y)amide	NO
H. microstoma	npp-4	HmN_000166500.1	GNYFRF-amide	R(F/Y)amide	YES
E. multilocularis	npp-5	EmuJ_000993900.1	MQRPAFLFDAW-amide; GAYLDLPW-amide	(A/P)Wamide	YES
E. granulosus	npp-5	EgrG_000993900.1	MQRPAFLFDAW-amide; GAYLDLPW-amide	(A/P)Wamide	YES
T. solium	npp-5	TsM_001041500.1	MQRPAFLFDAW-amide; GAYLDLPW-amide	(A/P)Wamide	YES
H. microstoma	npp-5	HmN_000072750	GAYLDLPW-amide	(A/P)Wamide	YES
E. multilocularis	npp-6	EmuJ_000759050	AIRLLRL-amide	(L/M/I)amide	YES
E. granulosus	npp-6	EgrG_000759050	AIRLLRL-amide	(L/M/I)amide	YES
T. solium	npp-6	TsM_000844500.1	AIRLLRL-amide	(L/M/I)amide	YES
H. microstoma	npp-6	HmN_000648800.1	AVRLLRL-amide	(L/M/I)amide	YES
E. multilocularis	spp-3	EmuJ_000185700	ARFRPRL-amide;	(L/M/I)amide	YES

			NYNFRARL-amide		
E. granulosus	spp-3	EgrG_000185700	ARFRPRL-amide; NYNFRARL-amide	(L/M/I)amide	YES
T. solium	spp-3	TsM_001117900.1*	ARFRPRL-amide	(L/M/I)amide	YES
H. microstoma	spp-3	HmN_000148600.1	MPFLSRL-amide; LYAFHSRL-amide	(L/M/I)amide	YES

(?) - not clear from current gene model; (*) - gene model corrected from original prediction; correction submitted to GeneDB; (SP after DS ATG) - signal peptide observed after downstream start (ATG) codon but not in the start (ATG) codon of the current prediction.

5.5.3. Expression and effects of NPs during metacestode growth and regeneration

In order to determine which NPs are expressed in the metacestode vesicles, we analyzed RNAseq data of this stage and of pre-gravid and gravid adults (Tsai et al. 2013); Table R5.2). As expected from the complex development of the nervous system in adult cestodes (Gustafsson 1992; Brownlee et al. 1994), expression of NP genes is higher in *E. multilocularis* pre-gravid and gravid adult stages as compared to metacestode vesicles (Table R5.2). However, expression of several NP genes could be detected in the metacestode transcriptomic data set (between 0.64% and 86.23% of the expression levels found in the gravid adult stage), and was confirmed by semi-quantitative RT-PCR for 6 genes (all RT-PCR products were confirmed by sequencing). For those genes for which no expression was detected in the transcriptomic data set of metacestode vesicles, no RT-PCR product was obtained (Table R5.2). As a control, RT-PCR in activated protoscoleces, which also have a developed peptidergic nervous system (Fairweather et al. 1994; Koziol, Krohne, and Brehm 2013), were positive for all of these genes except for *em-npp-4*, which may therefore be an adult-specific NP. This suggests that some of these NPs could have a biological role, perhaps as peptide hormones, in the metacestode stage.

We reasoned that if any NPs expressed in the metacestode vesicles had a role in the regulation of larval development, these might be up-regulated during regeneration from primary cell preparations. Several NP-genes were predicted to be expressed in the regenerating primary cells from RNAseq experiments (*em-npp2*, *em-npp-5*, *em-npp-6*, *em-npp-20.1*, *em-npp-20.2*, *em-npp-20.3*, *em-npp-20.4*, *em-npp-24*, *em-npp-27* and *em-npp-34*). Many of these genes appeared to be up-regulated in primary cells as compared to metacestode vesicles, but gave variable results in two different RNAseq replicates (data not shown). We analyzed three of these presumably up-regulated genes (*em-npp-2*, *em-npp-6*, and *em-npp-14*) and a NP gene which did not show any variation (*npp-20.3*), by semi-quantitative RT-PCR in primary cells and metacestode vesicles (Figure R5.6). No reproducible difference in expression could be detected for *em-npp-20.3* or *em-npp-14*, whereas *em-npp-2* and *em-npp-6* were reproducibly up-regulated in primary cells and were selected for further studies.

The predicted active peptides encoded by these genes (RGFIamide and AIRLLRLamide, respectively) were synthezised *in vitro* and tested at different concentrations on primary cell preparations. Addition of RGFIamide at concentrations of 10^{-7} to 10^{-6} M resulted in a significant increase in DNA synthesis, as measured by BrdU incorporation (Figure R5.7), whereas AIRLLRLamide did not show a reproducible effect at the same concentrations (data not shown). Therefore, RGFIamide could have a specific effect on cell proliferation in *E. multilocularis*, which is consistent with its up-regulation during regeneration.

Table R5.2. RNAseq and RT-PCR gene expression data for neuropeptide / peptide hormone genes in *E. multilocularis* larval and adult stages.

Gene	GeneDB code	Vesicles RT-PCR	Protoscolex RT-PCR	Vesicles RNAseq %	Pre-gravid RNAseq %	Gravid RNAseq %
spp-18	EmuJ_000092400	N/D	N/D	0.00	80.60	100.00
npp-14	EmuJ_000740500	YES (30 cycles)	N/D	3.35	51.33	100.00
npp-15.1	EmuJ_000945400	N/D	N/D	11.07	58.72	100.00
npp-15.2	EmuJ_000945300	N/D	N/D	86.23	34.19	100.00
npp-2	EmuJ_000530500	YES (30 cycles)	YES (30 cycles)	2.83	100.00	77.88
npp-20.1	EmuJ_001070600	NO (40 cycles)	YES (40 cycles)	0.00	67.22	100.00
npp-20.2	EmuJ_000043400	YES (30 cycles)	YES (30 cycles)	22.77	100.00	35.78
npp-20.3	EmuJ_001194600	YES (30 cycles)	YES (30 cycles)	10.53	70.15	100.00
npp-20.4	EmuJ_000926000	N/D	N/D	1.80	49.72	100.00
npp-20.5	EmuJ_000706000	N/D	N/D	1.61	100.00	55.85
npp-24	EmuJ_001046700	NO (30 cycles)	YES (30 cycles)	0.00	100.00	54.74
npp-27	EmuJ_000347700	YES (30 cycles)	YES (30 cycles)	2.56	96.99	100.00
npp-29	EmuJ_000229800	N/D	N/D	3.84	51.67	100.00
npp-30	EmuJ_000489700	N/D	N/D	10.90	56.74	100.00
npp-31	EmuJ_000076000	N/D	N/D	0.00	100.00	64.15
npp-32	EmuJ_000179900	N/D	N/D	2.56	95.61	100.00
npp-33	EmuJ_000829900	N/D	N/D	4.56	88.09	100.00
npp-34	EmuJ_000316500	NO (30 cycles)	YES (30 cycles)	0.00	100.00	37.55
npp-4	EmuJ_000240300	NO (40 cycles)	NO (40 cycles)	0.00	50.09	100.00
npp-5	EmuJ_000993900	N/D	N/D	0.64	100.00	54.96
npp-6	EmuJ_000759050	YES (30 cycles)	YES (30 cycles)	2.27	90.28	100.00
spp-3	EmuJ_000185700	N/D	N/D	0.94	100.00	80.31

Vesicles: metacestode vesicles. Pre-gravid and gravid refers to adults before and after egg production begins. RNAseq data are expressed as percentage of the stage with the highest RPKM (reads per kilobase per million reads) for each gene. Qualitative RT-PCR results are shown (yes: amplification after the indicated number of cycles; no, no amplification after the indicated number of cycles; N/D, not determined).

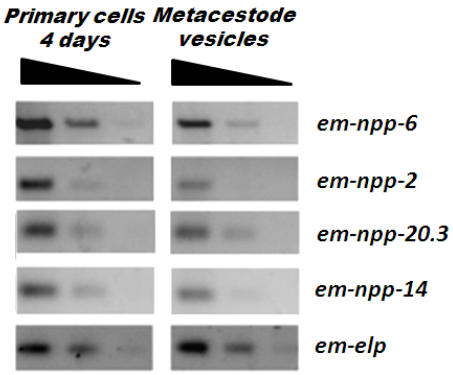

Figure R5.6. Semi-quantitative RT-PCR analysis of NP genes in primary cells and metacestode vesicles. RT-PCR was performed with serial ten-fold dilutions of cDNA from primary cells (after 4 days of culture) and metacestode vesicles (from axenic culture). The constitutive gene *em-elp* was used for normalization. The experiment was repeated three times with similar results.

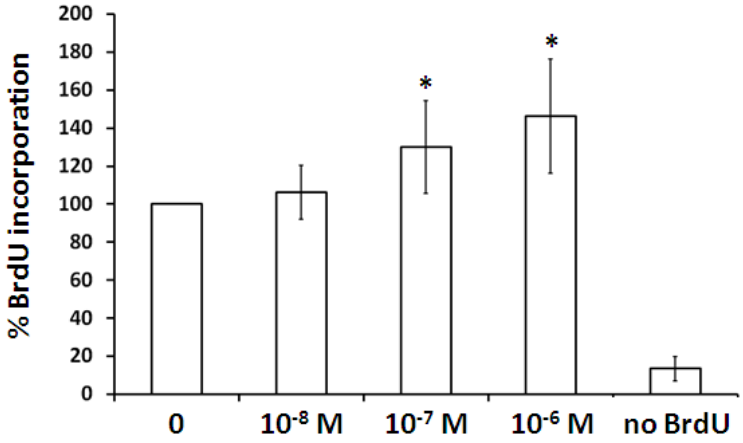

Figure R5.7. Effect of RGFIamide on primary cell proliferation. *E. multilocularis* primary cells were cultured in complete DMEM medium for a total of 44 hours in the presence of different concentrations of RGFIamide. BrdU (10 µM) was added during the last four hours of culture, and its incorporation was measured by ELISA (see the Materials and Methods section for more details). The control without RGFIamide was defined as 100 % of incorporation. A background control of cells that were not incubated with BrdU is included ("no BrdU"). Averages and standard deviations of 4 independent experiments are shown. *p<0.05 (Mann-Whitney-Wilcoxon Test) as compared to the control without RGFIamide.

6. Discussion

6.1. Tissue turnover and growth in *E. multilocularis* metacestodes depends on undifferentiated germinative cells

The results obtained in this work show that in the metacestode larva of *E. multilocularis*, germinative cells are the only cells in which proliferation can be detected. Therefore, they must be the only appreciable source of new cells for tissue growth and turnover under normal conditions and during regeneration. This mechanism of tissue growth and regeneration is rather unique to flatworms, as opposed to a combination of stem cells and self-duplicating differentiated cells as seen in most metazoans (Yanger and Stanger 2011). Confirming that this mechanism also operates for *E. multilocularis* larvae is not trivial: very little is known about cell proliferation and differentiation in larval cestodes, and since asexual reproduction is an evolutionary novelty of taeniids (Freeman 1973; Slais 1973; Moore and Brooks 1987), it was possible in principle that this adaptation could be accompanied by novel mechanisms of cell generation. Furthermore, in the cysticercus larva of the closely related *Taenia solium*, the results of autoradiographic studies after ^{3}H-thymidine labeling had been interpreted to support the presence of DNA synthesis in differentiated cells, even in cells that are usually considered to be terminally differentiated (*e.g.* calcareous corpuscle cells) (Merchant, Corella, and Willms 1997). It is possible that the labeled nuclei were misidentified in these histological studies, or that very fast cell differentiation processes could result in labeled differentiated cells after a period of mere hours of incubation with ^{3}H-thymidine.

Any contribution of differentiated cells to proliferation must therefore be negligible. Of course at this point we cannot rule out the occurrence of de-differentiation processes, in which germinative cells could be generated from differentiated cells under certain conditions. However, the results observed during regeneration from primary cell preparations suggest otherwise, since most differentiated

cells appeared to degenerate. If any de-differentiation occurs, then cell-cycle re-entry would occur only after de-differentiation, since the surviving differentiated cells were never labeled by EdU whereas germinative cell proliferation could be observed from the earliest time points. Ruling out the existence of de-differentiation will ultimately depend on unambiguous lineage tracing mediated by stable genetic markers. Unfortunately, reliable genetic manipulation of *E. multilocularis* is not as yet achievable, although retroviral-mediated transgene insertion has been shown in proof-of-principle experiments (M. Spiliotis and K. Brehm, unpublished results). The markers for germinative cells and differentiated cell types developed in this work could be an important tool for tracing the differentiation pathways of germinative cells if CreER-mediated lineage tracing techniques are developed (Jaisser 2000). In this way, stable genetic labeling of *ta-TRIM* expressing cells could be performed to determine the self-renewal and differentiation potential of individual germinative cells, and performing similar experiments with *em-nos-1* and *em-nos-2* would evidence the potency of these particular germinative cell sub-populations. Stable labeling of cells expressing *em-muc*, *em-alp-1*, *em-alp-2* and *em-tpm1.hmw* (which has a specific promoter different from the *em-tpm-1.lmw* isoform, from which specific CreER expression could be driven (Koziol et al. 2011)) would be able to conclusively demonstrate the lack of contribution to tissue turnover for individual differentiated cell types.

6.2. Gene expression patterns of germinative cells: molecular markers and population heterogeneity

This work represents the first description of gene expression patterns and molecular markers for cestode germinative cells, and the results obtained demonstrate that germinative cells are a morphologically similar but molecularly heterogeneous population. This heterogeneity includes the expression of *em-nos-1*, *em-nos-2*, *em-ago2* and *emfr3* in sub-populations of the germinative cells of diverse sizes (<<1% to *ca*. 50% of all proliferating germinative cells as judged from EdU co-labeling experiments). Because Argonaute, Nanos and FGFR proteins are well known regulators with important roles in stem cell biology (Juliano, Swartz, and Wessel 2010; Lanner and Rossant 2010; Coutu and Galipeau 2011), this indicates the existence of different sub-populations of germinative cells, with different self-renewal or differentiation potencies. Unfortunately, most of the germinative cell-specific genes studied (with the exception of *emfr3*) code for intracellular proteins and as such would not be appropriate for the isolation of live cells by FACS using specific antibodies, as is commonplace for other models (*e.g.* HSC). An important follow-up step would be to determine the functional relevance of these markers for the physiology of germinative cells. In principle, this could be achieved by RNAi, but the technique is only at a proof-of-concept stage for *E. multilocularis* (Spiliotis et al. 2010), and has given equivocal results in our laboratory so far (Sarah Hemer and Raphaël Duvoisin, personal communication).

It is possible that the heterogeneous germinative cell population contains a sizeable proportion of committed progenitors, as is common for many stem cell systems in metazoans (Bryder, Rossi, and Weissman 2006; Reddien 2013). The uniform structure of the germinal layer hinders the possible identification of such cells, since unlike other flatworm models (Collins et al. 2013; Rink 2013), there is no spatial segregation between the proliferating germinative cells and differentiated cells, nor are there any specific regions or organs which give rise to particular cell types. For example, in the plerocercoid larva of the cestode *Diphyllobothrium dendriticum*, a specific population of proliferating germinative cells has been described around the growing nerve cords, and these cells integrate into the cords to form new nerve cells

(Gustafsson 1976a). Similarly, neoblast subpopulations from free-living flatworms have been described close to and within particular organs, suggesting that they consist of lineage-restricted neoblasts which differentiate into organ-specific cell types. In *Macrostomum lignano*, gastrodermal neoblasts are found within the intestinal epithelium, and have been proposed to give rise to intestinal cells (Rieger et al. 1999). Perhaps the best evidence is found in planarians, for the existence of photoreceptor-specific progenitors and for progenitors of the excretory system. In both cases, the cells in question are situated close to the organs, while they proliferate and co-express neoblast markers with organ/tissue specific markers (Reddien 2013). In our results in *E. multilocularis*, the only association of proliferating germinative cells with a specific organ was observed in the formation of the suckers (during later stages of protoscolex development). At this stage, there is a massive accumulation of proliferating germinative cells (EdU^+, *em-h2b*$^+$, and *em-TRIM* $^+$ cells) at the base of the sucker, whereas differentiating cells accumulate in the adjacent exterior region of the sucker cup (including differentiating *em-tpm-1.hmw*$^+$ muscle cells, *emfr2*$^+$ cells and $AcTub^+$ nerve cells). This suggests that these germinative cells could be committed to the formation of the muscular suckers and their associated nervous structures.

So far, gene expression studies were performed for selected genes from a candidate-gene approach. In order to obtain a larger number of candidate genes that may be specifically expressed in the germinative cells, we have undertaken transcriptomic studies of tissues that are depleted of germinative cells (through HU treatment, this work) and of early primary cell preparations that are enriched in germinative cells ((Tsai et al. 2013), unpublished results). Genes enriched in transcriptomic studies of early primary cells and depleted in HU-treated metacestodes are therefore strong candidates for having a germinative cell-specific expression. The analysis of HU-treated metacestodes is analogous to the transcriptomic analyses performed in planarians and schistosomes after depleting all proliferating cells by means of ionizing irradiation or RNAi (Rossi et al. 2007; Eisenhoffer, Kang, and Sanchez Alvarado 2008; Solana et al. 2012; Wagner, Ho, and Reddien 2012; Collins et al. 2013). However, irradiated samples are usually studied within 24 hours when searching for neoblast-specific transcripts. In our case, because of the longer incubation period required with HU, the treatment will not only deplete the germinative cells, but probably also their differentiating progeny, as

these cells differentiate but are no longer generated from the germinative cell pool. Such effects were also observed with longer incubation periods after irradiation in planarians (Eisenhoffer, Kang, and Sanchez Alvarado 2008). Furthermore, differentiation of proliferating cells to some differentiated cell types can occur within seven days, as seen in continuous EdU labeling experiments (Koziol et al. 2014).

Given that both HU treatment and primary cell preparation are relatively harsh procedures, which could affect gene expression in many ways, it is remarkable that the observed results indicate a strong "stem cell-signature" in both data sets. This includes the specific depletion of markers of germinative cell sub-populations after HU treatment (see chapter 3 of the Results section), and the enrichment of germinative cell markers in the primary cell preparations (for example, *em-plk1* and *em-nos-2*; (Schubert et al. 2014) and unpublished results). Further work must now be performed to confirm that the candidate genes from RNAseq experiments are specifically expressed in germinative cells. The planned experiments include first a screening by quantitative RT-PCR of candidate genes, to confirm their decreased expression after other methods of germinative cell depletion (such as treatment with the PLK-1 inhibitor BI2536 (Schubert et al. 2014)). The rationale behind this is to show that the decrease of the transcripts is due to germinative cell depletion, and not a specific HU effect. Then, WMISH analysis of selected confirmed genes would follow. Finally, a method for FACS isolation of viable proliferative cells from the cestode *Mesocestoides corti* has been recently described, which allowed the purification of RNA of the isolated cells at the ng to µg scale (Dominguez et al. 2014). The adaptation of this method to *E. multilocularis* cells, in combination with RNAseq, would allow us to obtain the germinative cell-specific transcriptome with minimal alterations of gene expression or contamination from other cell types.

6.3. Self-renewal of the germinative cells

Because *E. multilocularis* metacestode larvae can be passaged indefinitely in intermediate hosts (Norman and Kagan 1961; Spiliotis and Brehm 2009), and new cells are originated from germinative cells (Koziol et al. 2014), it follows that at least a fraction of the germinative cells should be able to self-renew indefinitely. The capacity for self-renewal of at least some of the germinative cells is strongly suggested by the HU mediated depletion experiments, where growth of clones, presumptively arising from single proliferating cells, was observed in metacestode vesicles after partial germinative cell depletion (Chapter 1, (Koziol et al. 2014)). However, this is not an ideal experiment for the analysis of cell renewal, since reaching the appropriate level of depletion (*i.e*. high enough to promote extensive compensatory proliferation, but not so high that all germinative cells are eliminated) is technically difficult, and the differentiated post-mitotic progeny of each clone cannot be distinguished from pre-existing differentiated cells. Furthermore, it is not possible to determine the proportion of self-renewing cells among the germinative cell population, in particular since the HU-induced DNA damage may limit the proliferation of some of the surviving germinative cells for long periods.

Determination of the self-renewal and differentiation potency of individual *E. multilocularis* germinative cells will require clonal analyses, but other than the difficult tracing of surviving proliferating cells after HU-depletion, the techniques required are largely lacking. Lineage tracing of genetically labeled cells is not yet available, and *in vitro* analysis of cultured individual *E. multilocularis* cells has not been feasible so far, since cells do not seem to grow at low seeding densities under current standard culture conditions, and their lack of adherence and small size also makes experimental manipulation extremely difficult (*e.g.* media changing and tracking of individual cells). The demonstration that *emTRIM* $^{+}$ germinative cells from *E. multilocularis* cells can integrate into *T. crassiceps* tissues opens up the possibility of using this transplantation system to study the self-renewal of individual germinative cells, with the caveat that their potential may be different in this xenogeneic setting. For this, limiting dilutions of monodispersed primary cell preparations of *E. multilocularis* would be injected into the cavity of *T. crassiceps* metacestodes in order to obtain clones that originate from single

germinative cells. Then, the number of *em-TRIM* $^{+}$ germinative cells of the clones could be traced with a time-series of transplanted *T. crassiceps* metacestodes, and the production of differentiated cells could be determined using the markers developed in this work. Furthermore, treatment of primary cell preparations by RNAi before transplantation (which is possible for primary cells but not for complete metacestode tissues (Spiliotis et al. 2010)) would allow studying the specific functions of genes for germinative cell self-renewal and differentiation. An important addition to this method would be the development of species-specific antibodies for *E. multilocularis* cells, similarly to the quail-specific antibodies used in quail-chick chimera experiments (Lance-Jones and Lagenaur 1987). These antibodies would allow for the reliable determination of the *E. multilocularis* origin for all cells in the clones.

6.4. *E. multilocularis* germinative cells and the stem cell systems of other flatworms: similarities and differences

The analysis of the genomes of cestodes and trematodes has shown that they have lost components of the GMP which are otherwise highly conserved in metazoans, including in free-living flatworms (Tsai et al. 2013). Since trematodes and cestodes have been proposed from molecular phylogenetic studies to be sister groups (Olson and Tkach 2005), this suggests that at least *vasa*, and perhaps also *piwi* and group 9 *tudor* genes were lost in the last common ancestor of cestodes and trematodes.

The loss of conserved GMP components, combined with the lack of chromatoid bodies in the germinative cells, suggest that important differences exist in the regulation of stem cells between cestodes and planarians. Among the missing components of the GMP, the lack of orthologs of *piwi* and *vasa* are particularly striking, given the almost universal expression of these genes in the germ line of metazoans (Ewen-Campen, Schwager, and Extavour 2010; Juliano, Swartz, and Wessel 2010; Juliano, Wang, and Lin 2011), their specific expression and function in the planarian neoblasts and their progeny (Reddien et al. 2005; Palakodeti et al. 2008), and the conserved role of *piwi* in protecting the genome from the expansion of transposable elements (Juliano, Wang, and Lin 2011; Skinner et al. 2014). In the trematode *Schistosoma mansoni*, other paralogs of the Argonaute (*sm-ago2-1*) and DEAD box helicase families (*sm-vlg3*) are specifically expressed in neoblast-like cells of adults and larvae (Collins et al. 2013; Wang, Collins, and Newmark 2013). Furthermore, Sm-ago2.1 is associated with small RNAs derived of transposable elements (Cai et al. 2012). This suggests that these paralog genes may have functionally replaced the corresponding canonical GMP components (Skinner et al. 2014). In contrast, the data obtained so far indicates that this is not conserved in *E. multilocularis*, since (1) *em-ago2* genes (the orthologs of *sm-ago2-1*) are not expressed in all the proliferating germinative cells; (2) *em-ago2* genes are also expressed in post-mitotic cells; and (3) the "*vasa*-like" genes (*vlg*) of *E. multilocularis* do not seem to be specifically expressed in the germinative cells, since their expression is not affected by HU treatment. It is still possible that *em-ago2* genes have a similar function in the germinative cell sub-population in which they are expressed, and that the expression of *em-ago2* genes and *vlg* genes in post-mitotic cells serves new additional functions in *E.*

multilocularis. In general, however, these differences suggest important differences between *S. mansoni* neoblast-like cells and *E. multilocularis* germinative cells. The RNAseq experiments of HU-treated *E. multilocularis* vesicles indicate instead a preponderance of transcription factors in the transcriptome of germinative cells, as compared with the strong over-representation of post-transcriptional regulators in free-living flatworms and trematodes (Rouhana et al. 2010; Collins et al. 2013; Rink 2013).

One conserved aspect between the *S. mansoni* and *E. multilocularis* stem cells systems is the expression of *nanos* homologs in sub-populations of somatic stem cells in their larvae (and also in the adult of *S. mansoni*), in contrast with the germ-line specific expression of the *nanos* homolog of planarians. However, in *S. mansoni* the *nanos* homologue *sm-nanos2* is expressed in a large population of larval neoblast-like cells (and perhaps in all of the adult neoblast-like cells) (Collins et al. 2013; Wang, Collins, and Newmark 2013), whereas in *E. multilocularis* the populations of germinative cells expressing *nanos* homologs are very small (<5%). In the later stages of protoscolex development, the expression seems to be restricted to the developing nervous system, and is not seen in any sub-populations of the germinative cells. It would be very interesting to determine if *nanos* genes are activated during the formation of the reproductive systems in adult cestodes, and if so whether they show specific expression in the germ line.

In *E. multilocularis,* the number of genomic copies of transposable elements is very low, as are their transcript levels, suggesting that alternative mechanisms to the canonical Piwi pathway repress their activity (Tsai et al. 2013; Skinner et al. 2014). This dearth of transposable elements is also observed in *Hymenolepis microstoma* (also a cyclophyllidean cestode), but may not be a common characteristic of all cestodes, since larger, repeat-rich genomes are found in pseudophyllidean cestodes (Matt Berrimann, personal communication). The taeniid-specific family of *ta-TRIM* elements, which is massively expressed in the germinative cells, seems to have somehow escaped this mechanism of repression. It is likely that because *ta-TRIM* elements are non-autonomous, they are controlled instead by the repression of the elements that contribute to their retrotransposition *in trans*, or even that these elements may already be extinct in the genome of *E. multilocularis*. This could explain the absence of strong negative effects despite their massive expression levels. In any case, they are the best

markers for the *E. multilocularis* germinative cell population found so far, and determining which transcription factors drive their expression could lead to the identification of transcriptional regulators of the germinative cells.

To the best of my knowledge, *ta-TRIMs* are the first transposables elements shown to have a stem-cell specific expression in flatworms. Their expression in the somatic germinative cells of the metacestode would allow *ta-TRIM*s to propagate in their genome, and to be in turn transmitted to the next generation as these germinative cells contribute to the formation of protoscoleces. Because a similar contribution of somatic neoblasts to the germ line of planarians is known to occur during regeneration (Sato et al. 2006), it would be of interest to determine if any transposable elements may have a similar expression pattern and propagation strategy in these organisms. Indeed, the expression of *piwi* homologs in planarian neoblasts has been suggested to limit the expansion of transposable elements in the genome of these indefinitely self-renewing cells (Rink 2013). This would be of particular importance for asexual planarian strains in which new individuals are continuously generated from the somatic neoblast population.

6.5. Complex expression patterns of *E. multilocularis* FGFRs

At the moment when this project started, only a single FGFR gene was known in *E. multilocularis* (*emfr1*), which was thought to mediate all of the effects on growth and development of metacestodes that were observed by the addition of human FGF ligands (Förster 2012). This, in combination with the expression of FGFR genes in stem cells of planarians and schistosomes, prompted us to speculate that *emfr1* could be specifically expressed in the germinative cells.

However, the reality was far more complex, since three FGFR genes are now known to exist, and their expression patterns are very different from each other (as well as from the expression patterns of FGFR genes in other flatworms (Ogawa et al. 2002; Collins et al. 2013; Wang, Collins, and Newmark 2013)). The only FGFR gene that seems to be specific for germinative cells is *emfr3*, and it is only expressed in a very small sub-population, whereas the likely ortholog of *emfr3* in *S. mansoni* (*sm-fgfrA*) is expressed in all of the adult and larval neoblast-like cells, as well as in the gonads (Collins et al. 2013; Wang, Collins, and Newmark 2013). Similarly, planarian FGFR genes are expressed in the neoblasts and gonads, but also in the nervous system (Ogawa et al. 2002). In contrast, *emfr2* is exclusively expressed in post-mitotic cells. These cells could consist of differentiating lineage(s) of the germinative cells, given the decrease of *emfr2* transcripts after HU-mediated germinative cell depletion. Finally, *emfr1* has widespread expression in the germinal layer.

Because of these complex expression patterns, it is not easy to determine which of these receptors mediate the response of *E. multilocularis* to human FGF ligands, although the widespread expression of *emfr1* makes it a promising candidate for this role. This could occur by activation in the germinative cells, or by an indirect effect through the stimulation of differentiated cells. Such an indirect effect could also be mediated through EmFR2 stimulation in post-mitotic cells, and FGF addition could also promote the differentiation of *emfr2*$^{+}$ cells. Indirect effects of FGF signaling are commonplace for FGF-mediated stimulation of proliferation in other systems (Coutu and Galipeau 2011).

Eventually, RNAi experiments targeting each individual receptor in primary cells may identify their specific contributions. Incubation of metacestode vesicles with the inhibitor BIBF1120 (Vargatef), which inhibits all three *E. multilocularis* receptors, resulted in vesicle death (parasitocidal effect) (Förster 2012). This contrasts with the parasitostatic effect of HU and the PLK1 inhibitor BI2536, that target specifically the proliferating germinative cells (Koziol et al. 2014; Schubert et al. 2014). It seems therefore that FGFR activation is not only required for growth and proliferation of germinative cells, but also for parasite survival, presumably through effects that are germinative cell-independent.

6.6. Evolution of the *E. multilocularis* metacestode: asexual reproduction and the neuromuscular system

Whether the asexual formation of scoleces in the metacestodes of different taeniids is homologous or convergent is still a matter of debate (Moore and Brooks 1987; Swiderski et al. 2007). The distribution of asexual proliferation across the phylogeny of taeniids suggests that this trait was present in their last common ancestor, since it is present in *Echinococcus* spp. and in several basal *Taenia* spp., including *Taenia mustelae* (Freeman 1973), which is probably more related to *Echinococcus* than to *Taenia* (making *Taenia* paraphyletic) (Hoberg et al. 2000; Trouvé, Morand, and Gabrion 2003; Hoberg 2006; Lavikainen et al. 2008; Knapp et al. 2011) (Figure D.1). However, this would imply multiple independent losses of asexual reproduction.

On the other hand, some authors have concluded based on morphological grounds that asexual reproduction is a convergent phenomenon arising in several taeniid lineages (Hoberg et al. 2000; Swiderski et al. 2007). It may be, however, that these morphological differences can be reconciled. For example, the development of *Echinococcus* spp. has been described as fundamentally different to that of other taeniids since protoscoleces are formed ”endogenously” within the brood capsules (Freeman 1973), which were considered to be “daughter cysts”, originating in the interior of the “mother cyst” from solid buds of the germinal layer (Sakamoto and Sugimura 1970; Thompson 1976). Because brood capsules are actually invaginations of the germinal layer (Leducq and Gabrion 1992; Koziol, Krohne, and Brehm 2013) which is itself homologous to the bladder tissue of *Taenia* (Freeman 1973), it is possible that the last taeniid common ancestor already possessed the ability to generate multiple scoleces from the bladder wall, and that the formation of brood capsules was a posterior evolutionary development in *Echinococcus*, as a way to generate extensions of germinal layer that are free of the covering laminated layer, where protoscolex production could proceed. The posterior stages of scolex development are actually very similar in all taeniids, as discussed above (Koziol, Krohne, and Brehm 2013). If asexual reproduction was indeed ancestral for taeniids, it would imply that the huge proliferative potential of *E. multilocularis* larval germinative cells was derived from stem cells with similar potency found in the last common taeniid ancestor. Further studies of the developmental

mechanisms and genes involved in asexual proliferation in different taeniids would be of great importance to resolve this issue.

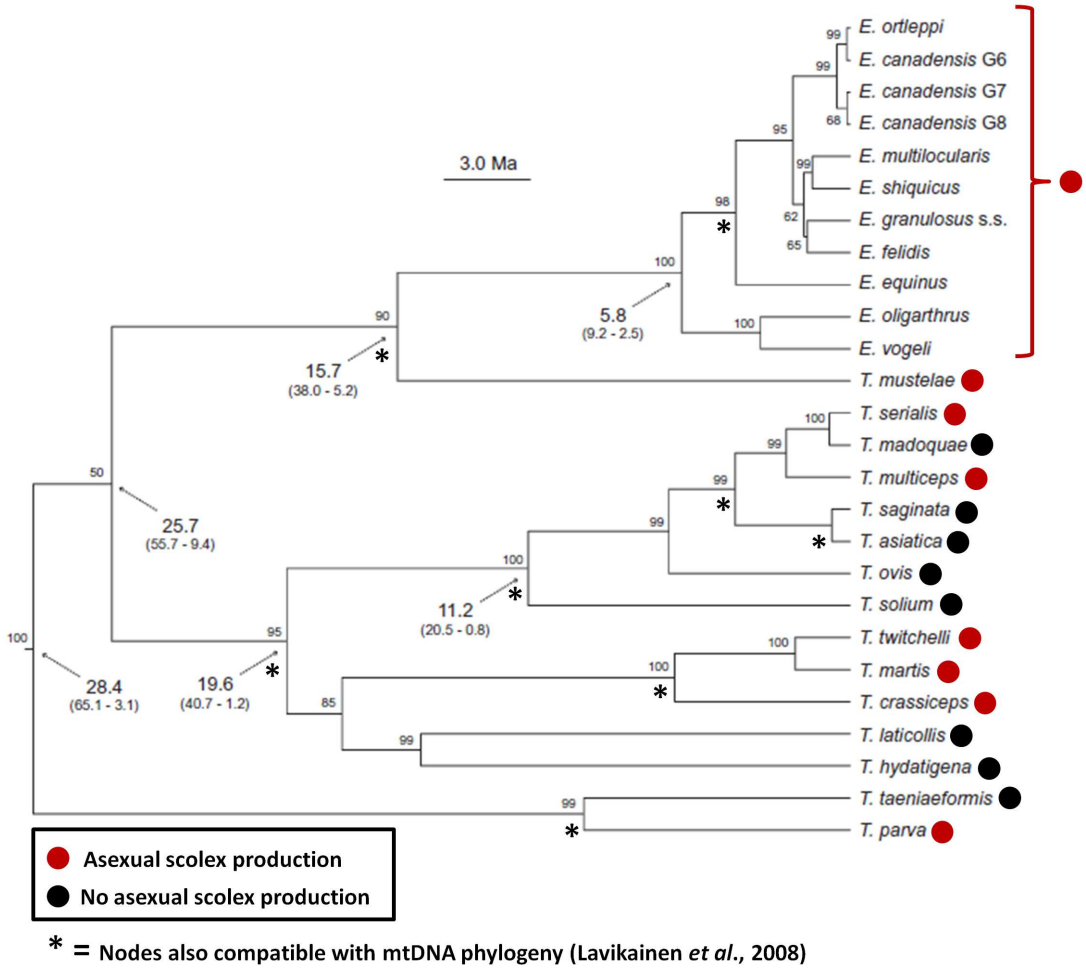

Figure D.1. Mapping of the capacity for asexual scolex production on the phylogeny of Taeniidae. Species with known asexual protoscolex production (Loos Frank, 2000; Swiderski et al., 2007) are indicated on the molecular phylogeny of Knapp et al. (2011), which was inferred from nuclear protein-coding genes. Nodes that are also congruent with a molecular phylogeny inferred from mitochondrial genes (Lavikainen et al. 2008) are indicated with an asterisk. The larval forms showing asexual scolex formation can be classified by their morphology (Swiderski et al., 2007, Hoberg et al., 2000) into: coenuri (with multiple scoleces invaginating into one large central cavity: *T. martis*, *T. multiceps*, *T. mustelae*, *T. serialis*); hydatids (with a laminated layer and protoscoleces originating from brood capsules; *Echinococcus* spp.); polycephalic larvae (with scoleces on external stalks connected to a central bladder that typically regresses: *T. parva*, *T. twitchelli*); and larvae with exogenous budding of scoleces from the posterior bladder tissue (*T. crassiceps*).

6. Discussion

The nervous and muscle systems in *E. multilocularis* are probably homologous to those present in the bladder tissue from *Taenia* spp. Because they have no function in motility, and since the nerve net in the germinal layer is not connected to the protoscolex nervous system, we have proposed that they may be instead a source of signals for metacestode development (Koziol, Krohne, and Brehm 2013). This is consistent with the presence of nerve cells and muscle cells in primary cell preparations, whereas many other differentiated cell types are depleted (Koziol et al. 2014). Furthermore, similar roles for the neuromuscular system in stem cell regulation and pattern formation have been proposed for free-living flatworms (Reuter and Gustafsson 1996; Rossi, Iacopetti, and Salvetti 2012; Witchley et al. 2013); see also the discussion for Koziol, Krohne and Brehm (2013)). It is also possible that the neuromuscular system of *E. multilocularis* metacestode vesicles represents a vestigial evolutionary remnant without a specific function, and further functional studies are required. As a first step towards this goal, we developed a novel strategy to identify NP-encoding genes in the *E. multilocularis* genome, and determined which are expressed in the germinal layer and primary cells. This strategy resulted in an increase from only 4 known or predicted NPs to 22 candidate NP gene groups conserved in cestodes. These NP-encoding genes from cestodes are particular in that only one or two mature peptides are encoded in most precursors, and many of them only seem to be conserved among flatworms. Furthermore, many metazoan NP and peptide hormone genes seem to have been lost in flatworm parasites. Because of these peculiarities, the novel strategy employed here was instrumental in their discovery. This strategy was only possible thanks to the availability of two sequenced cestode genomes that were at the appropriate evolutionary distance, so that the mature NP residues were still highly conserved, but the remaining of the CDS showed only modest conservation (Tsai et al. 2013). For instance, such an analysis would have been impossible between *E. multilocularis* and *T. solium*, since their close evolutionary proximity results in high similarity throughout the CDS of NP genes (thus any taeniid or *Echinococcus* specific NP genes will have been missed in this analysis), or between *E. multilocularis* and planarians, since the small mature NPs only show modest conservation. Given the current commonality of genome sequencing projects for metazoans, this strategy could also be applied for the *de novo* prediction of candidate NPs in other groups.

6. Discussion

One NP gene, coding for the predicted mature peptide RGFIamide, was shown to be up-regulated in primary cells. Furthermore, synthetic RGFIamide was shown to increase the proliferation of primary cells after addition *in vitro*. This indicates that endogenously produced RGFIamide could have a similar effect in primary cells and metacestode tissues, although the concentrations required (10^{-7} to 10^{-6} M) are at the higher end of what is typical for the activity of NPs (10^{-9} to 10^{-6} M) (Siegel et al. 2006). Its action could be either as a widely diffused "endocrine factor" (for example by secretion into the hydatid fluid), or as local, niche-like signals in the vicinity of the nerve cells. Future experiments should include the localization of cells producing RGFIamide, determining whether they are nerve cells, and confirming by mass-spectrometry analyses that RGFIamide can be found as a mature NP in *E. multilocularis* tissues. Finally, many other possible effects of this and other NPs should be addressed, such as their global effect on metacestode regeneration, their influence on the differentiation of germinative cells, and their effect on metacestode growth and protoscolex development.

7. Materials and Methods

7.1. Parasite culture and experimental manipulation

7.1.1. Media

Media	Description
DMEM	Dulbecco's Modified Eagle's Medium, high glucose (4.5 g/l) GlutaMAX (Life Technologies 10566-016)
Complete DMEM	DMEM + 10% Fetal Bovine Serum (Biochrom, S 0115) and antibiotics (Penicillin 100 U /ml, Life Technologies; Streptomycin, 100 µg/ml, Life Technologies; Levofloxacin (sold as Tavanic), 20 µg/ml, Sanofi-Aventis)
cDMEM-A (also known as A4)	Filter-sterilized supernatant of Reuber H35 culture ($1x10^6$ cells in 50 ml Complete DMEM for seven days in a 75 cm^2 flask, with the addition before using of reducing agents β-mercaptoethanol (1:100.000 v/v), batho-cuproine disulfonic acid (10 µM) and L-cysteine (100 µM))

7.1.2. *E. multilocularis* isolates

Isolate	Year of isolation	Original stage isolated	Original Host	Protoscolex production (*in vitro*)
H95	1995	Oncosphere (*ex*. adult worms)	*Vulpes vulpes*	No
Java	2005	Metacestode	*Macaca fascicularis*	No (since aprox. 2009)
Ingrid	2010	Metacestode	*Macaca fascicularis*	No (since aprox. 2012)
GH09	2009	Metacestode	*Macaca mulatta*	Yes

GT10	2010	Metacestode	*Macaca mulatta*	Rare
G8065	2009	Metacestode	*Macaca mulatta*	Rare
J2012	2012	Metacestode	*Macaca fascicularis*	Yes
DPZ13	2013	Metacestode	*Macaca fascicularis*	Yes
MS1010	2010	Metacestode	*Canis familiaris*	Yes

For most experiments with metacestode vesicles, recent isolates that are able to produce protoscoleces *in vitro* were used (mostly isolates GH09, MS1010, DPZ13, J2012). For primary cell preparations, older isolates that have largely lost the ability to produce protoscoleces *in vitro* (and sometimes also *in vivo*) were preferred, since they grow faster *in vitro* and give greater primary cell yields (isolates H95, Java and Ingrid).

7.1.3. *In vivo E. multilocularis* maintenance, isolation of parasite material and standard *in vitro* co-culture technique

The parasite isolates were maintained by serial intraperitoneal passage in *Meriones unguiculatus* and cultured *in vitro* under sterile conditions as previously described (Spiliotis and Brehm 2009). Briefly, the metacestode material was isolated under sterile conditions, cut into small pieces with a scalpel and passed through a metallic tea strainer for sieving. The material was then washed extensively with Phosphate-Buffered Saline (PBS: 2.67 mM KCl, 1.47 mM KH_2PO_4, 137 mM NaCl, 8.1 mM Na_2HPO_4; Life Technologies 21600-069). For routine maintenance of isolates, the parasite material was then kept in a minimum volume of PBS and incubated overnight at 4 °C with levofloxacin (sold as Tavanic, Sanofi-Aventis, and used at 20 µg/ml final concentration). The material was washed three times with PBS, and injected into the peritoneal cavity of *M. unguiculatus* (*ca*. 0.5 ml/ inoculum). For standard *in vitro* culture and amplification of parasite material in the co-culture system, the grounded material was added directly to T-75 culture flasks (Sarstedt, Germany) containing 50 ml of complete DMEM with *ca*. 10^6 Reuber H35 feeder cells (Rat hepatoma cell line, ATCC number CRL-1600). The flasks were incubated at 37 °C in a 5% CO_2

atmosphere (Hera cell 240 incubator, Heraeus), and the medium and cells were replaced weekly. When necessary, the material was split into more flasks or transferred into larger T-160 culture flasks (Sarstedt, Germany) with up to 150 ml of complete DMEM. Under these conditions, those isolates that are able to produce protoscoleces *in vitro* begin to do so after 2 to 3 months of culture.

7.1.4. Axenic culture of *E. multilocularis* metacestodes

Metacestode vesicles obtained from the co-culture system were cultured under axenic conditions as described (Koziol et al. 2014). For this, they were washed extensively with sterile PBS to remove any adhering Reuber H35 cells and cultured in conditioned medium cDMEM-A at 37 °C under a nitrogen atmosphere (obtained by bubbling pressurized nitrogen into the media and closing the lid of the culture flasks hermetically). The medium was changed every 48 to 72 hours, and initially the culture flask was also changed in order to remove any possible carryover of contaminating Reuber H35 cells.

7.1.5. Isolation and activation of *E. multilocularis* protoscoleces

Metacestode material obtained from *in vivo* culture in *M. unguiculatus* was isolated and minced as described above. Then, the protoscoleces were released from the metacestode vesicles by placing them in a 50 ml Falcon tube filled to up to 25 ml with PBS, and shaking the tube vigorously for 10 to 20 minutes. The parasite material is then first filtered through sterile 150 µm gauze to remove large pieces of tissue, and then filtered through 30 µm gauze with the aid of a pipette. The protoscoleces are retained in the second gauze filter and can be transferred with PBS and a pipette to a Petri dish. By swirling, the protoscoleces accumulate in the center of the dish, and can be collected separately from any remaining material (mostly calcareous corpuscles) in 1.5 ml microtubes. Some small vesicles may be co-isolated with protoscoleces, but they are usually destroyed if the activation treatment is performed (see below).

Protoscoleces can then be directly cultured under standard co-culture conditions (as described above for total metacestode material). Some will evaginate spontaneously

in culture, and many will begin the de-differentiation process to form metacestode vesicles (see chapter 5 of the Results section).

Protoscoleces can also be activated by mimicking the ingestion by the definitive host. For this, the isolated protoscoleces are treated with Pepsin under acidic conditions (15 mg of pepsin (Sigma Aldrich) in 30 ml of DMEM, with 200 µl of 25% HCl giving a final pH of 2.0; sterile filtered) for 1 hour at 37 ºC with shaking (125 RPM). Then, they are allowed to sediment, washed 3 times with sterile PBS, and treated with sodium taurocholate (60 mg in 30 ml of DMEM, checking that the pH remains at 7.4; sterile filtered) for three hours at 37ºC with shaking (125 RPM). Finally, they are once again washed 3 times with sterile PBS.

7.1.6. Primary cell isolation and culture

Primary cell isolation from axenic metacestode vesicles was performed as described (Koziol et al. 2014) with a protocol almost identical to the one originally published by Spiliotis and Brehm (2009). A working protocol for primary cell isolation is included in Appendix 1.

Echinococcus cells are very small, and difficult to distinguish from tissue debris that is generated during the isolation procedure, making their direct quantification by microscopy difficult in the absence of staining. Primary cells were therefore quantified by measuring their turbidity with a spectrophotometer (U-2000, Hitachi, USA). For this, one unit of parasite cells was defined as the amount of cells that increased the absorbance of light (λ = 600 nm) by 0.02 units after being diluted 125:10.000 in PBS. Typically, 1000 to 3000 units are obtained from 50 ml of metacestode vesicles. In one pilot assay, I estimated by direct counting with a Neubauer chamber after staining with Hoechst 33342 (Life Technologies) that 1 unit of primary cells is roughly equivalent to 65.000 cells. Although not absolutely precise, this method is very useful since it allows for reproducible culture development between different experiments (M. Spiliotis, unpublished results). Primary cells were cultured with cDMEM-A in multi-well culture plates (500 units for each well of a 6-well plate, 200 units for each well of a 12-well plate, 50-100 units for each well of a 48 well plate, and 30-60 units for each well of a 96-well plate, unless otherwise stated) under a nitrogen atmosphere (by placing the

plates in a Ziploc bag, purging the air with pressurized nitrogen, and sealing the bag). Media was changed every 48 to 72 h.

7.1.7. Live microscopy of parasite cultures

Parasite cultures were observed and photographed with a light stereomicroscope, (Leica DM IL LED, Germany) using the bright-field and phase-constrast settings.

7.1.8. 5-ethynyl-2′deoxyuridine (EdU) incubation and detection

Incubation of *in vitro* cultured parasite vesicles and primary cells with EdU (Life Technologies), as well as fluorescent detection of EdU with the Click-iT® EdU Alexa Fluor® 555 Imaging Kit (Life Technologies), was performed as described (Koziol et al. 2014). A working protocol for EdU detection in whole-mounts is included in Appendix 2. EdU detection was performed after the WMISH protocol in co-labeling experiments.

7.1.9. Treatment of primary cells and metacestode vesicles with hydroxyurea (HU)

Axenic metacestode vesicles were cultured in cDMEM-A medium with a nitrogen gas phase (40 vesicles in 5 ml of medium in T-25 25 cm^2 cell culture flasks (Sarstedt, Germany), vertically positioned). HU (Sigma-Aldrich) was added to a final concentration of 40 mM (from a 2 M stock prepared in DMEM; normal DMEM was added to controls). HU was added every day to the medium since it is not stable in solution at temperatures around 37°C, and the medium was changed completely every two days. After seven days of treatment, the vesicles were washed extensively with PBS. Some vesicles were fixed immediately for immunohistofluorescence and whole-mount in situ hybridization. The remaining vesicles were transferred to HU-free cDMEM-A medium and cultured under a nitrogen gas phase, taking samples for EdU labeling after 1, 4, 9 and 22 days. Surviving metacestodes were defined as vesicles being able to maintain turgency and with an apparently intact germinal layer as seen under a dissecting microscope.

Primary cells were cultured in 48 well plates in cDMEM-A in the presence of 10 or 40 mM HU (from a 2 M stock prepared in DMEM; normal DMEM was added to controls), changing half of the medium and HU each 48 to 72 h. The regeneration of metacestode vesicles was quantified after three weeks by direct microscopical inspection.

For the determination of the effect of HU on BrdU incorporation, primary cells from the Ingrid isolate were cultured in a 96 well-plate (8 units of cells per well) in 200 µl of cDMEM-A with 10 or 40 mM HU (from a 2 M stock prepared in DMEM; normal DMEM was added to controls) for 40 hours. After this time, half of the medium was replaced with fresh medium containing HU and BrdU (10 µM final concentration). The cells were cultured for 4 more hours and processed for detection with the Cell Proliferation Elisa, BrdU (Colorimetric) Kit (Roche), as indicated by the manufacturer, including the optional blocking step. The experiment was repeated four times (starting with fresh primary cell preparations each time), and in each experiment three technical replicates (*i.e.* three wells) were performed per experimental condition.

7.1.10. X-ray irradiation of metacestode vesicles

For X-ray irradiation, axenic metacestode vesicles in cDMEM-A medium were subjected to a 150 Gy dose with a Faxitron CP160 source (Faxitron). Vesicles were then set back into axenic culture, and samples were taken for EdU labeling after 2, 7, 20 and 48 days. Surviving metacestodes were defined as vesicles being able to maintain turgency and with an apparently intact germinal layer as seen under a dissecting microscope.

7.1.11. Treatment of primary cells with *in vitro* synthezised peptides

Predicted mature neuropeptides (cell-culture grade, minimum purity of 95% as determined by high pressure liquid chromatography) were synthezised by Metabion (Germany). The peptides synthesized were RGFIamide (dissolved in DMEM medium as an original stock solution of 2 mg/ml, equivalent to 4.08 mM) and AIRLLRLamide (dissolved in dimethylsulfoxide as an original-stock solution of 20 mg/ml, equivalent to 23.44 mM). Primary cells from the Ingrid isolate were cultured in 96 well-plates (8 units per well) in 200 µl of complete DMEM for 40 hours, in the presence of 10^{-8} to 10^{-6} M of each peptide (from 10^{-5} to 10^{-3} stock solutions; an equivalent volume of DMEM or dimethylsulfoxide was added to the controls for RGFIamide and AIRLLRLamide, respectively). After this time, half of the medium was replaced with fresh medium containing the peptides and BrdU (10 µM, final concentration). The cells were cultured for 4 more hours and processed for detection with the Cell Proliferation Elisa, BrdU (Colorimetric) Kit (Roche), as indicated by the manufacturer, including the optional blocking step. The experiment was repeated four times (starting with fresh primary cell preparations each time), and in each experiment three technical replicates (*i.e.* three wells) were performed per experimental condition. For this experiment, non-conditioned complete DMEM was chosen in order to be able to detect relatively minor effects of the peptides on the proliferation of primary cells, which may be masked by other factors present in the conditioned medium (where cells show optimal growth).

7.2. Manipulation of nucleic acids

7.2.1. Synthetic oligonucleotides used in this work

Gene or plasmid	GeneDB code	Primer name	Sequence	Experiment
em-ago2-A	EmuJ_000739100	911700_Fwd_1	ATGCTTCCTT CGCGTCCTG GTAG	To obtain the 5´region of em-ago2-A and probe for WMISH (ca. 1.35 Kb)
em-ago2-A	EmuJ_000739100	739100_Rev_700	ATTGCCAGG TCCACTCCCT TTGCA	To obtain the 5´region of em-ago2-A and probe for WMISH (ca. 1.35 Kb)
em-ago2-A	EmuJ_000739100	739100_1.6_Fwd	TTTGTGGTG CATGGATTG TCAAG	For sequencing and probe for WMISH (ca. 1.6 kb)
em-ago2-A	EmuJ_000739100	739100_1.6_Rev	ACATTTGGTC TTGTTGTCCA GGA	For sequencing and probe for WMISH (ca. 1.6 kb)
em-ago2-A	EmuJ_000739100	739100_sq_Fwd	GCTCCCCTCG TTGTTCAGA G	For semi-quantitative RT-PCR
em-ago2-A	EmuJ_000739100	AgoCommon_sq_ Rev	CACCCAACTT GGCGTTTAT C	For semi-quantitative RT-PCR
em-ago2-B	EmuJ_000911700	911700_sq_Fwd	CCAAAAACG TTAACCTCTT AATGGAC	For semi-quantitative RT-PCR
em-ago2-B	EmuJ_000911700	AgoCommon_sq_ Rev	CACCCAACTT GGCGTTTAT C	For semi-quantitative RT-PCR
em-ago2-C	EmuJ_000911600	911600_sq_Fwd	CACAAATGC TAATAAATTA TTGAAGGC	For semi-quantitative RT-PCR

em-ago2-C	EmuJ_000911600	AgoCommon_sq_Rev	CACCCAACTTGGCGTTTATC	For semi-quantitative RT-PCR
em-ago2-C	EmuJ_000911600	911600_sp_F2	GCGGTCGGACCAAGGAGC	For semi-quantitative RT-PCR, second set
em-ago2-C	EmuJ_000911600	911600_sp_F2	TCCCCCTATCAAGTTTCTTTGACCAAC	For semi-quantitative RT-PCR, second set
em-ago2-ψ	N/A	Pseudo_F	TTGTCCGGAAGGTGGAATGACTAG	For semi-quantitative RT-PCR
em-ago2-ψ	N/A	Pseudo_R	GTGCCCGGTAGAACATTCTTCC	For semi-quantitative RT-PCR
em-alp-1	EmuJ_000393300	1730AP-Fwd	AGAATTTGGCTCGCAAGGAG	For semi-quantitative RT-PCR
em-alp-1	EmuJ_000393300	1730AP-Rev	ACTGGACTCCCGCTGGATAG	For semi-quantitative RT-PCR
em-alp-2	EmuJ_000393400	emap2-CDS-F	AGCTCAGCTTCTTGATAATCATG	Full CDS + partial 5´UTR region for sequencing and probe for WMISH (1.6 kb)
em-alp-2	EmuJ_000393400	emap2-CDS-R	TTATTCACAGGGTGTCTTTTTCTG	Full CDS + partial 5´UTR region for sequencing and probe for WMISH (1.6 kb)
em-alp-2	EmuJ_000393400	emap2-F	GAGGGCTACTAGGGCTATCATTCTG	For semi-quantitative RT-PCR
em-alp-2	EmuJ_000393400	emap2-R	TTCCGAACGTAGCTCAGGAGG	For semi-quantitative RT-PCR
em-alp-3	EmuJ_000752700	emap3-F	AGAAGCAGCCCACGAGCAGTGAAG	For semi-quantitative RT-PCR

em-alp-3	EmuJ_000752700	emap3-R	GGACGGACT CTACTCTCTC CTCAGG	For semi-quantitative RT-PCR
em-alp-4	EmuJ_000752800	emap4-F	TGTGCTTTCA TGGGAGGTG C	For semi-quantitative RT-PCR
em-alp-4	EmuJ_000752800	emap4-R	CAGAAACGT AGGATTTATT TGTTGGAC	For semi-quantitative RT-PCR
em-elp	EmuJ_000485800	Em10-15	AATAAGGTC AGGGTGACT AC	RT-PCR
em-elp	EmuJ_000485800	Em10-16	TTGCTGGTA ATCAGTCGA TC	RT-PCR
emfr1	EmuJ_000833200	EmW_000833200 _Nd_Fwd	TCTCCTCTGC ATCATCGCAT C	Second round of nested RT-PCR for WMISH probe (ca. 1.7 kb)
emfr1	EmuJ_000833200	EmW_000833200 _Nd_Rev	GTAAATGTG GGCCGACAC TCAG	Second round of nested RT-PCR for WMISH probe (ca. 1.7 kb)
emfr1	EmuJ_000833200	EmW_000833200 _Fwd	GCAGTGGGC GTCTTCTTTC AC	First round of nested RT-PCR for WMISH probe
emfr1	EmuJ_000833200	EmW_000833200 _Rev	GAACTTTGA CAGTGTAGC GAGGATG	First round of nested RT-PCR for WMISH probe
emfr3	EmuJ_000893600	EmuJ_000893600 -HindIII-F	ATA AAGCTT GGAAGTCCC CGTTTTCACG G	Second round of nested RT-PCR for cloning into pSecTag2Hygro
emfr3	EmuJ_000893600	EmuJ_000893600 .2_R_NotI_nostop	ATAGCGGCC GCAAGGCTG AGGCGCCCA CG	Second round of nested RT-PCR for cloning into pSecTag2Hygro

emfr3	EmuJ_000893600	EmuJ_000893600.2_F_SP	GGATGTGTGAGGATTGAAGTCCC	First round of nested RT-PCR
emfr3	EmuJ_000893600	EmuJ_000893600.2_R_3U	TGGGCAGCCGATCATATTAAAG	First round of nested RT-PCR
emfr3	EmuJ_000893600	EmuJ_000893600-sq-R	GCAAGCGGTCATGAGGCTGTAG	Second round of nested RT-PCR for WMISH probe (ca. 1.9 kb)
emfr3	EmuJ_000893600	EmuJ_000893600-sq-F2	TTGCCCAGTCATCCGCTACAAG	Second round of nested RT-PCR for WMISH probe (ca. 1.9 kb)
emfr3	EmuJ_000893600	EmuJ_000893600_seq1215F	GCCATGTCGTTGTATGTGTC	Complete sequencing of cloned emfr3 fragment
emfr3	EmuJ_000893600	EmuJ_000893600_seq1314R	GCAGATGAGTAAGAAACCCTC	Complete sequencing of cloned emfr3 fragment
em-h2b-1	EmuJ_000387800	H2B-387800.1-F	ATGGCTCCTAAAGTAGTGTCAGGC	Sequencing and probe for WMISH (255 bp)
em-h2b-1	EmuJ_000387800	H2B-R	GGTCGACTTCTTATTGTAATGCG	Sequencing and probe for WMISH (255 bp)
em-h2b-2	EmuJ_000472800	H2B-472800.1-F	ATGGCACCTAAGGTTGTGTCAGGA	Sequencing and probe for WMISH (255 bp)
em-h2b-2	EmuJ_000472800	H2B-R	GGTCGACTTCTTATTGTAATGCG	Sequencing and probe for WMISH (255 bp)
em-hdac1	EmuJ_001102300	HD1-FullCDS-F	ATGGATCCTGCTGTTGACAAGAAAG	Full CDS sequencing and probe for WMISH (ca. 1.7 kb)

em-hdac1	EmuJ_001102300	HD1-FullCDS-R	TCAAGTACT ATTAGCCCA AGGGATAAT TAG	Full CDS sequencing and probe for WMISH (ca. 1.7 kb)
em-muc-1	EmuJ_000742900	2736Muc-Fwd	GCTACTAAC AGCCCATAC ATTTGC	For semi-quantitative RT-PCR, sequencing, and probe for WMISH (188 bp).
em-muc-1	EmuJ_000742900	2736Muc-Rev	TAGGAGGTG ATAAAGAGA AGGAGG	For semi-quantitative RT-PCR, sequencing, and probe for WMISH (188 bp).
em-nos-1	EmuJ_000861500	EmW_000861500 .1_CDS_F	ATGCCTGCC GGTTCTCTCT TG	Full CDS sequencing and probe for WMISH (684 bp)
em-nos-1	EmuJ_000861500	EmW_000861500 .1_CDS_R	TTAGCTGAG CGAGAAATT ACGG	Full CDS sequencing and probe for WMISH (684 bp)
em-nos-2	EmuJ_000606200	EmW_000606200 .1_CDS_F	ATGCGGGCG ATGATTCCA	Full CDS sequencing and probe for WMISH (720 bp)
em-nos-2	EmuJ_000606200	EmW_000606200 .1_CDS_R	CTACAAGGA TAGAAAGGA GATTTCTTG	Full CDS sequencing and probe for WMISH (720 bp)
em-npp-14	EmuJ_000740500	2738-(K/R)MR(I/M)NH2 -F	AGATTGGTA CACGAGGGC ACAG	RT-PCR
em-npp-14	EmuJ_000740500	2738-(K/R)MR(I/M)NH2 -R	TGTCGGTAC CTTTGGGCTT TC	RT-PCR
em-npp-2	EmuJ_000530500	RGFINH2-1880-QF	AGAACTTGT CTCCCTTCTC GTTTGC	RT-PCR
em-npp-2	EmuJ_000530500	RGFINH2-1880-QR	GCCTCTTCTG CAATCTAGT GCCAC	RT-PCR and 5´RACE (second round)

em-npp-2	EmuJ_000530500	1880_REV_UTR	TTTGTGGGACTCCTCTCTTCG	5´RACE (first round)
em-npp-20.1	EmuJ_001070600	NPF1-F	ATGGAGCAGCAACAACAGGATC	RT-PCR
em-npp-20.1	EmuJ_001070600	NPF1-R	TGTAAGGCCTCCACTAAAGAATCTTC	RT-PCR
em-npp-20.2	EmuJ_000043400.1	NPF2-3433-WF	ATGGTGGGCAGGCTTCATTG	RT-PCR
em-npp-20.2	EmuJ_000043400.1	NPF2-3433-WR	AGTTCCTGCCATCCTGACCTTC	RT-PCR
em-npp-20.3	EmuJ_001194600	NPF3-1768-CORR-F	CAATTTCGTGGTGTGGAATGGC	RT-PCR
em-npp-20.3	EmuJ_001194600	NPF3-1768-CORR-R	TGGTCGTCGAATTGTGAATCTTC	RT-PCR
em-npp-24	EmuJ_001046700.1	3405-FKPKMPIFLGLINH2-F	CAGATGCTCACAACTTTGTTGC	RT-PCR
em-npp-24	EmuJ_001046700.1	3405-FKPKMPIFLGLINH2-R	GGAAACAGCAATGTCAAATTCAAAG	RT-PCR
em-npp-27	EmuJ_000347700	3006-GG(I/V)RY-F	TCTGTCTAGGCCCCAAAATTTC	RT-PCR
em-npp-27	EmuJ_000347700	3006-GG(I/V)RY-R	TGATTGACAGAAGGATGATCGG	RT-PCR

em-npp-34	EmuJ_000316500	SPQFAWRPHSRFNH2-1680-WF	CCATTCTAACACTCTTCTACTTCGC	RT-PCR
em-npp-34	EmuJ_000316500	SPQFAWRPHSRFNH2-1680-WR	TACCGGGAAGTGAGGCATG	RT-PCR
em-npp-4	EmuJ_000240300	GNFFRNH2-1872-QF	ATCGATGCCCTGGAGAGTCG	RT-PCR
em-npp-4	EmuJ_000240300	GNFFRNH2-1872-QR	AATCCACATTCTCGATCATGACATG	RT-PCR
em-npp-6	EmuJ_000759050	NPP6-F	CTGTGACTTACCTACTTGCACACAG	RT-PCR
em-npp-6	EmuJ_000759050	NPP6-R	AGTGAGTCGTTGTTAATAGAGAGGC	RT-PCR
em-phb1	EmuJ_000738700	PHB-1F	TGGTTGCAGCTGGCAGTATC	Probe for WMISH (299 bp)
em-phb1	EmuJ_000738700	PHB-1R	CTCATAATCGAAGCCAAGGTTAG	Probe for WMISH (299 bp)
emplk1	EmuJ_000471700	AK0-55	CTCTCATGGAACTGCATAAGAG	RT-PCR for WMISH probe (1.3 kb)
emplk1	EmuJ_000471700	AK0-60	CGATCTATCATATCGTAGGCG	RT-PCR for WMISH probe (1.3 kb)
em-tpm-1.hmw	EmuJ_000958100	TPM1-HMW F	AGCGGAGTCTCGTTTGGAAAC	WMISH probe (278 bp)

em-tpm-1.hmw	EmuJ_000958100	TPM1-HMW R	TGATGGCTC GGTAACGTT CC	WMISH probe (278 bp)
ta-TRIM	N/A	3´RACE-Fn-1	TGTGTCTTCT TTCGTNTTCA GGGAG	nested 3´RACE of ta-TRIMs in *E. multilocularis*
ta-TRIM	N/A	3´RACE-Fn-2	TCAGGGAGT CYYGGGAYG CTACA	nested 3´RACE of ta-TRIMs in *E. multilocularis*
ta-TRIM **fusion "locus 2"**	EmuJ_000054900	Fusion-locus2-F	CCGAGTATT GTGTCTTCTT TCGTCTTC	Confirmation of fusion of CDS to solo-LTR
ta-TRIM **fusion "locus 2"**	EmuJ_000054900	Fusion-locus2-R	CGGAATGAC ATTTGGCAA AGTC	Confirmation of fusion of CDS to solo-LTR
ta-TRIM **fusion "locus 8"**	EmuJ_000118100	Fusion-locus8-F	TTCGTCTTCT TTCGTCTTCA GAGAG	Confirmation of fusion of CDS to solo-LTR
ta-TRIM **fusion "locus 8"**	EmuJ_000118100	Fusion-locus8-R	GCATCCTTG ATCGAAGTT TGGG	Confirmation of fusion of CDS to solo-LTR
ta-TRIM **fusion "locus 21"**	EmuJ_000465100	Fusion-locus21-F	CTTTTGTACT TTGAGTTAG CCCCTTGTAC	Confirmation of fusion of CDS to solo-LTR
ta-TRIM **fusion "locus 21"**	EmuJ_000465100	Fusion-locus21-R	CCATGGCGA AATCGACCA C	Confirmation of fusion of CDS to solo-LTR
ta-TRIM **fusion "locus 60"**	EmuJ_001025350	Fusion-locus60-F	CCTTGTACCT AGCTAAGAG GGCTGAC	Confirmation of fusion of CDS to solo-LTR
ta-TRIM **fusion "locus 60"**	EmuJ_001025350	Fusion-locus60-R	CGACGTAGG CACTCAAGC AAG	Confirmation of fusion of CDS to solo-LTR

***ta-TRIM* locus 39**	N/A	Inter-F	TTGGTGGCA GCGGAAAGC	PCR for probe for WMISH of ta-TRIM (region between LTRs of locus 39, 584 bp)
***ta-TRIM* locus 39**	N/A	Inter-R	CCTCTTTTGA GTGTTATCCC CAGC	PCR for probe for WMISH of ta-TRIM (region between LTRs of locus 39, 584 bp)
N/A	N/A	Smart CDS Primer IIA	AAGCAGTGG TATCAACGC AGAGTACT3 0VN	Reverse transcription
N/A	N/A	Smart PCR Primer IIA	AAGCAGTGG TATCAACGC AGAGT	3´RACEs
pJG4-5 (Invitrogen)	N/A	4-5 dw	GATGCCTCCT ACCCTTATGA TGTG	
pJG4-5 (Invitrogen)	N/A	pJG 4-5 SPR	CTTATGATGT GCCAGATTA TG	
pDrive (QIAGEN)	N/A	T7	GTAATACGA CTCACTATAG	
pDrive (QIAGEN)	N/A	SP6	CATTTAGGT GACACTATA G	
pJet1.2 (Fermentas)	N/A	pJetFwd	CGACTCACT ATAGGGAGA GCGGC	
pJet1.2 (Fermentas)	N/A	pJetRev	AAGAACATC GATTTTCCAT GGCA	
pSecTag2/HygroA (Invitrogen)	N/A	psecfw	CTAGTTATTG CTCAGCGGT GG	

pSecTag2/HygroA (Invitrogen)	N/A	psecrev	TAATACGAC TCACTATAG GG

7.2.2. General precautions for working with RNA

When working with RNA, powder-free latex gloves were always used. The surface of the working bench and of the pipettes was cleaned with RNAse Exitus Plus to remove traces of RNAses, followed by rinsing with 70% ethanol. A separate stock of chemicals and plastic material was reserved for working exclusively with RNA. Glassware was treated by dry heat (180 °C for 2 hours) to remove RNAses. Solutions and buffers were treated when possible with diethyl pyrocarbonate (DEPC, Applichem) to remove RNAse traces, by adding 0.1% DEPC to the solutions and incubating them with stirring overnight, followed by autoclaving the solutions two times to eliminate the DEPC. In the case of solutions that are incompatible with DEPC treatment, these were prepared with DEPC-treated water, and taking care not to introduce contaminations during their preparation by using clean disposable weighing material. Enzymatic reactions can be inhibited by small traces of DEPC. Therefore, commercial nuclease-free double distilled water (Qiagen) was used for enzymatic reactions instead.

7.2.3. RNA isolation and quantification

RNA was isolated from metacestode vesicles and protoscoleces (*ca*. 100 mg of material) and from primary cells (ca. 500 units) using 1 ml of Tri-Reagent (5 PRIME) as instructed by the manufacturer (in the case of protoscoleces, yield can be improved by using a glass pestle homogenizer, although this is not essential). The concentration of RNA was determined spectrophotometrically using the NanoDrop 1000 (Thermo Scientific) at a wavelength of 260 nm (using an extinction coefficient of 0.025 $(\mu g/ml)^{-1}$ cm^{-1} for single stranded RNA). The purity of the nucleic acids was determined on the basis of the ratios of absorbance at a wavelength of 260 nm over absorbance at a wavelength of 280 nm using the NanoDrop 1000 (this ratio is expected to be between *ca.* 1.8 and 2.0 for pure RNA at neutral pH). The integrity of the RNA was confirmed

by the lack of degradation of ribosomal RNAs, as evaluated by agarose gel electrophoresis (see below).

7.2.4. DNAse treatment of RNA

For RT-PCR experiments of genes lacking introns, traces of genomic DNA were removed before cDNA synthesis by treatment with RQ1 DNAse (Promega). RNA was incubated with RQ1 DNAse (2 units per µg of RNA to be treated) at 37 °C for 1 hour. The RNA was then re-purified by extraction with 1 volume of chloroform, followed by centrifugation at 12,000 g for 20 minutes at 4 °C. The aqueous phase was transferred to a new tube and precipitated by the addition of 0.1 volumes of sodium acetate (3 M, pH 5.2, RNAse free) and 2.5 volumes of 100% ethanol, followed by centrifugation at 12,000 g for 20 minutes at 4 °C. The supernatant was discarded, and the RNA pellet was washed twice with 70% ethanol and allowed to dry at room temperature for 5 to 10 minutes. Finally, the RNA pellet was dissolved in commercial RNAse-free water and its concentration determined by spectrophotometry as described above.

7.2.5. cDNA synthesis

First strand cDNA synthesis was performed with Prime Script reverse transcriptase (Takara) as instructed by the manufacturer, using typically 700 ng of total RNA and 50 pmol of primer Smart CDS Primer IIA (AAGCAGTGGTATCAACGCAGAGTAC-T_{30}-VN). For specific non-quantitative experiments, the amount of RNA was sometimes increased to up to 3000 ng.

7.2.6. PCR, RT-PCR, and semi-quantitative RT-PCR

For general purposes, Taq polymerase (New England Biolabs) was used for PCR, whereas the proofreading KOD Hot Start polymerase (Novagen) was used for cloning larger fragments (>1 kb), for which the chance of incorporating an incorrect nucleotide would be high in the absence of proofreading activity. For Taq polymerase, the reaction conditions consisted in 1 x reaction buffer (with 1.5 mM $MgCl_2$), 0.2 mM of each dNTP (Applichem), 0.8 µM of each primer (custom synthesized by Sigma-

Aldrich), 1 unit of Taq polymerase, DNA template, and sterile double-distilled water up to a final volume of 25 µl. Cycling conditions for Taq polymerase consisted of an initial denaturation step at 95 °C for 2 minutes, followed by 30 to 35 cycles of denaturation (95 °C for 30 s to 1 min), annealing (at the lowest primer Tm for 30 s o 1 min) and extension (at 72 °C, 1 min per kb of the amplicon), and finally a last extension step at 72 °C for 10 minutes. For KOD Hot Start polymerase, the reaction conditions consisted of 1 X reaction buffer, 1.5 mM $MgCl_2$, 0.2 mM of each dNTP (Applichem), 0.3 µM of each primer (custom synthesized by Sigma-Aldrich), 1 unit of KOD Hot Start Polymerase, DNA template, and sterile double-distilled water up to a final volume of 50 µl. Cycling conditions for KOD Hot Start polymerase consisted of an initial denaturation and polymerase activation step at 95 °C for 2 min, followed by 35 cycles of denaturation at 95 °C for 20 s, annealing at the lowest primer Tm for 10 s, and extension at 70 °C for between 10 and 20 s per kb of the amplicon. The amount of template used per reaction for both polymerases was 1 to 2 µl of cDNA synthesis reaction for cDNA amplification, and 100 ng for gDNA amplification.

For semi-quantitative RT-PCR, ten-fold serial dilutions of each cDNA were used for PCR with Taq polymerase (New England Biolabs), and the amplification was limited to 28 to 30 cycles. For normalization, RT-PCR with the constitutive gene *em-elp* (Brehm et al. 2003) was performed.

7.2.7. Rapid amplification of cDNA ends (RACE)

For 5´ RACE of the *em-npp-2* gene (EmuJ_000530500), a cDNA library previously generated in the laboratory with vector pJG4-5 was used. A nested PCR was performed using in the first reaction 2 µl of the library as template together with primers 1880_REV_UTR and 4-5 dw. In the second reaction 0.5 µl of the first reaction was used as template together with primers RGFINH2-1880-QR and pJG 4-5 SPR.

For 3´ RACE of the *ta-TRIM* elements, a semi-nested PCR was performed using in the first reaction 2 µl of cDNA as template (containing the AAGCAGTGGTATCAACGCAGAGTAC sequence at the 3´end of all cDNAs from the Smart CDS Primer IIA sequence) together with primers TGTGTCTTCTTTCGTNTTCAGGGAG and Smart PCR Primer IIA. For the second

reaction, 0.5 µl of the first reaction was used as template with primers TCAGGGAGTCYYGGGAYGCTACA and Smart PCR Primer IIA.

7.2.8. Electrophoresis of DNA and RNA

Electrophoresis of nucleic acids was performed by standard agarose gel electrophoresis in TAE buffer (40 mM Tris base, 20 mM acetic acid, 1 mM EDTA), and the gels were post-stained with ethidium bromide and photographed under UV light in a trans-illuminator (Sambrook, Fritsch, and Maniatis 1989). The molecular weight marker SmartLadder (Eurogentec, Germany) was included in the gels. For gel purification of DNA fragments, the regions of the agarose gel containing the DNA fragments of interest were excised from the gel with a clean scalpel, and the DNA was purified using the QIAEX II gel extraction kit (Qiagen) as instructed by the manufacturer. The DNA concentration was determined spectrophotometrically at 260 nm with the NanoDrop 1000 (Thermo-Scientific). The extinction coefficient used for double stranded DNA was 0.020 $(\mu g/ml)^{-1}$ cm^{-1}.

For the electrophoresis of RNA the same methods were used (non-denaturing agarose gels prepared in TAE Buffer), except that the buffer was specially prepared to be RNAse free, and the electrophoresis chamber was decontaminated by treating for 15 to 30 min with 3 % H_2O_2, followed by rinsing with 95% ethanol and with RNAse-free water.

7.2.9. Molecular Cloning

PCR and RT-PCR amplicons were cloned either directly or after gel purification with the PCR cloning kit vectors pDrive (T/A cloning vector, for Taq polymerase amplicons, Qiagen) and pJET1.2 (Thermo-Scientific; blunt end cloning vector, used for KOD Hot Start polymerase amplicons and also for Taq polymerase amplicons, by including the blunting step of the protocol) as instructed by the manufacturers.

For sub-cloning of the CDS of *emfr3* (minus the signal peptide region), the CDS was originally amplified from a pool of cDNA obtained from different developmental stages by a nested PCR approach, using primer combinations EmuJ_000893600.2_F_SP

and EmuJ_000893600.2_R_3U for the first reaction, and EmuJ_000893600-HindIII-F and EmuJ_000893600.2_R_NotI_nostop (containing *Hind*III and *Not*I adapters at their 5´ ends) for the second reaction. The amplified fragment was cloned into pJET1.2, and excised by restriction digestion with *Hind*III and *Not*I for sub-cloning into the *Hind*III and *Not*I sites of the pSecTag2/HygroA plasmid (Invitrogen). The resulting plasmid contains the *emfr3* CDS (minus its signal peptide) in frame with the murine Ig κ-chain signal peptide at its 5´ end and with the His-Tag and c-myc tag at its 3´ end. This fusion-CDS is downstream of T7 pol and Cytomegalovirus (CMV) promoters.

Chemically competent *Escherichia coli* Top 10 cells (Invitrogen) were previously prepared by a standard $CaCl_2$ protocol (Sambrook, Fritsch, and Maniatis 1989) and stored at -80 ºC. Transformation of *E. coli* Top 10 cells was performed as follows. First, the cells were thawed on ice, and the ligation mixture (no more than 10% of the total volume of the competent cell suspension) was added. The cells were incubated for 20 min on ice, followed by a 90 s incubation at 42 ºC (heat shock treatment), and a 90 s incubation on ice. Then, 500 µl of Luria Broth (LB, Invitrogen) or SOC (Invitrogen) medium (pre-warmed at 37 ºC) was added to the cells, and they were allowed to recover at 37 ºC for 45 minutes with shaking at 220 RPM. Finally, 20 to 80% of the cells were plated on LB agar plates (LB with 1.5% Bacto-Agar) containing 100 µg / ml ampicillin (Sigma-Aldrich) and incubated overnight at 37 ºC to allow clonal colonies to appear. When cloning into the pDrive vector, which has the blue/white *lacZ* mediated screening system, 5-bromo-4-chloro-3-indolyl-β-D-galactopyranoside (X-Gal, Fermentas) was added to the plates (40 µl per plate from a 40 mg/ml solution of X-Gal in N,N-dimethylformamide).

Screening for recombinant clones was done by colony-PCR followed by agarose gel electrophoresis of the amplicons. For this, individual colonies were picked and resuspended in 10 µl of sterile double-distilled water. 1 to 2 µl of each clone suspension were used directly for PCR with Taq polymerase (New England Biolabs) in a protocol identical to the one previously detailed, except that the initial denaturation step at 95 ºC was increased to 5 min. The primers used were T7 and SP6 for pDrive derived constructs, pJetFwd and pJetRev for pJET1.2 derived constructs, and psecfwd and psecrev for pSecTag2/HygroA derived constructs.

Positive clones were then inoculated into 5 ml of LB medium with 100 µg/ml ampicillin, and incubated overnight at 37 ºC with shaking (220 RPM). The bacterial cells were harvested by centrifugation and used for small-scale isolation of plasmid DNA ("minipreps") with the NucleoSpin Plasmid Kit (Macherey-Nagel). Sequencing with vector primers (and for large inserts, also with internal primers) was done by the Sanger dideoxy-termination method at the Institut für Hygiene und Mikrobiologie, Würzburg.

7.2.10. Restriction digestion

Restriction digestion was carried out with diverse enzymes purchased from New England Biolabs, using the buffer systems and temperatures recommended by the manufacturer. Reactions were incubated for 2 h to overnight.

7.2.11. High throughput RNA sequencing (RNAseq) and analysis

Samples for RNAseq were frozen in ten volumes of Tri-Reagent (5 PRIME) and shipped to the Wellcome Trust Sanger Institute (Cambridge, United Kingdom) with dry ice. There, RNA was isolated and processed for RNAseq. The following description of the methods used at the Wellcome Trust Sanger Institute was written by Magdalena Zarowiecki, and is transcribed here after minor editing.

Total RNA was isolated using TRIzol (Invitrogen, UK) according to manufacturer specifications (*E. multilocularis)*. Samples were treated with TURBO DNA-free DNase (Ambion) to reduce genomic DNA contamination, ethanol precipitated and re-suspended in nuclease free water. RNA quality was assessed using an Agilent RNA 6000 Nano-Bioanalyzer. The transcriptome libraries were sequenced following Illumina RNA-seq protocols on the Illumina Genome Analyser IIx or HiSeq, producing paired reads of 76 or 100 bp. Four fluorescently labeled nucleotides and a specialized polymerase were used to determine the clusters base by base in parallel. Paired end RNA-seq libraries (400-500 bp fragments) were produced using polyadenylated mRNA purified from total RNA from *E. multilocularis*. Image

deconvolution and quality value calculations were performed using the Illumina GA pipeline v1.6.

RNA-Seq reads were mapped to the reference genomes with Tophat v2.0.9, and the FPKM values (Fragments Per Kilobase of transcript per Million mapped reads) were calculated using the Cuffdiff programme v2.1.1 included in the Cufflinks package (http://cufflinks.cbcb.umd.edu/); default parameters plus -u and –b option. Reads per gene was calculated using BEDTools v 2.10.1 coverageBed, and duplicates were marked up and removed using custom scripts and SAMtools v.0.1.19+. Significantly differentially expressed genes between non-treated and stem-cell depleted samples was performed using DESeq v.1.12.1, which uses a negative binomial distribution model to test for differential expression, on the statistical programming platform R v.3.0.0. For normalization, size factors and dispersion were estimated separately for each library, and the negative binomial test applied. A DESeq q-value cutoff 1e-5 was applied.

GO-enrichment analysis on significantly differentially expressed genes was performed using topGO v.2.12.0 on biological processed (BP) using the "classic" algorithm under the Fisher statistic. The GO-annotation of genes was obtained from http://www.genedb.org.

7.3. Histological procedures and transmission electron microscopy

7.3.1. Preparation of cell suspensions (cell maceration) and staining

Cell suspensions from metacestodes and primary cells were prepared and fixed on SuperFrost Plus glass slides (Thermo-Scientific) for microscopical examination of their morphology, using a modification of the method of David (1973), as described (Koziol et al. 2014). A working protocol is included in Appendix 3. The staining procedures are also explained in detail by Koziol et al. (2014)

7.3.2. Fixation of metacestode vesicles and protoscoleces for histological sectioning and whole-mount procedures

Before fixation, metacestode vesicles were gently opened using a syringe tip in order to allow the fast entry of the fixative and other reagents. Total metacestode material, metacestode vesicles and protoscoleces were fixed in 4% paraformaldehyde (Sigma-Aldrich) prepared in PBS (PFA 4% - PBS) for 1 hour at room temperature (for EdU detection), 1 to 4 hours at room temperature (for IHF in whole-mounts, Paraplast sections and cryosections) or overnight at 4 ºC (for WMISH, in which case DEPC-treated PBS was used for preparing the PFA 4% - PBS solution).

7.3.3. Preparation of Paraplast sections

Fixed specimens were washed extensively with PBS, and embedded into Paraplast (Sigma-Aldrich) blocks according to the following protocol. First the samples were dehydrated in an ethanol dilution series (25 % ethanol in PBS, 50 % ethanol in PBS, 75 % ethanol, and 100% ethanol; 15 minutes each). They were then serially incubated in Peel-A-Way embedding molds (Sigma-Aldrich) with 100% isopropanol (2 incubations of 15 min each), a mixture of 1:1 isopropanol and Paraplast at 55-60 ºC (40 minutes) and Paraplast at 55-60 ºC (two incubations of 40 minutes each). Finally, the molds were put on ice for the solidification of the Paraplast into blocks, and once a layer of solid Paraplast could be observed over the top of the mold, the whole mold was covered with ice and the blocks were allowed to solidify overnight at 4 ºC. The

Paraplast blocks were cut into 6 to 10 µm thick sections with an RM 2065 microtome (Leica, Germany), transferred to a tray with warm distilled water (*ca.* 50 ºC), and collected on SuperFrost Plus glass slides (Thermo Scientific). After this, they were allowed to dry overnight at 37 ºC and stored at 4 ºC until further use.

7.3.4. Preparation of Cryosections

After fixation, specimens were embedded in OCT compound (Tissue-Tek), snap-frozen with liquid nitrogen, and the cryoblock was allowed to equilibrate to -20 ºC before cutting. Sections (5 to 15 µm thick) were obtained with a 2800 Frigocut E cryotome (Leica, Germany) and mounted on SuperFrost Plus glass slides (Thermo Scientific), allowing them to dry for 2 hours at room temperature before storing them at -20 ºC until further use. Sometimes, a cryoprotection step was added by pre-incubating the specimens in 30% sucrose at 4 °C for 48 hours before embedding.

7.3.5. Alkaline phosphatase histochemistry (ALP-HC)

ALP-HC on cryosections was performed according to the protocol of Cox and Singer (Cox and Singer 1999). In brief, cryosections were thawed for 30 min, and re-fixed with PFA 4% – PBS for 15 min. They were then washed 5 times with PBS, 3 min each, and permeabilized with PBS + 0.2 % Tween-20 for 10 min. After washing for 10 min with PBS, they were incubated with ALP Buffer (Tris.HCl 100 mM, NaCl 100 mM, $MgCl_2$ 5 mM, pH 9.5) for 5 min, and finally the reaction was initiated by incubating the slides with 20 µl/ml of NBT/BCIP substrate preparation (Fluka) in ALP buffer. The reaction was stopped with PBS + 25 mM ethylenediaminetetraacetic acid (EDTA, Applichem). All steps were carried out at room temperature.

ALP-HC of whole-mounts was performed by T. Rauschendörfer during her Bachellor Thesis using an equivalent protocol.

7.3.6. Acetylcholinesterase histochemistry (AChE-HC)

AChE-HC was performed on cryosections, according to the method of Karnovsky and Roots (Karnovsky and Roots 1964). Briefly, thawed cryosections were incubated at room temperature with the reaction solution, which must be prepared freshly as follows: first, 5 mg of acetylthiocholine (Sigma-Aldrich) are dissolved in 6.5 ml of 0.1 M phosphate buffer, pH 6.0. The following solutions are added in order, under continuous stirring: 0.5 ml of 0.1 M sodium citrate, 1 ml of 30 mM $CuSO_4$, 1 ml of distilled water and 1 ml of 5 mM potassium ferrycianide. The reaction solution is stable for hours at room temperature.

7.3.7. 4′,6-diamidino-2-phenylindole (DAPI) and phalloidin staining

Co-staining of cryosections and whole-mounts after IHF was done with DAPI dilactate (Sigma-Aldrich, 1 µg/ml in PBS for 10 to 15 min) and/or TRITC-conjugated phalloidin (Sigma-Aldrich, diluted 1:40 for metacestode vesicles and 1:40 to 1:200 for protoscoleces, in PBS + 1 % bovine serum albumin (BSA, Sigma Aldrich) for 20 minutes at room temperature), followed by several washes in PBS. DAPI co-staining was also performed for Paraplast sections after IHF and WMISH.

7.3.8. Processing of samples for Transmission Electron Microscopy (TEM)

The fixation of specimens was initiated at room temperature with Fixation solution A (2.5% gluteraldehyde; 50 mM cacodylate, pH 7.2; 50 mM KCl; 2,5 mM $MgCl_2$) for primary cell aggregates or with Fixation Solution B (2.5% gluteraldehyde and 2 % formaldehyde, 50 mM cacodylate, pH 7.2; 50 mM KCl; 2,5 mM $MgCl_2$) for metacestode vesicles. After 10 to 15 min of fixation, the samples were transferred to 4 °C and fixation was continued for 3 hours. Specimens were washed at 4 °C for 3 to 5 times (for primary cell aggregates and metacestode vesicles, respectively), each for 5 min, with cacodylate buffer (50 mM cacodylate, pH 7.2). Samples were stored overnight at 4°C, before continuing with fixation with 2% OsO_4 in cacodylate buffer for 90 to 120 min. After fixation, the specimens were washed 5 times with distilled water, 3 min each, and contrasted with 0.5% uranyl acetate overnight. The next day, the specimens were washed 5 times with distilled water, 3 min each, and dehydrated at 4 ºC

by serial incubations of 30 min each in 50% ethanol, 70% ethanol, 90% ethanol, 96% ethanol, and finally three 30 min incubations in 100% ethanol. The dehydrated specimens were transferred to propylene oxide at room temperature (three successive incubations of 30 min each) and then to a 1:1 mix of propylene oxide and Epon 812 for overnight incubation. Finally, the specimens were transferred to pure Epon 812 (three incubations of 2 hours each) and the Epon 812 was polymerized at 60 ºC for two days. Cutting of ultrathin sections and mounting of the specimens was performed by Daniela Bunsen and Prof. Georg Krohne, of the Department of Electron Microscopy, University of Würzburg. The sections were examined with an EM10 and an EM900 electron microscope (Zeiss, Germany).

7.4. Detection of protein and mRNA localization *in situ*

7.4.1. Antibodies used in this work

Antibody	Species origin and clonality	Dilution (Experiment)	Source
Anti-5-Hydroxytryptamine (Serotonin)	Rabbit polyclonal	1/300 (IHF)	Immunostar (20091)
Anti-Acetylated alpha-tubulin	Mouse monoclonal	1/100 (IHF)	Santa Cruz (clone 6-11B-1)
Anti-Digoxigenin Fab fragments, Alkaline Phosphatase conjugated	Sheep polyclonal	1/200 (WMISH)	Roche (11 093 274 910)
Anti-Digoxigenin Fab fragments, Horse Radish Peroxidase conjugated	Sheep polyclonal	1/50 (WMISH)	Roche (11 207 733 910)
Anti-FMRFamide	Rabbit polyclonal	1/300 (IHF)	Immunostar (20080)
Anti-FVamide	Rabbit polyclonal	1/125 (IHF)	Markus Conzelmann (Max Planck Institute for Developmental Biology, Tübingen, Germany)
Anti-HMW-tropomyosin	Rabbit polyclonal	1/500 (IHF)	Gabriela Alvite (Facultad de Ciencias, Montevideo, Uruguay)
Anti-mouse, FITC conjugated (secondary antibody)	Goat polyclonal	1/100 (IHF)	Jackson Immunoresearch (115-095-003)
Anti-mouse, FITC conjugated (secondary antibody)	Donkey polyclonal	1/100 (IHF)	Jackson Immunoresearch (715-095-150)
Anti-PHB1	Rabbit polyclonal	1/100 (IHF) 1/1000 (WB)	Sigma-Aldrich (HPA003280)

Anti-phospho-histone H3 (Ser10)	Rabbit polyclonal	1/100 (IHF)	Cell Signaling Technology (9701)
Anti-rabbit, FITC conjugated (secondary antibody)	Donkey polyclonal	1/100 (IHF)	Jackson Immunoresearch (711-095-152)
Anti-rabbit, Horse Radish Peroxidase conjugated (secondary antibody)	Goat polyclonal	1/5000 (WB)	Jackson Immunoresearch (111-055-003)
Anti-RYamide	Rabbit polyclonal	1/250 (IHF)	Markus Conzelmann (Max Planck Institute for Developmental Biology, Tübingen, Germany)

7.4.2. Immunohistofluorescence (IHF) and immunohistochemistry (IHC)

IHF (in sections and in whole-mounts) and IHC (in sections) were performed as described (Koziol et al. 2011; Koziol, Krohne, and Brehm 2013). Working protocols for these techniques are included in Appendices 4 to 6.

7.4.3. Whole-mount in situ hybridization (WMISH)

In vitro transcription of digoxigenin labeled riboprobes, quantification of riboprobes by dot blot, and WMISH were performed as described (Koziol et al. 2014). A detailed working protocol for all of these steps, including all of the reagents and solutions, is included in Appendices 7 to 9. The probes used for each gene are indicated above in the list of synthetic oligonucleotides used for this work, except for the probe used for *emfr2*, which consisted in a full-length CDS probe (minus the signal peptide region), from a clone previously obtained by Monika Bergmann.

7.4.4. Epifluorescence microscopy and confocal laser scanning microscopy

Samples were analyzed by confocal microscopy (Leica TCS SP5; Leica Microsystems, Germany) and by epifluorescence microscopy (ZeissAxio Imager.Z1 (Zeiss, Germany) and Keyence BZ9000 (Keyence, Germany)). For the quantification of

positive cells after different staining procedures, random fields were photographed and the total number of positive cells in a given area and/or the proportion of positive cells was manually counted (specific details for each experiment are included in the main text). ImageJ (Rasband 1997) was used for analyzing and merging different channels, adjusting brightness and contrast, and measuring lengths and areas.

7.5. Manipulation of proteins

7.5.1. Preparation of lysates for SDS-PAGE

Parasite material (4 to 5 metacestode vesicles) were lysed directly in 100 to 200 µl of 1 x sample buffer for SDS-PAGE (Tris-HCl (62.5 mM pH 6.8); 10 % Glycerol; 2 % (w/v) SDS, 5 % (v/v) ß-mercaptoethanol, 0.002 % Bromophenol Blue) by boiling for 15 minutes at 100 ºC.

7.5.2. Sodium Dodecyl Sulfate-Polyacrylamide Gel Electrophoresis (SDS-PAGE)

SDS-PAGE was performed as described (Sambrook, Fritsch, and Maniatis 1989), using a Biorad Mini-Protean system. The separation gel contained 10% acrylamide, and the stacking gel contained 4% acrylamide. The molecular weight marker Color Plus Prestained Protein Marker (10- 230 kDa) (New England Biolabs) was included in the gel.

7.5.3. Western Blot

The proteins from the SDS-PAGE gel were transferred onto a nitrocellulose membrane (GE Healthcare) using the Biorad Mini Trans-Blot Cell. The transfer was carried out for 1 h at 350 mA with running buffer (25 mM Tris, pH 8.3, 193 mM Glycin, and 20% methanol). The membrane was then blocked for 1 h at room temperature in blocking buffer (5 % skimmed milk in TBS-T: 20 mM Tris pH 8.0; 150 mM NaCl; 0.1 % Tween-20) with shaking. The anti-PHB1 antibody (Sigma-Aldrich) was diluted 1:1000 with blocking buffer and incubated with the membrane overnight at 4 ºC with gentle rocking. The membrane was washed 3 times, for 10 min each time, at room temperature with TBS-T with shaking, after which it was incubated with an anti-rabbit antibody conjugated with horse radish peroxidase (Jackson Immunoresearch, diluted 1:5000 in blocking buffer) for 1 h at room temperature with shaking. The membrane was washed again 3 times, for 10 min each time, with TBS-T at room temperature with shaking and the bound antibody was visualized with a

chemiluminescent substrate (ECL-Western Blot Substrate, Pierce) by exposing X-ray-films (Kodak). The films were developed with a Curix 60 automated developer (Agfa).

7.6. Bioinformatics and statistics

7.6.1. Datasets and programs

Genomic and predicted transcriptomic and proteomic datasets for *Echinococcus multilocularis*, *Echinococcus granulosus*, *Taenia solium*, *Hymenolepis microstoma* (Tsai et al. 2013) and *Schistosoma mansoni* (Berriman et al. 2009) were downloaded from GeneDB (http://www.genedb.org) and used locally for blast searches, motif searches, and alignments with Bioedit ((Hall 1999); in particular, alignments were done with the ClustalW program (Thompson, Gibson, and Higgins 2002) included in the Bioedit package). Visualization of predicted genes and RNAseq data was done with IGV (Thorvaldsdóttir, Robinson, and Mesirov 2013) and Artemis (Rutherford et al. 2000). Sequences and blast analyses for other organisms were obtained from the NCBI GenBank server (http://ncbi.nlm.nih.gov/), except for *Schmidtea mediterranea* (SmedGD, Robb et al. 2007; http://smedgd.neuro.utah.edu/).

In addition, an EST database for *Echinococcus* spp. (Echi-EST-DB) was assembled by Ferenc Kiss by combining the available ESTs from NCBI and diverse unpublished EST projects and collections: from the Wellcome trust Sanger Institute (ftp://ftp.sanger.ac.uk/pub/pathogens/Echinococcus/multilocularis/ESTs/ and ftp://ftp.sanger.ac.uk/pub/pathogens/Echinococcus/granulosus/ESTs/), the *Echinococcus* full length cDNA project (http://fullmal.hgc.jp/index_em_ajax.html), and samples of a yeast-two-hybrid library previously sequenced in our laboratory.

Analysis of domain structure for protein sequences was performed with Interpro Protein Sequence Analysis and Classification (http://www.ebi.ac.uk/interpro/) and Smart analysis searches (http://smart.embl-heidelberg.de).

Phylogenetic analyses of aligned protein sequences were performed using MEGA 5.0 (Tamura et al. 2011). Typically, maximum likelihood (ML) analyses were performed using a substitution model with the best fit to the datasets (using the “find best DNA/protein models (ML)” feature), and compared with Neighbor Joining (NJ) analyses using the JTT model. In most cases and for most nodes, the results were largely comparable and only the NJ JTT tree is shown. Bootstrap analysis of support for individual nodes was performed with 1000 replicates.

7.6.2. Discovery of neuropeptide and peptide hormone (NP) genes in the genomes of cestodes

Initially, a list of neuropeptides from diverse publications (McVeigh et al. 2009; Collins et al. 2010; Veenstra 2010; Veenstra 2011) and from Neuropedia (Kim et al. 2011) was used for blastp and tblastn searches against the *E. multilocularis* predicted proteins and genome contigs, respectively. A high expect value (100) was used, given the small size and low conservation of NPs, and the results were manually inspected.

Because the first strategy was only marginally successful, and because the initial results suggested that the usual *de novo* strategies for NP gene discovery would not work in cestodes (see the Results section), we searched for novel conserved cestode NP genes with the following strategy.

1) We searched for *E. multilocularis* genes with the motif {[K/R][K/R]X_{4-20}[K/R/stop codon]} as candidate neuropeptide encoding genes (that is, all possible peptides that could be released from a potential precursor by canonical cleavage by prohormone convertases).

2) We filtered these hits discarding a) Gene models with CDS coding for proteins longer than 200 amino acids; b) Gene models with significant similarity (blastp expect value < 10^{-5}) to uniprot reference proteins (since they will most likely not represent NP encoding genes, but rather other proteins with spurious similarity to the NP; if it was indeed a NP gene with high similarity to a Uniprot protein, then it should have been detected with the original blast strategy using well-known NP genes).

3) We analyzed all the filtered hits by tblastn against the *H. microstoma* genome contigs (expect value threshold = 0.1), and manually inspected the results, looking for high conservation within the putative mature neuropeptide sequences and proprotein convertase sites, but lower conservation in the rest of the CDS. (Figure R5.5 shows such an example). All hits were analyzed for the presence of 1) single or multiple copies of putative mature peptide sequences 2) Presence of a signal peptide (SignalP 4.0 server (Petersen et al. 2011; 2014)); 3) search for conservation of the putative mature peptides in other flatworms and lophotrochozoans. Finally, similar sequences were searched for by blastp and tblastn in *E. granulosus* and *T. solium*.

7.6.3. Statistics

Statistical analyses were performed using the non-parametric Mann-Whitney-Wilcoxon rank-sum test for comparing medians in diverse experiments. The chi-square test was used for comparing proportions of cells in cell maceration experiments, and to compare the proportion of surviving metacestode vesicles after hydroxyurea treatment.

8. Bibliography

Abbott, J. C., D. M. Aanensen, K. Rutherford, S. Butcher, and B. G. Spratt. 2005. WebACT--an online companion for the Artemis Comparison Tool. Bioinformatics 21:3665-3666.

al Nahhas, S., C. Gabrion, S. Walbaum, and A. F. Petavy. 1991. In vivo cultivation of *Echinococcus multilocularis* protoscoleces in micropore chambers. Int J Parasitol 21:383-386.

Alberts, B. 2000. Molecular biology of the cell. Garland Science.

Alvite, G., and A. Esteves. 2009. *Echinococcus granulosus* tropomyosin isoforms: from gene structure to expression analysis. Gene 433:40-49.

Aoki, Y., S. Nakamura, Y. Ishikawa, and M. Tanaka. 2009. Expression and syntenic analyses of four nanos genes in medaka. Zoolog Sci 26:112-118.

Archambault, V., and D. M. Glover. 2009. Polo-like kinases: conservation and divergence in their functions and regulation. Nat Rev Mol Cell Biol 10:265-275.

Ariz, M., R. Mainpal, and K. Subramaniam. 2009. *C. elegans* RNA-binding proteins PUF-8 and MEX-3 function redundantly to promote germline stem cell mitosis. Dev Biol 326:295-304.

Arsac, C., S. Walbaum, M. E. Sarciron, and A. F. Petavy. 1997. Histochemical observations of alkaline phosphatase activity of *Echinococcus multilocularis* during in vivo development in golden hamsters, an alternative definitive host. Exp Anim 46:25-30.

Attenborough, R. M., D. C. Hayward, M. V. Kitahara, D. J. Miller, and E. E. Ball. 2012. A "neural" enzyme in nonbilaterian animals and algae: preneural origins for peptidylglycine alpha-amidating monooxygenase. Mol Biol Evol 29:3095-3109.

Auladell, C., J. Garcia-Valero, and J. Baguña 1993. Ultrastructural localization of RNA in the chromatoid bodies of undifferentiated cells (neoblasts) in planarians by the RNase-gold complex technique. Journal of morphology 216:319-326.

Ax, P. 1996. Multicellular Animals - A New Approach to the Phylogenetic Order in Nature – Vol I, Springer Verlag, Berlin.

Baguna, J. 2012. The planarian neoblast: the rambling history of its origin and some current black boxes. Int J Dev Biol 56:19-37.

Baguñà, J., and M. Riutort. 2004. Molecular phylogeny of the Platyhelminthes. Canadian Journal of Zoology 82:168-193.

Baguñà, J., and R. Romero. 1981. Quantitative analysis of cell types during growth, degrowth and regeneration in the planarians *Dugesia (S) mediterranea* and *Dugesia (G) tigrina*. Hydrobiologia 84:181-194.

Baguñà, J., E. Saló, and C. Auladell. 1989. Regeneration and pattern formation in planarians. III. Evidence that neoblasts are totipotent stem cells and the source of blastema cells. Development 108:77-86.

Ballandras-Colas, A., H. Naraharisetty, X. Li, E. Serrao, and A. Engelman. 2013. Biochemical characterization of novel retroviral integrase proteins. PLoS One 8:e76638.

8. Bibliography

Barkauskas, C. E., M. J. Cronce, C. R. Rackley, E. J. Bowie, D. R. Keene, B. R. Stripp, S. H. Randell, P. W. Noble, and B. L. Hogan. 2013. Type 2 alveolar cells are stem cells in adult lung. J Clin Invest 123:3025-3036.

Barker, N., S. Bartfeld, and H. Clevers. 2010. Tissue-resident adult stem cell populations of rapidly self-renewing organs. Cell Stem Cell 7:656-670.

Barker, N., and H. Clevers. 2010. Leucine-rich repeat-containing G-protein-coupled receptors as markers of adult stem cells. Gastroenterology 138:1681-1696.

Barker, N., M. Huch, P. Kujala, M. van de Wetering, H. J. Snippert, J. H. van Es, T. Sato, D. E. Stange, H. Begthel, M. van den Born, E. Danenberg, S. van den Brink, J. Korving, A. Abo, P. J. Peters, N. Wright, R. Poulsom, and H. Clevers. 2010. Lgr5(+ve) stem cells drive self-renewal in the stomach and build long-lived gastric units in vitro. Cell Stem Cell 6:25-36.

Barker, N., J. H. van Es, J. Kuipers, P. Kujala, M. van den Born, M. Cozijnsen, A. Haegebarth, J. Korving, H. Begthel, P. J. Peters, and H. Clevers. 2007. Identification of stem cells in small intestine and colon by marker gene Lgr5. Nature 449:1003-1007.

Batut, P., A. Dobin, C. Plessy, P. Carninci, and T. R. Gingeras. 2013. High-fidelity promoter profiling reveals widespread alternative promoter usage and transposon-driven developmental gene expression. Genome Res 23:169-180.

Beard, T. C. 1973. The elimination of echinococcosis from Iceland. Bulletin of the World Health Organization 48:653.

Benovoy, D., and G. Drouin. 2009. Ectopic gene conversions in the human genome. Genomics 93:27-32.

Berriman, M., B. J. Haas, P. T. LoVerde, R. A. Wilson, G. P. Dillon, G. C. Cerqueira, S. T. Mashiyama, B. Al-Lazikani, L. F. Andrade, P. D. Ashton, M. A. Aslett, D. C. Bartholomeu, G. Blandin, C. R. Caffrey, A. Coghlan, R. Coulson, T. A. Day, A. Delcher, R. DeMarco, A. Djikeng, T. Eyre, J. A. Gamble, E. Ghedin, Y. Gu, C. Hertz-Fowler, H. Hirai, Y. Hirai, R. Houston, A. Ivens, D. A. Johnston, D. Lacerda, C. D. Macedo, P. McVeigh, Z. Ning, G. Oliveira, J. P. Overington, J. Parkhill, M. Pertea, R. J. Pierce, A. V. Protasio, M. A. Quail, M. A. Rajandream, J. Rogers, M. Sajid, S. L. Salzberg, M. Stanke, A. R. Tivey, O. White, D. L. Williams, J. Wortman, W. Wu, M. Zamanian, A. Zerlotini, C. M. Fraser-Liggett, B. G. Barrell, and N. M. El-Sayed. 2009. The genome of the blood fluke *Schistosoma mansoni*. Nature 460:352-358.

Bode, A., W. Salvenmoser, K. Nimeth, M. Mahlknecht, Z. Adamski, R. M. Rieger, R. Peter, and P. Ladurner. 2006. Immunogold-labeled S-phase neoblasts, total neoblast number, their distribution, and evidence for arrested neoblasts in *Macrostomum lignano* (Platyhelminthes, Rhabditophora). Cell Tissue Res 325:577-587.

Boeke, J. D., and J. P. Stoye. 1997. Retrotransposons, Endogenous Retroviruses, and the Evolution of Retroelements *in* J. M. Coffin, S. H. Hughes, and H. E. Varmus, eds. Retroviruses. Cold Spring Harbor Laboratory Press, Cold Spring Harbor (NY).

Bolla, R. I., and L. S. Roberts. 1971. Developmental physiology of cestodes. IX. Cytological characteristics of the germinative region of *Hymenolepis diminuta*. J Parasitol 57:267-277.

Bowen, N. J., and J. F. McDonald. 2001. Drosophila euchromatic LTR retrotransposons are much younger than the host species in which they reside. Genome Res 11:1527-1540.

8. Bibliography

Bowles, J., G. Schepers, and P. Koopman. 2000. Phylogeny of the SOX family of developmental transcription factors based on sequence and structural indicators. Dev Biol 227:239-255.

Bradbury, A. F., and D. G. Smyth. 1991. Peptide amidation. Trends Biochem Sci 16:112-115.

Brawley, C., and E. Matunis. 2004. Regeneration of male germline stem cells by spermatogonial dedifferentiation in vivo. Science 304:1331-1334.

Brehm, K. 2010a. The role of evolutionarily conserved signalling systems in *Echinococcus multilocularis* development and host-parasite interaction. Med Microbiol Immunol 199:247-259.

Brehm, K. 2010b. *Echinococcus multilocularis* as an experimental model in stem cell research and molecular host-parasite interaction. Parasitology 137:537-555.

Brehm, K., and M. Spiliotis. 2008a. Recent advances in the in vitro cultivation and genetic manipulation of *Echinococcus multilocularis* metacestodes and germinal cells. Exp Parasitol 119:506-515.

Brehm, K., and M. Spiliotis. 2008b. The influence of host hormones and cytokines on *Echinococcus multilocularis* signalling and development. Parasite 15:286-290.

Brehm, K., M. Wolf, H. Beland, A. Kroner, and M. Frosch. 2003. Analysis of differential gene expression in *Echinococcus multilocularis* larval stages by means of spliced leader differential display. Int J Parasitol 33:1145-1159.

Brennan, G. P., D. W. Halton, A. G. Maule, and C. Shaw. 1993. Electron immunogold labeling of regulatory peptide immunoreactivity in the nervous system of *Moniezia expansa* (Cestoda: Cyclophyllidea). Parasitol Res 79:409-415.

Brennand, K., D. Huangfu, and D. Melton. 2007. All beta cells contribute equally to islet growth and maintenance. PLoS Biol 5:e163.

Bresnick, E. H., K. R. Katsumura, H. Y. Lee, K. D. Johnson, and A. S. Perkins. 2012. Master regulatory GATA transcription factors: mechanistic principles and emerging links to hematologic malignancies. Nucleic Acids Res 40:5819-5831.

Brownlee, D. J., I. Fairweather, C. F. Johnston, and M. T. Rogan. 1994. Immunocytochemical localization of serotonin (5-HT) in the nervous system of the hydatid organism, *Echinococcus granulosus* (Cestoda, Cyclophyllidea). Parasitology 109 (Pt 2):233-241.

Brulet, P., P. Duprey, M. Vasseur, M. Kaghad, D. Morello, P. Blanchet, C. Babinet, H. Condamine, and F. Jacob. 1985. Molecular analysis of the first differentiations in the mouse embryo. Cold Spring Harb Symp Quant Biol 50:51-57.

Brunetti, E., P. Kern, and D. A. Vuitton. 2010. Expert consensus for the diagnosis and treatment of cystic and alveolar echinococcosis in humans. Acta Trop 114:1-16.

Brunmeir, R., S. Lagger, and C. Seiser. 2009. Histone deacetylase HDAC1/HDAC2-controlled embryonic development and cell differentiation. Int J Dev Biol 53:275-289.

Bryder, D., D. J. Rossi, and I. L. Weissman. 2006. Hematopoietic stem cells: the paradigmatic tissue-specific stem cell. Am J Pathol 169:338-346.

Buczacki, S. J., H. I. Zecchini, A. M. Nicholson, R. Russell, L. Vermeulen, R. Kemp, and D. J. Winton. 2013. Intestinal label-retaining cells are secretory precursors expressing Lgr5. Nature 495:65-69.

Cai, P., X. Piao, N. Hou, S. Liu, H. Wang, and Q. Chen. 2012. Identification and characterization of argonaute protein, Ago2 and its associated small RNAs in *Schistosoma japonicum*. PLoS Negl Trop Dis 6:e1745.

8. Bibliography

Cameron, H. A., T. G. Hazel, and R. D. McKay. 1998. Regulation of neurogenesis by growth factors and neurotransmitters. J Neurobiol 36:287-306.

Camicia, F., M. Herz, L. C. Prada, L. Kamenetzky, S. H. Simonetta, M. A. Cucher, J. I. Bianchi, C. Fernandez, K. Brehm, and M. C. Rosenzvit. 2013. The nervous and prenervous roles of serotonin in *Echinococcus* spp. Int J Parasitol 43:647-659.

Carmell, M. A., Z. Xuan, M. Q. Zhang, and G. J. Hannon. 2002. The Argonaute family: tentacles that reach into RNAi, developmental control, stem cell maintenance, and tumorigenesis. Genes Dev 16:2733-2742.

Carmon, K. S., X. Gong, Q. Lin, A. Thomas, and Q. Liu. 2011. R-spondins function as ligands of the orphan receptors LGR4 and LGR5 to regulate Wnt/beta-catenin signaling. Proc Natl Acad Sci U S A 108:11452-11457.

Clevers, H. 2006. Wnt/beta-catenin signaling in development and disease. Cell 127:469-480.

Cohen, C. J., W. M. Lock, and D. L. Mager. 2009. Endogenous retroviral LTRs as promoters for human genes: a critical assessment. Gene 448:105-114.

Cohn, L. 1899. Untersuchungen über das centrale Nervensystem der Cestoden. Zool. Jahrb. 12:89-160.

Collin, W. K. 1969. The cellular organization of hatched oncospheres of *Hymenolepis citelli* (Cestoda, Cyclophyllidea). J Parasitol 55:149-166.

Collins, J. J., 3rd, X. Hou, E. V. Romanova, B. G. Lambrus, C. M. Miller, A. Saberi, J. V. Sweedler, and P. A. Newmark. 2010. Genome-wide analyses reveal a role for peptide hormones in planarian germline development. PLoS Biol 8:e1000509.

Collins, J. J., 3rd, R. S. King, A. Cogswell, D. L. Williams, and P. A. Newmark. 2011. An atlas for *Schistosoma mansoni* organs and life-cycle stages using cell type-specific markers and confocal microscopy. PLoS Negl Trop Dis 5:e1009.

Collins, J. J., 3rd, B. Wang, B. G. Lambrus, M. E. Tharp, H. Iyer, and P. A. Newmark. 2013. Adult somatic stem cells in the human parasite *Schistosoma mansoni*. Nature 494:476-479.

Conzelmann, M., and G. Jekely. 2012. Antibodies against conserved amidated neuropeptide epitopes enrich the comparative neurobiology toolbox. Evodevo 3:23.

Coutelen, F., J. Biguet, J. M. Doby, and S. Deblock. 1952. Le systéme musculaire du scolex echinococcique. Mécanismes de dévagination et d´invagination du rostre et des ventouses. Ann Parasitol Hum Comp 27:86-104.

Coutu, D. L., and J. Galipeau. 2011. Roles of FGF signaling in stem cell self-renewal, senescence and aging. Aging (Albany NY) 3:920-933.

Cox, W. G., and V. L. Singer. 1999. A high-resolution, fluorescence-based method for localization of endogenous alkaline phosphatase activity. J Histochem Cytochem 47:1443-1456.

Craig, P. 2003. Echinococcus multilocularis. Curr Opin Infect Dis 16:437-444.

Crittenden, S. L., C. R. Eckmann, L. Wang, D. S. Bernstein, M. Wickens, and J. Kimble. 2003. Regulation of the mitosis/meiosis decision in the *Caenorhabditis elegans* germline. Philos Trans R Soc Lond B Biol Sci 358:1359-1362.

Crusz, H. 1947. The early development of the rostellum of *Cysticercus fasciolaris* Rud., and the chemical nature of its hooks. J Parasitol 33:87-98.

Cucher, M., G. Mourglia-Ettlin, L. Prada, H. Costa, L. Kamenetzky, C. Poncini, S. Dematteis, and M. C. Rosenzvit. 2013. *Echinococcus granulosus* pig strain (G7 genotype) protoscoleces did not develop secondary hydatid cysts in mice. Vet Parasitol 193:185-192.

8. Bibliography

Cunningham, L. J., and P. D. Olson. 2010. Description of *Hymenolepis microstoma* (Nottingham strain): a classical tapeworm model for research in the genomic era. Parasit Vectors 3:123.

Curtis, D., D. K. Treiber, F. Tao, P. D. Zamore, J. R. Williamson, and R. Lehmann. 1997. A CCHC metal-binding domain in Nanos is essential for translational regulation. Embo J 16:834-843.

Chen, J. M., D. N. Cooper, N. Chuzhanova, C. Ferec, and G. P. Patrinos. 2007. Gene conversion: mechanisms, evolution and human disease. Nat Rev Genet 8:762-775.

Chitnis, A. B., and J. Y. Kuwada. 1990. Axonogenesis in the brain of zebrafish embryos. J Neurosci 10:1892-1905.

D'Alessandro, A., and R. L. Rausch. 2008. New aspects of neotropical polycystic (*Echinococcus vogeli*) and unicystic (*Echinococcus oligarthrus*) echinococcosis. Clin Microbiol Rev 21:380-401, table of contents.

Daubert, E. A., and B. G. Condron. 2010. Serotonin: a regulator of neuronal morphology and circuitry. Trends Neurosci 33:424-434.

David, C. N. 1973. A Quantitative Method for Maceration of *Hydra* Tissue. Wilhelm Roux' Archiv 171:259-268.

de Lau, W., N. Barker, T. Y. Low, B. K. Koo, V. S. Li, H. Teunissen, P. Kujala, A. Haegebarth, P. J. Peters, M. van de Wetering, D. E. Stange, J. E. van Es, D. Guardavaccaro, R. B. Schasfoort, Y. Mohri, K. Nishimori, S. Mohammed, A. J. Heck, and H. Clevers. 2011. Lgr5 homologues associate with Wnt receptors and mediate R-spondin signalling. Nature 476:293-297.

De Mulder, K., G. Kuales, D. Pfister, B. Egger, T. Seppi, P. Eichberger, G. Borgonie, and P. Ladurner. 2010. Potential of *Macrostomum lignano* to recover from gamma-ray irradiation. Cell Tissue Res 339:527-542.

De Mulder, K., G. Kuales, D. Pfister, M. Willems, B. Egger, W. Salvenmoser, M. Thaler, A. K. Gorny, M. Hrouda, G. Borgonie, and P. Ladurner. 2009a. Characterization of the stem cell system of the acoel *Isodiametra pulchra*. BMC Dev Biol 9:69.

De Mulder, K., D. Pfister, G. Kuales, B. Egger, W. Salvenmoser, M. Willems, J. Steger, K. Fauster, R. Micura, G. Borgonie, and P. Ladurner. 2009b. Stem cells are differentially regulated during development, regeneration and homeostasis in flatworms. Dev Biol 334:198-212.

del Cacho, E., C. Causape, C. Sanchez-Acedo, and J. Quilez. 1996. Cytochemical study of the germinal membrane of the *Echinococcus granulosus* cyst. Vet Parasitol 62:101-106.

Desai, T. J., D. G. Brownfield, and M. A. Krasnow. 2014. Alveolar progenitor and stem cells in lung development, renewal and cancer. Nature 507:190-194.

Diaz, A., C. Casaravilla, F. Irigoin, G. Lin, J. O. Previato, and F. Ferreira. 2011. Understanding the laminated layer of larval *Echinococcus* I: structure. Trends Parasitol 27:204-213.

Dickinson, A. J., R. P. Croll, and E. E. Voronezhskaya. 2000. Development of embryonic cells containing serotonin, catecholamines, and FMRFamide-related peptides in *Aplysia californica*. Biological Bulletin 199:305-315.

Dirks, U., H. R. Gruber-Vodicka, B. Egger, and J. A. Ott. 2012a. Proliferation pattern during rostrum regeneration of the symbiotic flatworm *Paracatenula galateia*: a pulse-chase-pulse analysis. Cell Tissue Res 349:517-525.

8. Bibliography

Dirks, U., H. R. Gruber-Vodicka, N. Leisch, S. Bulgheresi, B. Egger, P. Ladurner, and J. A. Ott. 2012b. Bacterial symbiosis maintenance in the asexually reproducing and regenerating flatworm *Paracatenula galateia*. PLoS One 7:e34709.

Domen, J., A. Wagers, and I. L. Weissman. 2006. Bone marrow (hematopoietic) stem cells. Pp. 13. Regenerative medicine. Stem Cell Information from the National Institutes of Health Resource for Stem Cell Research. United States

Dominguez, M. F., U. Koziol, V. Porro, A. Costabile, S. Estrade, J. Tort, M. Bollati-Fogolin, and E. Castillo. 2014. A new approach for the characterization of proliferative cells in cestodes. Exp Parasitol 138:25-29.

Dor, Y., J. Brown, O. I. Martinez, and D. A. Melton. 2004. Adult pancreatic beta-cells are formed by self-duplication rather than stem-cell differentiation. Nature 429:41-46.

Dorrell, C., L. Erker, J. Schug, J. L. Kopp, P. S. Canaday, A. J. Fox, O. Smirnova, A. W. Duncan, M. J. Finegold, M. Sander, K. H. Kaestner, and M. Grompe. 2011. Prospective isolation of a bipotential clonogenic liver progenitor cell in adult mice. Genes Dev 25:1193-1203.

Dos Santos, L. V., M. V. de Queiroz, M. F. Santana, M. A. Soares, E. G. de Barros, E. F. de Araujo, and T. Langin. 2012. Development of new molecular markers for the *Colletotrichum* genus using RetroCl1 sequences. World J Microbiol Biotechnol 28:1087-1095.

Douglas, L. T. 1961. The development of organ systems in nematotaeniid cestodes. I. Early histogenesis and formation of reproductive structures in *Baerietta diana* (Helfer. 1948). J Parasitol 47:669-680.

Doupe, D. P., and P. H. Jones. 2013. Cycling progenitors maintain epithelia while diverse cell types contribute to repair. Bioessays 35:443-451.

Dupressoir, A., and T. Heidmann. 1996. Germ line-specific expression of intracisternal A-particle retrotransposons in transgenic mice. Mol Cell Biol 16:4495-4503.

Dykstra, B., D. Kent, M. Bowie, L. McCaffrey, M. Hamilton, K. Lyons, S. J. Lee, R. Brinkman, and C. Eaves. 2007. Long-term propagation of distinct hematopoietic differentiation programs in vivo. Cell Stem Cell 1:218-229.

Eckert, J., and P. Deplazes. 2004. Biological, epidemiological, and clinical aspects of echinococcosis, a zoonosis of increasing concern. Clin Microbiol Rev 17:107-135.

Eckert, J., R. C. Thompson, and H. Mehlhorn. 1983. Proliferation and metastases formation of larval *Echinococcus multilocularis*. I. Animal model, macroscopical and histological findings. Z Parasitenkd 69:737-748.

Egger, B., R. Gschwentner, and R. Rieger. 2007. Free-living flatworms under the knife: past and present. Dev Genes Evol 217:89-104.

Eisenhoffer, G. T., H. Kang, and A. Sanchez Alvarado. 2008. Molecular analysis of stem cells and their descendants during cell turnover and regeneration in the planarian *Schmidtea mediterranea*. Cell Stem Cell 3:327-339.

Evsikov, A. V., W. N. de Vries, A. E. Peaston, E. E. Radford, K. S. Fancher, F. H. Chen, J. A. Blake, C. J. Bult, K. E. Latham, D. Solter, and B. B. Knowles. 2004. Systems biology of the 2-cell mouse embryo. Cytogenet Genome Res 105:240-250.

Ewen-Campen, B., E. E. Schwager, and C. G. Extavour. 2010. The molecular machinery of germ line specification. Mol Reprod Dev 77:3-18.

Extavour, C. G., and M. Akam. 2003. Mechanisms of germ cell specification across the metazoans: epigenesis and preformation. Development 130:5869-5884.

8. Bibliography

Fairley, N. H., and R. J. Wright-Smith. 1929. Hydatid infestation (*Echinococcus granulosus*) in sheep, oxen and pigs, with special reference to daughter cyst formation. The Journal of Pathology and Bacteriology 32:309-335.

Fairweather, I., A. E. A. Campbell, P. J. Skuce, C. F. Johnston, and C. Shaw. 1991. Development of the peptidergic nervous system during ontogeny of the cysticercus larva of the tapeworm *Taenia crassiceps*. Regulatory Peptides 35:235.

Fairweather, I., G. A. Macartney, C. F. Johnston, D. W. Halton, and K. D. Buchnan. 1988. Immunocytochemical demonstration of 5-hydroxytryptamine (serotonin) and vertebrate neuropeptides in the nervous system of excysted cysticercoid larvae of the rat tapeworm, *Hymenolepis diminuta* (Cestoda, Cyclophyllidea). Parasitol Res 74:371-379.

Fairweather, I., M. T. McMullan, C. F. Johnston, M. T. Rogan, and R. E. Hanna. 1994. Serotoninergic and peptidergic nerve elements in the protoscolex of *Echinococcus granulosus* (Cestoda, Cyclophyllidea). Parasitol Res 80:649-656.

Farber, E., and R. Baserga. 1969. Differential effects of hydroxyurea on survival of proliferating cells in vivo. Cancer Res 29:136-139.

Faulkner, G. J., Y. Kimura, C. O. Daub, S. Wani, C. Plessy, K. M. Irvine, K. Schroder, N. Cloonan, A. L. Steptoe, T. Lassmann, K. Waki, N. Hornig, T. Arakawa, H. Takahashi, J. Kawai, A. R. Forrest, H. Suzuki, Y. Hayashizaki, D. A. Hume, V. Orlando, S. M. Grimmond, and P. Carninci. 2009. The regulated retrotransposon transcriptome of mammalian cells. Nat Genet 41:563-571.

Fausto, N., and J. S. Campbell. 2003. The role of hepatocytes and oval cells in liver regeneration and repopulation. Mech Dev 120:117-130.

Feschotte, C., N. Jiang, and S. R. Wessler. 2002. Plant transposable elements: where genetics meets genomics. Nat Rev Genet 3:329-341.

Förster, S. 2012. Nuclear Hormone Receptors and Fibroblast Growth Factor Receptor Signaling in *Echinococcus multilocularis*. University of Würzburg, Würzburg.

Fort, A., K. Hashimoto, D. Yamada, M. Salimullah, C. A. Keya, A. Saxena, A. Bonetti, I. Voineagu, N. Bertin, A. Kratz, Y. Noro, C. H. Wong, M. de Hoon, R. Andersson, A. Sandelin, H. Suzuki, C. L. Wei, H. Koseki, Y. Hasegawa, A. R. Forrest, and P. Carninci. 2014. Deep transcriptome profiling of mammalian stem cells supports a regulatory role for retrotransposons in pluripotency maintenance. Nat Genet 46:558-566.

Franchini, A. 2005. The distribution of cells containing FMRFamide- and 5-HT-related molecules in the embryonic development of *Viviparus ater* (Mollusca, Gastropoda). Eur J Histochem 49:301-308.

Freeman, R. S. 1973. Ontogeny of cestodes and its bearing on their phylogeny and systematics. Adv Parasitol 11:481-557.

Friedl, A. A., M. Kiechle, H. G. Maxeiner, R. H. Schiestl, and F. Eckardt-Schupp. 2010. Ty1 integrase overexpression leads to integration of non-Ty1 DNA fragments into the genome of *Saccharomyces cerevisiae*. Mol Genet Genomics 284:231-242.

Frooninckx, L., L. Van Rompay, L. Temmerman, E. Van Sinay, I. Beets, T. Janssen, S. J. Husson, and L. Schoofs. 2012. Neuropeptide GPCRs in *C. elegans*. Front Endocrinol (Lausanne) 3:167.

Gafni, O., L. Weinberger, A. A. Mansour, Y. S. Manor, E. Chomsky, D. Ben-Yosef, Y. Kalma, S. Viukov, I. Maza, A. Zviran, Y. Rais, Z. Shipony, Z. Mukamel, V. Krupalnik, M. Zerbib, S. Geula, I. Caspi, D. Schneir, T. Shwartz, S. Gilad, D.

Amann-Zalcenstein, S. Benjamin, I. Amit, A. Tanay, R. Massarwa, N. Novershtern, and J. H. Hanna. 2013. Derivation of novel human ground state naive pluripotent stem cells. Nature 504:282-286.

Galindo, M., R. Paredes, C. Marchant, V. Mino, and N. Galanti. 2003. Regionalization of DNA and protein synthesis in developing stages of the parasitic platyhelminth *Echinococcus granulosus*. J Cell Biochem 90:294-303.

Galindo, M., G. Schadebrodt, and N. Galanti. 2008. *Echinococcus granulosus*: cellular territories and morphological regions in mature protoscoleces. Exp Parasitol 119:524-533.

Gelmedin, V. 2008. Targeting flatworm signaling cascades for the development of novel anthelmintic drugs. University of Würzburg, Würzburg.

Gelmedin, V., R. Caballero-Gamiz, and K. Brehm. 2008. Characterization and inhibition of a p38-like mitogen-activated protein kinase (MAPK) from *Echinococcus multilocularis*: antiparasitic activities of p38 MAPK inhibitors. Biochem Pharmacol 76:1068-1081.

Gelmedin, V., M. Spiliotis, and K. Brehm. 2010. Molecular characterisation of MEK1/2- and MKK3/6-like mitogen-activated protein kinase kinases (MAPKK) from the fox tapeworm *Echinococcus multilocularis*. Int J Parasitol 40:555-567.

Gilbert, S. F. 2006. Developmental Biology, 8th edition. Sinauer Sunderland, Massachusetts.

Gillooly, J. F., A. P. Allen, G. B. West, and J. H. Brown. 2005. The rate of DNA evolution: effects of body size and temperature on the molecular clock. Proc Natl Acad Sci U S A 102:140-145.

Glinka, A., C. Dolde, N. Kirsch, Y. L. Huang, O. Kazanskaya, D. Ingelfinger, M. Boutros, C. M. Cruciat, and C. Niehrs. 2011. LGR4 and LGR5 are R-spondin receptors mediating Wnt/beta-catenin and Wnt/PCP signalling. EMBO Rep 12:1055-1061.

Goldschmidt, R. 1900. Zur Entwicklungsgeschichte der Echinococcusköpfchen. Zool. Jahrb. 13.

Greenspan, P., E. P. Mayer, and S. D. Fowler. 1985. Nile red: a selective fluorescent stain for intracellular lipid droplets. J Cell Biol 100:965-973.

Guo, T., A. H. Peters, and P. A. Newmark. 2006. A Bruno-like gene is required for stem cell maintenance in planarians. Dev Cell 11:159-169.

Gustafsson, M. K. 1976a. Observations on the histogenesis of nervous tissue in *Diphyllobothrium dendriticum* Nitzsch, 1824 (Cestoda, Pseudophyllidea). Z Parasitenkd 50:313-321.

Gustafsson, M. K. 1976b. Studies on cytodifferentiation in the neck region of *Diphyllobothrium dendriticum* Nitzsch, 1824 (Cestoda, Pseudophyllidea). Z Parasitenkd 50:323-329.

Gustafsson, M. K. 1992. The neuroanatomy of parasitic flatworms. Adv Neuroimmunol. 2:267-286.

Gustafsson, M. K. S. 1976c. Basic cell types in *Echinococcus granulosus* (Cestoda, Cyclophyllidea). Acta Zool. Fenn. 146:1-16.

Gustafsson, M. K. S. 1990. The cells of a cestode. *Diphyllobothrium dendriticum* as a model in cell biology. Acta Acad Abo Ser B 50:13-44.

Haag, K. L., P. B. Marin, D. A. Graichen, and M. L. De La Rue. 2011. Reappraising the theme of breeding systems in *Echinococcus*: is outcrossing a rare phenomenon? Parasitology 138:298-302.

8. Bibliography

Halton, D. W., and M. K. S. Gustafsson. 1996. Functional morphology of the Platyhelminth Nervous System. Parasitology 113:547-572.

Halton, D. W., and A. G. Maule. 2003. Flatworm nerve–muscle: structural and functional analysis. Can J Zool 82:316-333.

Hall, T. A. 1999. BioEdit: a user-friendly biological sequence alignment editor and analysis program for Windows 95/98/NT. Pp. 95-98. Nucleic acids symposium series.

Handberg-Thorsager, M., and E. Salo. 2007. The planarian nanos-like gene Smednos is expressed in germline and eye precursor cells during development and regeneration. Dev Genes Evol 217:403-411.

Hanna, J. H., K. Saha, and R. Jaenisch. 2010. Pluripotency and cellular reprogramming: facts, hypotheses, unresolved issues. Cell 143:508-525.

Haraguchi, S., M. Tsuda, S. Kitajima, Y. Sasaoka, A. Nomura-Kitabayashid, K. Kurokawa, and Y. Saga. 2003. nanos1: a mouse nanos gene expressed in the central nervous system is dispensable for normal development. Mech Dev 120:721-731.

Hartenstein, V., and M. Jones. 2003. The embryonic development of the bodywall and nervous system of the cestode flatworm *Hymenolepis diminuta*. Cell Tissue Res 311:427-435.

Harzsch, S., and C. H. Muller. 2007. A new look at the ventral nerve centre of *Sagitta*: implications for the phylogenetic position of Chaetognatha (arrow worms) and the evolution of the bilaterian nervous system. Front Zool 4:14.

Hastings, K. E. 2005. SL trans-splicing: easy come or easy go? Trends Genet 21:240-247.

Havecker, E. R., X. Gao, and D. F. Voytas. 2004. The diversity of LTR retrotransposons. Genome Biol 5:225.

Hay, E. D., and S. J. Coward. 1975. Fine structure studies on the planarian, *Dugesia*. I. Nature of the "neoblast" and other cell types in noninjured worms. J Ultrastruct Res 50:1-21.

Hayashi, T., M. Asami, S. Higuchi, N. Shibata, and K. Agata. 2006. Isolation of planarian X-ray-sensitive stem cells by fluorescence-activated cell sorting. Dev Growth Differ 48:371-380.

Heeney, M. M., M. R. Whorton, T. A. Howard, C. A. Johnson, and R. E. Ware. 2004. Chemical and functional analysis of hydroxyurea oral solutions. J Pediatr Hematol Oncol 26:179-184.

Hemer, S., C. Konrad, M. Spiliotis, U. Koziol, D. Schaack, S. Forster, V. Gelmedin, B. Stadelmann, T. Dandekar, A. Hemphill, and K. Brehm. 2014. Host insulin stimulates *Echinococcus multilocularis* insulin signalling pathways and larval development. BMC Biol 12:5.

Henderson, D. J., and R. E. Hanna. 1988. *Hymenolepis nana* (Cestoda:Cyclophyllidea): DNA, RNA and protein synthesis in 5-day-old juveniles. Int J Parasitol 18:963-972.

Hendzel, M. J., Y. Wei, M. A. Mancini, A. Van Hooser, T. Ranalli, B. R. Brinkley, D. P. Bazett-Jones, and C. D. Allis. 1997. Mitosis-specific phosphorylation of histone H3 initiates primarily within pericentromeric heterochromatin during G2 and spreads in an ordered fashion coincident with mitotic chromosome condensation. Chromosoma 106:348-360.

8. Bibliography

Higuchi, S., T. Hayashi, I. Hori, N. Shibata, H. Sakamoto, and K. Agata. 2007. Characterization and categorization of fluorescence activated cell sorted planarian stem cells by ultrastructural analysis. Dev Growth Differ 49:571-581.

Hindmarsh, P., and J. Leis. 1999. Retroviral DNA integration. Microbiol Mol Biol Rev 63:836-843, table of contents.

Hoberg, E. P. 2006. Phylogeny of *Taenia*: Species definitions and origins of human parasites. Parasitol Int 55 Suppl:S23-30.

Hoberg, E. P., A. Jones, R. L. Rausch, K. S. Eom, and S. L. Gardner. 2000. A phylogenetic hypothesis for species of the genus *Taenia* (Eucestoda : Taeniidae). J Parasitol 86:89-98.

Hock, J., and G. Meister. 2008. The Argonaute protein family. Genome Biol 9:210.

Hoffman, M. M., and E. Birney. 2007. Estimating the neutral rate of nucleotide substitution using introns. Mol Biol Evol 24:522-531.

Hopman, A. H., F. C. Ramaekers, and E. J. Speel. 1998. Rapid synthesis of biotin-, digoxigenin-, trinitrophenyl-, and fluorochrome-labeled tyramides and their application for In situ hybridization using CARD amplification. J Histochem Cytochem 46:771-777.

Hoyer, D., and T. Bartfai. 2012. Neuropeptides and neuropeptide receptors: drug targets, and peptide and non-peptide ligands: a tribute to Prof. Dieter Seebach. Chem Biodivers 9:2367-2387.

Huch, M., S. F. Boj, and H. Clevers. 2013. Lgr5(+) liver stem cells, hepatic organoids and regenerative medicine. Regen Med 8:385-387.

Hyman, L. H. 1951. The Invertebrates: Platyhelminthes and Rhynchocoela The Acoelomate Bilateria. Volume II McGraw-Hill.

Inoue, C., S. K. Bae, K. Takatsuka, T. Inoue, Y. Bessho, and R. Kageyama. 2001. Math6, a bHLH gene expressed in the developing nervous system, regulates neuronal versus glial differentiation. Genes Cells 6:977-986.

Jabbar, A., S. Crawford, D. Mlocicki, Z. P. Swiderski, D. B. Conn, M. K. Jones, I. Beveridge, and M. W. Lightowlers. 2010. Ultrastructural reconstruction of *Taenia ovis* oncospheres from serial sections. Int J Parasitol.

Jaeger, S., S. Barends, R. Giege, G. Eriani, and F. Martin. 2005. Expression of metazoan replication-dependent histone genes. Biochimie 87:827-834.

Jaisser, F. 2000. Inducible gene expression and gene modification in transgenic mice. J Am Soc Nephrol 11 Suppl 16:S95-S100.

Jaruzelska, J., M. Kotecki, K. Kusz, A. Spik, M. Firpo, and R. A. Reijo Pera. 2003. Conservation of a Pumilio-Nanos complex from *Drosophila* germ plasm to human germ cells. Dev Genes Evol 213:120-126.

Jellies, J., D. M. Kopp, K. M. Johansen, and J. Johansen. 1996. Initial Formation and Secondary Condensation of Nerve Pathways in the Medicinal Leech. J Comp Neurol 373:1-10.

Jiang, N., I. K. Jordan, and S. R. Wessler. 2002. Dasheng and RIRE2. A nonautonomous long terminal repeat element and its putative autonomous partner in the rice genome. Plant Physiol 130:1697-1705.

Jones, S. 2004. An overview of the basic helix-loop-helix proteins. Genome Biol 5:226.

Juliano, C., J. Wang, and H. Lin. 2011. Uniting germline and stem cells: the function of Piwi proteins and the piRNA pathway in diverse organisms. Annu Rev Genet 45:447-469.

Juliano, C. E., S. Z. Swartz, and G. M. Wessel. 2010. A conserved germline multipotency program. Development 137:4113-4126.

8. Bibliography

Jura, H., A. Bader, M. Hartmann, H. Maschek, and M. Frosch. 1996. Hepatic tissue culture model for study of host-parasite interactions in alveolar echinococcosis. Infect Immun 64:3484-3490.

Kadyrova, L. Y., Y. Habara, T. H. Lee, and R. P. Wharton. 2007. Translational control of maternal Cyclin B mRNA by Nanos in the *Drosophila* germline. Development 134:1519-1527.

Kalendar, R., J. Tanskanen, W. Chang, K. Antonius, H. Sela, O. Peleg, and A. H. Schulman. 2008. Cassandra retrotransposons carry independently transcribed 5S RNA. Proc Natl Acad Sci U S A 105:5833-5838.

Kamachi, Y., and H. Kondoh. 2013. Sox proteins: regulators of cell fate specification and differentiation. Development 140:4129-4144.

Kanska, J., and U. Frank. 2013. New roles for Nanos in neural cell fate determination revealed by studies in a cnidarian. J Cell Sci 126:3192-3203.

Karnovsky, M. J., and L. Roots. 1964. A "Direct-Coloring" Thiocholine Method for Cholinesterases. J Histochem Cytochem 12:219-221.

Kass, D. H., M. A. Batzer, and P. L. Deininger. 1995. Gene conversion as a secondary mechanism of short interspersed element (SINE) evolution. Mol Cell Biol 15:19-25.

Kelley, D., and J. Rinn. 2012. Transposable elements reveal a stem cell-specific class of long noncoding RNAs. Genome Biol 13:R107.

Kidwell, M. G., and D. R. Lisch. 2001. Perspective: transposable elements, parasitic DNA, and genome evolution. Evolution 55:1-24.

Kijima, T. E., and H. Innan. 2010. On the estimation of the insertion time of LTR retrotransposable elements. Mol Biol Evol 27:896-904.

Kim, Y., S. Bark, V. Hook, and N. Bandeira. 2011. NeuroPedia: neuropeptide database and spectral library. Bioinformatics 27:2772-2773.

Klaver, B., and B. Berkhout. 1994. Comparison of 5' and 3' long terminal repeat promoter function in human immunodeficiency virus. J Virol 68:3830-3840.

Klein, A. M., and B. D. Simons. 2011. Universal patterns of stem cell fate in cycling adult tissues. Development 138:3103-3111.

Knapp, J., M. Nakao, T. Yanagida, M. Okamoto, U. Saarma, A. Lavikainen, and A. Ito. 2011. Phylogenetic relationships within *Echinococcus* and *Taenia* tapeworms (Cestoda: Taeniidae): an inference from nuclear protein-coding genes. Mol Phylogenet Evol 61:628-638.

Koch, U., R. Lehal, and F. Radtke. 2013. Stem cells living with a Notch. Development 140:689-704.

Konrad, C., A. Kroner, M. Spiliotis, R. Zavala-Gongora, and K. Brehm. 2003. Identification and molecular characterisation of a gene encoding a member of the insulin receptor family in *Echinococcus multilocularis*. Int J Parasitol 33:301-312.

Kornienko, A. E., P. M. Guenzl, D. P. Barlow, and F. M. Pauler. 2013. Gene regulation by the act of long non-coding RNA transcription. BMC Biol 11:59.

Koziol, U., and E. Castillo. 2011. Cell proliferation and differentiation in cestodes. Pp. 121-138 *in* A. Esteves, ed. Research in Helminths. Transworld Research Network, Kervala, India.

Koziol, U., A. Costabile, M. F. Dominguez, A. Iriarte, G. Alvite, A. Kun, and E. Castillo. 2011. Developmental expression of high molecular weight tropomyosin isoforms in *Mesocestoides corti*. Mol Biochem Parasitol 175:181-191.

Koziol, U., M. F. Dominguez, M. Marin, A. Kun, and E. Castillo. 2010. Stem cell proliferation during in vitro development of the model cestode *Mesocestoides corti* from larva to adult worm. Front Zool 7:22

Koziol, U., A. Iriarte, E. Castillo, J. Soto, G. Bello, A. Cajarville, L. Roche, and M. Marin. 2009. Characterization of a putative hsp70 pseudogene transcribed in protoscoleces and adult worms of *Echinococcus granulosus*. Gene 443:1-11.

Koziol, U., G. Krohne, and K. Brehm. 2013. Anatomy and development of the larval nervous system in *Echinococcus multilocularis*. Front Zool 10:24.

Koziol, U., M. Marin, and E. Castillo. 2008. Pumilio genes from the Platyhelminthes. Dev Genes Evol 218:47-53.

Koziol, U., T. Rauschendorfer, L. Zanon Rodriguez, G. Krohne, and K. Brehm. 2014. The unique stem cell system of the immortal larva of the human parasite *Echinococcus multilocularis*. Evodevo 5:10.

Krakoff, I. H., N. C. Brown, and P. Reichard. 1968. Inhibition of ribonucleoside diphosphate reductase by hydroxyurea. Cancer Res 28:1559-1565.

Kultz, D. 1998. Phylogenetic and functional classification of mitogen- and stress-activated protein kinases. J Mol Evol 46:571-588.

Labbe, R. M., M. Irimia, K. W. Currie, A. Lin, S. J. Zhu, D. D. Brown, E. J. Ross, V. Voisin, G. D. Bader, B. J. Blencowe, and B. J. Pearson. 2012. A comparative transcriptomic analysis reveals conserved features of stem cell pluripotency in planarians and mammals. Stem Cells 30:1734-1745.

Ladurner, P., R. Rieger, and J. Baguna. 2000. Spatial distribution and differentiation potential of stem cells in hatchlings and adults in the marine platyhelminth *Macrostomum* sp.: a bromodeoxyuridine analysis. Dev Biol 226:231-241.

Lance-Jones, C. C., and C. F. Lagenaur. 1987. A new marker for identifying quail cells in embryonic avian chimeras: a quail-specific antiserum. J Histochem Cytochem 35:771-780.

Lander, A. D. 2011. The individuality of stem cells. BMC Biol 9:40.

Lander, A. D., J. Kimble, H. Clevers, E. Fuchs, D. Montarras, M. Buckingham, A. L. Calof, A. Trumpp, and T. Oskarsson. 2012. What does the concept of the stem cell niche really mean today? BMC Biol 10:19.

Lander, E. S., L. M. Linton, B. Birren, C. Nusbaum, M. C. Zody, J. Baldwin, K. Devon, K. Dewar, M. Doyle, W. FitzHugh, R. Funke, D. Gage, K. Harris, A. Heaford, J. Howland, L. Kann, J. Lehoczky, R. LeVine, P. McEwan, K. McKernan, J. Meldrim. J. P. Mesirov. C. Miranda, W. Morris, J. Naylor, C. Raymond, M. Rosetti, R. Santos, A. Sheridan, C. Sougnez, N. Stange-Thomann, N. Stojanovic, A. Subramanian, D. Wyman, J. Rogers, J. Sulston, R. Ainscough, S. Beck, D. Bentley, J. Burton, C. Clee, N. Carter, A. Coulson, R. Deadman, P. Deloukas, A. Dunham, I. Dunham, R. Durbin, L. French, D. Grafham, S. Gregory, T. Hubbard, S. Humphray, A. Hunt, M. Jones, C. Lloyd, A. McMurray, L. Matthews, S. Mercer, S. Milne, J. C. Mullikin, A. Mungall, R. Plumb, M. Ross, R. Shownkeen, S. Sims, R. H. Waterston, R. K. Wilson, L. W. Hillier, J. D. McPherson, M. A. Marra, E. R. Mardis, L. A. Fulton, A. T. Chinwalla, K. H. Pepin, W. R. Gish, S. L. Chissoe, M. C. Wendl, K. D. Delehaunty, T. L. Miner, A. Delehaunty, J. B. Kramer, L. L. Cook, R. S. Fulton, D. L. Johnson, P. J. Minx, S. W. Clifton, T. Hawkins, E. Branscomb, P. Predki, P. Richardson, S. Wenning, T. Slezak, N. Doggett, J. F. Cheng, A. Olsen, S. Lucas, C. Elkin, E. Uberbacher, M. Frazier, R. A. Gibbs, D. M. Muzny, S. E. Scherer, J. B. Bouck, E. J. Sodergren, K. C. Worley, C. M. Rives, J. H. Gorrell, M. L. Metzker, S. L.

Naylor, R. S. Kucherlapati, D. L. Nelson, G. M. Weinstock, Y. Sakaki, A. Fujiyama, M. Hattori, T. Yada, A. Toyoda, T. Itoh, C. Kawagoe, H. Watanabe, Y. Totoki, T. Taylor, J. Weissenbach, R. Heilig, W. Saurin, F. Artiguenave, P. Brottier, T. Bruls, E. Pelletier, C. Robert, P. Wincker, D. R. Smith, L. Doucette-Stamm, M. Rubenfield, K. Weinstock, H. M. Lee, J. Dubois, A. Rosenthal, M. Platzer, G. Nyakatura, S. Taudien, A. Rump, H. Yang, J. Yu, J. Wang, G. Huang, J. Gu, L. Hood, L. Rowen, A. Madan, S. Qin, R. W. Davis, N. A. Federspiel, A. P. Abola, M. J. Proctor, R. M. Myers, J. Schmutz, M. Dickson, J. Grimwood, D. R. Cox, M. V. Olson, R. Kaul, C. Raymond, N. Shimizu, K. Kawasaki, S. Minoshima, G. A. Evans, M. Athanasiou, R. Schultz, B. A. Roe, F. Chen, H. Pan, J. Ramser, H. Lehrach, R. Reinhardt, W. R. McCombie, M. de la Bastide, N. Dedhia, H. Blocker, K. Hornischer, G. Nordsiek, R. Agarwala, L. Aravind, J. A. Bailey, A. Bateman, S. Batzoglou, E. Birney, P. Bork, D. G. Brown, C. B. Burge, L. Cerutti, H. C. Chen, D. Church, M. Clamp, R. R. Copley, T. Doerks, S. R. Eddy, E. E. Eichler, T. S. Furey, J. Galagan, J. G. Gilbert, C. Harmon, Y. Hayashizaki, D. Haussler, H. Hermjakob, K. Hokamp, W. Jang, L. S. Johnson, T. A. Jones, S. Kasif, A. Kaspryzk, S. Kennedy, W. J. Kent, P. Kitts, E. V. Koonin, I. Korf, D. Kulp, D. Lancet, T. M. Lowe, A. McLysaght, T. Mikkelsen, J. V. Moran, N. Mulder, V. J. Pollara, C. P. Ponting, G. Schuler, J. Schultz, G. Slater, A. F. Smit, E. Stupka, J. Szustakowski, D. Thierry-Mieg, J. Thierry-Mieg, L. Wagner, J. Wallis, R. Wheeler, A. Williams, Y. I. Wolf, K. H. Wolfe, S. P. Yang, R. F. Yeh, F. Collins, M. S. Guyer, J. Peterson, A. Felsenfeld, K. A. Wetterstrand, A. Patrinos, M. J. Morgan, P. de Jong, J. J. Catanese, K. Osoegawa, H. Shizuya, S. Choi, and Y. J. Chen. 2001. Initial sequencing and analysis of the human genome. Nature 409:860-921.

Lanner, F., and J. Rossant. 2010. The role of FGF/Erk signaling in pluripotent cells. Development 137:3351-3360.

Lascano, E. F., E. A. Coltorti, and V. M. Varela-Diaz. 1975. Fine structure of the germinal membrane of *Echinococcus granulosus* cysts. J Parasitol 61:853-860.

Lasko, P. 2013. The DEAD-box helicase Vasa: evidence for a multiplicity of functions in RNA processes and developmental biology. Biochim Biophys Acta 1829:810-816.

Lavikainen, A., V. Haukisalmi, M. J. Lehtinen, H. Henttonen, A. Oksanen, and S. Meri. 2008. A phylogeny of members of the family Taeniidae based on the mitochondrial cox1 and nad1 gene data. Parasitology 135:1457-1467.

Le Douarin, N. M., and M. A. Teillet. 1974. Experimental analysis of the migration and differentiation of neuroblasts of the autonomic nervous system and of neurectodermal mesenchymal derivatives, using a biological cell marking technique. Dev Biol 41:162-184.

Leducq, R., and C. Gabrion. 1992. Developmental changes of *Echinococcus multilocularis* metacestodes revealed by tegumental ultrastructure and lectin-binding sites. Parasitology 104 Pt 1:129-141.

Lenhard, B., A. Sandelin, and P. Carninci. 2012. Metazoan promoters: emerging characteristics and insights into transcriptional regulation. Nat Rev Genet 13:233-245.

Li, C., and K. Kim. 2008. Neuropeptides. WormBook:1-36.

Li, L., and H. Clevers. 2010. Coexistence of quiescent and active adult stem cells in mammals. Science 327:542-545.

8. Bibliography

Lo Celso, C., and D. T. Scadden. 2011. The haematopoietic stem cell niche at a glance. J Cell Sci 124:3529-3535.

Loehr, K. A., and R. W. Mead. 1979. A Maceration Technique for the Study of Cytological Development in *Hymenolepis citelli*. J Parasitol 65:886-889.

Loos-Frank, B. 2000. An up-date of Verster's (1969) 'Taxonomic revision of the genus *Taenia* Linnaeus' (Cestoda) in table format. Syst Parasitol 45:155-183.

Losick, V. P., L. X. Morris, D. T. Fox, and A. Spradling. 2011. *Drosophila* stem cell niches: a decade of discovery suggests a unified view of stem cell regulation. Dev Cell 21:159-171.

Lowe, T. M. and S. R. Eddy. 1997. tRNAscan-SE: A Program for Improved Detection of Transfer RNA Genes in Genomic Sequence. Nucl Acids Res 25:955-964

MacDonald, J. L., and A. J. Roskams. 2008. Histone deacetylases 1 and 2 are expressed at distinct stages of neuro-glial development. Dev Dyn 237:2256-2267.

Macfarlan, T. S., W. D. Gifford, S. Driscoll, K. Lettieri, H. M. Rowe, D. Bonanomi, A. Firth, O. Singer, D. Trono, and S. L. Pfaff. 2012. Embryonic stem cell potency fluctuates with endogenous retrovirus activity. Nature 487:57-63.

Mak, J., and L. Kleiman. 1997. Primer tRNAs for reverse transcription. J Virol 71:8087-8095.

Mankau, S. K. 1956. Studies on *Echinococcus alveolaris* (Klemm, 1883), from St. Lawrence Island, Alaska. III. The histopathology caused by the infection of *E. alveolaris* in white mice. Am J Trop Med Hyg 5:872-880.

Marin, M., B. Garat, U. Pettersson, and R. Ehrlich. 1993. Isolation and characterization of a middle repetitive DNA element from *Echinococcus granulosus*. Mol Biochem Parasitol 59:335-338.

Marks, N. J., and A. G. Maule. 2010. Neuropeptides in helminths: occurrence and distribution. Adv Exp Med Biol 692:49-77.

Martin-Duran, J. M., and B. Egger. 2013. Developmental diversity in free-living flatworms. Evodevo 3:7.

Maule, A. G., N. J. Marks, and T. A. Day. 2006. Signalling Molecules and Nerve–Muscle Function *in* A. G. Maule, and N. J. Marks, eds. Parasitic Flatworms. Molecular Biology, Biochemistry, Immunology and Physiology. CABI Publishing, Oxfordshire.

McVeigh, P., G. R. Mair, L. Atkinson, P. Ladurner, M. Zamanian, E. Novozhilova, N. J. Marks, T. A. Day, and A. G. Maule. 2009. Discovery of multiple neuropeptide families in the phylum Platyhelminthes. Int J Parasitol 39:1243-1252.

McVeigh, P., G. R. Mair, E. Novozhilova, A. Day, M. Zamanian, N. J. Marks, M. J. Kimber, T. A. Day, and A. G. Maule. 2011. Schistosome I/Lamides--a new family of bioactive helminth neuropeptides. Int J Parasitol 41:905-913.

Mead, R. W. 1982. Changes in germinative cell frequencies in the germinative region of *Hymenolepis diminuta* during development. J Parasitol 68:95-99.

Mehlhorn, H., J. Eckert, and R. C. Thompson. 1983. Proliferation and metastases formation of larval *Echinococcus multilocularis*. II. Ultrastructural investigations. Z Parasitenkd 69:749-763.

Melamed, C., Y. Nevo, and M. Kupiec. 1992. Involvement of cDNA in homologous recombination between Ty elements in *Saccharomyces cerevisiae*. Mol Cell Biol 12:1613-1620.

Mercer, T. R., M. E. Dinger, and J. S. Mattick. 2009. Long non-coding RNAs: insights into functions. Nat Rev Genet 10:155-159.

Merchant, M. T., C. Corella, and K. Willms. 1997. Autoradiographic analysis of the germinative tissue in evaginated *Taenia solium* metacestodes. J Parasitol 83:363-367.

Merkwirth, C., and T. Langer. 2009. Prohibitin function within mitochondria: essential roles for cell proliferation and cristae morphogenesis. Biochim Biophys Acta 1793:27-32.

Metcalf, D. 2007. Concise review: hematopoietic stem cells and tissue stem cells: current concepts and unanswered questions. Stem Cells 25:2390-2395.

Mochizuki, K., H. Sano, S. Kobayashi, C. Nishimiya-Fujisawa, and T. Fujisawa. 2000. Expression and evolutionary conservation of nanos-related genes in Hydra. Dev Genes Evol 210:591-602.

Moore, J., and D. R. Brooks. 1987. Asexual Reproduction in Cestodes (Cyclophyllidea: Taeniidae): Ecological and Phylogenetic Influences. Evolution 41:882-891.

Moraczewski, J. 1977. Asexual reproduction and regeneration of *Catenula* (Turbellaria, Archoophora). Zoomorphologie 88:65-80.

Morita, M., J. B. Best, and J. Noel. 1969. Electron microscopic studies of planarian regeneration. I. Fine structure of neoblasts in *Dugesia dorotocephala*. J Ultrastruct Res 27:7-23.

Moro, P., and P. M. Schantz. 2009. Echinococcosis: a review. Int J Infect Dis 13:125-133.

Morrison, S. J., and A. C. Spradling. 2008. Stem cells and niches: mechanisms that promote stem cell maintenance throughout life. Cell 132:598-611.

Morseth, D. J. 1967a. Observations on the fine structure of the nervous system of *Echinococcus granulosus*. J Parasitol 53:492-500.

Morseth, D. J. 1967b. Fine structure of the hydatid cyst and protoscolex of *Echinococcus granulosus*. J Parasitol 53:312-325.

Mount, P. M. 1970. Histogenesis of the rostellar hooks of *Taenia crassiceps* (Zeder, 1800) (Cestoda). J Parasitol 56:947-961.

Mousley, A., A. G. Maule, D. W. Halton, and N. J. Marks. 2005. Inter-phyla studies on neuropeptides: the potential for broad-spectrum anthelmintic and/or endectocide discovery. Parasitology 131 Suppl:S143-167.

Muller, M. C., and W. Westheide. 2000. Structure of the nervous system of *Myzostoma cirriferum* (Annelida) as revealed by immunohistochemistry and cLSM analyses. J Morphol 245:87-98.

Murko, C., S. Lagger, M. Steiner, C. Seiser, C. Schoefer, and O. Pusch. 2010. Expression of class I histone deacetylases during chick and mouse development. Int J Dev Biol 54:1527-1537.

Nakao, M., A. Lavikainen, T. Iwaki, V. Haukisalmi, S. Konyaev, Y. Oku, M. Okamoto, and A. Ito. 2013. Molecular phylogeny of the genus *Taenia* (Cestoda: Taeniidae): proposals for the resurrection of *Hydatigera* Lamarck, 1816 and the creation of a new genus *Versteria*. Int J Parasitol 43:427-437.

Nakao, M., T. Yanagida, M. Okamoto, J. Knapp, A. Nkouawa, Y. Sako, and A. Ito. 2010. State-of-the-art *Echinococcus* and *Taenia*: phylogenetic taxonomy of human-pathogenic tapeworms and its application to molecular diagnosis. Infect Genet Evol 10:444-452.

Nathoo, A. N., R. A. Moeller, B. A. Westlund, and A. C. Hart. 2001. Identification of neuropeptide-like protein gene families in *Caenorhabditis elegans* and other species. Proc Natl Acad Sci U S A 98:14000-14005.

8. Bibliography

Newmark, P. A., and A. Sanchez Alvarado. 2002. Not your father's planarian: a classic model enters the era of functional genomics. Nat Rev Genet 3:210-219.

Newmark, P. A., and A. Sanchez Alvarado. 2000. Bromodeoxyuridine specifically labels the regenerative stem cells of planarians. Dev Biol 220:142-153.

Nguyen, L., J. M. Rigo, V. Rocher, S. Belachew, B. Malgrange, B. Rogister, P. Leprince, and G. Moonen. 2001. Neurotransmitters as early signals for central nervous system development. Cell Tissue Res 305:187-202.

Norman, L., and I. G. Kagan. 1961. The maintenance of *Echinococcus multilocularis* in gerbils (Meriones unguiculatus) by intraperitoneal inoculation. J Parasitol 47:870-874.

Nusse, R., C. Fuerer, W. Ching, K. Harnish, C. Logan, A. Zeng, D. ten Berge, and Y. Kalani. 2008. Wnt signaling and stem cell control. Cold Spring Harb Symp Quant Biol 73:59-66.

Ogawa, K., C. Kobayashi, T. Hayashi, H. Orii, K. Watanabe, and K. Agata. 2002. Planarian fibroblast growth factor receptor homologs expressed in stem cells and cephalic ganglions. Dev Growth Differ 44:191-204.

Oh, I. H., and E. P. Reddy. 1999. The myb gene family in cell growth, differentiation and apoptosis. Oncogene 18:3017-3033.

Ohbayashi, M. 1960. Studies on echinococcosis. X. Histological observations on experimental cases of multilocular echinococcosis. Japanese Journal of Veterinary Research 8:134-160.

Olson, P. D., and V. V. Tkach. 2005. Advances and trends in the molecular systematics of the parasitic Platyhelminthes. Adv Parasitol 60:165-243.

Olson, P. D., M. Zarowiecki, F. Kiss, and K. Brehm. 2011. Cestode genomics - progress and prospects for advancing basic and applied aspects of flatworm biology. Parasite Immunol.

Onal, P., D. Grun, C. Adamidi, A. Rybak, J. Solana, G. Mastrobuoni, Y. Wang, H. P. Rahn, W. Chen, S. Kempa, U. Ziebold, and N. Rajewsky. 2012. Gene expression of pluripotency determinants is conserved between mammalian and planarian stem cells. Embo J 31:2755-2769.

Orii, H., T. Sakurai, and K. Watanabe. 2005. Distribution of the stem cells (neoblasts) in the planarian *Dugesia japonica*. Dev Genes Evol 215:143-157.

Orrhage, L., and C. M. Müller. 2005. Morphology of the nervous system of Polychaeta (Annelida). Hydrobiologia 535/536:79–111.

Palakodeti, D., M. Smielewska, Y. C. Lu, G. W. Yeo, and B. R. Graveley. 2008. The PIWI proteins SMEDWI-2 and SMEDWI-3 are required for stem cell function and piRNA expression in planarians. Rna 14:1174-1186.

Palmberg, I. 1990. Stem cells in microturbellarians. Protoplasma 158:109-120.

Parisi, M., and H. Lin. 2000. Translational repression: a duet of Nanos and Pumilio. Curr Biol 10:R81-83.

Parkinson, J., J. D. Wasmuth, G. Salinas, C. V. Bizarro, C. Sanford, M. Berriman, H. B. Ferreira, A. Zaha, M. L. Blaxter, R. M. Maizels, and C. Fernandez. 2012. A transcriptomic analysis of *Echinococcus granulosus* larval stages: implications for parasite biology and host adaptation. PLoS Negl Trop Dis 6:e1897.

Peaston, A. E., A. V. Evsikov, J. H. Graber, W. N. de Vries, A. E. Holbrook, D. Solter, and B. B. Knowles. 2004. Retrotransposons regulate host genes in mouse oocytes and preimplantation embryos. Dev Cell 7:597-606.

Pellettieri, J., and A. Sanchez Alvarado. 2007. Cell turnover and adult tissue homeostasis: from humans to planarians. Annu Rev Genet 41:83-105.

8. Bibliography

Peng, J. C., and H. Lin. 2013. Beyond transposons: the epigenetic and somatic functions of the Piwi-piRNA mechanism. Curr Opin Cell Biol 25:190-194.

Persson, D. K., K. A. Halberg, A. Jorgensen, N. Mobjerg, and R. M. Kristensen. 2012. Neuroanatomy of *Halobiotus crispae* (Eutardigrada: Hypsibiidae): Tardigrade brain structure supports the clade Panarthropoda. J Morphol 273:1227-1245.

Peter, R., R. Gschwentner, W. Schürmann, R. M. Rieger, and P. Ladurner. 2004. The significance of stem cells in free-living flatworms: one common source for all cells in the adult. Journal of Applied Biomedicine 2:21-35.

Peter, R., P. Ladurner, and R. M. Rieger. 2001. The Role of Stem Cell Strategies in Coping with Environmental Stress and Choosing Between Alternative Reproductive Modes: Turbellaria Rely on a Single Cell Type to Maintain Individual Life and Propagate Species. Marine Ecology 22:35-51.

Petermann, E., M. L. Orta, N. Issaeva, N. Schultz, and T. Helleday. Hydroxyurea-stalled replication forks become progressively inactivated and require two different RAD51-mediated pathways for restart and repair. Mol Cell 37:492-502.

Petersen, T. N., S. Brunak, G. von Heijne, and H. Nielsen. 2011. SignalP 4.0: discriminating signal peptides from transmembrane regions. Nat Methods 8:785-786.

Pfister, D., K. De Mulder, V. Hartenstein, G. Kuales, G. Borgonie, F. Marx, J. Morris, and P. Ladurner. 2008. Flatworm stem cells and the germ line: developmental and evolutionary implications of macvasa expression in *Macrostomum lignano*. Dev Biol 319:146-159.

Pfister, D., K. De Mulder, I. Philipp, G. Kuales, M. Hrouda, P. Eichberger, G. Borgonie, V. Hartenstein, and P. Ladurner. 2007. The exceptional stem cell system of *Macrostomum lignano*: screening for gene expression and studying cell proliferation by hydroxyurea treatment and irradiation. Front Zool 4:9.

Piperno, G., and M. T. Fuller. 1985. Monoclonal antibodies specific for an acetylated form of alpha-tubulin recognize the antigen in cilia and flagella from a variety of organisms. J Cell Biol 101:2085-2094.

Pohle, S., R. Ernst, C. MacKenzie, M. Spicher, T. Romig, A. Hemphill, and S. Gripp. 2011. *Echinococcus multilocularis*: the impact of ionizing radiation on metacestodes. Exp Parasitol 127:127-134.

Powell, D. W., R. C. Mifflin, J. D. Valentich, S. E. Crowe, J. I. Saada, and A. B. West. 1999. Myofibroblasts. I. Paracrine cells important in health and disease. Am J Physiol 277:C1-9.

Prouse, M. B., and M. M. Campbell. 2012. The interaction between MYB proteins and their target DNA binding sites. Biochim Biophys Acta 1819:67-77.

Rais, Y., A. Zviran, S. Geula, O. Gafni, E. Chomsky, S. Viukov, A. A. Mansour, I. Caspi, V. Krupalnik, M. Zerbib, I. Maza, N. Mor, D. Baran, L. Weinberger, D. A. Jaitin, D. Lara-Astiaso, R. Blecher-Gonen, Z. Shipony, Z. Mukamel, T. Hagai, S. Gilad, D. Amann-Zalcenstein, A. Tanay, I. Amit, N. Novershtern, and J. H. Hanna. 2013. Deterministic direct reprogramming of somatic cells to pluripotency. Nature 502:65-70.

Rasband, W. S. 1997. ImageJ. U. S. National Institutes of Health, Bethesda, Maryland, USA.

Rausch, R. 1954. Studies on the helminth fauna of Alaska. XX. The histogenesis of the alveolar larva of *Echinococcus* species. J Infect Dis 94:178-186.

Rausch, R. L., and A. D'Alessandro. 1999. Histogenesis in the metacestode of *Echinococcus vogeli* and mechanism of pathogenesis in polycystic hydatid disease. J Parasitol 85:410-418.

Rebscher, N., F. Zelada-Gonzalez, T. U. Banisch, F. Raible, and D. Arendt. 2007. Vasa unveils a common origin of germ cells and of somatic stem cells from the posterior growth zone in the polychaete *Platynereis dumerilii*. Dev Biol 306:599-611.

Reddien, P. W. 2013. Specialized progenitors and regeneration. Development 140:951-957.

Reddien, P. W., N. J. Oviedo, J. R. Jennings, J. C. Jenkin, and A. Sanchez Alvarado. 2005. SMEDWI-2 is a PIWI-like protein that regulates planarian stem cells. Science 310:1327-1330.

Reddien, P. W., and A. Sanchez Alvarado. 2004. Fundamentals of planarian regeneration. Annu Rev Cell Dev Biol 20:725-757.

Reuter, M., and M. Gustafsson. 1996. Neuronal signal substances in asexual multiplication and development in flatworms. Cell Mol Neurobiol 16:591-616.

Reuter, M., and N. Kreshchenko. 2004. Flatworm asexual multiplication implicates stem cells and regeneration. Canadian Journal of Zoology 82:334-356.

Reuter, M., K. Mäntylä, and M. K. S. Gustafsson. 1998. Organization of the orthogon – main and minor nerve cords. Hydrobiologia 383:175-182.

Ribeiro, P., F. El-Shehabi, and N. Patocka. 2005. Classical transmitters and their receptors in flatworms. Parasitology 131 Suppl:S19-40.

Rieger, R. M., A. Legniti, P. Ladurner, D. Reiter, E. Asch, W. Salvenmoser, W. Schürmann, and R. Peter. 1999. Ultrastructure of neoblasts in microturbellaria: significance for understanding stem cells in free-living Platyhleminthes. Invertebrate Reproduction and Development 35:127-140.

Rink, J. C. 2013. Stem cell systems and regeneration in planaria. Dev Genes Evol 223:67-84.

Ritsma, L., S. I. Ellenbroek, A. Zomer, H. J. Snippert, F. J. de Sauvage, B. D. Simons, H. Clevers, and J. van Rheenen. 2014. Intestinal crypt homeostasis revealed at single-stem-cell level by in vivo live imaging. Nature 507:362-365.

Robb, S. M., E. Ross, and A. Sanchez Alvarado. 2008. SmedGD: the *Schmidtea mediterranea* genome database. Nucleic Acids Res 36:D599-606.

Rogan, M. T., and K. S. Richards. 1986. In vitro development of hydatid cysts from posterior bladders and ruptured brood capsules of equine *Echinococcus granulosus*. Parasitology 92 (Pt 2):379-390.

Rogan, M. T., and K. S. Richards. 1989. Development of the tegument of *Echinococcus granulosus* (Cestoda) protoscoleces during cystic differentiation in vivo. Parasitol Res 75:299-306.

Rompolas, P., K. R. Mesa, and V. Greco. 2013. Spatial organization within a niche as a determinant of stem-cell fate. Nature 502:513-518.

Ross, R. J., M. M. Weiner, and H. Lin. 2014. PIWI proteins and PIWI-interacting RNAs in the soma. Nature 505:353-359.

Rossi, L., P. Iacopetti, and A. Salvetti. 2012. Stem cells and neural signalling: the case of neoblast recruitment and plasticity in low dose X-ray treated planarians. Int J Dev Biol 56:135-142.

Rossi, L., A. Salvetti, R. Batistoni, P. Deri, and V. Gremigni. 2008. Planarians, a tale of stem cells. Cell Mol Life Sci 65:16-23.

Rossi, L., A. Salvetti, F. M. Marincola, A. Lena, P. Deri, L. Mannini, R. Batistoni, E. Wang, and V. Gremigni. 2007. Deciphering the molecular machinery of stem cells: a look at the neoblast gene expression profile. Genome Biol 8:R62.

Rouhana, L., N. Shibata, O. Nishimura, and K. Agata. 2010. Different requirements for conserved post-transcriptional regulators in planarian regeneration and stem cell maintenance. Dev Biol 341:429-443.

Rutherford, K., J. Parkhill, J. Crook, T. Horsnell, P. Rice, M.-A. Rajandream, and B. Barrell. 2000. Artemis: sequence visualization and annotation. Bioinformatics 16:944-945.

Rybicka, K. 1966. Embryogenesis in cestodes. Adv Parasitol 4:107-186.

Sakamoto, H., and M. Sugimura. 1969. Studies on Echinococcosis XXI. Electron Microscopical Observations on General Structure of Larval Tissue of Multilocular Echinococcus. Jap J vet Res 17:67-80.

Sakamoto, T., and M. Sugimura. 1970. Studies on echinococcosis XXIII. Electron microscopical observations on histogenesis of larval *Echinococcus multilocularis*. Jap J vet Res 18:131-144.

Salic, A., and T. J. Mitchison. 2008. A chemical method for fast and sensitive detection of DNA synthesis in vivo. Proc Natl Acad Sci U S A 105:2415-2420.

Salo, E., and J. Baguna. 1984. Regeneration and pattern formation in planarians. I. The pattern of mitosis in anterior and posterior regeneration in *Dugesia (G) tigrina*, and a new proposal for blastema formation. J Embryol Exp Morphol 83:63-80.

Salvetti, A., L. Rossi, L. Bonuccelli, A. Lena, C. Pugliesi, G. Rainaldi, M. Evangelista, and V. Gremigni. 2009. Adult stem cell plasticity: neoblast repopulation in non-lethally irradiated planarians. Dev Biol 328:305-314.

Salvetti, A., L. Rossi, P. Deri, and R. Batistoni. 2000. An MCM2-related gene is expressed in proliferating cells of intact and regenerating planarians. Dev Dyn 218:603-614.

Salvetti, A., L. Rossi, A. Lena, R. Batistoni, P. Deri, G. Rainaldi, M. T. Locci, M. Evangelista, and V. Gremigni. 2005. DjPum, a homologue of *Drosophila* Pumilio, is essential to planarian stem cell maintenance. Development 132:1863-1874.

Sambrook, J., E. F. Fritsch, and T. Maniatis. 1989. Molecular cloning. Cold spring harbor laboratory press.

Santoni, F. A., J. Guerra, and J. Luban. 2011. HERV-H RNA is abundant in human embryonic stem cells and a precise marker for pluripotency. Retrovirology 9:111.

Sato, K., N. Shibata, H. Orii, R. Amikura, T. Sakurai, K. Agata, S. Kobayashi, and K. Watanabe. 2006. Identification and origin of the germline stem cells as revealed by the expression of nanos-related gene in planarians. Dev Growth Differ 48:615-628.

Sato, T., and H. Clevers. 2013. Growing self-organizing mini-guts from a single intestinal stem cell: mechanism and applications. Science 340:1190-1194.

Sato, T., J. H. van Es, H. J. Snippert, D. E. Stange, R. G. Vries, M. van den Born, N. Barker, N. F. Shroyer, M. van de Wetering, and H. Clevers. 2011. Paneth cells constitute the niche for Lgr5 stem cells in intestinal crypts. Nature 469:415-418.

Sawyer, S. 1989. Statistical tests for detecting gene conversion. Mol Biol Evol 6:526-538.

Sawyer, S. A. 1999. GENECONV: A computer package for the statistical detection of gene conversion http://www.math.wustl.edu/~sawyer/.

8. Bibliography

Schrom, E. M., R. Moschall, M. J. Hartl, H. Weitner, D. Fecher, J. Langemeier, J. Bohne, B. M. Wohrl, and J. Bodem. 2013. U1snRNP-mediated suppression of polyadenylation in conjunction with the RNA structure controls poly (A) site selection in foamy viruses. Retrovirology 10:55.

Schubert, A., U. Koziol, K. Calilliau, M. Vanderstraete, C. Dissous, and K. Brehm. 2014. Targeting *Echinococcus multilocularis* Stem Cells by Inhibition of the Polo-Like Kinase EmPlk1. PLoS Negl Trop Dis 8:e2870.

Schulman, A. H. 2012. Hitching a Ride: Nonautonomous Retrotransposons and Parasitism as a Lifestyle. Topics in Current Genetics 24:71-88.

Schürmann, W., and R. Peter. 2001. Planarian cell culture: a comparative review of methods and an improved protocol for primary cultures of neoblasts. Belg. J. Zool 131:123-130.

Seidah, N. G., G. Mayer, A. Zaid, E. Rousselet, N. Nassoury, S. Poirier, R. Essalmani, and A. Prat. 2008. The activation and physiological functions of the proprotein convertases. Int J Biochem Cell Biol 40:1111-1125.

Seita, J., and I. L. Weissman. 2010. Hematopoietic stem cell: self-renewal versus differentiation. Wiley Interdiscip Rev Syst Biol Med 2:640-653.

Shibata, N., L. Rouhana, and K. Agata. 2010. Cellular and molecular dissection of pluripotent adult somatic stem cells in planarians. Dev Growth Differ 52:27-41.

Shibata, N., Y. Umesono, H. Orii, T. Sakurai, K. Watanabe, and K. Agata. 1999. Expression of vasa(vas)-related genes in germline cells and totipotent somatic stem cells of planarians. Dev Biol 206:73-87.

Shield, J. M. 1969. Dipylidium caninum, *Echinococcus granulosus* and *Hydatigera taeniaeformis*: histochemical identification of cholinesterases. Exp Parasitol 25:217-231.

Shield, J. M., D. D. Heath, and J. D. Smyth. 1973. Light microscope studies of the early development of *Taenia pisiformis* cysticerci. Int J Parasitol 3:471-480.

Siddiqui, S. S., E. Aamodt, F. Rastinejad, and J. Culotti. 1989. Anti-tubulin monoclonal antibodies that bind to specific neurons in *Caenorhabditis elegans*. J Neurosci 9:2963-2972.

Siddle, K. 2011. Signalling by insulin and IGF receptors: supporting acts and new players. J Mol Endocrinol 47:R1-10.

Siegel, G. J., B. W. Agranoff, R. W. Albers, S. K. Fisher, and M. D. Uhler. 2006. Basic Neurochemistry: Molecular, Cellular and Medical Aspects. Philadelphia: Lippincott Williams and Wilkins.

Sinclair, W. K. 1965. Hydroxyurea: differential lethal effects on cultured mammalian cells during the cell cycle. Science 150:1729-1731.

Skinner, D. E., G. Rinaldi, U. Koziol, K. Brehm, and P. J. Brindley. 2014. How might flukes and tapeworms maintain genome integrity without a canonical piRNA pathway? Trends Parasitol 30:123-129.

Skinner, D. E., G. Rinaldi, S. Suttiprapa, V. H. Mann, P. Smircich, A. A. Cogswell, D. L. Williams, and P. J. Brindley. 2012. Vasa-Like DEAD-Box RNA Helicases of *Schistosoma mansoni*. PLoS Negl Trop Dis 6:e1686.

Slais, J. 1973. Functional morphology of cestode larvae. Adv Parasitol 11:395-480.

Smith, S. A., and K. S. Richards. 1993. Ultrastructure and microanalyses of the calcareous corpuscles of the protoscoleces of *Echinococcus granulosus*. Parasitol Res 79:245-250.

Smyth, J. D., A. B. Howkins, and M. Barton. 1966. Factors controlling the differentiation of the hydatid organism, *Echinococcus granulosus*, into cystic or strobilar stages in vitro. Nature 211:1374-1377.

Smyth, J. D., and D. P. McManus. 2007. The physiology and biochemistry of cestodes. Cambridge University Press.

Snippert, H. J., L. G. van der Flier, T. Sato, J. H. van Es, M. van den Born, C. Kroon-Veenboer, N. Barker, A. M. Klein, J. van Rheenen, B. D. Simons, and H. Clevers. 2010. Intestinal crypt homeostasis results from neutral competition between symmetrically dividing Lgr5 stem cells. Cell 143:134-144.

Solana, J. 2013. Closing the circle of germline and stem cells: the Primordial Stem Cell hypothesis. Evodevo 4:2.

Solana, J., D. Kao, Y. Mihaylova, F. Jaber-Hijazi, S. Malla, R. Wilson, and A. Aboobaker. 2012. Defining the molecular profile of planarian pluripotent stem cells using a combinatorial RNAseq, RNA interference and irradiation approach. Genome Biol 13:R19.

Spangrude, G. J., S. Heimfeld, and I. L. Weissman. 1988. Purification and characterization of mouse hematopoietic stem cells. Science 241:58-62.

Specht, D., and M. Voge. 1965. Asexual Multiplication of *Mesocestoides* Tetrathyridia in Laboratory Animals. J Parasitol 51:268-272.

Spiliotis, M., and K. Brehm. 2009. Axenic in vitro cultivation of *Echinococcus multilocularis* metacestode vesicles and the generation of primary cell cultures. Methods Mol Biol 470:245-262.

Spiliotis, M., C. Konrad, V. Gelmedin, D. Tappe, S. Bruckner, H. U. Mosch, and K. Brehm. 2006. Characterisation of EmMPK1, an ERK-like MAP kinase from *Echinococcus multilocularis* which is activated in response to human epidermal growth factor. Int J Parasitol 36:1097-1112.

Spiliotis, M., A. Kroner, and K. Brehm. 2003. Identification, molecular characterization and expression of the gene encoding the epidermal growth factor receptor orthologue from the fox-tapeworm *Echinococcus multilocularis*. Gene 323:57-65.

Spiliotis, M., S. Lechner, D. Tappe, C. Scheller, G. Krohne, and K. Brehm. 2008. Transient transfection of *Echinococcus multilocularis* primary cells and complete in vitro regeneration of metacestode vesicles. Int J Parasitol 38:1025-1039.

Spiliotis, M., C. Mizukami, Y. Oku, F. Kiss, K. Brehm, and B. Gottstein. 2010. *Echinococcus multilocularis* primary cells: Improved isolation, small-scale cultivation and RNA interference. Mol Biochem Parasitol.

Spiliotis, M., D. Tappe, S. Bruckner, H. U. Mosch, and K. Brehm. 2005. Molecular cloning and characterization of Ras- and Raf-homologues from the fox-tapeworm Echinococcus *multilocularis*. Mol Biochem Parasitol 139:225-237.

Spiliotis, M., D. Tappe, L. Sesterhenn, and K. Brehm. 2004. Long-term in vitro cultivation of *Echinococcus multilocularis* metacestodes under axenic conditions. Parasitol Res 92:430-432.

Stange, D. E. 2013. Intestinal stem cells. Dig Dis 31:293-298.

Stange, D. E., B. K. Koo, M. Huch, G. Sibbel, O. Basak, A. Lyubimova, P. Kujala, S. Bartfeld, J. Koster, J. H. Geahlen, P. J. Peters, J. H. van Es, M. van de Wetering, J. C. Mills, and H. Clevers. 2013. Differentiated Troy+ chief cells act as reserve stem cells to generate all lineages of the stomach epithelium. Cell 155:357-368.

Steiner, D. F. 1998. The proprotein convertases. Curr Opin Chem Biol 2:31-39.

8. Bibliography

Subramaniam, K., and G. Seydoux. 1999. nos-1 and nos-2, two genes related to *Drosophila* nanos, regulate primordial germ cell development and survival in *Caenorhabditis elegans*. Development 126:4861-4871.

Subramanian, S., and S. Kumar. 2003. Neutral substitutions occur at a faster rate in exons than in noncoding DNA in primate genomes. Genome Res 13:838-844.

Sulgostowska, T. 1972. The development of organ systems in cestodes. I. A study of histology of *H. diminuta* (Rud., 1819). Acta Parasit Pol 20:449.462.

Swiderski, Z. 1983. *Echinococcus granulosus*: hook-muscle systems and cellular organisation of infective oncospheres. Int J Parasitol 13:289-299.

Swiderski, Z., J. Miquel, D. Mlocicki, B. B. Georgiev, C. Eira, B. Grytner-Ziecina, and C. Feliu. 2007. Post-embryonic development and ultrastructural characteristics of the polycephalic larva of *Taenia parva* Baer, 1926 (Cyclophyllidea, Taeniidae). Acta Parasitol 52:31-50.

Tachibana, M., P. Amato, M. Sparman, N. M. Gutierrez, R. Tippner-Hedges, H. Ma, E. Kang, A. Fulati, H. S. Lee, H. Sritanaudomchai, K. Masterson, J. Larson, D. Eaton, K. Sadler-Fredd, D. Battaglia, D. Lee, D. Wu, J. Jensen, P. Patton, S. Gokhale, R. L. Stouffer, D. Wolf, and S. Mitalipov. 2013. Human embryonic stem cells derived by somatic cell nuclear transfer. Cell 153:1228-1238.

Takahashi, K., and S. Yamanaka. 2006. Induction of pluripotent stem cells from mouse embryonic and adult fibroblast cultures by defined factors. Cell 126:663-676.

Takashima, S., D. Gold, and V. Hartenstein. 2013. Stem cells and lineages of the intestine: a developmental and evolutionary perspective. Dev Genes Evol 223:85-102.

Takizawa, H., U. Schanz, and M. G. Manz. 2011. Ex vivo expansion of hematopoietic stem cells: mission accomplished? Swiss Med Wkly 141:w13316.

Tamura, K., D. Peterson, N. Peterson, G. Stecher, M. Nei, and S. Kumar. 2011. MEGA5: molecular evolutionary genetics analysis using maximum likelihood, evolutionary distance, and maximum parsimony methods. Mol Biol Evol 28:2731-2739.

Tanaka, E. M., and P. W. Reddien. 2011. The cellular basis for animal regeneration. Dev Cell 21:172-185.

Tantin, D. 2013. Oct transcription factors in development and stem cells: insights and mechanisms. Development 140:2857-2866.

Tappe, D., K. Brehm, M. Frosch, A. Blankenburg, A. Schrod, F. J. Kaup, and K. Matz-Rensing. 2007. *Echinococcus multilocularis* infection of several Old World monkey species in a breeding enclosure. Am J Trop Med Hyg 77:504-506.

Tappe, D., and M. Frosch. 2007. Rudolf Virchow and the recognition of alveolar echinococcosis, 1850s. Emerg Infect Dis 13:732-735.

Telesnitsky, A., and S. P. Goff. 1997. Reverse Transcriptase and the Generation of Retroviral DNA *in* J. M. Coffin, S. H. Hughes, and H. E. Varmus, eds. Retroviruses. Cold Spring Harbor Laboratory Press, Cold Spring Harbor (NY).

ten Berge, D., D. Kurek, T. Blauwkamp, W. Koole, A. Maas, E. Eroglu, R. K. Siu, and R. Nusse. 2011. Embryonic stem cells require Wnt proteins to prevent differentiation to epiblast stem cells. Nat Cell Biol 13:1070-1075.

Thompson, J. D., T. J. Gibson, and D. G. Higgins. 2002. Multiple sequence alignment using ClustalW and ClustalX. Curr Protoc Bioinformatics Chapter 2:Unit 2 3.

Thompson, J. D., D. G. Higgins, and T. J. Gibson. 1994. CLUSTAL W: improving the sensitivity of progressive multiple sequence alignment through sequence

weighting, position-specific gap penalties and weight matrix choice. Nucleic Acids Res 22:4673-4680.

Thompson, R. C. 1976. The development of brood capsules and protoscolices in secondary hydatid cysts of *Echinococcus granulosus*. A histological study. Z Parasitenkd 51:31-36.

Thompson, R. C., J. D. Dunsmore, and A. R. Hayton. 1979. *Echinococcus granulosus*: secretory activity of the rostellum of the adult cestode in situ in the dog. Exp Parasitol 48:144-163.

Thompson, R. C. A. 1986. Biology and systematics of *Echinococcus*. Pp. 5-43 *in* R. C. A. Thompson, ed. The Biology of *Echinococcus* and hydatid disease. George Allen & Unwin.

Thorel, F., V. Nepote, I. Avril, K. Kohno, R. Desgraz, S. Chera, and P. L. Herrera. 2010. Conversion of adult pancreatic alpha-cells to beta-cells after extreme beta-cell loss. Nature 464:1149-1154.

Thorvaldsdóttir, H., J. T. Robinson, and J. P. Mesirov. 2013. Integrative Genomics Viewer (IGV): high-performance genomics data visualization and exploration. Briefings in bioinformatics 14:178-192.

Toledo, A., C. Cruz, G. Fragoso, J. P. Laclette, M. T. Merchant, M. Hernandez, and E. Sciutto. 1997. In vitro culture of *Taenia crassiceps* larval cells and cyst regeneration after injection into mice. J Parasitol 83:189-193.

Torgerson, P. R., K. Keller, M. Magnotta, and N. Ragland. 2010. The global burden of alveolar echinococcosis. PLoS Negl Trop Dis 4:e722.

Trouvé, S., S. Morand, and C. Gabrion. 2003. Asexual multiplication of larval parasitic worms: a predictor of adult life-history traits in Taeniidae? Parasitol Res 89:81-88.

Tsai, I. J., M. Zarowiecki, N. Holroyd, A. Garciarrubio, A. Sanchez-Flores, K. L. Brooks, A. Tracey, R. J. Bobes, G. Fragoso, E. Sciutto, M. Aslett, H. Beasley, H. M. Bennett, J. Cai, F. Camicia, R. Clark, M. Cucher, N. De Silva, T. A. Day, P. Deplazes, K. Estrada, C. Fernandez, P. W. Holland, J. Hou, S. Hu, T. Huckvale, S. S. Hung, L. Kamenetzky, J. A. Keane, F. Kiss, U. Koziol, O. Lambert, K. Liu, X. Luo, Y. Luo, N. Macchiaroli, S. Nichol, J. Paps, J. Parkinson, N. Pouchkina-Stantcheva, N. Riddiford, M. Rosenzvit, G. Salinas, J. D. Wasmuth, M. Zamanian, Y. Zheng, X. Cai, X. Soberon, P. D. Olson, J. P. Laclette, K. Brehm, and M. Berriman. 2013. The genomes of four tapeworm species reveal adaptations to parasitism. Nature 496:57-63.

Uchikawa, M., Y. Kamachi, and H. Kondoh. 1999. Two distinct subgroups of Group B Sox genes for transcriptional activators and repressors: their expression during embryonic organogenesis of the chicken. Mech Dev 84:103-120.

Valverde-Islas, L. E., E. Arrangoiz, E. Vega, L. Robert, R. Villanueva, O. Reynoso-Ducoing, K. Willms, A. Zepeda-Rodriguez, T. I. Fortoul, and J. R. Ambrosio. 2011. Visualization and 3D reconstruction of flame cells of *Taenia solium* (cestoda). PLoS One 6:e14754.

van der Flier, L. G., M. E. van Gijn, P. Hatzis, P. Kujala, A. Haegebarth, D. E. Stange, H. Begthel, M. van den Born, V. Guryev, I. Oving, J. H. van Es, N. Barker, P. J. Peters, M. van de Wetering, and H. Clevers. 2009. Transcription factor achaete scute-like 2 controls intestinal stem cell fate. Cell 136:903-912.

Vasantha, S., B. V. Kumar, S. D. Roopashree, S. Das, and S. K. Shankar. 1992. Neuroanatomy of *Cysticercus cellulosae* (Cestoda) as revealed by

acetylcholinesterase and nonspecific esterase histochemistry. Parasitol Res 78:581-586.

Veenstra, J. A. 2010. Neurohormones and neuropeptides encoded by the genome of *Lottia gigantea*, with reference to other mollusks and insects. Gen Comp Endocrinol 167:86-103.

Veenstra, J. A. 2011. Neuropeptide evolution: neurohormones and neuropeptides predicted from the genomes of *Capitella teleta* and *Helobdella robusta*. Gen Comp Endocrinol 171:160-175.

Voronezhskaya, E. E., and K. Elekes. 1996. Transient and sustained expression of FMRFamide-like immunoreactivity in the developing nervous system of *Lymnaea stagnalis* (Mollusca, Pulmonata). Cell Mol Neurobiol 16:661-676.

Wachtler, F., and A. Stahl. 1993. The nucleolus: a structural and functional interpretation. Micron:473-505.

Wagner, D. E., J. J. Ho, and P. W. Reddien. 2012. Genetic regulators of a pluripotent adult stem cell system in planarians identified by RNAi and clonal analysis. Cell Stem Cell 10:299-311.

Wagner, D. E., I. E. Wang, and P. W. Reddien. 2011. Clonogenic neoblasts are pluripotent adult stem cells that underlie planarian regeneration. Science 332:811-816.

Wahlberg, M. H. 1998. The distribution of F-actin during the development of *Diphyllobothrium dendriticum* (Cestoda). Cell Tissue Res 291:561-570.

Wang, B., J. J. Collins, 3rd, and P. A. Newmark. 2013. Functional genomic characterization of neoblast-like stem cells in larval *Schistosoma mansoni*. Elife 2:e00768.

Wang, Y., R. M. Zayas, T. Guo, and P. A. Newmark. 2007. nanos function is essential for development and regeneration of planarian germ cells. Proc Natl Acad Sci U S A 104:5901-5906.

Watabe, T., and K. Miyazono. 2009. Roles of TGF-beta family signaling in stem cell renewal and differentiation. Cell Res 19:103-115.

Werren, J. H. 2011. Selfish genetic elements, genetic conflict, and evolutionary innovation. Proc Natl Acad Sci U S A 108 Suppl 2:10863-10870.

Wickens, M., D. S. Bernstein, J. Kimble, and R. Parker. 2002. A PUF family portrait: 3'UTR regulation as a way of life. Trends Genet 18:150-157.

Wicker, T., F. Sabot, A. Hua-Van, J. L. Bennetzen, P. Capy, B. Chalhoub, A. Flavell, P. Leroy, M. Morgante, O. Panaud, E. Paux, P. SanMiguel, and A. H. Schulman. 2007. A unified classification system for eukaryotic transposable elements. Nat Rev Genet 8:973-982.

Wikgren, B.-J., and M. K. S. Gustafsson. 1971. Cell proliferation and histogenesis in *diphyllobothrid tapeworms* (Cestoda). Acta Acad Abo Ser B 31:1-10.

Wikgren, B. J., and M. K. Gustafsson. 1967. Duration of the cell cycle of germinative cells in plerocercoids of *Diphyllobothrium dendriticum*. Z Parasitenkd 29:275-281.

Wilson, A., E. Laurenti, G. Oser, R. C. van der Wath, W. Blanco-Bose, M. Jaworski, S. Offner, C. F. Dunant, L. Eshkind, E. Bockamp, P. Lio, H. R. Macdonald, and A. Trumpp. 2008. Hematopoietic stem cells reversibly switch from dormancy to self-renewal during homeostasis and repair. Cell 135:1118-1129.

Willms, K., M. T. Merchant, M. Gomez, and L. Robert. 2001. *Taenia solium*: germinal cell precursors in tapeworms grown in hamster intestine. Arch Med Res 32:1-7.

8. Bibliography

Winkles, J. A., and G. F. Alberts. 2005. Differential regulation of polo-like kinase 1, 2, 3, and 4 gene expression in mammalian cells and tissues. Oncogene 24:260-266.

Witchley, J. N., M. Mayer, D. E. Wagner, J. H. Owen, and P. W. Reddien. 2013. Muscle cells provide instructions for planarian regeneration. Cell Rep 4:633-641.

Witte, C. P., Q. H. Le, T. Bureau, and A. Kumar. 2001. Terminal-repeat retrotransposons in miniature (TRIM) are involved in restructuring plant genomes. Proc Natl Acad Sci U S A 98:13778-13783.

Wu, X., Y. Li, B. Crise, S. M. Burgess, and D. J. Munroe. 2005. Weak palindromic consensus sequences are a common feature found at the integration target sites of many retroviruses. J Virol 79:5211-5214.

Xie, T. 2008. Germline stem cell niches *in* L. Girard, ed. Stembook. Harvard University.

Yamashita, J., M. Ohbayashi, and T. Sakamoto. 1960. STUDIES ON ECHINOCOCCOSIS XI.: OBSERVATIONS ON SECONDARY ECHINOCOCCOSIS. Japanese Journal of Veterinary Research 8:315-322.

Yamashita, J., M. Ohbayashi, T. Sakamoto, and M. Orihara. 1962. STUDIES ON ECHINOCOCCOSIS. XIII: OBSERVATIONS ON THE VESICULAR DEVELOPMENT OF THE SCOLEX OF E. MULTILOCULARIS IN VITRO. Japanese Journal of Veterinary Research 10:85-96.

Yanger, K., and B. Z. Stanger. 2011. Facultative stem cells in liver and pancreas: fact and fancy. Dev Dyn 240:521-529.

Ye, B., C. Petritsch, I. E. Clark, E. R. Gavis, L. Y. Jan, and Y. N. Jan. 2004. Nanos and Pumilio are essential for dendrite morphogenesis in *Drosophila* peripheral neurons. Curr Biol 14:314-321.

Ying, Q. L., J. Wray, J. Nichols, L. Batlle-Morera, B. Doble, J. Woodgett, P. Cohen, and A. Smith. 2008. The ground state of embryonic stem cell self-renewal. Nature 453:519-523.

Yokota, Y. 2001. Id and development. Oncogene 20:8290-8298.

Yoshida-Kashikawa, M., N. Shibata, K. Takechi, and K. Agata. 2007. DjCBC-1, a conserved DEAD box RNA helicase of the RCK/p54/Me31B family, is a component of RNA-protein complexes in planarian stem cells and neurons. Dev Dyn 236:3436-3450.

Younossi-Hartenstein, A., U. Ehlers, and V. Hartenstein. 2000. Embryonic Development of the Nervous System of the Rhabdocoel Flatworm *Mesostoma lingua* (Abildgaard, 1789). J Comp Neurol 416:461-474.

Younossi-Hartenstein, A., and V. Hartenstein. 2000. The embryonic development of the polyclad flatworm *Imogine mcgrathi*. Dev Genes Evol 210:383-398.

Younossi-Hartenstein, A., M. Jones, and V. Hartenstein. 2001. Embryonic development of the nervous system of the temnocephalid flatworm *Craspedella pedum*. J Comp Neurol 434:56-68.

Zavala-Gongora, R., B. Derrer, V. Gelmedin, P. Knaus, and K. Brehm. 2008. Molecular characterisation of a second structurally unusual AR-Smad without an MH1 domain and a Smad4 orthologue from *Echinococcus multilocularis*. Int J Parasitol 38:161-176.

Zhao, B., L. Li, and K. L. Guan. 2010. Hippo signaling at a glance. J Cell Sci 123:4001-4006.

Zhou, H., G. J. Rainey, S. K. Wong, and J. M. Coffin. 2001. Substrate sequence selection by retroviral integrase. J Virol 75:1359-1370.

Zhou, Y., and S. H. Cahan. 2012. A novel family of terminal-repeat retrotransposon in miniature (TRIM) in the genome of the red harvester ant, *Pogonomyrmex barbatus*. PLoS One 7:e53401.

Zhu, S. J., and B. J. Pearson. 2013. The Retinoblastoma pathway regulates stem cell proliferation in freshwater planarians. Dev Biol 373:442-452.

Appendix 1: *E. multilocularis* primary cell isolation

1) Transfer axenic metacestode vesicles (≥ 5 mm in diameter) to one or several 50 ml Falcon tubes (25 ml of vesicles or less per tube) and wash extensively with PBS (at least 10 washes). Remove any dead vesicles with a sterile 1 ml plastic pipette. At the last wash, retain the vesicles with sterile gauze in order to remove all the PBS).

2) Break the vesicles by passing them once through a sterile plastic 5 ml pipette (for small vesicles, if needed, add a blue p1000 tip at the pipette´s end).

3) Centrifuge the vesicles for 6 minutes at 600 g at room temperature and remove the supernatant

4) Wash the broken vesicles for at least three times with PBS (let them settle by gravity).

5) Centrifuge the vesicles for 6 minutes at 600 g at room temperature and remove the supernatant

6) Add 4 to 8 volumes of Trypsin/ethylenediaminetetraacetic acid (EDTA) solution (0.05%/0.02% (w/v) respectively, in PBS) to 1 volume of broken vesicles, and incubate at 37 ºC for 15 minutes with periodic shaking. By the end, most vesicle fragments should float, and the solution should become turbid from the released cells.

7) Filter through a 30 µm mesh (with the aid of pipettes and adding PBS) and transfer to a new 50 ml Falcon tube.

8) Centrifuge for 1 minute at room temperature at 100 g in a centrifuge with a tilting-rotor to remove the calcium corpuscles. Transfer the supernatant with the cells to a new 50 ml Falcon tube.

9) Centrifuge the cells for 6 minutes at 600 g

10) Discard the supernatant and carefully re-suspend the cells in cDMEM-A. Take a 12.5 µl aliquot and dilute it to a total volume of 1000 µl with PBS. Measure the absorbance at 600 nm with a spectrophotometer (U-2000, Hitachi, USA) to quantify the cells.

Appendix 2: EdU detection in Whole-mounts

1) Fix the samples for 1 h in paraformaldehyde 4 % prepared in PBS at room temperature (RT), with shaking.

2) Wash 3 times with PBS, 15 min each, with shaking.

3) Block with 2 incubations of 10 min each in PBS + 3% bovine serum albumin (BSA, Sigma-Aldrich), with shaking.

4) Permeabilize with 2 incubations of 20 min each in PBS + 0.5% Triton X-100 (Sigma-Aldrich), with shaking.

5) Block with 2 incubations of 10 min each in PBS + 3% BSA, with shaking.

6) Incubate for 1 hour in the dark with the Click-iT reaction cocktail (Click-iT® EdU Alexa Fluor® 555 Imaging Kit (Life Technologies), prepared as described by the manufacturer), with shaking.

7) Wash for 10 min with PBS + 3% BSA, with shaking.

8) Incubate for 10 min in PBS + 1 μg/ml DAPI (Sigma-Aldrich), with shaking.

9) Wash 3 times with PBS, 10 min each, with shaking.

10) Mount in Fluoprep (Biomérieux)

Appendix 3: Preparation of cell macerates (cell suspensions) for microscopy

Starting from metacestode vesicles

1) Wash the vesicles with PBS and transfer them to a 1.5 ml microtube
2) Break the vesicles with a syringe tip, and wash again with PBS
3) Remove all of the PBS and add cell maceration solution (13:1:1 water : glacial acetic acid : glycerol). Use 500 µl for *ca.* 5 vesicles (of 5 mm diameter). Pipette up and down with a p1000 tip to gently break the tissue.

Starting from 2 day-old cell aggregates

1) Transfer the aggregates to a 1.5 ml microtube, let them sediment for 5 minutes.
2) Wash with PBS
3) Let the aggregates sediment again for 5 minutes, remove all of the PBS and add cell maceration solution (13:1:1 water : glacial acetic acid : glycerol); use 500 µl for one well of a 6 well plate (500 units). Pipette up and down with a p1000 to gently break the tissue.

Then, for both kinds of samples

4) Leave in maceration solution overnight at 4 °C
5) Pipette up and down extensively with p1000 to macerate the tissues
6) Dilute 1:10 in maceration solution
7) Spot 10-20 µl of the dilution on Superfrost Plus Slides (Thermo-Scientific) and leave to dry overnight at room temperature (cover them with a tray to prevent dust from falling on the slides)
8) Store at 4 °C until further use

Appendix 4: Immunohistochemistry of Paraplast sections

1) Remove Paraplast with two incubations of 5 min each in Xylol

2) Rehydrate through a series of ethanol dilutions: 100% ethanol, 75% ethanol, 50% ethanol in PBS, and 25% ethanol in PBS (2 min each)

3) Wash 2 times with PBS (5 min each) at room temperature

4) For those antibodies that require it (Anti-PHB1 and Anti-phospho-histone H3 (Ser10)), perform **Heat Induced Epitope Retrieval (HIER)** as follows. Place the slides in a plastic box covered with a lid and filled with HIER Buffer (Sodium Citrate Buffer 10 mM pH 6.0 + 0.1% Tween-20). Heat in a microwave at 700 Watts until it boils, and then continue heating for 20 more min. Keep more HIER buffer at hand at 100 ºC and use it to add periodically to the box during the incubation, if too much HIER buffer evaporates from the box.

5) Eliminate endogenous peroxidases with 3% H_2O_2 in PBS for 10 min at room temperature

6) Wash in PBS for 5 min at room temperature

7) Wash two times, 5 min each, with PBS + 0.1% Triton X-100

8) Block with PBS + 3 % bovine serum albumin (BSA, Sigma-Aldrich) + 5% Sheep serum (Sigma-Aldrich) for 1 hour at room temperature

9) Incubate with the primary antibody at the appropriate dilution in PBS + 3 % BSA for 2 hours at room temperature in a humid chamber, covering with Parafilm.

10) Wash 4 times, 15 min each, with PBS (the Parafilm will detach from the slide with the first wash).

11) Incubate with the secondary antibody, conjugated to horse radish peroxidase, at the appropriate dilution in PBS + 3 % BSA for 2 hours at room temperature in a humid chamber, covering with Parafilm.

12) Wash 4 times, 15 min each, with PBS (the Parafilm will detach from the slide with the first wash).

13) Perform a quick incubation with sodium acetate buffer 50 mM, pH 5.0

14) Develop the colorimetric reaction with **3-Amino-9-ethylcarbazole (AEC, Sigma-Aldrich A6926)** as follows. Dissolve 1 tablet in 2.5 ml of N.N-dimethylformamide and mix with 47.5 ml of 50 mM sodium acetate buffer, pH 5.0, with stirring. Add 25 µl of fresh 30% (w/w) hydrogen peroxide immediately prior to use. If not all the reaction solution will be used at once, a smaller aliquot can be prepared with a stoichiometrically reduced amount of hydrogen peroxide, and the remaining solution can be stored for two months at 4 ºC in the dark. Cover the slide with the solution and incubate in the dark in a humid chamber to allow the reaction to proceed, checking the reaction development from time to time under a microscope.

15) If desired, perform nuclear staining (*e.g.* DAPI staining).

16) Mount with Fluoprep (Biomérieux) or with 80% glycerol diluted with PBS.

Appendix 5: Immunohistofluorescence on cryosections

1) Thaw cryosections for 30 min at room temperature (RT)

2) Incubate 15 min with PFA 4% - PBS at room temperature

3) Wash 3 times, 5 min each, with PBS

4) Permeabilize with 0.1% Triton X-100 (Sigma-Aldrich) in PBS for 10 min at RT

5) Block with PBS + 1% bovine serum albumin (BSA, Sigma-Aldrich) + 5 % sheep serum (Sigma-Aldrich) + 0.05% Tween-20 (Sigma-Aldrich) for 1 h at RT in a humid chamber

6) Incubate with the primary antibody at the appropriate dilution in PBS + 1 % BSA for 2 h at room temperature in a humid chamber. For some antibodies, it is recommended to do an overnight incubation in a humid chamber, covering the slide with Parafilm at 4 º C (*e.g.* anti-FMRFamide, anti-5-HT).

7) Wash 4 times, 15 min each, with PBS (optional: add 0.05% Tween-20)

8) Incubate with the fluorophore-conjugated secondary antibody at the appropriate dilution in PBS + 1 % BSA for 2 h at RT in a humid chamber

9) Remove antibody solution, and add PBS + 1 % BSA + 1:40 TRITC Phalloidin (Sigma-Aldrich) + 1 µg/ml DAPI (Sigma-Aldrich), incubating for 20 min at RT in a humid chamber

10) Wash 4 times, 15 min each, with PBS (optional: add 0.05% Tween-20)

11) Mount with Fluoprep (Biomérieux)

Appendix 6: Whole-mount Immunohistofluorescence protocols for protoscoleces and small metacestodes

DAY 1

1) Fix protoscoleces or pierced and opened metacestode vesicles with 4% PFA - PBS for 1 hour at room temperature (RT), with shaking.

2) Wash 3 times, 10 min each with PBS + 0.3% Triton X-100 (PBS-T) at RT, with shaking. (Optional: at this point the protocol can be paused by keeping the samples overnight at 4 °C).

3) Permeabilization: two different protocols, for each kind of sample. Use protocol A for protoscoleces and protocol B for vesiculated protoscoleces and metacestode vesicles.

    - Protocol A (with proteinase K):
        - 5 min PBS-T + 0.5% SDS + 2 µg/ml Proteinase K (Fermentas) at RT
        - Quick wash with PBS-T
        - 10 min of re-fixation with 4% PFA / PBS-T at RT, with shaking

    - Protocol B: without proteinase K:
        - 20 min PBS + 1% SDS at RT

4) Wash 3 x 10 min each in PBS-T at RT, with shaking

5) Block 2 hours with PBS-T + 3% bovine serum albumin (BSA, SIGMA) + 5% sheep serum (SIGMA) at RT, with shaking

6) Incubate with PBS-T + 3% BSA + primary antibody at the appropriate concentration overnight at 4 °C with slow rocking

DAY 2

7) Wash 5 times, 30 min each with PBS-T at RT, with shaking

8) Incubate with PBS-T + 3 % BSA + secondary antibody (conjugated to a fluorophore) at the appropriate concentration overnight at 4 °C with slow rocking. From now on protect samples from light.

DAY 3

9) Wash briefly with PBS-T

10) Incubate 30 min with PBS + 1 % BSA + DAPI 1 μg/ml + Phalloidin-TRITC (Sigma) diluted 1:40 at RT with shaking

11) Wash 4 times, 30 min each with PBS-T at RT, with shaking

12) Mount with Fluoprep (Biomérieux)

Appendix 7: Fluorescent Whole-Mount in situ Hybridization (WMISH) for *E. multilocularis* metacestodes

This protocol is a modification of the WMISH protocol for *Hymenolepis microstoma* developed in the laboratory of Dr. Peter Olson (http://www.olsonlab.com/).

General Notes

• Work under RNAse-free conditions. This includes: clean the working bench and the exterior of the pipettes with RNAse-Exitus Plus (Applichem) followed by rinsing with 70% ethanol, use RNAse free plastics, and use gloves at all stages. All solutions up to and including the hybridization step are treated with DEPC or prepared with DEPC treated water under clean conditions.

• Unless stated otherwise, always incubate the specimens under mild shaking for washes and processing.

• Pre-warm buffers using a hot water bath where necessary.

• The solutions and reagents for this protocol are provided at the end

Fixation of *Echinococcus multilocularis* metacestodes for WMISH

1) Wash the metacestodes with PBS and transfer to a Petri dish (the vesicles should be larger than 4 mm but smaller vesicles can also be used, although they have a tendency to be difficult to wash in the following steps).

2) Open gently using a syringe tip and clean fine pincettes.

3) Transfer to a 15 ml Falcon (Greiner) tube with PBS (DEPC-treated), exchange the buffer for 4% PFA/ PBS (DEPC) and leave overnight at 4 ºC.

4) Replace with 100% methanol and agitate on a roller or shaker for 10 min.

5) Exchange methanol and store at -20°C. Specimens can now be stored for long periods (at least six months) at -20 °C or used directly for *in situ* hybridization.

Whole-Mount In Situ Hybridization

DAY 1

Rehydrate the specimens by washing in an ethanol dilution series:

1) 100% ethanol, 5 min on a roller.

2) Wash once in 75% ethanol/distilled water (DEPC), 10 min on a roller.

3) Wash once in 50% ethanol/PBS-T (DEPC), 10 min on a roller.

4) Wash three times in PBS-T for 5 min on a roller.

Proteinase K treatment and re-fixing

5) Take the Proteinase K (Fermentas, 20 mg/ml in 50% Glycerol, stored at -20°C) and put it into ice.

6) Add 7.5 µl of Proteinase K (20 mg/ml) to each vial containing 10 ml of PBS-T.

7) Incubate at room temperature for 10 min, **without** shaking.

8) Rinse twice in 5 ml of 0.1 M Triethanolamine (TEA), pH 7.8, for 5 min (mix by inverting the specimens from time to time).

9) Add 12.5 µl of acetic anhydride to the second wash and swirl often. After 5 min add 12.5 µl more acetic anhydride, and incubate for 5 min.

10) Wash twice for 5 min with PBS-T on roller (mix by inverting the specimens from time to time).

11) Re-fix for 20 min, in 4% paraformaldehyde in PBS-T, on roller.

12) Wash five times for 5 min or longer in PBS-T, to wash off excess paraformaldehyde.

Equilibration of specimens in hybridization buffer

13) Add 500 µl of hybridization buffer to 2 ml PBS-T and allow specimens to settle.

14) Remove the buffer and replace with 1 ml of hybridization buffer. Transfer carefully to 1.5 ml tubes using blue tips that have the tip cut off with clean scissors (for that,

clean the scissors with RNase Exitus Plus and 70% Ethanol and allow to dry). Transfer 5-10 vesicles per tube, depending on vesicle size.

15) Incubate at 60 °C for 10 min (use the shaking Eppendorf thermomixer, 600 RPM). Check the real temperature with a thermometer. Usually the real temperature is 2-3 degrees below what it says on the screen.

Pre-hybridization

16) Replace the hybridization buffer with 0.5 to 1 ml of fresh hybridization buffer (warmed to 60 °C).

17) Pre-hybridize for at least 6 hours at 60 °C using the Eppendorf thermomixer, at 600 RPM. It can be left pre-hybridizing overnight.

DAY 2

Hybridization

18) Prepare the DIG-labeled RNA probe: Denature the probe (10 µl) at 80°C for 3 min, centrifuge and place on ice. Add the probe to 490 µl of pre-warmed hybridization buffer (57-58 °C). Remove the pre-hybridization solution and add the hybridization solution containing the probe to the samples. The resulting probe concentration should be 0.2 to 1 ng/µl. When re-using a probe (that is, the probe is already diluted in hybridization buffer), denature at 80°C for 3 min, and place at 58 °C for 5 minutes before adding to the specimens.

Use approximately 0.2 ng/ul of probe **as measured by dot blot comparing to the Roche standard (see below).**

19) For "short" (up to 250 bp) riboprobes hybridize at 53-54 ºC overnight (24 hours) in the Eppendorf thermomixer, 600 RPM.

20) For all other probes, hybridize at 57-58 °C overnight (24 hours) in the Eppendorf thermomixer, 600 RPM.

DAY 3

Probe removal and washing

21) Carefully remove the probe from the vial and place on ice. Store at - 80°C in a microtube. The probe can be reused several times.

22) Rinse in 1 ml of pre-warmed hybridization buffer (pre-warmed to 57-58 °C), and wash at 57-58°C for 10 min, twice, in the Eppendorf thermomixer, at 600 RPM. *Note:* While changing solutions keep the tubes on the thermomixer to keep specimens at 57-58 °C at all times.

For "short" (up to 250 bp) riboprobes, wash at 53-54 ºC

23) Wash three times in 2 x SSC + 0.1% Tween-20 (pre-warmed to 57-58 °C) at 57-58 °C for 20 min in the Eppendorf thermomixer, 600 RPM.

For "short" (up to 250 bp) riboprobes, wash at 53-54 ºC

24) Wash three times in 0.2 x SSC + 0.1% Tween-20 (pre-warmed to 57-58 °C) at 57-58 °C for 30 min in the Eppendorf thermomixer, 600 RPM.

For "short" (up to 250 bp) riboprobes, wash at 53-54 ºC

25) Wash twice in Maleic acid buffer (MAB) for 15 mins at room temperature on a roller (standard shaker with 70 RPM or Blot shaker at 200 RPM).

Antibody incubation and washing

26) Pre-incubate for 2 hours in 0.5 ml of MAB + 1% Blocking reagent + 5% Sheep serum. This whole blocking solution must be previously heated to 60 ºC for 30 minutes to inactivate the serum, and then cooled down on ice before adding to the samples.

27) Remove the solution and replace with MAB + 1% Blocking Reagent (without sheep serum) containing 1:50 dilution of **Roche Anti-DIG Peroxidase (POD) conjugate**. Place on a rocker overnight at 4°C.

DAY 4

Washing

28) Remove the antibody.

29) Wash three times for 5 min with MAB at room temperature, mixing gently.

30) Wash three times for 1 hour (3 x 1 hour washes) at room temperature, with shaking during the washes (Blue Shaker with 70 RPM or Blot Shaker at 200 RPM).

31) Wash once for 3 min at room temperature with PBS + 0.1 M Imidazole, pH 7.6 at room temperature.

32) Wash once for 10 min at room temperature in PBS + 0.1 M Imidazole, pH 7.6 at room temperature.

Fluorescent Colour Reaction

33) Prepare the fluorescent reaction solution by mixing PBS + 0.1 M imidazole, pH 7.6 with 1:100 Fluorescein Tyramide (prepared as described by Hopman et al., 1998, see also the working protocol below) and 0.001 % final concentration H_2O_2 (for that, it is better to make a 1:300 initial dilution of the 30% H_2O_2 and then use that in a 1:100 dilution for the final solution).

34) Add the fluorescent reaction solution to the specimens, mix by inversion (5-10 times) and incubate 5 minutes in the dark without shaking.

35) Wash 4 times for 5 minutes with PBS-T in the dark. RNAse free conditions are no longer necessary (the FISH is sold). After this, EdU detection and/or DAPI staining (1 µg/ml for 10 minutes, followed by washes in PBS-T) can be done.

36) Mount with Fluoprep (Biomérieux) or with 80% Glycerol in PBS, and seal the borders with nail polish to prevent evaporation.

Modifications of the fluorescent WMISH protocol for the colorimetric alkaline phosphatase WMISH protocol

DAY 3

27) Remove the solution and replace with MAB + 1% Blocking Reagent (without sheep serum) containing 1:200 dilution of **Roche Anti-DIG Alkaline Phosphatase (AP) conjugate (Roche 11 093 274 910).** Place on a rocker overnight at 4 °C.

DAY 4

31) Wash once for 3 min in 100 mM Tris-HCl, 100 mM NaCl, 50 mM $MgCl_2$ (pH=9.5)

32) Wash once for 10 min in 100 mM Tris-HCl, 100 mM NaCl, 50 mM $MgCl_2$ (pH=9.5)

33-36) Perform the detection with nitro-blue tetrazolium and 5-bromo-4-chloro-3'-indolyphosphate (NBT/BCIP, Sigma, B1911) for 2 hours to overnight (for highly expressed genes, signal will be apparent after 15-30 minutes). Perform DAPI staining and mount in Fluoprep.

Reagents and solutions for the WMISH protocol

DEPC treated H_2O

Add 0.1% DEPC to double-distilled water, and stir overnight (leave the lid slightly open). Autoclave twice.

PBS

Add 0.1% DEPC to a bottle of PBS, and stir overnight (leave the lid slightly open). Autoclave twice.

PFA 4% / PBS (DEPC)

Dissolve 4 g of paraformaldehyde (Sigma-Aldrich P-6148) in 100 ml of DEPC-treated PBS by incubating at 65 °C for 1-2 hours and shaking periodically. Make 10 ml aliquots, and store at -20 °C.

PBS-T

PBS + 0.1% Tween-20 (SIGMA P-9416)

Proteinase K (Fermentas, Thermo Scientific # EO0491)

0.1 M Triethanolamine (TEA), pH 7 to 8

From stock TEA (90278, Sigma-Aldrich), concentration 7.53 M, prepare a 1:75.3 dilution (0.665 ml TEA in 50 ml of DEPC-treated water). Adjust pH with freshly aliquoted 25% HCl (usually *ca*. 200 µl are needed) and confirm the pH by placing a drop on a pH strip.

Acetic anhydride (Sigma-Aldrich A-6404)

10% CHAPS (Sigma-Aldrich C-3023)

Dissolve 5 g of CHAPS in 50 ml total volume with DEPC treated H_2O.

10% Tween-20 (Sigma-Aldrich P-9416)

Dissolve 5 ml of Tween-20 in 50 ml total volume with DEPC treated H_2O.

Heparin 100 mg/ml stock (Sigma-Aldrich H-3393)

Dissolve 0.5 g of Heparin in 5 ml of sterile (not DEPC-treated) double-distilled water. Store at -20 °C in 0.2 ml aliquots.

***Torula* RNA 100 mg/ml (Sigma-Aldrich R-6625)**

1) Dissolve Torula RNA at 10 mg/ml in DEPC-treated water (dissolve at 65 °C, *ca*. 1 hour). Start with 40 ml or less.
2) Extract with one volume of Phenol:Chloroform:Isoamyl alcohol (25:24:1), centrifuge 20 minutes at 10,000 g at 4 °C, and transfer the aqueous phase to a new tube.
3) Extract with one volume of Chloroform and centrifuge 20 minutes at 10,000 g at 4 °C, and transfer the aqueous phase to a new tube.
4) Precipitate the RNA by adding 0.1 volume of sodium acetate 3 M (pH 5.2, RNAse-free) and 2.5 volumes of 100% ethanol , and centrifuge 20 minutes at 10,000 g at 4 °C.
5) Wash the pellet twice with 70% ethanol (RNAse-free).
6) Remove all the ethanol with a pipette. Dry the pellet (usually around 5 minutes by placing at 42 °C), and resuspend in 1 ml of DEPC-treated water (pipette up and down, this can take a while; heat for 5-10 minutes at 65 °C if needed).
7) Quantify and estimate purity with the NanoDrop.
8) Dilute to 100-200 mg/ml and store at -20 °C.

Formamide, de-ionized (Sigma-Aldrich F9037)

Aliquot in Falcon (Greiner) tubes and store a -20 °C.

20 X SSC (3 M NaCl, 0.3 M tri-sodium citrate)

175.3 g NaCl (Sigma-Aldrich)

88.2 g Tri-sodium citrate (Sigma-Aldrich)

Add double-distilled water to 800 ml, and adjust pH to 7.0 with HCl. Complete the volume to 1 l with H_2O.

Add 0.1% DEPC and stir overnight, leave the lid slightly opened. Autoclave twice. Store at 4 °C.

Denhardt´s Solution 50X concentrate (Sigma-Aldrich, D2532).

Hybridization solution

Final concentration	Stock	Volume for 10 ml
50 % Formamide	100%	5 ml
5 X SSC	20 X SSC	2.5 ml
1 mg/ml Torula RNA	100-200 mg/ml	50 – 100 µl
100 µg/ml Heparin	100 mg/ml	10 µl
1 X Denhardt´s	50 X Denhardt´s	0.2 ml
0.1% Tween-20	10% Tween-20	0.1 ml
0.1% CHAPS	10% CHAPS	0.1 ml
DEPC-treated water		Up to 10 ml

SSC 2X + 0.1% Tween-20

Prepare with DEPC water.

SSC 0.2X + 0.1% Tween-20

Prepare with DEPC water.

Maleic Acid Buffer (MAB)

100 mM Maleic Acid (23.21 g/l) (Sigma-Aldrich)

150 mM NaCl (17.53 g/l) (Sigma-Aldrich)

Add double-distilled water to 800 ml. Adjust pH to 7.5 and complete the volume to 1 liter. Autoclave and store at 4 °C.

Before use, add Tween-20 to 0.1% (v/v)

MAB + 1% Blocking reagent (Roche, 11 096 176 001)

Dissolve by placing at 65 °C for 30 – 60 minutes, with frequent shaking. Store at -20 °C.

MAB + 1% Blocking reagent + 5% Sheep serum (Sigma-Aldrich, S3772)

The whole blocking solution is heated to 60 º C for 30 minutes to inactivate the serum and then cooled down on ice before adding to the samples.

Roche anti-digoxigenin, POD conjugated (Roche 11 207 733 910, store at 4 °C after reconstitution)

PBS + 0.1 M Imidazole, pH 7.6

Add 0.1 M imidazole (Sigma-Aldrich) to sterile PBS, autoclave, and keep at 4 °C.

Appendix 8: Fluorescein-tyramide synthesis (Hopman et al., 1998[4])

Materials

Fluorescein-NHS ester (NHS-Fluorescein, Thermo Scientific 46410, 100 mg scale, enough for 2 preparations to be done in parallel). Once opened dissolve entire contents in N,N-dimethylformamide and use at once.

Tyramine (Sigma-Aldrich T-2879)

N,N-dimethylformamide (DMFA, Sigma-Aldrich T-8654)

Triethylamine (Sigma-Aldrich T-0886)

100% ethanol

Solutions

Fluorescein-NHS ester solution: dissolve at 10 mg/ml in DMFA in a 15 ml Falcon tube. Because we buy a 100 mg package of NHS-Fluorescein, the easiest thing to do is to dissolve everything in 10 ml DMFA, and from there do two reactions, with 4 ml of the NHS-Fluorescein stock each (2 ml remain, discard them). Keep in the dark.

DMFA-triethylamine solution: Add 50 µl of triethylamine to 5 ml of DMFA

Tyramine solution: Dissolve 50 mg of tyramine in 5 ml of DMFA-triethylamine solution

Reaction

In a 15 ml Falcon Tube, mix 4 ml fluorescein-NHS ester solution (in DMFA) and 1.37 ml tyramine solution (in DMFA-triethylamine), and incubate in the dark at room temp for 2 hours. Add 4.6 ml of 100% ethanol, and store in dark at -20 °C. Use as a 1:100 dilution as detailed in the WMISH working protocol.

[4] Hopman, A. H., F. C. Ramaekers, and E. J. Speel. 1998. Rapid synthesis of biotin-, digoxigenin-, trinitrophenyl-, and fluorochrome-labeled tyramides and their application for In situ hybridization using CARD amplification. J Histochem Cytochem **46**:771-777.

Appendix 9: in vitro synthesis and quantification of Digoxigenin-labeled RNA probes

1) Cloning of the probe cDNA

Although other protocols recommend shorter probes for improved tissue penetration, in my experience it is better to use full-length probes, for greater signal intensity. For shorter genes that are highly expressed (*e.g. em-h2b*, *em-muc*), probes of *ca*. 200 bases worked fine. For genes of low expression, probes of 1 kb or more are recommended.

Clone the cDNA from a RT-PCR reaction into a PCR cloning vector such as pDrive (Qiagen) or pJet1.2 (Thermo Scientific). For pDrive, only one clone is needed, since it has T7 and SP6 promoters upstream and downstream of the multiple cloning site (MCS), respectively. When cloning into pJet1.2, one needs to make sure to have one clone with each insert orientation, since it only has a T7 promoter upstream of the MCS.

2) Linearizing the plasmid

Digest the plasmid with an enzyme that cuts in the MCS right after the insert, on the opposite side of the RNA polymerase promoter, so that the probe only includes the insert sequence. For example, with pJet1.2, only *Xba*I and *Nco*I (of the usual enzymes) are useful.

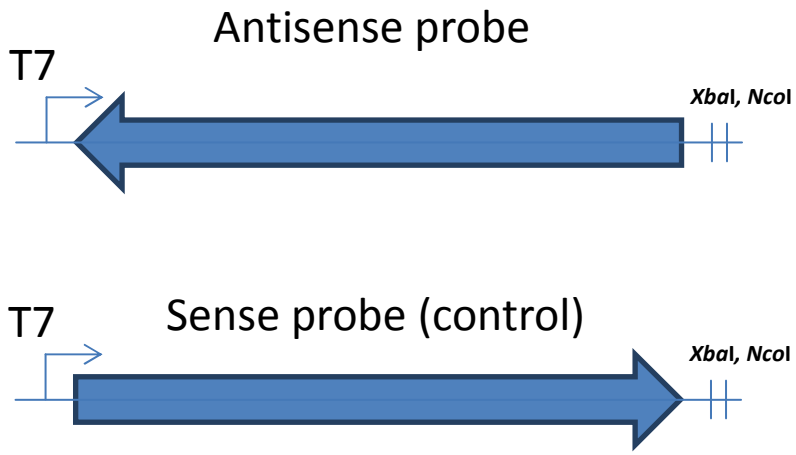

Digest at least 4 µg of plasmid for two hours with 40 units of enzyme, and run 100 ng on a 1% agarose gel to confirm that it is completely linearized. Then purify the linearized plasmid DNA with a Kit (a simple DNA clean-up kit is sufficient). Quantify by Nanodrop. Keep the plasmid as clean as possible (use clean plastic tips and elution buffer).

Note: check that the insert does not have a restriction site for that enzyme. If no enzyme can be used, amplify the insert plus the promoter using flanking primers, and purify by gel extraction after agarose electrophoresis.

3) *In vitro* transcription

- **Set up the following reaction on ice and mix well by pipetting:**

  Transcription Buffer 10 X (New England Biolabs) – 2 µl

  DIG RNA labeling mix 10 X (Roche 11 277 073 910) – 2 µl

  T7 OR SP6 polymerase (50,000 units/ml, New England Biolabs) – 2 µl

  RNAse out (40 units/µl, Invitrogen) – 0.5 µl

  Linearized plasmid DNA – 1 µg

  Bovine Serum Albumin 1 mg/ml, molecular biology grade (New England Biolabs) – 2 µl

  Water, RNAse free – enough for a 20 µl final reaction volume (do not use DEPC-treated water, but instead use commercial RNAse free water, since traces of DEPC can inhibit the reaction).

- Incubate for 2 hours at 37 °C
- Add 2 µl of RQ1 DNAse (Promega) and incubate for 15 minutes at 37 °C
- Purify each reaction with the Pure Link RNA Mini Kit (Ambion). Elute in 30 µl of RNAse free water. Alternatively, if many probes are being synthesized and a cheaper alternative is needed, precipitate the probe overnight at -80 °C with 0.1 volumes of sodium acetate 3 M, pH 5.2 and 2.5 volumes of 100% ethanol. Centrifuge at 12,000 g for 20 min at 4 °C, wash the RNA pellet with 70% ethanol, dry the pellet and dissolve it in 30 µl of RNAse free water (use RNAse free reagents).
- Run 3 µl of each sample in a 1% agarose gel to confirm the integrity of the probe (it does not need to be a denaturing gel, but it must be RNAse free).

4) Probe quantification by Dot-blot

In a Hybond-N membrane, spot 1 µl drops of serial dilutions of the probe (undiluted, 1:10, 1:100, 1:1000) and of the control DIG-RNA probe (Roche 11585746910, dilutions 10, 1.0, 0.1 and 0.01 ng/µl).

Dry for 1 hour at 60 °C between two Whatman Paper sheets, and cross-link under UV light for 1 minute in a trans-illuminator.

Then perform the following detection protocol:

- Wash 5 minutes in Buffer 1 (Tris-HCl 100 mM, NaCl 150 mM, pH 7.5), with shaking
- Block 10 minutes in Buffer 2 (Buffer 1 + 0.5% w/v Blocking Reagent, Roche), with shaking.
- Incubate with Anti-DIG, alkaline phosphatase conjugated (Roche 11 093 274 910), 1:2000 dilution in Buffer 2, for 20 minutes, with shaking.
- 2 washes of 10 minutes each in Buffer 1, with shaking
- Brief wash in Buffer 3 (Tris-HCl 100 mM, NaCl 100 mM, MgCl2 50 mM, pH 9.5), with shaking
- Detection with nitro-blue tetrazolium and 5-bromo-4-chloro-3'-indolyphosphate (NBT/BCIP, Sigma 72091, dilute 20 µl/ml in Buffer 3). Usually the detection is ready after 5 to 10 minutes in the dark without shaking.

Curriculum Vitae

Personal information

Name: Koziol Antmann, Uriel Bensión.
Birth Date: 10/10/1982, Montevideo, Uruguay.
Nationality: Uruguayan and Italian

Education

Currently performing my doctoral studies in the Graduate School of Life Sciences, University of Würzburg (Germany). Thesis supervisor: Prof. Dr. Klaus Brehm. (Since April 2011).
Thesis title: Molecular and developmental characterization of stem cells in the human parasite *Echinococcus multilocularis*,

Master in Science in Biology, with specialization in Cell and Molecular Biology (PEDECIBA Biología, Uruguay). Thesis supervisor: Dr. Estela Castillo, Sección Bioquímica, Facultad de Ciencias, Uruguay (from December 2006 until December 2009).
Thesis title: Caracterización de células proliferantes en *Mesocestoides corti* (Cestoda), y de genes *pumilio* como posibles marcadores moleculares de las mismas. ***(Characterization of proliferative cells in Mesocestoides corti (Cestoda) and of pumilio genes as possible molecular markers of these cells)***. Approved with the maximum qualification.

Bachellor in Sciences (Orientation: Invertebrate Zoology). (Facultad de Ciencias, Universidad de la República, Uruguay)
Graduation date: 30th August 2006.
Average grade: 10.94 over 12

Selected Post-graduate courses

Short Course for Young Parasitologists. Organized by the Deutsche Gesellschaft für Parasitologie (Heidelberg, Germany, 2012).

"Transferable skill courses" in the Graduate School of Life Sciences (Würzburg, Germany) such as "Poster design", "Scientific writing and publishing" "Statistical Data Analysis", "Good scientific Practices", and "Writing Grant Proposals". (Since April 2011).

Curso Internacional de Biología del Desarrollo. ***(International Course on Developmental Biology).*** Universidad Nacional Andrés Bello (Quintay, Chile, 2010).

Working with Pathogen Genomes. Wellcome Trust – Sanger Institute (Instituto de Higiene, Montevideo, Uruguay 2009).

Salud, Bienestar y Producción en Animales de Laboratorio ***(Health, well-being and production in laboratory animals).*** Universidad de la República - Comisión Honoraria de Experimentación Animal, Uruguay (CHEA) (2008).

"Real time PCR". Un método eficiente para caracterizar el genoma. ***(Real time PCR; an efficent method for genome characterization)***. PEDECIBA, Uruguay. (2008).

Regulación de la expresión génica en eucariotas. ***(Regulation of gene expression in eukaryotes).*** PEDECIBA, Uruguay (2008).

Curso Básico de Cultivo de Células. ***(Basic course in cell culture).*** PEDECIBA, Uruguay. (2007).

Microscopía Confocal. Principios y Aplicaciones. ***(Confocal microscopy. Principles and applications).*** PEDECIBA, Uruguay (2007).

Expresión y Silenciamiento de Genes en Células Animales y Vegetales. ***(Expression and silencing of genes in animal and vegetal cells)*** CABBIO (Universidad Nacional de Córdoba, Argentina, 2007).

Positions

Assistant Professor, second level, of Sección Bioquímica (Biochemistry department), Facultad de Ciencias, Universidad de la República, Uruguay (since December 2009, currently on a leave for the duration of my doctoral studies).

Research assistant in the project "Aplicación de la metagenómica para la obtención de enzimas de uso potencial en industrias procesadoras de pulpa de papel" *("Application of metagenomics for the obtention of enzymes of potenital use in paper pulp production")*, under the direction of Dr. Elena Fabiano and Dr. Francisco Noya. (Biochemistry department, IIBCE, Uruguay) (From January 2007 until July 2008).

Research internship in the laboratory of Dr. Michael Kahn, Institute of Biological Chemistry, Washington State University. Partially financed by CSIC, Uruguay (Pullman, U.S.A, from October until December 2007)

Research and teaching assistant of Sección Bioquímica (Biochemistry department) Facultad de Ciencias, Universidad de la República, Uruguay. (from November 2006 until december 2009).

Interim Teaching Assistant of Sección Bioquímica (Biochemistry department) (Facultad de Ciencias, Universidad de la República) (From April 2006 until July 2006).

Research assistant in the project "Búsqueda de reguladores globales del metabolismo del hierro en Sinorhizobium meliloti 1021" *("Search for global regulators of iron metabolism in Sinorhizobium meliloti 1021")* under the direction of Dr. Elena Fabiano and Dr. Francisco Noya. (Biochemistry department, IIBCE, Uruguay) (From May 2005 until February 2007)

Publications

Schubert, A., **Koziol, U**., Cailliau, K., Vanderstraete, M., Dissous. C., Brehm, K. (2014). **Targeting *Echinococcus multilocularis* Stem Cells by Inhibition of the Polo-Like Kinase EmPlk1.** PloS Neglected Tropical Diseases, 8(6):e2870.

Koziol, U., Rauschendorfer, T., Zanon-Rodríguez, L., Krohne, G., Brehm, K. (2014). **The unique stem cell system of the immortal larva of the human parasite *Echinococcus multilocularis.*** *EvoDevo*, 5:10.

Domínquez, M.F.*, **Koziol, U.***, Porro, V., Costábile, A., Estrade, S., Tort, J., Bollati-Fogolin, M., Castillo, E (2014). **A new approach for the characterization of proliferative cells in cestodes.** *Experimental Parasitology*, 138:25–29. (* Both authors contributed equally to this work).

Skinner, D.E., Rinaldi, G., **Koziol, U.**, Brehm, K., Brindley, P.J. **How might flukes and tapeworms maintain genome integrity without a canonical piRNA pathway?** *Trends in Parasitology*, 30:123-129.

Hemer, S., Konrad, C., Spiliotis, M., **Koziol, U.**, Schaack, D., Förster, S., Gelmedin, V., Stadelmann, B., Dandekar, T., Hemphill, A., Brehm, K. **Host insulin stimulates *Echinococcus multilocularis* insulin signalling pathways and larval development.** *BMC Biology*, 12:5.

Koziol U., Krohne G., Brehm K. (2013)**. Anatomy and development of the larval nervous system in *Echinococcus multilocularis*.** *Frontiers in Zoology* 10:24.

Tsai I.J., Zarowiecki M., Holroyd N., Garciarrubio A., Sanchez-Flores A., Brooks K.L., Tracey A., Bobes R.J., Fragoso G., Sciutto E., Aslett M., Beasley H., Bennett H.M., Cai J., Camicia F., Clark R., Cucher M., De Silva N., Day T.A., Deplazes P., Estrada K., Fernández C., Holland P.W., Hou J., Hu S., Huckvale T., Hung S.S., Kamenetzky L., Keane J.A., Kiss F., **Koziol U.**, Lambert O., Liu K., Luo X., Luo Y., Macchiaroli N., Nichol S., Paps J., Parkinson J., Pouchkina-Stantcheva N., Riddiford N., Rosenzvit M., Salinas G., Wasmuth J.D., Zamanian M., Zheng Y.; Taenia solium Genome Consortium, Cai X., Soberón X., Olson P.D., Laclette J.P., Brehm K., Berriman M. (2013). **The genomes of four tapeworm species reveal adaptations to parasitism.** *Nature* 496:57-63

Koziol, U., Costábile, A., Domínguez, M. F., Iriarte, A., Alvite, G., Kun, A., Castillo, E. (2011). **Developmental expression of high molecular weight tropomyosin isoforms in *Mesocestoides corti***. *Molecular and Biochemical Parasitology* 175:181-91.

Koziol, U., Domínguez, M. F., Marín, M., Kun, A., Castillo, E. (2010). **Stem cell proliferation during in vitro development of the model cestode *Mesocestoides corti* from larva to adult worm**. *Frontiers in Zoology* 7:22.

Amarelle, V., **Koziol, U.**, Rosconi, F., Noya, F., O´Brian, M.R., Fabiano, E. (2010). **A new small regulatory protein, HmuP, modulates hemin acquisition in *Sinorhizobium meliloti*.** *Microbiology* 156:1873-1882.

Koziol, U., Hannibal, L., Rodríguez, M. C., Fabiano, E., Kahn, M. L., Noya, F. (2009). **Deletion of citrate synthase restores growth in *Sinorhizobium meliloti* 1021 aconitase mutants.** *Journal of Bacteriology* 191:7581-7586.

Koziol, U., Iriarte, A., Castillo, E., Soto, J., Bello, G., Cajarville, A., Roche, L., Marín, M. (2009) **Characterization of a putative *hsp70* pseudogene transcribed in protoscoleces and adult worms of *Echinococcus granulosus*.** *Gene* 443:1-11.

Koziol, U., Lalanne, A. I., Castillo, E. (2009). **Hox genes in the parasitic Platyhelminthes *Mesocestoides corti*, *Echinococcus multilocularis* and *Schistosoma mansoni.* Evidence for a reduced Hox complement.** *Biochemical genetics* 47:100-116.

Koziol, U., Marín, M., y Castillo, E. (2008). ***Pumilio* genes from the Platyhelminthes**. *Development Genes and Evolution* 218(1):47-53.

Book Chapters

Koziol, U., Castillo, E. (2010). **Cell proliferation and differentiation in cestodes**. In: Research in Helmiths, Esteves, A. Ed. Transworld Research Network, Kerala, India.

Selected Presentations and Conferences

Koziol, U., Krohne, G., Castillo, E., Brehm, K. **Cell proliferation and differentiation in cestode larval and adult development.** Oral presentation at the Euro Evo Devo Conference (Lisbon, Portugal, 10th to 13th July 2012).

Koziol, U., Amarelle, V., Rosconi, F., Noya, F., O´Brian, M. R., Fabiano, E. (2010). **Discovery of a new conserved tandem motif upstream of outer membrane hemin transporters in alpha and beta-proteobacteria.** Poster in International Society for Computational Biology Latin America Conference (Montevideo, Uruguay, 13th to 16th March 2010).

Koziol, U., Domínguez, M. F., Costábile, A., Marín, M., Castillo, E. (2009) **Characterization of proliferative cells in cestodes by BrdU labelling and molecular markers.** Poster and oral presentation in the XXIII World Congress of the International Association of Hydatidology. (Colonia del Sacramento, Uruguay, December 2009).

Koziol, U., Domínguez, M.F., Costábile, A., Caurla, G., Marín, M., Kun, A., Castillo, E. **Proliferación celular durante el desarrollo de *Mesocestoides corti* (Cestoda).** ***(Cell proliferation during the development of Mesocestoides corti (Cestoda))*.** Oral and poster presentation in the molecular parasitology session in the VI meeting of the Sociedad de Bioquímica y Biología Molecular (Montevideo, November 2009).

Amarelle, V., Senatore, D., Koziol, U., Noya, F., Fabiano, E. **Functional metagenomics of termite gut bacteria**. poster presentation by V. Amarelle in Genomes 2008: Functional Genomics of Microorganisms, 2008 (Paris, France, April 2008)

Koziol, U., Yurgel, S., Kahn, M., Noya, F. ***Sinorhizobium meliloti* 1021 mutations that link nitrogen and osmotic stress responses**. Poster in the 8th European Nitrogen Fixation Conference (Ghent, Belgium, September 2008).

Awards and Mentions

NEB Price for the best Student Presentation, 6th Short Course for Young Parasitologists (Heidelberg, Germany, March 2012).

Eugenio Prodanov Award (PEDECIBA Biology, Uruguay) for the best M.Sc. thesis in basic research in biology in the period from May 2009 to May 2010. The award is given to a student whose thesis, developed mainly in Uruguay, constitutes an important contribution to scientific knowledge in his research subject.

Special mention for the oral presentation "Caracterización genética y molecular de locus *acnA* de *Sinorhizobium meliloti*. Esencialidad de la aconitasa para la viabilidad celular" (Genetic and molecular characterization of the *acnA* locus of *Sinorhizobium meliloti*. Essentiality of aconitase for cell viability). Award for Young researchers, XII meeting of the Sociedad Uruguaya de Biociencias (Minas, Uruguay, September 2007).

EMBO Poster Prize, Outstanding poster presentation, Genomes 2008: **Functional Genomics of Microorganisms.** (Paris, France, April 2008) (poster presentation performed by V. Amarelle).

Scholarships and Grants

PhD fellowship, Graduate School of Life Sciences, University of Würzburg (Since April 2011, extended until July 2014).

M.Sc. Degree scholarship from the Sistema Nacional de Becas, ANII, Uruguay. (Awarded in 2009 but not accepted by me)

Scholarship for M.Sc. post-graduate studies, awarded by CSIC, Universidad de la República, Uruguay (November 2008 to November 2009).

Travel grant for the course "Expresión y Silenciamiento de Genes en Células Animales y Vegetales". *(Expression and silencing of genes in animal and vegetal cells)* (Universidad Nacional de Córdoba, Argentina, 2007), awarded by CABBIO, Argentina-Brasil.

Travel grant for the 8th Nitrogen Fixation Conference, Ghent, Belgium, awarded by FEMS, 2008.

Appendices and C.V.

Statement of individual author contributions and of legal second publication rights

Publication (complete reference): **Koziol, U.**, Rauschendorfer, T., Zanon-Rodríguez, L., Krohne, G., Brehm, K. (2014). **The unique stem cell system of the immortal larva of the human parasite *Echinococcus multilocularis.*** *EvoDevo**, 5:10***

Participated in	**Author Initials,** Responsibility decreasing from left to right				
Study Design	KB	UK			
Data Collection	UK	TR	LZR	GK	
Data Analysis and Interpretation	UK	KB	GK		
Manuscript Writing	UK	KB			

Explanations (if applicable):

Publication (complete reference): **Koziol U.**, Krohne G., Brehm K. (2013)**. Anatomy and development of the larval nervous system in *Echinococcus multilocularis*.** *Frontiers in Zoology* 10:24.

Participated in	**Author Initials,** Responsibility decreasing from left to right				
Study Design	UK	KB			
Data Collection	UK	GK			
Data Analysis and Interpretation	UK	KB	GK		
Manuscript Writing	UK	KB			

Explanations (if applicable):

Publication (complete reference): Koziol, U., Radio, S., Smircich, P., Zarowiecki, M., Fernández, C., Brehm, K. (in preparation, provisional title). A novel terminal-repeat transposon in miniature (TRIM) is massively expressed in *Echinococcus multilocularis* stem cells.

Participated in	**Author Initials,** Responsibility decreasing from left to right				
Study Design	UK	KB	CF		
Data Collection	UK	SR	MZ	PS	
Data Analysis and Interpretation	UK	SR	PS	MZ	KB CF
Manuscript Writing	UK	KB	CF		

Explanations (if applicable):

I confirm that I have obtained permission from both the publishers and the co-authors for legal second publication.

I also confirm my primary supervisor's acceptance.

Uriel Koziol	11.04.2014	Würzburg	
Doctoral Researcher's Name	Date	Place	Signature